THE LONG TERM IMPACT OF THE SELI ONE SHIPWRECK ON THE TABLE BAY BEACHES

by Christian Seifart

Thesis presented in fulfilment of the requirements for the degree of Master of Science in the Faculty of Civil Engineering at Stellenbosch University

Supervisor: Mr Geoffrey Toms

December 2012

DECLARATION

By submitting this thesis electronically, I declare that the entirety of the work contained therein is my own, original work, that I am the owner of the copyright thereof (unless to the extent explicitly otherwise stated) and that I have not previously in its entirety or in part submitted it for obtaining any qualification.

....

Christian Seifart Date

ABSTRACT

On the 9th September 2009, the 178 m Panamanian bulk carrier, the Seli One, ran aground off the coast of Blouberg in Table Bay, South Africa. Due to failed salvage attempts, the vessel has remained stranded approximately 500 m off the Blouberg beachfront. Since the vessel ran aground, a gradual change in the Blouberg beach shape in the lee of the wreck has been observed. The local coastline, which has traditionally been fairly uniform, has assumed a curved shape, with significant sediment accretion being observed in the wave shadow of the wreck. Initially, the Seli One wreck remained intact. However, during a storm on the 4th September 2011, the vessel split up into three separate pieces.

The impact that the wreck is having on the local wave, current and sediment transport dynamics remains undefined. This lack of knowledge results in significant risks, relating to shoreline stability and beach amenity. The objective is this study was therefore the determination of the long-term impact of the Seli One shipwreck on the Blouberg beachfront.

A review of existing literature has indicated that no empirical relationships are available which could be used to calculate the impact of a shipwreck on nearby coastal processes. Numerous methods are available which can be used to determine the net longshore transport rates, but these cannot be used to quantify the impacts of shipwrecks on the local sediment transport regime. Numerical models were therefore used to determine the impact of the Seli One shipwreck.

Through the analysis of simulation results, it was concluded that, as expected, the shipwreck has resulted in a significant reduction in the net longshore sediment transport rate in her lee, resulting in sediment deposition in this area. It was further concluded that the vessel does not result in the complete blockage of longshore sediment transport, and that sediment is able to periodically pass through the lee of the vessel.

The simulated beach salient on the 3rd July 2011 was compared to results of a beach survey, performed on the same date specifically for this study. The simulated accretion of approximately 27 m in the lee of the shipwreck agrees well with the measured salient. It has been shown that approximately 75% of the salient accretion occurred within the first two months of the vessel's arrival. Furthermore, shoreline erosion on the northern side of the salient resulting directly from the shipwreck has been shown to be approximately 15 m. This too occurs relatively rapidly, within approximately two months of the vessels arrival.

Following the initial impact of the wreck in its intact configuration, the long-term potential impact of the vessel in its broken-up configuration was determined. This included the assumption that the vessel does not undergo any additional breaking-up, and remains in its three-piece configuration indefinitely. This has shown that the salient width resulting from the shipwreck is reduced to approximately 20 m, compared to the initial 27 m. However, shoreline erosion on the northern side of the wreck has increased from approximately 15 m initially to approximately 18 m in the long-term, which is caused by the continuous sedimentation between the vessel and the beach.

A two-dimensional coupled wave, current and sediment transport model has been developed and has shown that the wave shelter resulting from the Seli One results in the formation of a submerged salient between the vessel and the shoreline.

It was found that shipwrecks have the potential of significantly altering local longshore sediment transport characteristics in general. Depending on local conditions, this may pose serious risks, both in terms of jeopardizing local seaside infrastructure, as well as creating dangerous swimming conditions.

Considering the impact that a shipwreck can have on local shoreline changes, with special regard to the rate at which these shoreline changes can occur, it is recommended that the results obtained from the current study be used to estimate the impact of potential future shipwreck scenarios in Table Bay.

OPSOMMING

Op die 9de September 2009 het die 178 m lange Panamese vragskip, die Seli Een, aan die kus van Bloubergstrand in Tafelbaai, Suid Afrika, gestrand. Weens mislukte reddingspogings, het die skip ongeveer 500 m van die kuslyn gestrande gebly. Sedertdien, is ‘n geleidelike verandering in die vorm van Bloubergstrand se kuslyn waargeneem. Die kuslyn, wat tradisioneel redelik uniform en reguit was, het onlangs ‘n aansienlike geboë vorm aangeneem, met ‘n beduidende hoeveelheid sand wat in die skip se lykant neerset. Aanvanklik het die Seli Een wrak ongeskonde gebly, maar tydens ‘n storm op die 4de September 2011, het die skip in drie afsonderlike stukke opgebreek.

Die impak wat die wrak op die golf, strome en sediment vervoer dinamika het,bly ongedefinieërd. Hierdie gebrek aan kennis veroorsaak ‘n aansienlike hoeveelheid risiko’s met spesifieke betrekking tot kuslyn stabiliteit en strand gerief. Die doel van hierdie studie was dus om die langtermyn-impak van die Seli Een skeepswrak op Bloubergstrand te bepaal.

'n Hersiening van bestaande literatuur het aangedui dat geen empiriese verhoudings beskikbaar is wat gebruik kan word om die impak van 'n skeepswrak op die nabygeleë kustelike prosesse te bereken nie, maar wel versekeie metodes wat gebruik kan word om die netto langsstroom sediment vervoer te bepaal. Hierdie verhoudings kan egter nie gebruik word om die impak van ‘n skeepswrak op die sediment vervoer meganisme te kwantifiseer nie, dus is numeriese modelle gebruik om die impak van die Seli Een skeepswrak te bepaal.

Die skeepswrak het ‘n aansienlike vermindering in the netto langsstroom sediment vervoer veroorsaak, wat tot die afsetting van sediment in hierdie gebied lei. Dit is ook verder bepaal dat die Seli Een nie die volledige verstopping van langsstroom sedimentvervoer veroorsaak nie, maar dat sediment van tyd tot tyd in staat is om deur die lykant van die skeepswrak te beweeg.

Die gesimuleerde strand aanwas van die 3de Julie 2011 is vergelyk met resultate van ‘n strand-opmeting, wat uitgevoer is op dieselfde datum, spesifiek vir hierdie studie. Die gesimuleerde aanwas, van ongeveer 27 m in die lykant van die skeepswrak, stem saam met die gemete aanwas. Ongeveer 75% van die aanwas het binne twee maande van die aankoms van die Seli Een plaasgevind. Verder is dit getoon dat aan die noordelike kant van die aanwas, ongeveer 15 m van die kuslyn weggespoel het as gevolg van die Seli Een.

Na die aanvanklike impak van die wrak in sy ongeskonde konfugirasie, is die potensiële langtermyn impak van die skip in sy opgebreekte konfugirasie bepaal. Dit sluit die aanname in dat die skip nie enige bykomende breke ondergaan nie, en in sy drie-stuk konfigurasie bly. Dit het getoon dat die breedte van die aanwas, wat veroorsaak is deur die skip, verminder tot ongeveer 20 m in vergelyking met die aanvanklike 27 m. Verder is dit getoon dat die erosie aan die noordelike kant van die Seli Een vermeerder het van die aanvanklike 15 m na ongeveerder 18 m in die langtermyn. Die oorsaak hiervaan is die aaneenlopende sedimentasie tussen die wrak en die strand.

'n Twee-dimensionele gekoppelde golf, stroom en sediment vervoer model is ontwikkel en het getoon dat die golf skuiling, as gevolg van die Seli Een, sedimentasie tussen die skip en die kuslyn veroorsaak.

Daar is gevind dat skeepswrakke die potensiaal het om aansienlike veranderinge aan die nabygeleë langstroom sediment vervoer stelsel te veroorsaak. Afhangende van die plaaslike omstandighede, kan hierdie ernstige risiko’s veroorsaak, beide in terme van die gevaar vir plaaslike kustelike infrastruktuur, sowel as die generasie van gevaarlike swem toestande.

Met inagneming van die impak wat 'n skeepswrak op plaaslike kuslyn veranderinge kan hê, met spesiale verwysing na die tempo waarteen hierdie kuslyn veranderinge kan plaasvind, word dit aanbeveel dat die resultate wat verkryg is vanuit die huidige studie, gebruik word om die impak van moontlike, toekomstige skeepswrakke in Tafelbaai te bepaal.

ACKNOWLEDGEMENTS

The completion of this thesis would not have been possible without the contribution of others.

First and foremost, I would like to thank my wife, Romy. Without her understanding and patience over the past three years, this study would not have come to completion. Her continued support and enthusiasm has been a great motivator to keep going.

My study leader, Geoff Toms, has provided invaluable guidance and leadership during the course of this investigation, and has kept me focused and determined throughout.

I would like to express my sincere gratitude to Prestedge Retief Dresner Wijnberg (PRDW) for financing my studies, as well as granting me time off work to attend lectures, seminars and to finish off this report during the latter stages of this investigation. I would especially like to thank Mr Stephen Luger of PRDW, who has provided many hours of invaluable technical input into this study, and has retained a keen interest in my results and progress.

Dr Nicholas Grunnet has greatly assisted with one-on-one training on the use of the LITPACK numerical models, as well as providing invaluable input into the understanding of the Table Bay sediment transport system.

Professor William Kamphuis, Emeritus Professor in Coastal Engineering at the Queens University in Canada, has provided expert advice towards the understanding of the Table Bay longshore sediment transport system, which is greatly appreciated.

The Danish Hydraulics Institute has provided me with an academic license for the numerical modelling software used during this investigation, without which, this study would most certainly not have been possible. Special thanks to Mr Andrew Pott for facilitating this.

Mr Magenthran Ruthenavelu, Port Engineer at the Port of Cape Town, and the Transnet National Ports Authority has provided historic beach profile measurements and measured offshore wave data for use in this study, without which, the detailed investigation of the Table Bay sediment transport system would not have been possible. Their contribution is greatly appreciated.

Eskom is thanked for providing additional measured wave data, which was used for the calibration of the wave transformation model.

The beach survey performed on the 3rd July 2011 was enabled by equipment provided free of charge by Mr Aubrey Price of C&C Technologies. The validation of this survey was enabled by knowledge of fixed town benchmarks, details of which were received from Mr Tim Painter of Lloyd and Hill Surveyors. Both are thanked for their respective contribution to this study.

THE LONG-TERM IMPACT OF THE SELI ONE SHIPWRECK ON THE TABLE BAY BEACHES

TABLE OF CONTENTS

LIST OF FIGURES

Page No

LIST OF TABLES

1. INTRODUCTION

1.1 The Seli One Shipwreck

On the 9th September 2009, the 178 m Panamanian bulk carrier, the Seli One, ran aground off the coast of Blouberg in Table Bay, South Africa. Due to failed salvage attempts, the vessel has remained stranded approximately 500 m off the Blouberg beachfront.

Figure 1-1: Table Bay and Location of Seli One Shipwreck

Image: Google Earth (Google Inc., 2010)

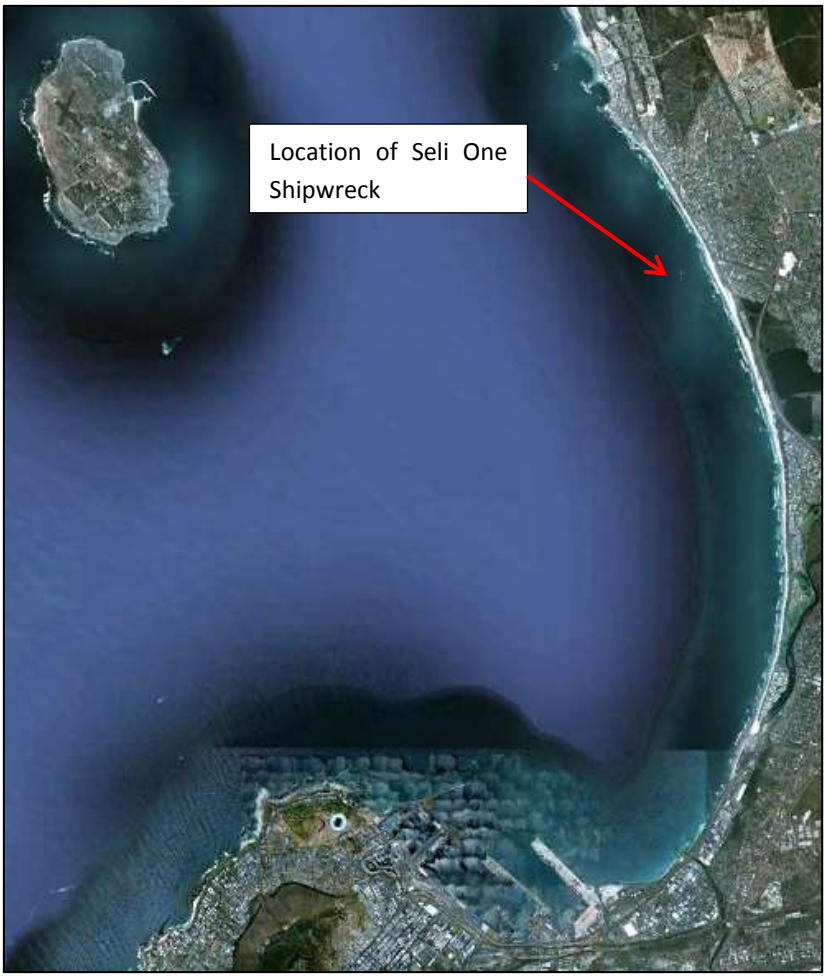

Since the vessel ran aground, a gradual change in the Blouberg beach shape in the lee of the wreck has been observed. The local coastline, which has traditionally been fairly uniform, has assumed a curved shape, with significant sediment accretion being observed in the wave shadow of the wreck.

Figure 1-2: Aerial View of Influence of Seli One on Table Bay Shoreline

Image Google Earth (Google Inc., 2010)

Figure 1-3: Seli One Shipwreck Shortly After Running Aground in September 2009

Figure 1-4: Seli One Shipwreck During Beach Survey (3rd July 2011)

Due to the vessel's orientation, it has been subjected to a relentless side-on wave attack, especially during the winter months when larger south-westerly swells arrive, accompanied by locally generated seas created by strong north-westerly winds. In September 2011, one such storm resulted in the vessel breaking up into three sections, as can be seen in Figure 1-5. It is unclear whether this break was only along the upper sections of the

vessel, i.e. the freeboard, or whether it is a complete disconnection between the three pieces. During this study, it was assumed that the break was complete.

Figure 1-5: Broken Up Seli One after a Storm in September 2011 (4th September 2011)

1.2 Hypothesis

It is hypothesized that the Seli One shipwreck acts in a similar manner as a detached offshore breakwater. Offshore breakwaters are usually designed to create calm wave and current conditions in the lee of the structure for a variety of reasons, including the stabilization of the local shoreline. However, the Seli One wreck was neither planned nor was it designed as an offshore breakwater. As such, the impact that the wreck is having on the local wave, current and sediment transport dynamics remains undefined. This lack of knowledge results in significant risks. One such risk relates to the potential generation of dangerous conditions for swimmers, surfers and other beach users. In addition to this, the sediment transport dynamics remain unclear, which means that the potential impact of the wreck on the local shoreline morphology requires quantification.

Regarding the sediment transport behaviour in the lee of offshore breakwaters, the calm wave and current conditions generally result in sediment deposition in this area. This is usually identified as shoreline accretion in the lee of offshore breakwaters, with shoreline erosion occurring along the adjacent beaches. In addition to this, sedimentation between the structure and the beach is also caused.

The impact of the Seli One shipwreck on the local Table Bay shoreline is shown in Figure 1-6. Shoreline accretion in the lee, as well as to the south of the vessel is evident. Additional accretion can be identified in the lee of the vessel between the Seli One and the shoreline. Furthermore, it can be identified that shoreline erosion is occurring immediately to the north of the ship, the extent of which reduces with increased distance away from the vessel. The altered wave climate in the lee of the Seli One shipwreck is visible in Figure 1-6, with wave crests rotating in a clockwise and anti-clockwise direction at the northern and southern ends of the vessel respectively. A limited amount of wave reflection is also visible in the figure.

Since the typical effects of an offshore breakwater are similar to those being observed at the Seli One, this study is expected to indicate that the changes in the shoreline morphology, including both the changes in the

shoreline position, as well as the apparent accretion between the wreck and the beach, are forming as a direct result of the presence of the Seli One shipwreck on the local sediment transport regime. This may therefore lead to the conclusion that procedures for the design of offshore breakwaters could be used to quantify the impacts of shipwreck on the local shoreline.

Figure 1-6: Impact of Seli One Shipwreck on Shoreline Morphology

1.3 Study Objective

The primary objective is the investigation of the impact of the Seli One shipwreck on the shoreline stability of Table Bay. This includes an investigation into the short-term impact of the wreck, prior to the vessel breaking up into three sections in September 2011, followed by an investigation into long-term potential impact, assuming that the vessel remains in the current three-piece configuration. The end of this long-term potential investigation was arbitrarily chosen as the 31st December 2024.

In addition to this, the impact of two "worst-case" potential grounding events on the local shoreline morphology is tested, to determine what the Table Bay shoreline may look like following a worst-case shipwreck event.

1.4 Study Overview

The study objective discussed in Section 1.3 is achieved through the execution of several sub-tasks, the details of which will be covered in Section 4 later. In general, these sub-tasks can be categorized as researching historic vessel groundings that have occurred both in Table Bay and internationally. Secondly, a review of existing literature was performed, which was followed by the case study of the Seli One shipwreck near the Blouberg beachfront. The impacts of the shipwreck on the nearby coastal processes, including the impacts on the waves, currents and sediment transport characteristics, were computed using numerical models, supported by field observations and the analysis of aerial photography. Results of this analysis were used to evaluate the study hypothesis.

1.5 Thesis Structure

This thesis is structured into twelve sections, including the current section. Background to the current investigation is given in Section 2, whilst the review of applicable literature is discussed in Section 3. The study methodology is summarized in Section 4. Important public and private developments which may have an impact on the longshore sediment transport characteristics of Table Bay are introduced in Section 5. Sections 6 and 7 continue to discuss the beach profile analysis performed to investigate the historic behaviour of the Table Bay shoreline, as well as the Table Bay sediment transport system. Sections 8 to 11 introduce the local shoreline modelling and two-dimensional sediment transport modelling performed as part of this study. Study findings and recommendations are covered in Section 12.

Throughout the course of this thesis, reference is made to various maps showing details of the study area. These are given in Appendix C to Appendix E.

2. BACKGROUND

2.1 Introduction

As general background to the current investigation, the history of shipwrecks in Table Bay is researched. This is done to determine how often such events occur, as well as identifying the need for this research to understand the potential impacts of shipwrecks on nearshore coastal processes in general. In addition to this, two specific shipwrecks which have had an impact on the nearshore sediment transport dynamics are highlighted.

2.2 Historic Vessel Groundings

2.2.1 Table Bay Shipwrecks

Shipwrecks are not an uncommon feature of the Table Bay coastline, especially during the 17th, 18th and early 19th century prior to the construction of the Port of Cape Town. The Dutch East India Company (VOC) used Table Bay as an anchorage, primarily due to its proximity to a fresh water supply from the "Varsche River", which flowed down from Table Mountain into the bay (Harris, 1993).

Despite its convenience, Table Bay was a dangerous anchorage, especially during the winter months. Before the construction of a breakwater near Green Point, which later became the root of the Port of Cape Town breakwater, the bay did not provide shelter during violent winter storms (Harris, 1993). These storms were accompanied by gale force onshore north-westerly winds. Vessels would drag their anchors in these conditions, eventually being wrecked along the southern half of Table Bay.

During the first decade of the VOC having established itself in Cape Town, the company lost two vessels, namely the *Mauritius Eylandt* and the *Haarlem* (Harris, 1993). During an especially violent storm in mid-June 1722, the company lost seven vessels due to strong north-westerly winds. Large waves crashed against the hulls, causing each of the seven timber vessels to break apart. One of the vessels, the *Standvastigheid*, lost 219 of her crew of 234, whilst the *Rotterdam* only had thirteen survivors (Harris, 1993).

These significant losses forced the VOC to consider the construction of a breakwater to create a shelter for vessels during violent winter storms. The breakwater was however not constructed, due to insufficient labour and funding for such a large project (Harris, 1993).

In the meantime, ships continued to wreck along the shores of Table Bay, until, in 1857, Captain Vetch, Harbour Surveyor of the Admiralty, stated that "...the value of a secure and ample harbour at the Cape cannot be overlooked." (Harris, 1993). Following this, the construction of a breakwater, which now forms the root of the current breakwater of the Port of Cape Town, started in 1860. By the end of the nineteenth century, a safe harbour was constructed.

Figure 2-1 shows the approximate locations of the shipwrecks in Table Bay during the 17th and 18th century. The dotted line in the figure indicates the current position of the reclaimed port. Of the 37 vessels that ran aground in that period, sixteen wrecked during two events in 1722 and 1737 (Harris, 1993).

Following the construction of the Port of Cape Town in the late 19th century, the number of shipwrecks in Table Bay has significantly reduced. Nevertheless, vessels continue to run aground in Table Bay and the greater Western Cape area. Figure 2-2 shows an aerial image of a few more recent shipwrecks located along the shores of the Western Cape (Anonomous, 2009).

Figure 2-1: Approximate Locations of Shipwrecks in the Vicinity of Cape Town

(Harris, 1993)

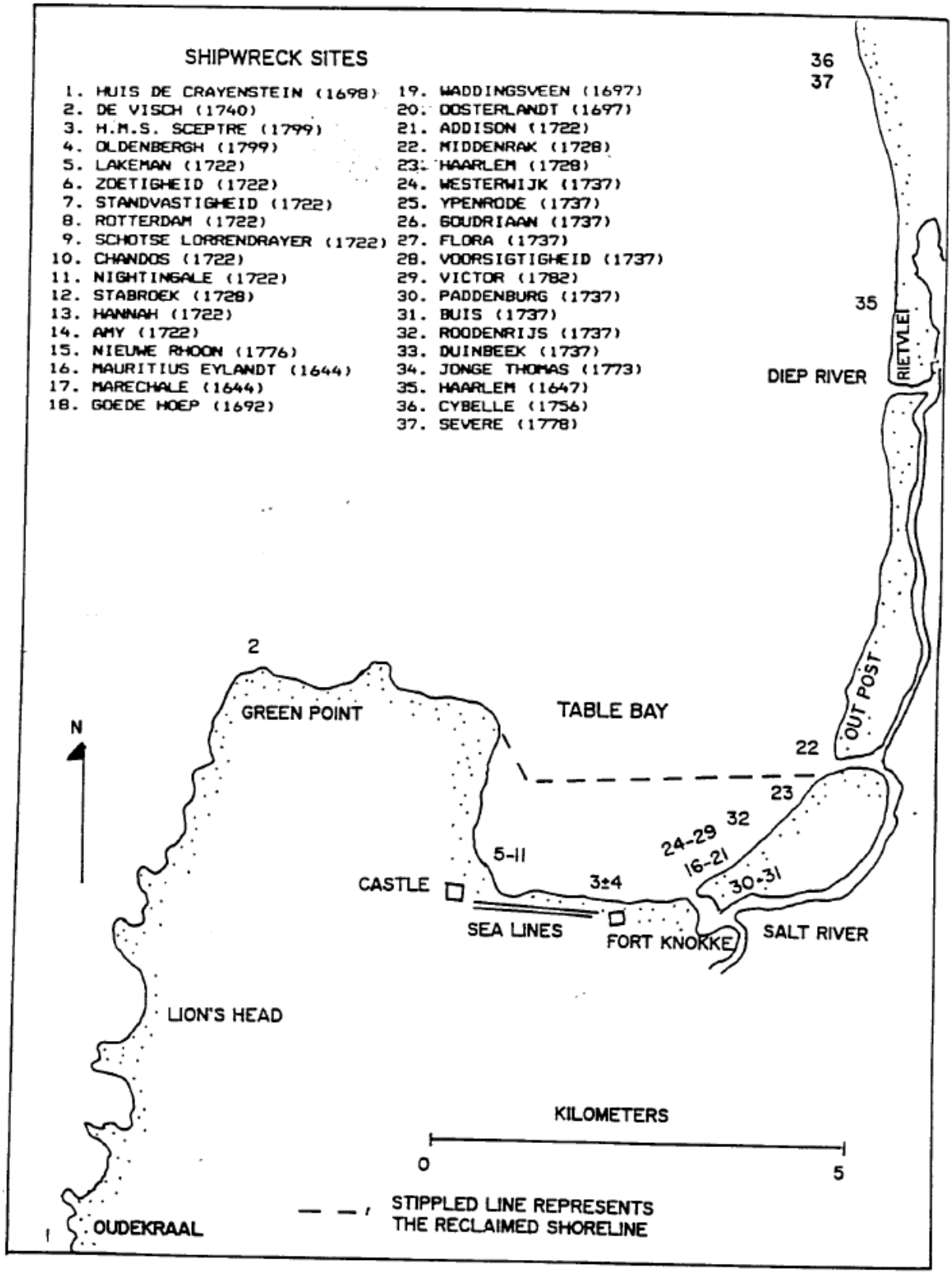

The dates on which these vessels ran aground is shown in parentheses in the figure, indicating that, although the frequency of these events has reduced since the 19th century, they continue to occur. Five vessels have run aground along the Western Cape since 1990.

Figure 2-2: Shipwrecks along the Western Cape Coastline

(Google Inc., 2010), (Anonomous, 2009)

Due to the frequency with which vessels run aground in Table Bay and the greater Western Cape area, an understanding of the potential impact that a shipwreck can have on local shoreline dynamics is important.

2.2.2 The Sealand Express

The US flagged container ship, the *Sealand Express*, ran aground off Sunset Beach in Table Bay early on the 19th August 2003. The vessel, with 1 037 containers on board, started dragging her anchor in winds gusting in excess of 100 km/hour (Main, 2003).

The container ship was re-floated during the mean high water spring tide on the 13th September 2003, following the dredging of a channel using a small Trailer Hopper Suction Dredger (Main, 2003). The vessel therefore remained stranded for approximately one month.

As can be seen from the photographs shown below, the Sealand Express grounded during high water, meaning that she drifted closer to the shore compared to the Seli One, and into the breaker zone. The potential effect that the Sealand Express could have had on local sediment transport characteristics was therefore much greater than the Seli One.

Figure 2-3: Grounded Sealand Express off Sunset Beach in August 2003

(Main, 2003)

During the approximately month-long period of the Sealand Express being wrecked off Sunset Beach, shoreline accretion would have occurred in the lee of the vessel. No explicit beach survey data immediately prior to the vessel's arrival and immediately after the vessel's removal is available, which means that the exact impact of the Sealand Express on the local shoreline morphology cannot be quantified. However, referring to Figure 2-4, slight shoreline accretion in the lee of the ship can be identified. It should be noted that it is not clear when this photograph was taken. If the photograph was taken fairly soon following the wrecking event, morphological changes would have been fairly limited.

Figure 2-4: Onset of Shoreline Accretion in the Lee of the Sealand Express

(Main, 2003)

From the introduction of sediment transport dynamics which will be given in Section 3, it will become clear that the surfzone is the most active in terms of sediment transport. The failure to re-float the Seli One could therefore have had a significant impact of the Table Bay sediment transport regime.

2.2.3 The Pasha Bulker

On the 8th June 2007, the coal carrier *Pasha Bulker* ran aground on Nobby's Beach at Newcastle in Australia. The ship was unloaded, with only 700 tonnes of heavy fuel oil (HFO), 34 tonnes of diesel and 16 tonnes of lube oil on board (AMSA, 2009). Due to the light loading condition of the vessel, and corresponding low draft, the vessel grounded very close to the shore, within the surfzone, as can be seen in Figure 2-5 below.

Three attempts were made to re-float the vessel. The first attempt started at 19h00 on the 1st July 2007, approximately three weeks after the vessel ran aground. This attempt was unsuccessful due to a tow-line, between the vessel and a tug, breaking (AMSA, 2009). The second attempt was started later on the same day. Whilst being unsuccessful in re-floating the vessel, the stranded vessel was turned perpendicular to the shoreline. This position was maintained overnight, with salvage tugs maintaining tension on the towing lines. The final attempt followed the next day, during which the vessel was re-floated with only small amounts of oil and lube leakage being detected (AMSA, 2009).

The Pasha Bulker remained stranded on Nobby's Beach for approximately three weeks before being salvaged.

Figure 2-5: The Grounded Pasha Bulker, Causing Shoreline Accretion in her Lee

(AMSA, 2009)

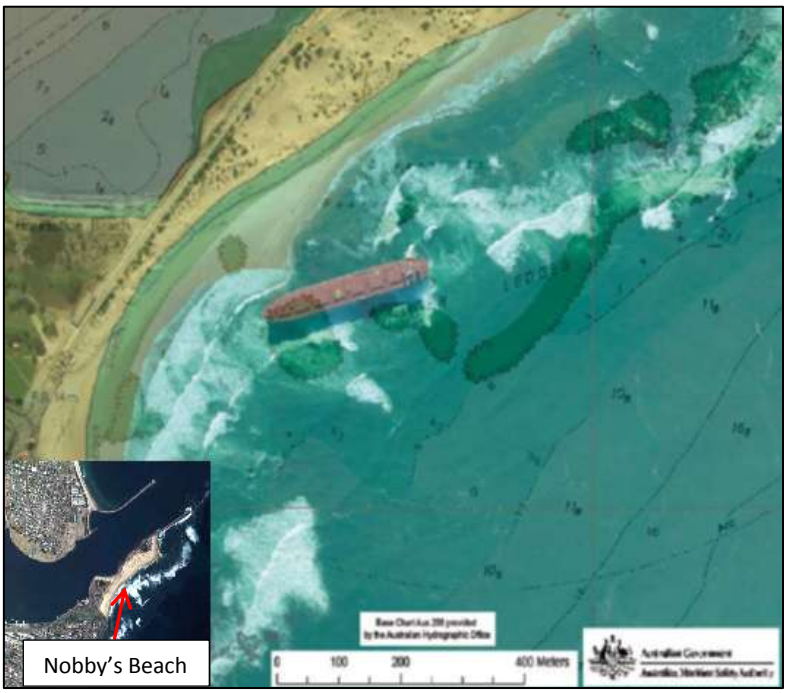

Similarly to the Seli One, the Pasha Bulker ran aground within the surfzone, thereby having a significant impact on the nearshore coastal processes. Figure 2-6 shows an aerial image taken on the 20th June 2005, indicating that without the shipwreck, the beach had a fairly uniform shape. Comparing this to the shoreline shown in Figure 2-5, it is evident that the shipwreck has resulted in significant shoreline accretion in the lee of the vessel, not dissimilar to what is currently being observed along the Table Bay shoreline.

The area to the north of the Newport Harbour entrance has historically been under severe threat of shoreline erosion. Because of this, numerous sediment transport studies have been performed to identify and quantify the longshore sediment transport regime of the area, mainly to develop shoreline stabilization measures for the northern beaches. The latest of these studies was performed by the Danish Hydraulics Institute (DHI, 2006).

The modelling results obtained by DHI are shown in Figure 2-7, showing a northern movement of sediment within the littoral zone. It is further clear that the Pasha Bulker was located within an area of strong longshore sediment transport, to the south of the harbour's entrance.

Figure 2-6: Nobby's Beach on the 20th June 2005

(Google Inc., 2010)

Figure 2-7: Sediment Transport Regime near Newport, Australia

(DHI, 2006)

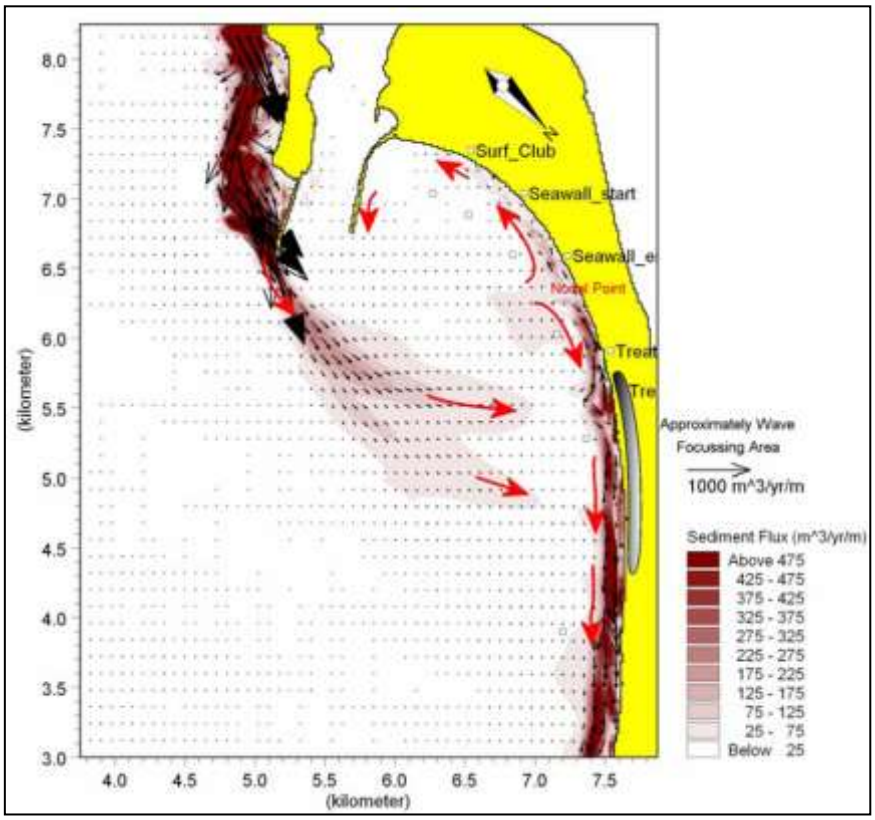

From these results, it can be argued that the non-removal of the Pasha Bulker would have resulted in severe shoreline erosion along the northern half of Nobby's Beach, whilst it is likely that the southern half would have accreted. This is because the sediment moving from south to north was blocked, thereby starving the northern half of Nobby's beach. Conversely, sediment was "piled up" on the southern side of the Pasha Bulker, causing shoreline accretion in the lee of the vessel as well as in the area further to the south.

It is further possible, considering the proximity of the vessel to the shoreline, that the accretion in the lee of the vessel would have connected with the vessel, thereby cutting off all sediment transport in the lee of the ship.

However, it is unlikely that the vessel would have resulted in the complete blockage of all longshore sediment transport moving from south to north. Most of the sediment would have bypassed the vessel further offshore, thereby maintaining the sediment feed to the beaches to the north of the Newport Harbour entrance. The impact of the shipwreck on the coastline to the north of the port is therefore expected to have been negligible.

2.3 Conclusions

It has been shown that ships running aground in the nearshore environment are a fairly common occurrence. This is especially the case near ports, where vessels are required to sail fairly close to the shoreline to enter the harbour.

Historically, prior to the construction of the Port of Cape Town, shipwrecks were very common along the Table Bay shoreline, especially during violent winter storms when strong north-westerly winds would drive vessels onto the beaches. Recently however, since the provision of the shelter of the Port of Cape Town, the frequency of these events has reduced. However, ships continue to run aground in Table Bay and the surrounding Western Cape shorelines, with five vessels having wrecked there since 1990.

Two shipwreck events have been highlighted, one of which, namely the Sealand Express, occurred only a few kilometres from the spot where the Seli One is currently located. The second event occurred near the Newport Harbour entrance in Australia. Although both of these vessels were salvaged after approximately one month, both cases exhibited similar traits as the Seli One. Shoreline accretion in the lee of the vessel could be observed at both the Sealand Express, as well as at the Pasha Bulker, with some adjacent erosion.

Due to the frequency with which shipwrecks occur globally, it is important to investigate the potential impact that a shipwreck could have on a shoreline and to simulate the long-term potential equilibrium shoreline that could result from the non-removal of a shipwreck. It is also important to investigate the rate at which shoreline changes occur as a result of shipwrecks near the coast, as this may guide the understanding of the window of opportunity for salvaging nearshore shipwrecks.

It was not the intention of this investigation to determine the impacts of shipwrecks on coastline stability. This is because each shipwreck will have unique characteristics such as the depth at which the vessel is stranded, the length and beam of the vessel, local wave climate and local sediment characteristics. As such, conclusions made from the investigation of the impact of the Seli One are only used to inform a general understanding of the impacts of shipwrecks, rather than deriving explicit guidelines.

3. LITERATURE REVIEW

3.1 Introduction

Considering the hypothesis of this thesis, being that the Seli One acts in a similar manner as an offshore breakwater, an in-depth discussion of the coastal processes surrounding such a structure is given in this section of the report. Figure 3-1 shows a schematic of the main coastal processes occurring near an offshore breakwater. These include:

- Wave diffraction in the lee of the structure
- Reduction of wave heights in the lee of the structure due to the structure's sheltering effect
- Water level variations due to wave height differentials
- Generation of currents due to water level variations

Figure 3-1: Schematic of Main Coastal Processes at an Offshore Breakwater

Based on (USACE, 2006b)

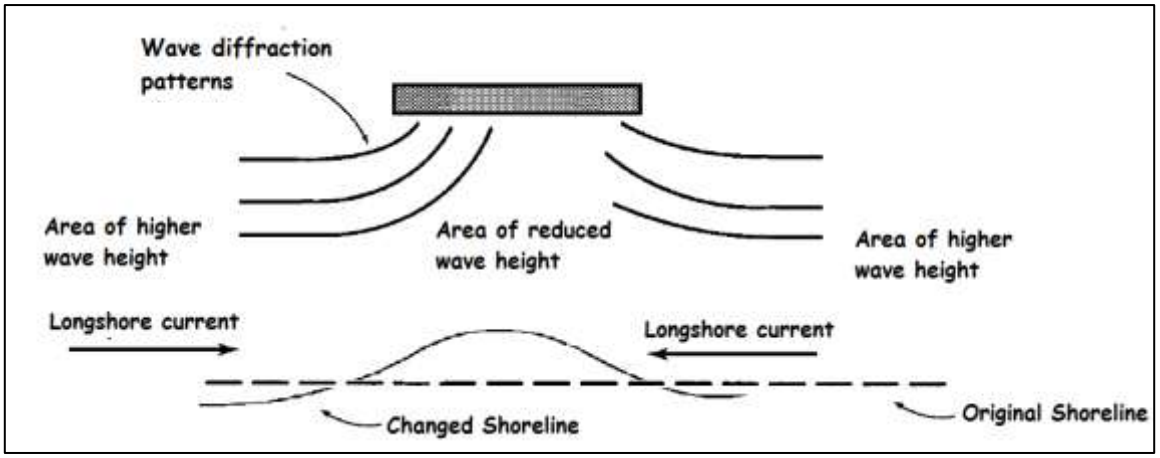

Further to the discussion of waves and currents, an in-depth review of sediment transport mechanics is given. In addition, guidelines for the design of offshore breakwaters are then introduced, in an attempt to shape an understanding of the potential impact that the Seli One shipwreck may have on the Blouberg shoreline.

3.2 Nearshore Wave Mechanics

Littoral sand transport is driven primarily by the nearshore wave and current climate. Higher waves deliver more energy to the surfzone, which have the potential to create stronger longshore currents, resulting in larger transport volumes. In addition to this, higher waves break further offshore which widens the surfzone, therewith suspending more sediment and increasing sediment transport volumes. The angle between the breaking wave crest and the shoreline is naturally a critical parameter (CERC, 1984).

Considering the scope of this investigation, only the aspects of nearshore wave mechanics, which directly influence the nearshore sediment transport characteristics around an obstruction like the wreck, are pointed out in this paragraph.

3.2.1 Incipient Wave Breaking

The width of the surfzone, the wave height and water depth at the breaking point are parameters which need to be considered when assessing the longshore sediment transport characteristics of a site, and are therefore introduced in the following paragraphs. This theory will be applied during a "hand-calculation" approach to determine the longshore sediment transport characteristics of Table Bay, which is required to ground-truth results obtained from numerical modelling simulations.

As waves approach shallow water, their wavelength decreases due to the effect of bottom friction and the shallowing of the seabed. Although the wave height will also decrease due to this decrease in wave energy, the wave steepness, being the ratio between wave height and wavelength (H/L), generally increases towards the shoreline. Wave breaking occurs when a limiting wave steepness is reached, which is a function of the depth and beach slope (Holthuijsen, 2007).

The breaker height index (Ω_b) correlates the breaking wave height to the deepwater wave height (USACE, 2003),

$$\boldsymbol{\Omega_b = \frac{H_b}{H_0} = 0.56 \left(\frac{H_0'}{L_0}\right)^{-0.2}} \qquad \text{Equation 3-1}$$

where H_0' is the refracted deepwater wave height and L_0 is the deepwater wave length. From this relationship, H_b can be determined.

The breaker index (γ_b) is used to relate the breaking wave height (H_b) with the depth at which this wave breaks (d_b), shown in Equation 3-2 below (USACE, 2003).

$$\boldsymbol{\gamma_b = \frac{H_b}{d_b} = b - a\frac{H_b}{gT^2}}, \text{ where} \qquad \text{Equation 3-2}$$

$$\boldsymbol{a = 43.8\left(1 - e^{-19\tan\beta}\right)} \text{ and} \qquad \text{Equation 3-3}$$

$$\boldsymbol{b = \frac{1.56}{1 + e^{-19.5\tan\beta}}}, \text{ where} \qquad \text{Equation 3-4}$$

T wave period,
g gravitational acceleration and
β beach slope.

From these relationships, the breaking wave height and depth at breaking can be determined. McCowan (1983) theoretically determined the breaker index as $\gamma_b = 0.78$ for a solitary wave travelling over a horizontal bottom. This value is commonly used in practical engineering projects as a first estimate of the breaking wave height given a certain depth (USACE, 2003).

3.2.2 Wave Diffraction

A sound understanding of wave diffraction is critical for the current investigation, since it plays an important role in the coastal processes occurring around the Seli One shipwreck. Although the calculation of diffraction effects are included in the numerical modelling tools, and will not be "hand calculated" as such, model results need to be evaluated to ensure their correctness. A view of what the wave and current patters should look like around the wreck is therefore required, necessitating a sound understanding of the coastal processes such as diffraction.

Wave diffraction is the process of lateral energy transfer along a wave's crest. The energy transfer takes place from an area of larger- to an area of smaller wave height (USACE, 2006c). Although this process occurs in offshore and coastal regions, it is most prominently observed in nearshore areas, especially at coastal structures such as breakwaters.

The small energy gradient in offshore areas results in diffraction playing an insignificant role. In nearshore areas however, where large energy gradients can occur due to the wave sheltering of natural headlands or man-made breakwaters, diffraction becomes plainly visible, and important to include in coastal engineering studies (USACE, 2006c).

As shown in the figure below, the wave changes direction due to diffraction. This is caused by the reduction in wave energy from the unsheltered to the sheltered areas. Due to this, wave heights are significantly reduced (USACE, 2006c).

Figure 3-2: Wave Diffraction – Definition of Terms (USACE, 2006c)

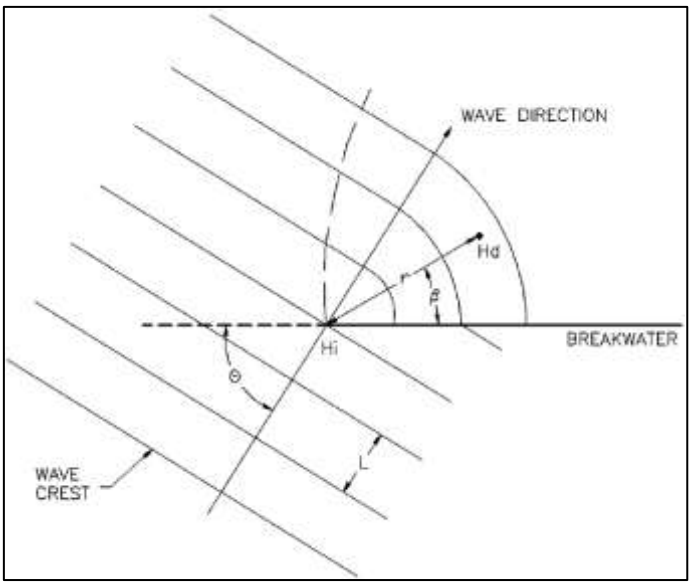

Wave diffraction diagrams, an example of which is shown in Figure 3-3, are generally used to obtain a first estimate of the diffraction effects of hard structures. The diffraction coefficient, K', shown in the figure, is the factor by which the wave height at the tip of the breakwater structure needs to be multiplied with to determine the wave height at a location in the lee of the structure (USACE, 2006c). Although this does not indicate the effect of the resulting wave angle in the lee of the structure, it does provide insight into the effectiveness in terms of wave sheltering of a structure for a given wave scenario.

Figure 3-3: Wave Diffraction – 60^o Wave Angle (USACE, 2006c)

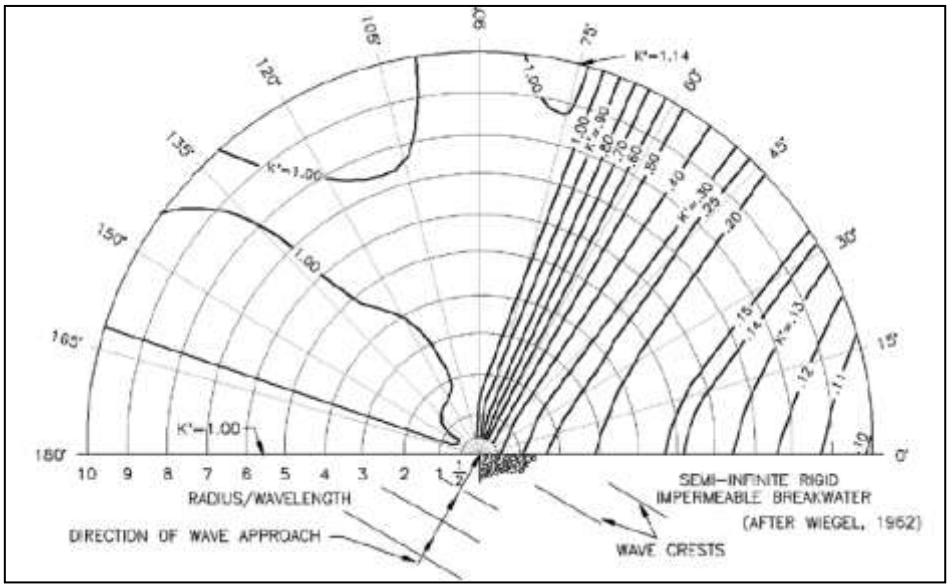

3.2.3 Wave-Induced Set-Up, Set-Down and Currents

From the discussion below, it will become clear that calculating the wave set-up, set-down and longshore current is a complex and time-consuming exercise, especially since these parameters vary spatially and temporally. In practice, this is therefore not usually done manually, but rather through the application of advanced numerical models. The same approach is used during this study. However, a sound understanding of these coastal processes is however required to accurately interpret simulation results.

A wave is a combination of potential and kinetic energy, which is transported through the water body. The potential energy component is due to the variation in water level of the wave crest compared to the surrounding water surface. The kinetic energy component is a resultant of the orbital motion of water particles within the wave (Holthuijsen, 2007). In addition to the generation of kinetic energy, the orbital motion of the water particles generates a momentum, which is transported with the wave as it moves through the water body. The total momentum in the x-direction (direction perpendicular to the shoreline) is dependent on the mass-density of the water, as well as the speed in the x-direction, and can be written as follows (Holthuijsen, 2007) (note that it is assumed here that the wave ray is perpendicular to the shoreline):

$\boldsymbol{Q_x = \int_{-d}^{\eta} \rho u_x dz}$, where Equation 3-5

Q_X total momentum in the x-direction (perpendicular to shoreline)

ρ seawater density

$-d$ water depth below still water level

η water surface elevation above still water level

u_x particle velocity in the x-direction (perpendicular to shoreline)

z vertical dimension

The momentum perpendicular to the x-direction, Q_y, is zero, since the orbital velocities in that direction are zero. The total horizontal momentum beneath the wave is therefore described by Q_x (Holthuijsen, 2007).

The transportation of momentum is equivalent to a stress acting on the water, known as "radiation stress". A variation in this stress, i.e. a variation in the transportation of momentum, generates a resultant force on the water body. This force causes local water level variations or the generation of wave-induced currents (Holthuijsen, 2007).

The total momentum transported through a vertical plane is not only dependent on the orbital motion of water particles within the wave, but also by wave induced pressure, which can be represented by the relationship shown in Equation 3-6 (Holthuijsen, 2007). Note that the subscript 'xx' denotes the x-momentum in the x-direction.

$$\boldsymbol{S_{xx}} = \int_{-d}^{\eta} (\boldsymbol{\rho u_x} + \boldsymbol{p_{wave}}) \boldsymbol{dz} \qquad \text{Equation 3-6}$$

A similar derivation process can be followed to determine the y-momentum in the y-direction. It should be noted that although the orbital velocities perpendicular to the wave propagation are zero, which means that the momentum in the y-direction is zero, the wave-induced pressure in the y-direction is not zero. The radiation stress in the y-direction is therefore also not equal to zero (Holthuijsen, 2007).

$$\boldsymbol{S_{yy}} = \int_{-d}^{\eta} (\boldsymbol{p_{wave}}) \boldsymbol{dz} \qquad \text{Equation 3-7}$$

In addition to S_{xx} and S_{yy}, the transportation of x-momentum in the y-direction (S_{xy}) and transportation of y-momentum in the x-direction (S_{yx}) can also be determined (Holthuijsen, 2007). The assumptions for the derivation of these equations is similar to the ones discussed previously, and will not be repeated here.

$$\boldsymbol{S_{xy}} = \int_{-d}^{\eta} (\boldsymbol{\rho u_x u_y} + \boldsymbol{\tau_{xy}}) \boldsymbol{dz} \qquad \text{Equation 3-8}$$

$$\boldsymbol{S_{yx}} = \int_{-d}^{\eta} (\boldsymbol{\rho u_y u_x} + \boldsymbol{\tau_{yx}}) \boldsymbol{dz} \qquad \text{Equation 3-9}$$

Orbital velocities in the y-direction are zero and shear stresses τ_{xy} and τ_{yx} are zero since it is assumed that the water is an ideal fluid. For the case in which the wave ray is perpendicular to the shoreline, both S_{xy} and S_{yx} are zero (Holthuijsen, 2007).

However, if the wave ray is not perpendicular to the shoreline, meaning that the wave crest approaches the shoreline obliquely, the orbital velocities in the y-direction are not zero. As mentioned previously, a decrease in radiation stresses results in an opposite force acting on the water body. This can be represented by the following relationships (Holthuijsen, 2007):

$$\boldsymbol{F_x} = \frac{\partial \boldsymbol{S_{xx}}}{\partial \boldsymbol{x}} - \frac{\partial \boldsymbol{S_{xy}}}{\partial \boldsymbol{y}} \text{and} \qquad \text{Equation 3-10}$$

$$\boldsymbol{F_y} = \frac{\partial \boldsymbol{S_{yy}}}{\partial \boldsymbol{y}} - \frac{\partial \boldsymbol{S_{yx}}}{\partial \boldsymbol{x}} \qquad \text{Equation 3-11}$$

Considering now the situation where a wave with wave ray perpendicular to the shoreline with shore-parallel contours, the force in the y-direction is zero since the radiation stresses S_{yy} and S_{yx} do not vary. This means that no longshore current is developed. The force F_x is not zero, with radiation stresses decreasing shoreward of the breaker line. This means that a shoreward force is generated, which tilts the water level as shown in Figure 3-4 (Holthuijsen, 2007).

Considering the situation where the wave ray is not perpendicular to the shoreline, the following can be deduced: The force in the y-direction cannot tilt the still water level since there is no beach for the water to

pile up against. F_y therefore generates a current, commonly known as the longshore current. This current is the main contributor to longshore sediment transportation (Holthuijsen, 2007).

Figure 3-4: Wave Set-Down and Set-Up With Shore-Normal Wave Ray

(Holthuijsen, 2007)

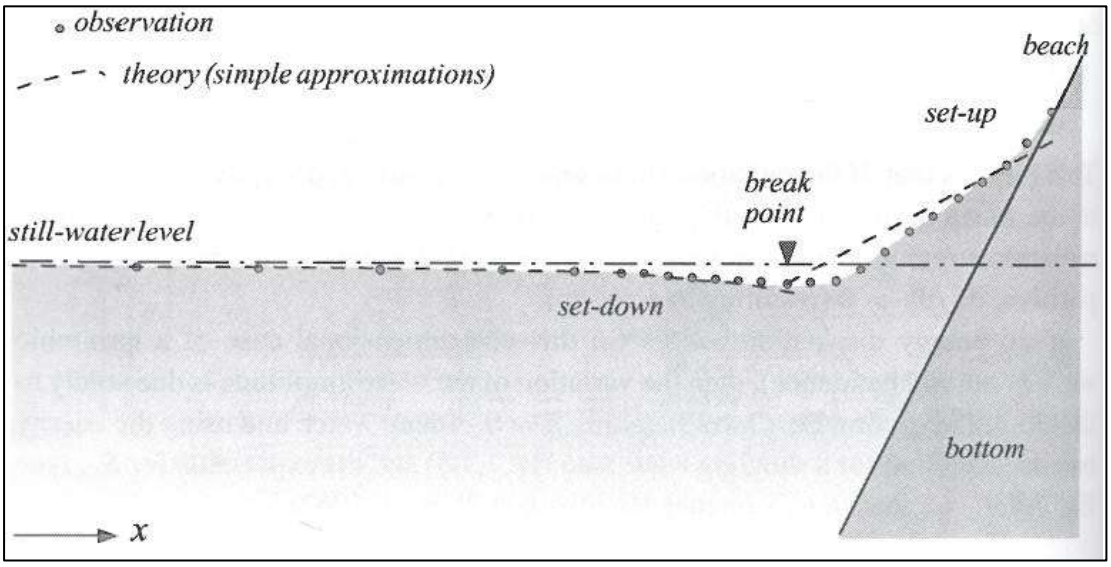

3.3 Sediment Transport Mechanics

"Littoral transport is the movement of sedimentary material in the littoral zone by waves and currents. The littoral zone extends from the shoreline to just beyond the seaward-most breakers." (CERC, 1984).

Local currents and forces combine to transport beach sediment both in a parallel and normal direction to the beach. Transport parallel to the beach is called longshore transport, whilst transport normal to the beach is called cross-shore transport. In certain circumstances, these local forces and currents result only the local rearrangement of sediment, whereas in other scenarios, they can combine to transport hundreds of thousands of cubic metres of sand up or down the coast each year (USACE, 2002).

3.3.1 Longshore Sediment Transport

The rate at which sediment is transported is dependent on the wave height, wave length, depth of water, water density and viscosity, gravitational acceleration, space and time and the sediment particle density. Including all these aspects in a methodology to estimate sediment transport rates is however impossible since not all are sufficiently understood. Simplified methods have therefore been developed to estimate the magnitude of longshore sediment transport (Kamphuis, et al., 1985).

Potential longshore drift is defined as the sediment movement parallel to the shoreline, assuming that an unlimited supply of sand is available for transportation. It should be noted that transport rates determined by the methods covered below are typically significantly larger than actual measured longshore transport rates. Consideration to the availability of sediment, the effect of local shoreline features (rock outcrops etc) needs to be included to estimate a more realistic longshore sediment transport rate (Kamphuis, et al., 1985).

Numerous methods have been developed to calculate longshore sediment transport rates, which can broadly be categorized into empirical and deterministic methods. A further categorization can be made between the

so-called "bulk" and "detailed" transport equations. The bulk equations calculate the total transport volume, integrated over the entire cross-shore profile. A detailed description of the cross-shore variability of the longshore sediment transport is however not determined by the bulk equations. The detailed transport equation on the other hand allows the determination of the longshore sediment transport rate as a function of offshore distance.

3.3.1.1 Empirical Methods

Two of the more commonly used empirical methods to calculate the bulk longshore sediment transport are the so-called "CERC" and "Kamphuis" equations.

The "CERC" Formulation

The CERC formulation simply states that the potential immersed weight transport rate (which is given as force per unit time) is calculated by

$$\boldsymbol{I_l = KP_l}\,, \qquad \text{Equation 3-12}$$

where K is a proportionality coefficient and P_l is the longshore component of the wave energy flux. The longshore component of the wave energy flux is the rate at which wave energy is transmitted across a plane of unit width perpendicular to the direction of wave advance, and can be determined using the following relationship (CERC, 1984).

$$\boldsymbol{P_l = \left(EC_g\right)_b \sin\alpha_b \cos\alpha_b} \qquad \text{Equation 3-13}$$

where E_b is the wave energy at the breaker line $\left(E_b = \frac{\rho g {H_b}^2}{8}\right)$ and C_{gb} is the wave group speed at the breaker line $\left(C_{gb} = \left(g\frac{H_b}{\kappa}\right)^{\frac{1}{2}}\right)$. κ is defined as the breaker index $\left(\kappa = \frac{H_b}{d_b}\right)$. The angle between the shoreline and the breaking wave crest is defined as α_b (USACE, 2002).

It should be noted that Equation 3-13 and its supporting equations are valid if there is one wave train with one height and period. However, since wave conditions are characterized by a combination of waves, the root mean square breaking wave height $H_{b\text{-}rms}$ should be used (USACE, 2002).

These equations are used to calculate the immersed weight transport, which is the weight of the sediment being transported parallel to the shoreline per unit time (USACE, 2002).

$$\boldsymbol{I_l = KP_l = K\left(EC_g\right)_b \sin\alpha_b \cos\alpha_b} \qquad \text{Equation 3-14}$$

The above equation can be rewritten in terms of volume of sand transportation,

$$\boldsymbol{Q_l = K\left(\frac{\rho\sqrt{g}}{16\kappa^{0.5}(\rho_s-\rho)(1-n)}\right){H_{b-rms}}^{2.5}\sin(2\alpha_b)} \qquad \text{Equation 3-15}$$

where 'n' is the in-place porosity of the non-cohesive sediment and $H_{b\text{-}rms}$ is the root-mean-square wave height at breaking (USACE, 2002).

It will be noticed from both Equations 3-14 and 3-15 that the immersed weight and volumetric longshore transport rates are dependent on a dimensionless proportionality coefficient, K. Since this dependency is linear, meaning that a 20% variation in the proportionality coefficient will result in a 20% variation in the predicted sediment transport rate, the choice of this coefficient is of great importance.

An early design value for the K-coefficient, which has been widely used in sediment transport calculations, is K = 0.39. This value was developed by Komar and Inman in the 1970's (USACE, 2002).

A further approximation of the proportionality coefficient can be made by incorporating the median grain size of the sediment, as well as the angle between the shoreline and the breaking waves. The relationship shown below was developed by Bailard in the 1980's, and is applicable to breaker wave heights between 0.5 and 2.0m, with grain sizes ranging between 0.2 and 1.0mm (USACE, 2002).

$$\boldsymbol{K = 0.05 + 2.6\ \sin(2\alpha_b) + 0.007\frac{u_{mb}}{w_f}}$$ Equation 3-16

In the above equation, u_{mb} is defined as the maximum oscillatory velocity $\left(u_{mb} = \frac{\kappa}{2}\sqrt{gd_b}\right)$ and w_f is the fall speed of the non-cohesive sediment. The fall speed of the sediment is dependent on the sediment grain size, as well as the Reynold's number of the flow regime (USACE, 2002). Detailed relationships to determine the grain fall speed can be found in USACE 2002a, and will not be discussed here.

A final approximation of the proportionality coefficient was made in 1993 by del Valle et al. This relationship is dependent only on the median grain diameter of the sediment. It should be noted that this relationship is based on a limited number of aerial photographs and is limited to a sediment grain size range of between 0.4 and 1.5 mm (USACE, 2002).

$$\boldsymbol{K = 1.4\ e^{-2.5D_{50}}}$$ Equation 3-17

Referring now to Equation 3-15, it will be noticed that the volumetric bulk longshore sediment transport rate determined by the CERC equation is dependent only on the local wave conditions. This formulation therefore ignores any external ocean currents. This needs to be taken into consideration when evaluating the results obtained through this method, since the additional volume of sediment which can be transported due to local currents can be significant.

The "Kamphuis" Equation

Another commonly used empirical method to determine the bulk potential longshore sediment transport is the Kamphuis equation. This equation relates the mass of sediment transported parallel to the beach to the significant breaking wave height and angle that this wave makes with the shoreline (Kamphuis, et al., 1985).

$$\boldsymbol{Q_s = 1.28\ \frac{m{H_{bs}}^{3.5}}{D}\sin 2\alpha_{bs}}$$ Equation 3-18

where

m	beach slope between breaker line and still water shoreline
H_{bs}	significant breaking wave height
α_{bs}	angle between breaking wave and shoreline
D	grain diameter

It should be noted here that the constant 1.28 relates to the use of SI units.

Of the methods introduced in this report, the Kamphuis equation is arguably the simplest method to implement. This is since most parameters, such as the sand's falling velocity, the wave's Reynold's Number or the longshore current speed, each of which is notoriously difficult to calculate, is not required. From Equation 3-18 it is clear that the required input into this equation is relatively simple to determine, which makes this method effective to determine a first estimate at the bulk longshore sediment transport rate.

Figure 3-5 shows calculated potential longshore sediment transport compared to measured values. From this figure, a slight trend of over-prediction of the lower transport rates can be identified, whilst an under-prediction of the higher transport rates can be seen. Overall however, it seems as though the Kamphuis equation represents the observed longshore transport rates well.

Similarly to the CERC formulation, the Kamphuis equation does not incorporate any local current fields. Results therefore need to be evaluated depending on the local site conditions, and adjusted if need be.

In summary, the CERC formulation which makes use of the energy flux method is highly dependent on a proportionality factor, which changes the net transport rate linearly with the choice of factor. In comparison to this, the Kamphuis equation requires only wave parameters, as well as knowledge of the sediment characteristics and beach slope, all of which are available during the current study. The Kamphuis method was therefore used rather than the CERC formulation to perform the desk assessment of the net longshore sediment transport rates in Table Bay.

Figure 3-5: Kamphuis Measured vs Calculated Longshore Sediment Transport Rate (Kamphuis, et al., 1985)

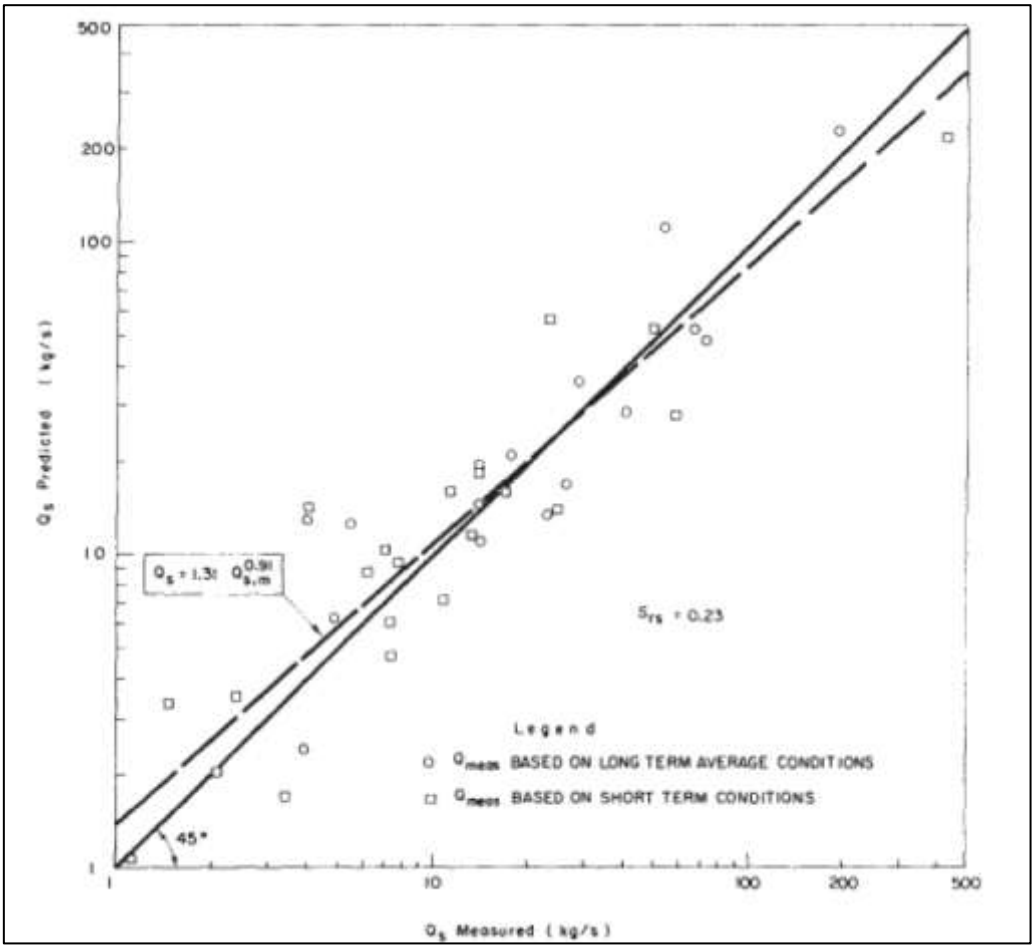

3.3.1.2 Deterministic Methods

One of the deterministic models available to determine the longshore sediment transport rate is based on the Longuet-Higgins longshore current model, developed in the 1970 (Longuet-Higgins, 1970). This model enables the calculation of the longshore current as a function of offshore distance, thereby enabling a detailed

description of the longshore sediment transport characteristics across the surfzone. Waves, currents and the effects of bottom friction are deterministically included in the model.

Incorporating this model, the longshore energy flux previously indicated becomes

$$\boldsymbol{P_l} = \frac{\rho g H_b W V_l C_f}{\left(\frac{5\pi}{2}\right)\left(\frac{V}{V_0}\right)}, \qquad \text{Equation 3-19}$$

in which W is the width of the surfzone, V_l is the measured (or modelled) longshore current at a point in the surfzone, C_f (=0.01) is a friction coefficient dependent on the Reynold's number and bottom roughness, whilst V_0 is the theoretical longshore velocity at breaking for no-lateral mixing (USACE, 2002).

$$\frac{V}{V_0} = \mathbf{0.2}\left(\frac{Y}{W}\right) - \mathbf{0.714}\left(\frac{Y}{W}\right)\ln\left(\frac{Y}{W}\right) \qquad \text{Equation 3-20}$$

In Equation 3-20 above, Y equals the distance from the shoreline to the measured current, whilst V/V_0 is the dimensionless longshore current velocity for an assumed mixing coefficient of 0.4.

The volumetric transport rate can be calculated by using the following relationship (USACE, 2002a).

$$\boldsymbol{Q_l} = \frac{K}{(\rho_s - \rho)(1-n)}\boldsymbol{P_l} \qquad \text{Equation 3-21}$$

Applying this method, the volumetric transport rate as a function of the offshore position can be calculated. During this study however, the above theoretical relationships were not directly applied. The detailed sediment transport rates were calculated using numerical modelling tools, which will be introduced in later sections of this report.

3.3.1.3 Variability of Longshore Sediment Transport

It has been established from the discussion above that the sediment movement along a coastline is dependent mainly on the wave conditions at that site, as well as local current patterns. Considering the variability of those conditions, the magnitude and direction of the coupled longshore sediment transport will be equally variable and cognisance of this should be taken when applying the equations presented above.

The net longshore transport is defined as the difference between the transports up and down the coast, whereas the gross longshore transport is defined as the sum of the two transport volumes (USACE, 2002). Both of these are applicable in a coastal engineering sense. For example, the gross longshore sediment transport rate may be important when investigating the siltation of an unprotected port entrance channel, where the net longshore transport rate will be important when investigating the accretion of sediment on the up-drift side of a breakwater. Shown below are the equations used to determine the time-averaged gross and net longshore sediment transport rates (USACE, 2002).

$$\boldsymbol{Q_{l-net}} = \frac{1}{T_0}\int_0^{T_0} \boldsymbol{Q_t(t)dt} \qquad \text{Equation 3-22}$$

$$\boldsymbol{Q_{l-gross}} = \frac{1}{T_0}\int_0^{T_0} \boldsymbol{|Q_t|(t)dt} \qquad \text{Equation 3-23}$$

A typical variability of longshore sediment transport is shown in Figure 3-6 below. The main variability may be caused due to seasonal variations in wave directions and/or currents, whereas the small peaks and troughs may be caused due to daily variations in weather patterns.

During the current study, both the net and gross longshore sediment transport rates are important. The net rate is considered when evaluating the historic long-term evolution of the Table Bay sediment transport system, which, in turn, is used to calibrate the one-dimensional shoreline evolution model. The gross transport rate is important since the magnitude of the sedimentation occurring in the lee of the Seli One shipwreck is linked to the total volume of sediment which is transported into the lee of the vessel, regardless from which direction it arrives.

Figure 3-6: Longshore Sediment Transport Definitions (USACE, 2002)

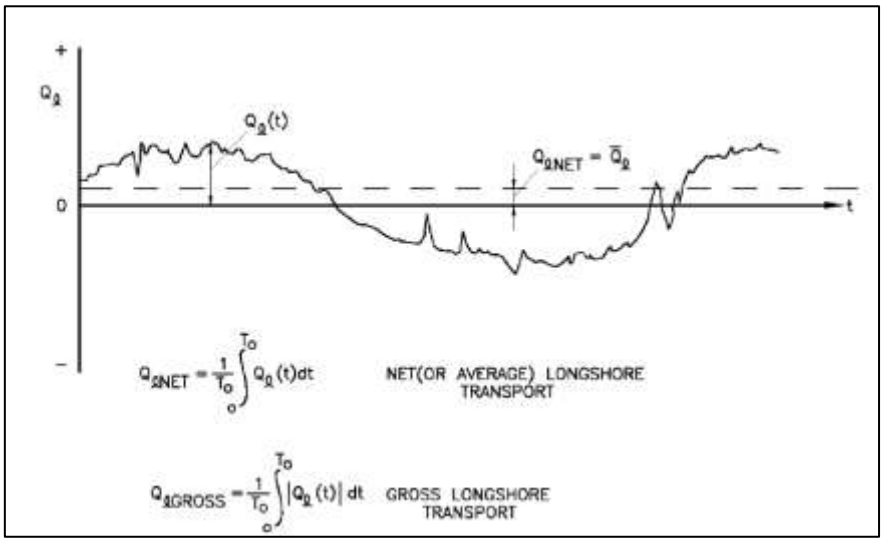

3.3.1.4 Cross-Shore Distribution of Longshore Sediment Transport

The relationships pointed out in the previous sections of this report present relationships to determine the total potential longshore sediment transport. This transport is however not distributed evenly across the surf zone (USACE, 2002). This is an important factor to consider, since many engineering applications require knowledge of the cross-shore distribution of the longshore sediment transport. The placement of a sand trap at a port for example needs to be carefully chosen in order to catch the bulk of the transported sediment to prevent the siltation of the entrance channel.

From field analysis, three transport modes were observed. The first mode has its maximum transport within the swash zone or near the shoreline; the second has its maximum within a few meters of the breaker line, whereas the final mode is a combination of the first two (USACE, 2002).

It was later determined that these modes are dependent on the type of breaking wave. For plunging waves, sediment concentrations peaks within a few meters of the breaker line, whilst for spilling waves, longshore transport occurs predominantly within the swash zone. Transport is also seen to move closer to the shoreline as the wave condition varies from spilling to collapsing (USACE, 2002).

Consideration of the cross-shore distribution of the longshore transport is an important aspect to consider during the analysis of historic beach profiles, which are used to calibrate numerical shoreline models. Beach profiles, which usually extend from the top of the primary dune to approximately -1 m MSL, do not include the entire littoral zone. Because of this, an estimate had to be made with regards to what percentage of the littoral zone is represented by the profile. An understanding of the cross-shore distribution of the longshore transport is therefore critical to this study.

3.3.2 Cross-Shore Sediment Transport

Cross-shore sediment transport occurs when the hydrodynamic conditions in the nearshore environment are altered, resulting in the forces acting on the sediment changing as well. Cross-shore transport can be categorized into two physical phenomena. The first is offshore transport, which occurs during storms and is responsible for beach erosion, whilst the second phenomenon is known as onshore transport and occurs during mild-weather periods. Forces responsible for onshore transport are known as constructive forces, whist offshore transport results from destructive forces (USACE, 2006a).

It will be discussed in later sections of this report that the numerical models used to determine the impact of the Seli One on the local shoreline generally do not include cross-shore processes. The assumption here is that cross-shore transport is in equilibrium over a long timeframe. Storm events cause erosion, whilst during calm conditions sand is brought back to the shoreline. Over a long time, the two components are assumed to cancel each other out (USACE, 2006a).

3.3.3 Cross-Shore Beach Profiles

The shape of a cross-shore beach profile has a significant impact on the magnitude of longshore sediment transport. As such, a general understanding of the parameters which influence with shape is required. Equilibrium beach profiles are useful to investigate what a beach would look like if there was no net cross-shore sediment transport. Generally observed trends of an equilibrium beach profile are as follows (USACE, 2006a):

- they have an upward concave shape
- slopes are milder when sediment is finer
- beach slopes tend to be flatter for steeper waves
- coarse sediment is in shallower water, whilst finer sediment is in deeper water

The seaward limit of profile fluctuation is known as the depth of closure (h_c). It should be noted that significant amounts of sediment movement occurs at greater depths than this, however, the variation in profile shape is limited and assumed negligible. The magnitude of this depth is based on the effective significant wave height (H_e) and effective peak period (T_e), which are exceeded only 12 hours each year. The closure depth can be calculated as (USACE, 2006a)

$$\boldsymbol{h_c = 2.28H_e - 68.5\left(\frac{H_e^2}{gT_e^2}\right)} \qquad \text{Equation 3-24}$$

Various models have been proposed for the calculation of the dynamic equilibrium cross-shore profile. Bruun was arguably the first to develop an expression in 1954, which is still widely used today. His expression relates the depth of the seabed (h), as a function of the offshore distance (y) to the sediment grain size (USACE, 2006a).

$$\boldsymbol{h = Ay^n} \qquad \text{Equation 3-25}$$

where

A sediment scale parameter which depends on the sediment size D (USACE 2006a, Table III-3-3)
h water depth [m]
y distance offshore from the still water line [m]
n exponent [-]

This equation was later refined by Dean in the mid 1970's. Applying Bruun's equation to approximately 500 measured profiles, he determined that an exponent of 2/3 gave a best fit. Dean's rule is therefore commonly applied today as a first estimate to describe the equilibrium cross-shore profile (USACE, 2006a).

$$h = Ay^{\frac{2}{3}}$$ Equation 3-26

Two aspects regarding Equation 3-26 should be clear immediately; firstly, wave characteristics are excluded, and secondly, the method assumes an even sediment size distribution across the profile. Although these assumptions are not entirely correct, the method has proven to be a useful starting point to determine the equilibrium beach profile.

From the discussion in Section 4.3.5, it will become clear that the numerical models used to calculate the shoreline morphology do not incorporate cross-shore processes, assuming that the cross-shore profile is stable. To ensure this is in fact true for Table Bay, an assessment of the stability of the cross-shore profiles used in the shoreline modelling will be made.

3.4 Effects of Shore-Parallel Structures on the Shoreline

The presence of shore-parallel structures significantly alters the nearshore wave and current pattern in the lee of the structure, resulting in the change of sediment transport characteristics in that area. Cross-shore sediment transport is reduced, if not nullified. Longshore currents are affected significantly, resulting in a pronounced change in longshore sediment transport (USACE, 2006b).

Since the Seli One is hypothesized to be acting similarly to a detached offshore breakwater, an understanding of both the coastal processes and functional design principals of these structures are of critical importance to understand what is happening at the Seli One shipwreck.

3.4.1 Coastal Processes at a Detached Breakwater

The following paragraphs discuss the physical processes surrounding a detached breakwater system, as shown in Figure 3-7 below. This figure is an appended version of Figure 3-1, including some of the processes which have been introduced in the preceding discussions.

As discussed previously, waves that arrive at the shoreline at an oblique angle create a time-averaged longshore current, resulting in the transportation of sediment in the downdrift direction (USACE, 2006b). Referring to Figure 3-7, assuming net longshore sediment transport is from left to right, the following can be observed:

Waves in the lee of the structure are smaller than in the adjacent areas. This is caused by the process of diffraction (USACE, 2006b). As indicated in Section 3.3.1, the magnitude of longshore sediment transport is dependent on wave height and direction, with a larger wave resulting in a larger volume of sediment being transported. The reduction in the wave height in the lee of the offshore breakwater therefore results in a longshore sediment transport capacity gradient between the updrift, downdrift and lee of the structure. The comparatively low sediment transport capacity in the lee of the structure results in sediment being deposited in this area.

A secondary cause for sedimentation in the lee of offshore breakwaters, also caused by the differential wave height distribution in the lee of offshore breakwaters, is the generation of an opposing current, which enters

the lee of the structure from the adjacent areas. Due to the process of wave induced setup introduced earlier, the differential wave height distribution results in a lower mean water level in the lee of the breakwater than in the adjacent areas, since the magnitude of setup is directly linked to wave height (USACE, 2006b).Naturally, water flows from the elevated areas towards the lower areas, resulting in an opposing current at either end of the structure. This means that at the left hand side of the breakwater, the current due to water level variation flows from left to right towards the shelter of the structure, whilst on the right hand side, the current flows from right to left, again towards the shelter of the structure. These two current patterns converge in the lee of the structure (USACE, 2006b). Depending on the strength of these currents, the colliding currents may be deflected in an offshore direction, thereby generating a so-called rip-current.

Figure 3-7: Coastal Processes at a Detached Breakwater

Based on (USACE, 2006b)

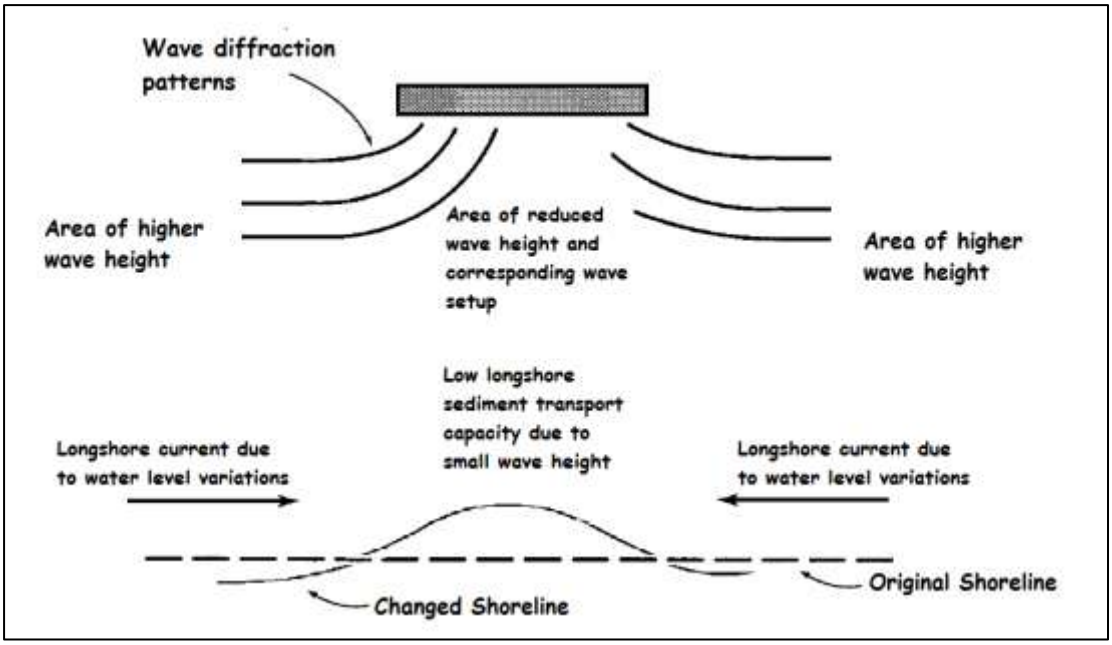

Combining the setup induced current with the background longshore current, a current acceleration is observed on the updrift side of the structure, which generally results in local erosion in that area. On the downdrift side of the structure, the current is reversed, now flowing towards the lee of the structure. This therefore leads to local erosion on the downdrift side of the structure (USACE, 2006b). The sediment eroded from either side of the breakwater settles in the lee of the structure (USACE, 2006b).

3.4.2 Functional Design of Detached Breakwater

Numerous investigations have been undertaken to quantify the effect of detached breakwaters on coastal morphology, but as yet, empirical methods are limited to classifying the response to being either a salient or tombolo. A salient is a defined as a bulge in the shoreline, whereas a tombolo is generated when the salient attached to the offshore breakwater.

The design of offshore breakwaters, normally done as an iterative approach, therefore requires significant engineering judgement and local knowledge of both longshore and cross-shore sediment transport characteristics (USACE, 2006b).

Figure 3-8: Definition Sketch for Detached Breakwater Functional Design Variables

(Chasten, et al., 1993)

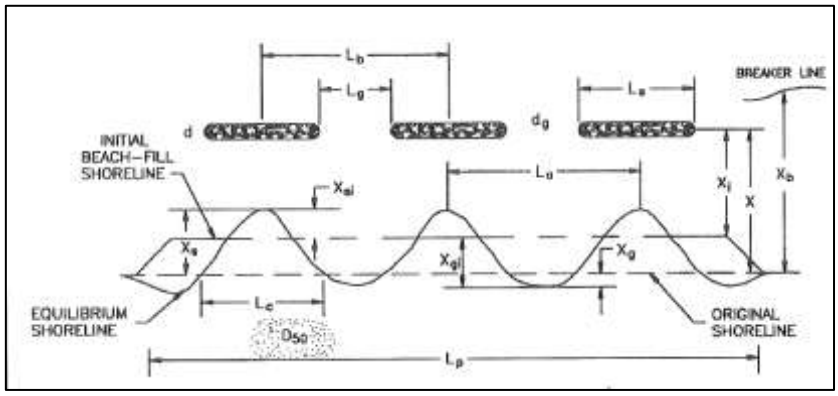

This determination is generally made by investigating the dimensionless ratio of the length of the structure (L_s) compared to the distance from the shoreline (X). The following guidelines, based on work done by Ahrens and Cox in 1990, can be used to predict the behaviour of a single offshore breakwater (USACE, 2006b).

$\frac{L_s}{X} > 1.5$ Well-developed salient / tombolo Equation 3-27

$\frac{L_s}{X} \leq 0.8 \; to \; 1.5$ Subdued salient Equation 3-28

$\frac{L_s}{X} \leq 0.27$ No sinuosity Equation 3-29

Ahrens and Cox further developed the so-called 'beach response index' (I_s) to develop a predictive relationship for beach response to a detached breakwater structure. This is approach is described as follows (USACE, 2006b).

$$I_s = e^{\left(1.72 - 0.41\frac{L_s}{X}\right)}$$ Equation 3-30

The following classification can now be made (USACE, 2006b):

$I_s = 1$ permanent tombolo formation

$I_s = 2$ periodic tombolo (tidal)

$I_s = 3$ well-developed salient

$I_s = 4$ subdued salient

$I_s = 5$ no sinuosity

Suh and Dalrymple developed the following relationship for the prediction of salient length in response to segmented offshore breakwaters (Chasten, et al., 1993).

$$X_s = X(14.8)\frac{L_g X}{{L_s}^2} e^{\left(-2.83\sqrt{\frac{L_g X}{{L_s}^2}}\right)}$$ Equation 3-31

It should be noted that Equation 3-31 is not applicable to single offshore structures.

Considering the development of the Seli One wreck, in the sense that initially the wreck was acting as a single offshore breakwater, whilst later on after the vessel broke up into three pieces, the vessel acted as a series of three breakwaters, each of the guidelines presented in this section will be used to estimate the potential impact of the vessel on the shoreline.

The estimates will then be compared to on-site measurements to investigate the applicability and accuracy of each of the calculations to the given case study.

3.4.3 Impact of Shipwreck as Detached Offshore Breakwater

Under normal conditions, offshore breakwaters are carefully designed to achieve the required beach, be it a gentle salient or tombolo which eventually connects to the offshore structure. Under these conditions, detached breakwaters can be used as extremely effective tools for the protection of sediment starved beaches. Normally though, these offshore breakwaters are not used in singularity, but rather in combination with a beach nourishment programme. This is done since, as discussed previously, although offshore breakwaters result in shoreline accretion in the lee of the structure, they also cause shoreline erosion in the adjacent areas. Beach nourishment is therefore used to prevent or limit the extent of shoreline erosion in the adjacent areas.

Under uncontrolled conditions, such as the grounding of a vessel within the surfzone, the morphological characteristics can be adversely affected, resulting in large scale erosion.

3.5 Summary and Conclusions

The importance of the nearshore wave climate on the sediment transport characteristics has been identified. Both the longshore and cross-shore sediment transport regimes are governed almost entirely by the nearshore wave characteristics. As such, to be able to accurately identify and quantify the sediment transport characteristics at a site, a detailed investigation of the nearshore wave climate has to be performed.

It has been shown that the physical processes governing longshore and cross-shore sediment transport are vast and complex. It has been further pointed out that although the effects of cross-shore processes can be significant in the short-term, they are of lesser importance in the long-term, and were therefore not considered during the Seli One case study.

Due to the sheer number of calculations required to determine longshore sediment transport rates, considering especially that these calculations need to be repeated for each time-step, relationships used to calculate longshore sediment transport rates are generally of an empirical nature. Many of these equations rely heavily on so-called engineering judgement, requiring the choice of critical empirical coefficients for the determination of transport rates. The Kamphuis equation has been identified as being the most user-friendly, since it does not require the user to input any debateable coefficients, but rather information based solely on the nearshore wave climate, beach sediment properties and beach gradients.

Considering that the Seli One fulfils a similar function as a detached offshore breakwater, the coastal processes surrounding such a structure have been discussed. This review has confirmed that this type of structure does, in fact, result in the formation of a beach salient, as well as resulting in the deposition of sediment between the structure and the beach. The postulated sedimentation caused by the Seli One shipwreck can therefore in principal be confirmed.

It has further been introduced that, as yet, no deterministic methods are available to quantify the effect of detached breakwaters on nearby coastal processes. The empirical methods currently available are limited to classifying the response to being either a salient or tombolo, but do not allow the determination of beach responses in terms of meters.

4. METHODOLOGY

4.1 Introduction

As previously indicated, the main objective of this investigation is the determination of the short- and long-term potential impact of the Seli One shipwreck on the Table Bay beaches. The methodology used to achieve this objective, as well as an introduction into the technical aspects of the numerical models used during this investigation, is discussed in the following paragraphs.

4.2 General Approach

The history of Table Bay in terms of shipwrecks has been highlighted in Section 2, whilst relevant literature was pointed out in Section 3. These two study components have developed the theoretical basis for this investigation, following which the case study of the Seli One was investigated.

In general, the case study of the Seli One is investigated by performing the following sub-tasks:

- Sediment budget calculation through the analysis of beach profile measurements
- Review of historic aerial photography to ground-truth observations from beach profile measurements
- Blouberg beach survey to determine the time-related impact of the Seli One shipwreck
- Wave modelling to determine the nearshore wave climate
- One-dimensional shoreline evolution modelling, to determine the impact of the wreck on the shoreline behaviour
- Two-dimensional sediment transport modelling, to determine the impact of the wreck on the coastal processes (waves, currents, sediment transport) in the lee of the vessel

Each of these tasks is discussed in more detail in the following sections.

4.2.1 Beach Profile Measurements

As with any numerical simulation, accurate input information is critical to the correct functioning of the model. As such, a sediment budget calculation was performing using beach profile measurements. These surveys have been performed along the Table Bay coastline since the mid-1960s. Results of this investigation are used to identify long-term shoreline trends, including the identification of the net longshore sediment transport characteristics of the bay. This information is used to calibrate the longshore sediment transport model used during this study.

4.2.2 Aerial Photography

A detailed review of aerial photography of Table Bay, dating back to 1968, was performed. Results of this investigation were used to ground-truth observations made from the analysis of the beach profile measurements. This was done by comparing the shoreline excursions observed from the photographs to those measured by the beach profile surveys.

4.2.3 Blouberg Beach Survey

Field data was collected by performing a survey of the Blouberg beachfront following the running aground of the Seli One, performed specifically for this investigation. The intention of this was to measure what the actual time-based impact of the Seli One shipwreck on the Blouberg shoreline was. This information was subsequently used to evaluate the results obtained through numerical simulations. The figure below shows the author surveying the bottom of a cross-section situated in the lee of the shipwreck.

Figure 4-1: The Author Surveying the Bottom Portion of a Cross-Section

4.2.4 Numerical Modelling Strategy

Various suites of numerical models are available to simulate the transformation of waves, currents and longshore sediment transport. This includes the wave model SWAN (Simulating Waves Nearshore) developed by the Delft University of Technology, as well as the one-dimensional shoreline evolution model UNIBEST (Uniform Beach Sediment Transport) developed by Deltares. A further suite of models is developed by the Danish Hydraulics Institute, including the so-called "MIKE by DHI" suite, as well as the "LITPACK by DHI" suite of models. MIKE by DHI includes, amongst others, two- and tree-dimensional wave, current and sediment transport models, whilst LITPACK by DHI is a set of one-dimensional sediment transport models. For the current study, the numerical models developed by the Danish Hydraulics Institute were used, for the simple reason that this is the software which is currently being used by the University of Stellenbosch. The details of each of the numerical models are discussed in greater detail in Section 4.3.

The first numerical modelling step was the simulation of the nearshore wave climate using MIKE21 SW. This model made use of an offshore wave dataset, performing wave refraction calculations to determine the nearshore wave climate along Table Bay. These wave conditions were used as input information to the sediment transport models. Details of this modelling exercise are introduced in Appendix A.

Following the successful simulation of the nearshore wave climate along the Table Bay coastline, a bay-wide one-dimensional shoreline model was developed, including the entire Table Bay littoral zone from the Port of Cape Town to the Blouberg rock headland. The intention of this bay-wide shoreline model was to reproduce the historic long-term shoreline trends of Table Bay. This was done by using longshore sediment transport rates and shoreline excursions as determined from beach profile measurements and aerial photographs, which will be discussed in more detail in Section 6. The calibration period of this bay-wide model was taken from May 1977 to May 2005, a period of 28 years. The validation period followed on from this until the 8th September 2009, the day prior to the arrival of the Seli One shipwreck.

The results of the bay-wide shoreline model were used to generate a smaller sub-model, focussing in on the Seli One wreck area. The smaller domain allowed a higher resolution of the coastal processes near the wreck, thereby allowing a more detailed analysis of the impact of the vessel on the local shoreline behaviour. This local model was re-validated using the same validation period as the bay-wide model, from May 2005 to the 8th September 2009. Note that this validation period excluded the influence of the Seli One wreck, since the wreck only arrived on the 9th September 2009.

The validated shoreline model was then used to investigate the short-term impact of the Seli One shipwreck, between the 9th September 2009 (date the vessel wrecked) and the 3rd July 2011 (date on which the Blouberg beach survey was performed). The simulated shoreline excursions were compared to measured shoreline changes, to perform a second validation of the local shoreline evolution model.

Following this step, two local shoreline evolution models had been developed; the first excluding the Seli One shipwreck, and the second including the vessel. The direct long-term impact of the Seli One shipwreck could now be modelled by comparing the results of the two simulations, excluding and including the vessel.

In addition to investigating the long-term potential impact of the Seli One shipwreck, two worst-case vessel grounding scenarios occurring in the same area as the Seli One were simulated. These scenarios included the largest vessel likely to sail in the Table Bay waters, running aground in a parallel and perpendicular fashion.

The final modelling task included the simulation of the two-dimensional sediment transport surrounding the wreck, using the coupled MIKE21 SW, MIKE21 HD and MIKE21 ST model. The intention of this model was to identify the changes in the coastal processes occurring as a direct result of the Seli one shipwreck, as well as identifying bed level changes offshore of the beach between the wreck and the beach.

4.3 Numerical Modelling Tools

Two modelling suites were applied during the course of this thesis, the first being MIKE21 by DHI, and the second being LITPACK by DHI. MIKE21 is made up of a number of different computational modules, which can be interlinked depending on modelling goals (DHI, 2011f). During this thesis, the spectral waves, as well as coupled spectral waves, hydrodynamic and non-cohesive sediment transport models were applied.

LIPACK is a suite of one-dimensional sediment transport models, of which the LITDRIFT and LITLINE models were applied during this study. LITDRIFT calculates the longshore sediment transport distribution across a given cross-shore profile (DHI, 2011b), whilst LITLINE is a one-dimensional shoreline model which determines the evolution of a shoreline over time (DHI, 2011d). Both of these models make use of the same sediment transport “engine”.

4.3.1 MIKE21 Spectral Waves by DHI

During this investigation, MIKE21 SW will be used to transform the offshore wave data to the required nearshore locations, taking into account the effects of wind, bottom friction, white capping and others to be listed later. The results of MIKE21 SW will form the input into LITDRFIT and LITLINE, as well as the coupled non-cohesive sediment transport computations.

The MIKE21 Spectral Waves (MIKE21 SW) model simulates the growth, decay and transformation of wind-generated waves and swells in nearshore and offshore applications. These applications include the design of offshore and coastal port structures where accurate knowledge of the local wave climate is required (DHI, 2011a). The model allows the user to refine the computational mesh in areas of interest, in order to refine the accuracy of the calculation in those areas, whilst minimizing computational requirements in other areas which are not of interest and which do not impact on the area of interest.

MIKE21 SW is also used in connection with the calculation of local and regional sediment transport. The radiation stresses calculated by MIKE21 SW are used as input into MIKE21 HD, which will be discussed later, to determine the wave-induced flow (DHI, 2011a).

MIKE21 SW incorporates the following physical phenomena (DHI, 2011a):

- Wave and wind forcing
- Non-linear wave-wave interaction (triads and quads)
- Dissipation due to white-capping, bottom friction and depth-induced wave breaking
- Diffraction
- Water-level variation

Figure 4-2: Typical Application Areas of Mike21 SW (DHI, 2011a)

MIKE21 SW includes the following physical computational features (DHI, 2011a):

- Fully spectral and directionally decoupled parametric formulations
- Instationary and quasi-stationary solutions
- Flexibility in describing bathymetry using unstructured mesh
- Coupling with hydrodynamic model in calculation wave-current interaction in time-varying depths
- Flooding and drying in connection with water-level variation

The user can obtain the simulated wave climate at each of the nodes within the model domain. This data can be given as either parametric data, or a fully spectral description. The spectral description is however only possible if the input wave climate at the model boundary is also a two-dimensional spectrum (DHI, 2011a).

4.3.2 MIKE21 Hydrodynamic Model by DHI

During this investigation, MIKE21 HD will not be used in singularity, but rather as one of the components of the coupled two-dimensional MIKE21 model, to be introduced later.

The MIKE21 Hydrodynamic (MIKE21 HD) module is the basic computational module for all the flow models of the MIKE modelling software, and provides the hydrodynamic input information to the transport modules such as MIKE21 non-cohesive sediment transport (MIKE21 ST). It is based on the numerical solution of the two-dimensional shallow water equations; the depth integrated incompressible Reynolds averaged Navier-Stokes equation. These equations arise from applying Newton's second law ($F = ma$) to fluid motion (DHI, 2011e).

The solver of the model makes use of the continuity, momentum, temperature, salinity and density equations (DHI, 2011e), the details of which do not form of the scope of this study.

MIKE21 HD incorporates the following physical phenomena (DHI, 2011e):

- Flooding and drying of shallow areas
- Water density variations (effects of salinity)
- Eddy viscosity
- Bed resistance
- Coriolis forcing
- Wind forcing
- Ice coverage
- Tidal potential
- Precipitation and evaporation
- Wave radiation
- Sources and Sinks
- Structures

Similarly to the MIKE21 SW model, MIKE21 HD allows the user to refine the mesh in the areas of interest, whilst minimizing the computational load in areas of non-interest, and which do not affect the area of interest. In this way run-times can be minimized (DHI, 2011f).

4.3.3 MIKE21 Non-Cohesive Sediment Transport by DHI

Similarly to MIKE21 HD, MIKE21 ST will not be used in singularity in this investigation, but rather as one of the components of the coupled two-dimensional MIKE21 model.

The MIKE21 non-cohesive sediment transport model (MIKE21 ST) describes the transportation of sand under the forces generated by waves and/or currents. This is performed by including the hydrodynamics of the given area through results of MIKE21 HD, whilst wave forcing is included by incorporating results of MIKE21 SW (DHI, 2011f).

Three main categories of non-cohesive sediment transport can, in general, be defined as bed load, suspended load and wash load transport. The first two of these transportation modes are well described in the model, whilst the third is excluded. The volume of sand transported within the wash load is relatively small compared to that transported by the bed load and suspended load transport modes (DHI, 2011f).

The following physical phenomena are included in MIKE21 ST in addition to those included in MIKE21 HD and MIKE21 SW (DHI, 2011f):

- Sediment properties (mean grain diameter and grading coefficient)
- Bed resistance
- Dispersion
- Sources and Sinks

4.3.4 MIKE21 Coupled Spectral Waves, Hydrodynamic and Sediment Transport Model by DHI

As mentioned previously, the MIKE21 coupled model gives the user the opportunity to combine the effects of waves and currents on two-dimensional sediment transport into one single simulation. During this study, the following modules will be combined to investigate the effect of the Seli One shipwreck on the sediment transport regime of Table Bay:

- MIKE21 Spectral Waves
- MIKE21 Hydrodynamics
- MIKE21 Sand Transport

The advantage of coupling the three processes listed above is that a more realistic representation of the system is obtained. Depending on the forces calculated by MIKE21 SW and MIKE21 HD, a certain amount of sediment transport may occur. This results in changes to the bathymetry. In the coupled model, this change in bathymetry influences the wave and current calculations performed during the next time step, resulting in a much more realistic representation of the system (DHI, 2011g).

This bathymetric feedback is especially important in shallow areas, where small changes in bathymetry may have a significant impact on local wave and current patterns. Since the area of interest for the current project is located near the coastline, the morphological feedback is deemed an important aspect to include in the simulations.

The disadvantage of the coupled model is an extremely high computational effort, since the hydrodynamics and waves need to be recalculated for each time step. This can result in simulations taking in the order of weeks rather than a few hours.

4.3.5 LITPACK by DHI

As mentioned previously, two modules of the LITPACK by DHI suite of models are used during this investigation, namely LITDRIFT and LITLINE. Both of these modules make use of the “Sediment Transport Program” or STP. The sediment transport magnitudes are calculated as the sum of the total suspended load transport and the bed load transport. In the STP, the Engelund and Fredsoe bed load transport model is used (DHI, 2011c). The bed load transport, Φ_b, is found through a deterministic approach.

$$\Phi_b = 5p\left(\sqrt{\theta'} - 0.7\sqrt{\theta_c}\right)$$ Equation 4-1

where

$$p = \left[1 + \left(\frac{\frac{\pi}{6}\beta}{\theta' - \theta_c}\right)^4\right]^{-0.25}$$ Equation 4-2

p relative density of the sediment
β beach slope
Θ' Shield's parameter determined for a plane bed (this is the time-varying parameter)
Θ_c Critical Shield's Parameter

The suspended sediment transport is calculated as the product of the instantaneous flow velocities and the instantaneous sediment concentration:

$$\mathbf{q_s} = \frac{1}{T}\int_0^T \int_{2d}^D (uc)\,dz\,dt$$ Equation 4-3

These two components are added together to determine the total sediment transport rate for a given time step. As such, the above calculations are repeated for each time-step during the simulation.

4.3.5.1 LITDRIFT by DHI

LITDRIFT calculates the longshore sediment transport in a cross-shore direction, assuming that conditions are uniform along a straight coastline (DHI, 2011b). This means that the model calculates the potential longshore sediment transport volumes, assuming an unlimited sand supply from both the updrift and downdrift side of the cross-section.

Essentially, LITDRIFT consists of two main computational components, namely (DHI, 2011b)

- a hydrodynamic model and
- a sediment transport model (STP, covered earlier).

The following physical phenomena are included in the LITDRIFT calculations (DHI, 2011b)

- Shoaling
- Refraction
- Bottom dissipation
- Wave breaking
- Wind generation
- Spectral wave description
- Wave-current interaction.

The cross-shore profile is described by the bathymetry at regular distance intervals perpendicularly to the coastline, as well as the sediment characteristics at each of those positions (DHI, 2011b).

For each time step, the hydrodynamic model calculates the radiation stresses, wave-induced setup and resulting longshore current at each node in the cross-shore profile. These parameters are then applied to the sediment characteristics to determine the resulting longshore transport at each node (DHI, 2011b).

The model then performs two integrations. The first is the integration of the longshore transport at each node over the entire profile, to determine the total bulk volume of sand transport through the cross-sectional plane for a given time step. This is saved to an output file to determine the time-dependant total longshore transport (DHI, 2011b).

The second integration is the longshore transport at each cross-shore node over the model simulation. This gives an indication of what percentage of the total longshore transport occurs at each cross-shore position of the profile (DHI, 2011b).

Additionally, LITDRIFT is used to determine the net longshore transport north of Table Bay.

4.3.5.2 LITLINE by DHI

LITLINE by DHI is a one-dimensional sediment transport model which calculates the evolution of the shoreline, assuming that shore cross-sections remain constant during accretion or erosion. The coastal morphology is therefore described by the coastline position in a cross-shore direction (DHI, 2011d). This means that the cross-shore profile, both in terms of bathymetry and sediment characteristics, remains constant throughout the simulation.

The shoreline is defined as the distance from a so-called baseline to the shoreline position, as shown in Figure 4-3. This distance is given at constant intervals along the baseline, thereby allowing a realistic representation of the coast. The position of the dune is also given as the distance from the baseline, and is naturally less than the distance to the shoreline.

Different shore cross-sections can be defined along different positions in the longshore direction (DHI, 2011d). This means that the profile shape, as well as sediment characteristics can be varied along the coastline to mimic reality. To reduce computational requirements, the number of cross-shore profiles is limited to five, which means that five representative profiles (bathymetry and sediment characteristics) need to be chosen to describe the entire coastline being simulated.

Figure 4-3: Definition of Components in Coastline Description (DHI, 2011d)

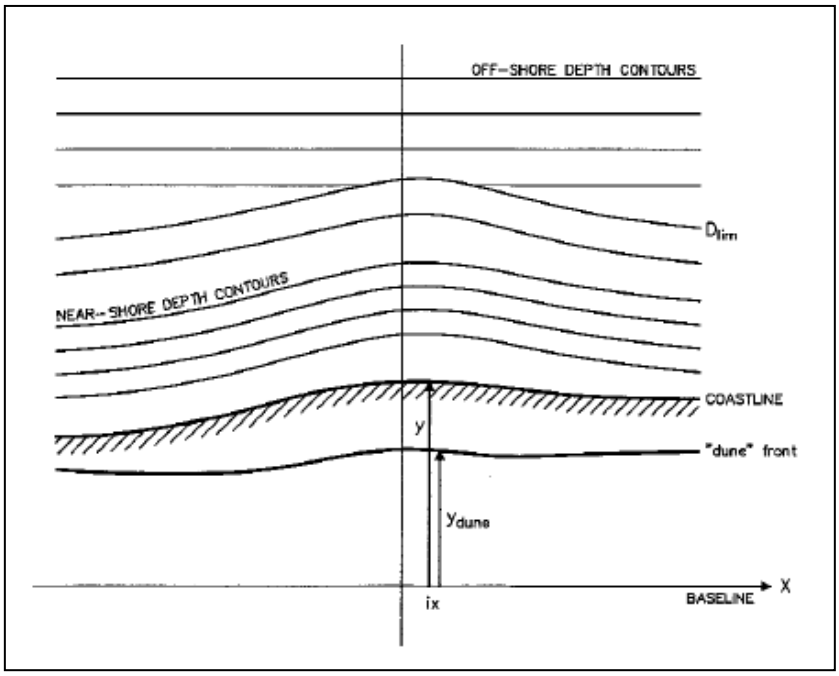

The four structures listed below are available for application in LITLINE (DHI, 2011d). Although only the offshore breakwater structure is applicable during this study, the others are included here for completeness.

- Groynes
  - Short structure extending in the offshore direction perpendicular to the shoreline
  - Littoral current and sediment transport is blocked
  - Structure has a sheltering effect for the wave action on the downdrift beach (sediment transport capacity is reduced)
- Jetties
  - Long structure extending in the offshore direction perpendicular to the shoreline
  - Partial of full blockage of littoral current and sediment transport
  - Structure has a sheltering effect for the wave action on the downdrift beach (wave action in this area is determined by diffraction)
- Offshore Breakwaters
  - Surface piercing structure running near-parallel to the shoreline
  - Structure is assumed to be impermeable and non-reflective
  - Wave heights reduced and wave angles altered due to diffraction, refraction and shoaling
- Shoreline Revetments
  - Structure that restricts the landward movement of the shoreline
  - When an eroding shoreline reaches a revetment, shoreline retreat is stopped, but the depth in front of the structure is increased
  - When local depth is equal to active depth in front of the revetment, longshore transport is set to zero at this location

The following physical phenomena are included in the computations performed by LITLINE:

- Shoaling, refraction and diffraction
- Dissipation by bottom friction and wave breaking
- Wave spreading
- Wave-current interaction

The main equation in LITLINE is the continuity equation for sediment volumes (DHI, 2011d):

$$\frac{\partial y_c}{\partial t} = -\frac{1}{h_{act}}\frac{\partial Q}{\partial x} + \frac{Q_{sou}}{h_{act}\Delta x} \qquad \text{Equation 4-4}$$

where

y_c coastline position
t time
Q longshore transport rates
X longshore position
h_{act} active height of profile
Q_{sou} supply of sediment from sources

Equation 4-4 is simply a balance equation of sediment transport at one specific longshore position. The equation determines the net volume of sand which remains at the longshore position, which is equal to the volume arriving minus the volume leaving, plus any sediment sources applied at the given position.

Once this volume has been determined, the shoreline evolution is determined, by adding the net volume to the active cross-shore profile. Note that during this calculation, both the active height and active depth of the profile remains constant, i.e. the profile is either accreted seaward or eroded landward parallel to its original orientation (DHI, 2011d).

There are numerous limitations of LITLINE, which need to be carefully considered to ensure both the applicability of the model, as well as to enable the correct evaluation of model results.

The first and most important limitation is that LITLINE is a one-dimensional model. This generates two secondary limitations, as listed below:

- Cross-shore effects, such as undertow, are not included in the simulation
- The shape of cross-shore profiles remains constant throughout the simulation. This means that phenomena like beach steepening, which is common in eroding shorelines, are not incorporated in the simulations.

A second limitation is that LITLINE was developed to determine the evolution of semi-infinite and straight coastlines (DHI, 2011d). This means that, firstly, the model calculates potential longshore sediment transport, and secondly, the geometric calculations to determine accretion and/or erosion are based on the assumption that the angle between the baseline and the shoreline is negligible (see Figure 4-3). For the present study, this is clearly not the case since the Table Bay shoreline is curved. This limitation was negated by incorporating a schematization approach, which will be discussed in greater detail in later sections of this report.

Furthermore, LITLINE does not take the differential wave setup and the resulting water level variations into account. This means that the opposing currents entering the lee of the vessel from either side of an offshore breakwater are not incorporated. The corresponding sediment transport resulting from these currents are therefore also not included, which means that LITLINE may slightly underestimate the extent of salient formation in the lee of offshore breakwaters, as well as excluding a portion of the erosion which can occur along the areas adjacent to an offshore breakwater (DHI, 2011d). Results obtained from the numerical model

therefore need to be analysed, taking the potential underestimation of sedimentation in the lee of offshore structures into account.

The final limitation introduced during this discussion is the manner in which LITLINE performs diffraction calculations. Since LITLINE is a one-dimensional model, it is unable to resolve the real wave climate in the lee of an offshore breakwater, being a two-dimensional effect. It therefore resorts to diffraction diagrams, covered in Section 3.2.2 to estimate the sheltered wave climate in the lee of the structure (DHI, 2011d). It will be remembered that the diffraction diagrams, as shown in Figure 3-3, make a critical assumption that the structure is semi-infinite, which means that it extends infinitely long to one end.

This is clearly not the case at an offshore breakwater, which is not infinitely long at either end. However, if the relative distance of the length of the breakwater compared to the distance offshore is long, i.e. the breakwater is longer than the distance offshore, the assumption still holds. This is because the diffraction effects of either end of the structure do not interact with each other, since they do not have sufficient distance behind the structure to develop. However, if the offshore breakwater is short compared to the distance offshore, irregularities may occur (DHI, 2011d). In general therefore, in shielded zones, i.e. in the lee of an offshore breakwater or shipwreck, the results of a coastline model may depend largely on the selected location and depth of the wave output points. Caution is therefore required when making the decision as to where to choose these output points, to ensure that the shoreline changes are simulated in a more representative manner in the coastline model.

This limitation is compensated for by determining the diffracted wave climate in the lee of the shipwreck with the wave transformation model, applying this diffracted wave climate to the shoreline model. In this way, the correct wave forcing is applied to the shoreline model.

LITLINE will be used to simulate the shoreline evolution resulting from the Seli One shipwreck, and is therefore the main numerical tool being employed during this project.

4.4 Summary and Conclusions

The general approach and methodology followed during the current study has been introduced, including an in-depth review of the numerical modelling tools used to simulate coastal processes. The DHI suite of numerical models was used during this study, including wave, hydrodynamic and both one- and two-dimensional sediment transport models. It has been ascertained that these models are applicable to assess the impact of the Seli One shipwreck on local waves, current and sediment transport characteristics.

It has been shown that, compared to the most common sediment transport relationships which are generally of an empirical nature, the numerical models are based on deterministic relationships. The models therefore include the physics behind the coastal processes, and are therefore more accurate than the empirical relationships.

Finally, it has been shown that some of the numerical models have a number of limitations, especially the shoreline evolution model. It has however also been pointed out that each of these limitations can be accommodated to still achieve the correct modelling procedure, to accurately simulate the physical processes of Table Bay.

It is therefore determined that the proposed methodology discussed in the preceding paragraphs is adequate to quantify the impact of the long-term impact of the Seli One shipwreck on the Table Bay beaches.

Figure 4-4: Study Flow Chart

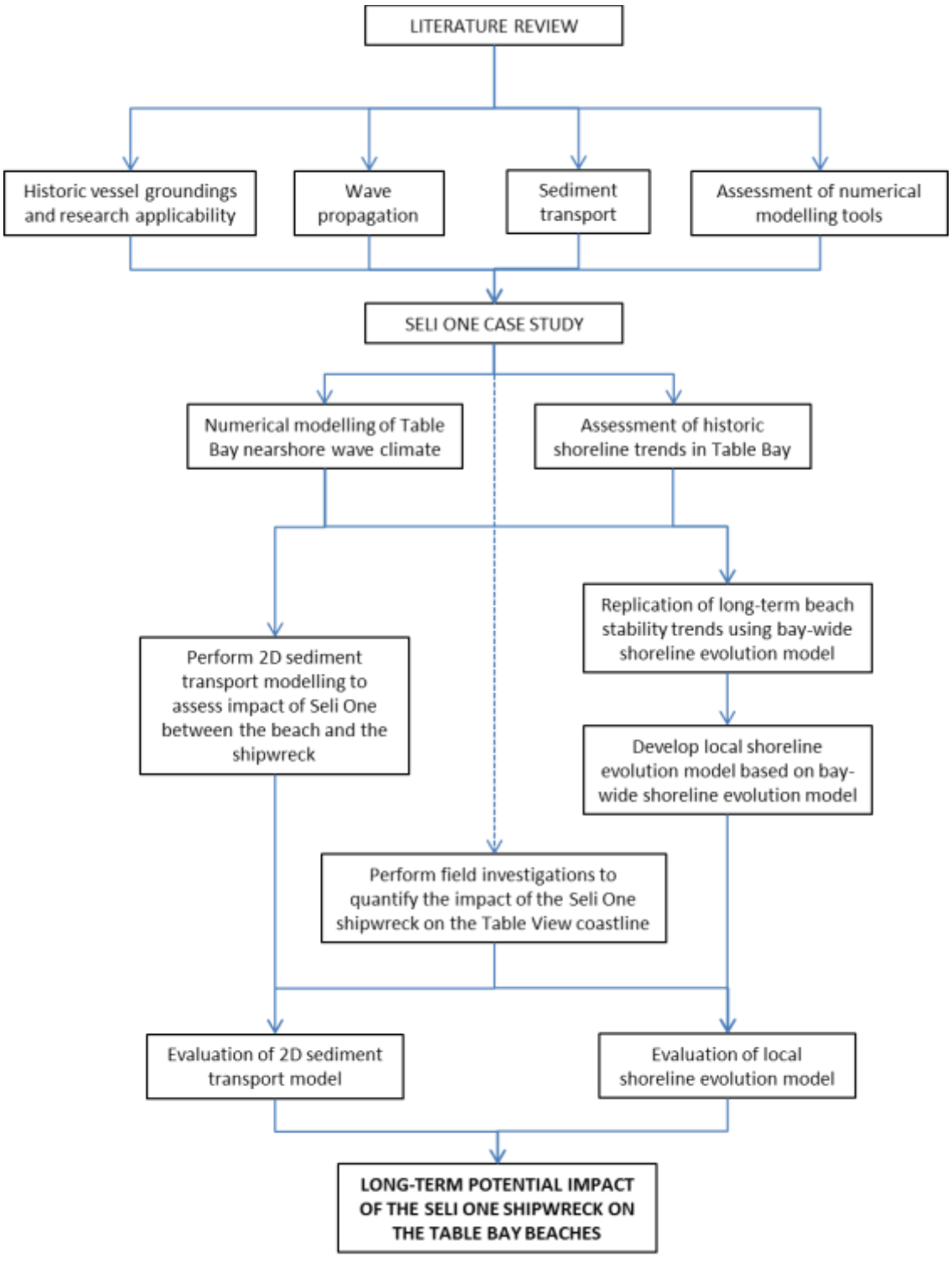

5. DEVELOPMENT OF THE PORT OF CAPE TOWN AND THE TABLE BAY SHORELINE

5.1 Introduction

The Seli One shipwreck is situated within a complex sediment transport system being Table Bay, and can therefore not be analysed in singularity. A high-level description of Table Bay is therefore a necessity to enable to correct understanding of the impact of the wreck on the local sediment transport system along the Blouberg shoreline. During the following discussions, reference is made to the fold-out maps of the study area, given in Appendix C, Appendix D and Appendix E.

5.2 Table Bay

Table Bay is a curved bay facing westward into the Atlantic Ocean, located along the west coast of South Africa. Table Bay, for purposes of this study, is defined as extending northwards from the rocky outcrop at Mouile Point to the rocky outcrop at Blouberg, as shown in Figure 5-1. The Port of Cape Town, which has undergone significant expansion since its original inception, is shown in the figure as well.

Figure 5-1: Table Bay – Image: Google Earth (Google Inc., 2010)

5.3 Development of the Port of Cape Town

Since the Dutch landed in 1652, the bay has been used as an important stop-over and replenishing station, as well as a safe haven port for vessels sailing between the Far East and Europe. More recently, the Port of Cape Town, located at the southernmost extent of Table Bay, has become a commercially important port, with large amounts of cargo being handled annually.

Due to this, the harbour has undergone extensive expansion since the original version was built in the 1870's. Below follows a brief overview of the expansion phases of the Port of Cape Town, as summarized by Entech (1995). This development is shown graphically in Figure 5-2.

1870's	Construction of Alfred Basin
1870 – 1920	Construction of 350 m of main breakwater Reclamation in the Cape Town vicinity
1905	Construction of Victoria Basin
1920 – 1933	Construction of A, B, C and D berths in Duncan Dock
1933	Extension of Main Breakwater by approximately 400 m
1933 – 1945	Reclamation of the Foreshore, Royal Cape Yacht Club area and the present crane repair depot Construction of eastern side of Duncan Dock
1965	Construction of eastern mole tanker berths and lay-up basin in Duncan Dock
1968 – 1972	Extension of Main Breakwater by 150 m to present day situation Construction of sea wall from Lagoongate Site to present entrance of Ben Schoeman Dock
1972 – 1977	Construction of Ben Schoeman Dock, including concrete dolos revetment up to 900 m south of Diep River mouth

It is clear from Figure 5-2 that extensive reclamation works have taken place during the phased construction of the Port of Cape Town. The Castle, shown as the star in Figure 5-2, was originally located fairly close to the sandy shoreline, but is now approximately 1.2 km behind the quay walls of the port.

Furthermore, an extensive stretch of originally sandy beaches has been hardened up due to the construction of the port. This stretch has therefore been excluded from the longshore sediment transport system of the bay. The development of the port therefore plays an important role in the longshore sediment transport system of Table Bay.

Figure 5-2: Development Phases of the Port of Cape Town – based on (CSIR, 1996)

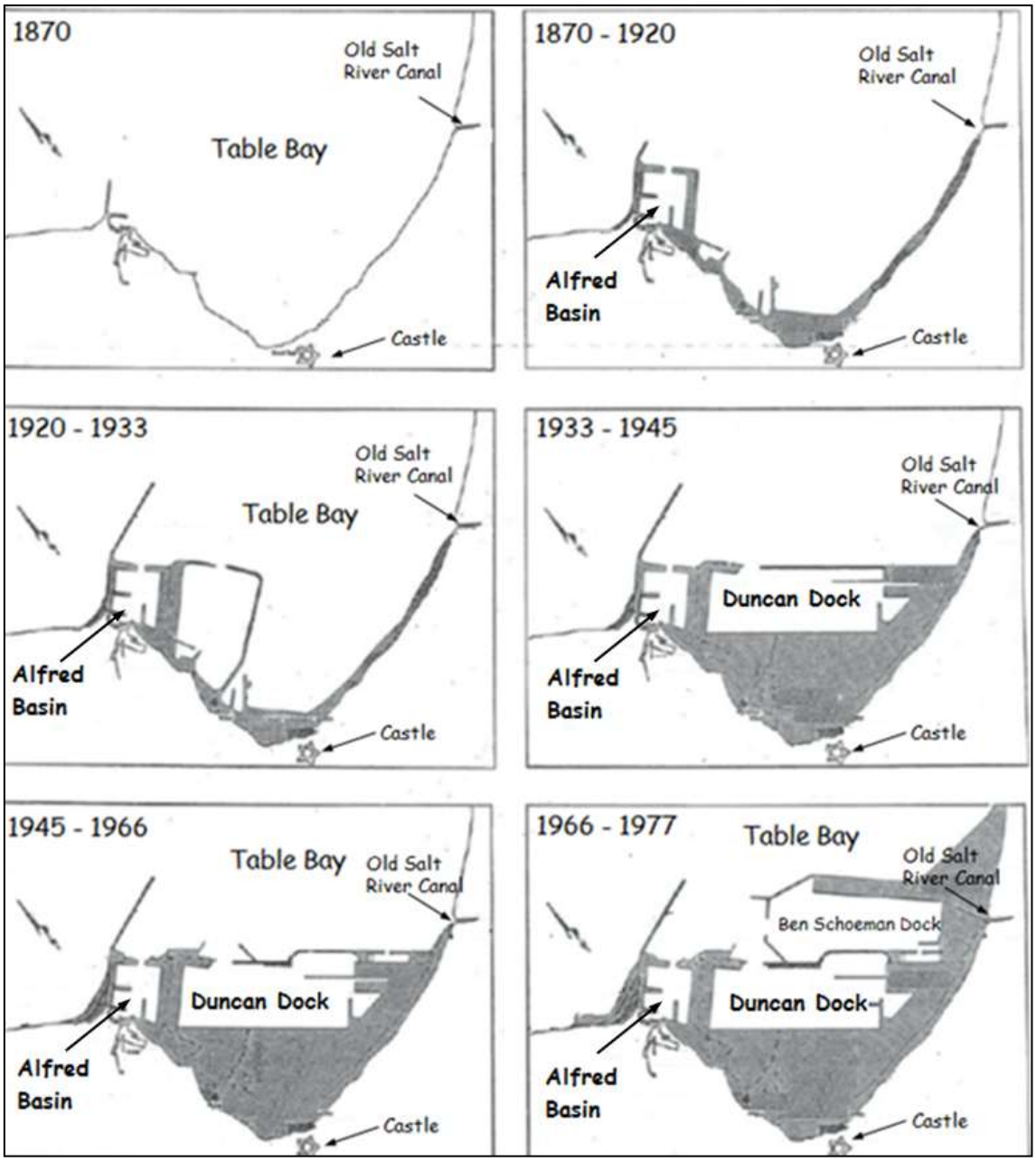

Comparing Figure 5-1 and Figure 5-2, it will further be observed that, originally, the Salt River mouth was located at the far southern end of Table Bay, within the area that has been reclaimed during the expansion of the Port of Cape Town. Since then, the river has been canalized, with the mouth now situated a few hundred metres north of the port boundaries.

5.4 Developments along the Table Bay Shoreline

Concurrent with the development of the port, extensive infrastructure development, both public and private, has taken place along the beaches of Table Bay. In addition, the two rivers draining into Table Bay, the Diep- and Salt River have undergone significant re-routing in the past. Similar to the port expansion, it is thought that both the infrastructure developments and the re-routing of the rivers have had an influence on the

longshore sediment transport dynamics of Table Bay. These developments are therefore of importance during the current study, and are subsequently discussed here.

The following paragraphs give a brief overview of the state of the shoreline along Table Bay. A general understanding of the state of the Table Bay shoreline is useful during the analysis of the historic beach profile measurements, which will be introduced in Section 6. This discussion is performed by separating the Table Bay into five coastal sectors, as shown in Figure 5-3 below (this figure is repeated in Appendix E as a fold-out map for ease of reference).

Figure 5-3: Coastal Sectors of Table Bay

5.4.1 Port of Cape Town to Diep River Mouth

The first and most southerly sector extends from the Port of Cape Town to the Diep River mouth, covering the southern 2.9 km of the Table Bay coast. The shoreline in this sector is characterized by a revetment constructed of concrete dolosse, as well as by the canalized outlet of the Salt River. The concrete canal is kept

clear of northwards-moving sediment by a groyne at its southern end. The northern 800 m of this sector is a sandy beach.

Figure 5-4: Concrete Dolos Revetment along Southern 2.9 km of Table Bay

Two coastal developments are situated along the sandy coastline of this sector (near profile station S06), being the Leisure Bay residential apartment block, as well as the Lagoon Beach Hotel. These are located immediately south of the Diep River mouth. Judging from aerial imagery, the Leisure Bay residential development was constructed between 1996 and 2000. The Lagoon Beach Hotel was constructed at a later stage, with construction starting mid-2003 (Figure 5-5).

Figure 5-5: Leisure Bay and Lagoon Beach Hotel Developments

Figure 5-5a: Leisure Bay Apartments on 12th July 2002
Image: Google Earth (Google Inc., 2010)

Figure 5-5b: Leisure Bay Apartments and Lagoon Beach Hotel on 30th November 2010
Image: Google Earth (Google Inc., 2010)

As can be seen onFigure 5-5a, the Leisure Bay residential development is set back from the beach, a distance of approximately 20 m. As such, a certain measure of dune protection has been retained on the seaward side of the apartments.

The Lagoon Beach Hotel, shown in Figure 5-5b, was constructed immediately to the south of the Diep River mouth, protected by a concrete seawall along its northern and western borders. The lack of primary dune makes this development susceptible to storm erosion by wave attack.

It will be shown in later sections of this report that this area has experienced significant shoreline erosion in the past. Recently, a sandbag revetment has been constructed in an attempt to limit further shoreline erosion Figure 5-6. Both of these developments are therefore severely impacted by longshore sediment transport processes.

Figure 5-6: Sandbag Revetment in front of the Leisure Bay Apartment Complex

5.4.2 Woodbridge Island and Milnerton Golf Club Clubhouse

The second sector stretches from the Diep River Mouth to north of the Milnerton Golf Club clubhouse, a length of approximately 1.5 km. The shoreline in this area is a sandy beach, backed by partially vegetated dunes. Currently, the dunes along Woodbridge Island and in front of the Milnerton Golf Club Clubhouse are fenced off with dedicated walkways spaced intermittently, in an attempt to promote shoreline stabilization and accretion.

The dunes north of the Milnerton Golf Club clubhouse are not artificially maintained, nor are they fenced off. The state of dune vegetation in this area is therefore visibly reduced compared to the dunes at Woodbridge Island.

The dune field fronting the residential houses at Woodbridge Island are in the order of 30 m wide. The so-called “Zonnekus House”, which can be seen in Figure 5-7 and Figure 5-8, has virtually no dune protection, and is therefore at risk of storm erosion.

Figure 5-7: Woodbridge Island Residential Development

The Milnerton Golf Club clubhouse, located at the southern end of the golf course, shown in Figure 5-9, is located well seaward of a reasonable setback line, with the most seaward edge of the clubhouse being seaward of the vegetation line of the northern dunes (see Figure 5-9). It will be shown in later sections of this report that the coastline in this area has receded between approximately 30 m and 50 m since the mid-1970s. Nevertheless, even prior to the shoreline erosion experienced in this area, the Milnerton Golf Club clubhouse was situated well seaward of a reasonable setback line. These buildings are therefore at high risk from both short term storm erosion, as well as long term shoreline fluctuations. A sandbag revetment has been constructed in front of the clubhouse in an attempt to limit damage from storm erosion.

Figure 5-8: Erosion of Woodbridge Island Shoreline - October 2001 (CSIR, 2003)

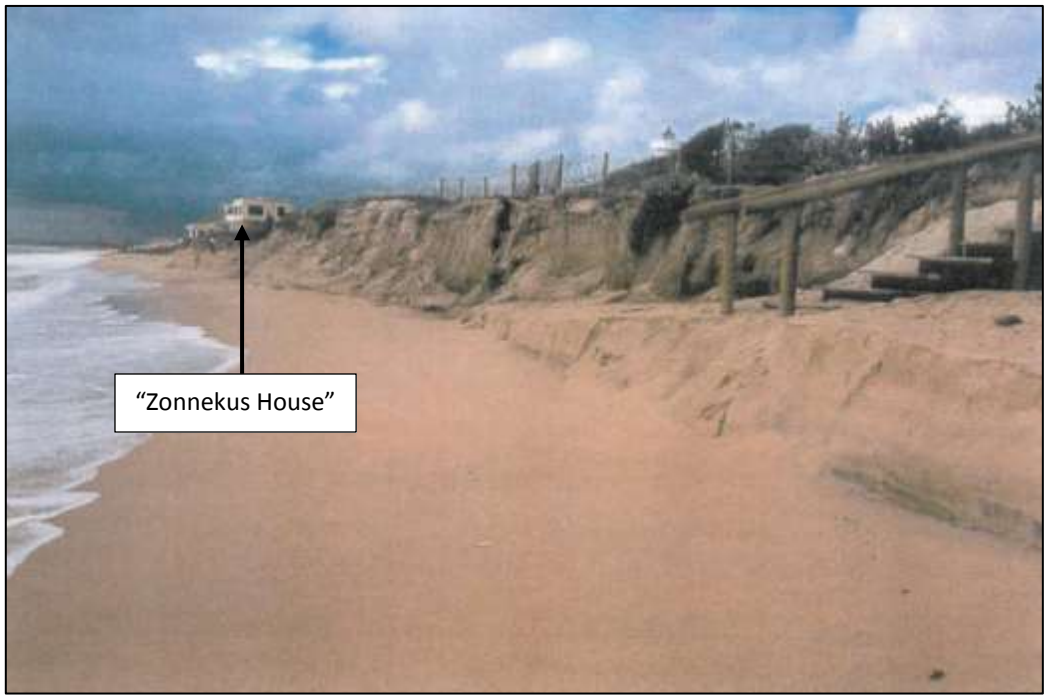

Figure 5-9: Milnerton Golf Club Clubhouse

5.4.3 Milnerton Golf Course and Sunset Beach

The third sector runs adjacent to the Milnerton Golf Course, extending to the northern end of Sunset Beach, a total length of approximately 3.85 km. The shoreline in this sector is a sandy beach, backed by partially vegetated dunes. The dune field fronting the Milnerton Golf Course is relatively narrow, reducing to a width of 3 m in some areas.

Judging again from aerial photography, the golf course was constructed during the late 1960's and early 1970's, and was later expanded to the current extents.

Properties along the Sunset Beach coastline have been set back substantially compared to the rest of the bay, and are therefore the least susceptible to damage due to shoreline excursions and storm erosion. The dune width ranges between 60 m and 110 m. Vegetation tramping is minimized by the erection of dedicated walkways, as shown in Figure 5-10.

Figure 5-10: Dedicated Walkways through Sunset Beach Dune Field

5.4.4 Sunset Beach to Dolphin Beach

The fourth sector extends approximately 2 km from Sunset Beach to the Dolphin Beach Hotel. The shoreline in this sector is a sandy beach. Arterial road R27 runs behind the approximately 100 m wide dune field, which is naturally vegetated. Access to this piece of coastline is limited, resulting in beach goers generally preferring to visit the Table View beaches further north. As such, the human impact on dune stability is very limited, resulting in good dune vegetation.

Prior to the construction of the Dolphin Beach Hotel, the R27 linked to the coastal road running along the Blouberg beachfront. This link was removed, as shown inFigure 5-11 andFigure 5-11b, to enable the construction of the hotel.

Comparing Figure 5-11a and Figure 5-11b further, it is clear that the hotel was constructed in the active littoral zone, with the beach in 1977 being significantly wider than that in 2009. To prevent both short-term and long-term shoreline erosion, an approximately 75 m wide dune field is artificially maintained.

Figure 5-11: Dolphin Beach Hotel Pre- and Post- Construction

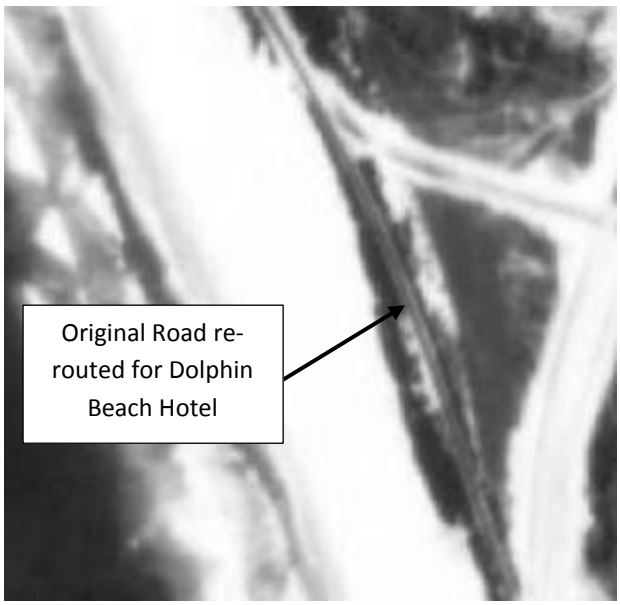

Figure 5-11a: Pre-Construction: 1977

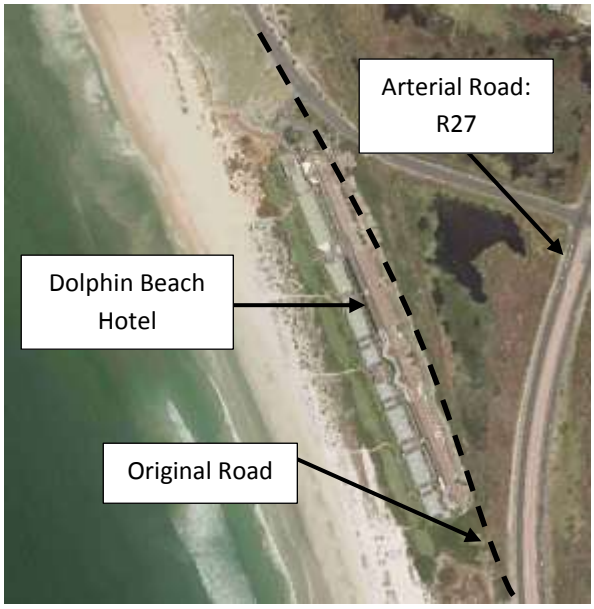

Figure 5-11b: Post Construction: 2009

5.4.5 Dolphin Beach to Blouberg Rocks

The most northern sector in Table Bay extends from the Dolphin Beach Hotel to the rocks at Blouberg, a distance of approximately 3 km. The shoreline south of the intersection between Blouberg Road and Marine Drive is a sandy beach, backed by a vegetated dune. The dune is backed by a grass embankment and parking lot, which has a width of 65 m at the Dolphin Beach Hotel, tapering off to approximately 10 m south of the intersection.

The shoreline north of the intersection is a fairly steep beach, backed by a narrow, partially vegetated dune. The width of the dune is between 10 m and 20 m, and backed by public parking lots and a coastal road.

The Seli One shipwreck is located within this final sector of Table Bay, in front of the intersection between Blouberg Road and Marine Drive.

5.4.6 Salt- and Diep River

Prior to the end of the 18th century, the Diep River mouth was located at the current location of the canalized Salt River mouth, in the far south of Table Bay (CSIR, 1983). During the 19th century, a new mouth formed near the present Diep River delta, although the Diep River was still connected to the Salt River by a natural channel. Siltation of this connection however followed, resulting in the opening near the current Diep River mouth being the only delta of the Milnerton Lagoon (CSIR, 1983).

To increase the water depth in the lagoon to permit pleasure boating, a concrete weir was constructed near the mouth in 1928. The weir was subsequently damaged during flood events, and because of inundations of the Milnerton area caused by the weir, it was subsequently demolished (CSIR, 1983).

The alongshore location of the Salt- and Diep River mouths have therefore been fixed. A certain variability of the Diep River mouth is still possible, but is limited to about 200 m.

5.5 Summary and Conclusions

It can be concluded that Table Bay has undergone significant changes within the past 150 years, one of which is the construction and continued expansion of the Port of Cape Town. The port, which was originally constructed in the 1870's has seen the construction of additional basins, new lengths of breakwater, as well as significant amounts of reclamation works to provide the required back of quay space for the port's cargo handling operations. The reclamation works have changed the appearance of the southern portion of Table Bay dramatically, with a significant length of originally sandy coastline being stabilized by a concrete dolos revetment.

Furthermore, it has been discussed that significant amounts of public and private developments have occurred all along the Table Bay coastline, some of which are thought to have an impact on the longshore sediment transport dynamics of the bay.

Finally, it has been pointed out that the two rivers draining into Table Bay have been rerouted from their original paths, and that this rerouting has taken place in conjunction with port development projects.

6. OBSERVED SHORELINE TRENDS

6.1 Introduction

Beach profile measurements have been performed by the CSIR on behalf of the Transnet National Ports Authority (TNPA) between the Port of Cape Town and Blouberg Rocks since the late 1960's. Permission has been obtained from Mr Magenthran Ruthenavelu, TNPA Port Engineer for the Port of Cape Town, to use this data for the current investigation.

The review of the beach profile measurements is considered a critical part of this investigation, since it forms the backbone to the shoreline evolution modelling. Beach surveys are used to identify long-term shoreline trends, which will be used directly in the shoreline models. The correct interpretation of this data is therefore a necessity to the correct understanding of the Table Bay longshore sediment transport system, which, in turn, is a necessity to accurately replicate and predict the impact of the Seli One shipwreck on the Blouberg coastline.

Observations and conclusions drawn from beach profile measurements are validated through a comparison with aerial photography. Table 6-1 gives a summary of the images used during the study.

Table 6-1: Summary of Aerial Photography

Date	Source	Extents
1968	CSIR	From the eastern breakwater (not constructed at that stage) to the Milnerton Golf Club Clubhouse
1972	CSIR	From slightly south of the Diep River Mouth to approximately 2 km north of the Milnerton Golf Club Clubhouse
1977	Chief Directorate, Surveys and Mapping, Mowbray	From the Port of Cape Town to north of the Koeberg Power Station (not constructed at that stage)
1987	CSIR	From approximately 1 km south of the Diep River mouth to approximately 2km north of the Diep River mouth
1996	City of Cape Town	From the Port of Cape Town to north of the Koeberg Power Station
2005	City of Cape Town	From the Port of Cape Town to north of the Koeberg Power Station
2008	Chief Directorate, Surveys and Mapping, Mowbray	From the Port of Cape Town to north of the Koeberg Power Station
2009	Chief Directorate, Surveys and Mapping, Mowbray	From the Port of Cape Town to the southern end of Big Bay

Not all image sets listed in Table 6-1 cover the entire extent of the bay. The oldest set covering the entire bay was taken in 1977. Very good coverage of the Woodbridge Island area is however available. Coverage of the entire bay has been improved during the more recent campaigns.

6.2 Beach Profile Measurements

6.2.1 Summary and Description of Data

Twenty-six so-called survey stations are spaced intermittently along the Table Bay beaches, with stations being most densely spaced in front of Woodbridge Island and the Milnerton Golf Club clubhouse. As shown on the fold-out map of Appendix C, station S03 is located adjacent to the Port of Cape Town, whilst station S44 is located immediately south of the rock outcrop at Blouberg.Table 6-2 summarizes the profile beacon coordinates, which make reference to the following coordinate system:

Map Projection	Gauss Conformal
Datum	Hartebeesthoek 94
Spheroid	WGS84
Central Meridian	19^{o}
Reference System	WG19
Co-ordinates	X, increasing eastwards
	Y, increasing northwards
Distance units	International metre

Table 6-2: Profile Beacon Coordinates

Profile	X [m]	Y [m]	Profile	X [m]	Y [m]
S03	-49187.3	-3753977.0	S16	-47247.0	-3749353.0
S04	-48747.4	3753533.0	S18	-47244.0	-3748766.0
S05	-48369.6	-3752922.0	S20	-47274.4	-3748156.0
S06	-48014.3	-3752067.0	S22	-47309.4	-3747527.0
S07	-47688.5	-3751311.0	S24	-47404.0	-3746967.0
S08	47654.2	-3751197.0	S28	-47587.0	-3746333.0
S09	-47609.2	-3751118.0	S31	-47791.0	-3745789.0
S10	-47548.8	-3750815.0	S35	-47994.0	-3745157.0
S11	-47472.9	-3750603.0	S38	-48283.0	-3744514.0
S12	-47398.3	-3750339.0	S41	-48531.7	-3744019.0
S13	-47347.8	-3750105.0	S42	-48811.0	-3743435.0
S14	-47314.8	-3749816.0	S43	-49127.0	-3742852.0
S15	-47278.1	-3749523.0	S44	-49482.1	-3742297.0

Table 6-3 below summarizes the survey data available for this study. It is clear that there is a large gap in survey data between the initial surveys performed in 1965 and 1967, and the recommencement of regular surveying in the early 1990's. Station S09 has been surveyed fairly continuously since May 1965. Furthermore, it is clear that profile measurements have been most regularly taken along the Woodbridge Island beachfront, at stations S07 to S12.

Table 6-3: Summary of Survey Data

	May-65	Apr-67	Sep-83	Jun-84	Jun-85	Jun-86	Apr-88	Sep-88	May-91	Aug-91	May-92	Nov-92	Jun-93	Apr-95	Feb-99	Nov-02	May-05	Aug-05	Oct-05	Dec-05	Mar-06	May-06	Jul-07	Oct-07	Jan-08	Mar-08	May-08	Aug-08	Dec-08	Mar-09	Oct-09	Dec-09	Feb-10
S03																			√	√	√	√								√		√
S04																			√	√	√	√								√	√	√
S05	√													√					√			√										√
S06	√	√									√		√	√	√	√	√	√	√	√	√	√		√	√		√	√	√	√	√		
S07	√	√				√		√		√			√	√	√	√	√	√	√	√	√	√		√	√	√	√	√	√	√	√	√	
S08	√	√				√				√			√	√	√	√	√	√	√	√	√	√	√	√	√	√	√	√	√	√	√	√	√
S09	√	√	√	√	√	√	√	√	√	√		√	√	√	√	√	√	√	√	√	√	√	√	√	√	√	√	√	√	√	√	√	√
S10	√	√											√	√	√	√	√	√	√	√	√	√	√	√	√	√	√	√	√	√	√	√	√
S11	√	√												√	√	√	√	√	√	√	√	√		√	√	√	√	√	√	√	√	√	√
S12	√	√						√	√			√	√	√	√	√	√	√	√	√	√	√	√	√	√	√	√	√	√	√	√	√	√
S13	√	√										√	√	√	√	√	√	√	√	√	√	√		√	√	√	√	√	√	√	√	√	√
S14	√	√										√	√	√	√	√	√	√	√	√	√	√	√	√	√	√	√	√	√	√	√	√	√
S15	√	√											√	√	√	√	√	√	√	√	√	√	√	√	√	√	√	√	√	√	√	√	√
S16	√	√											√	√	√	√	√	√	√	√	√	√	√	√	√	√	√	√	√	√	√	√	√
S18																			√	√	√	√		√	√	√	√	√	√	√	√	√	√
S20																			√	√	√	√		√	√	√	√	√	√	√	√	√	√
S22	√	√													√	√	√	√	√	√	√	√	√	√	√	√	√	√	√	√	√	√	√
S24																			√	√	√	√	√	√	√	√	√	√	√	√	√	√	√
S28																			√	√	√	√		√	√	√	√	√	√	√	√	√	√
S31	√	√											√			√	√	√	√	√	√	√		√	√	√	√	√	√	√	√	√	√
S35																			√	√	√	√	√	√	√	√	√	√	√	√	√	√	√
S38																			√	√	√	√		√	√	√	√	√	√	√	√	√	√
S41	√	√											√			√	√		√	√	√	√		√	√	√	√	√	√	√	√	√	√
S42																			√	√	√	√	√	√	√	√	√	√	√	√	√		√
S43																																	
S44																			√	√	√	√	√	√	√	√	√	√	√	√	√	√	√

Profile measurements between May 1965 and April 1995 are described by a horizontal distance measured from a beacon position, with the corresponding vertical level given at the various survey locations. Eastings and Northings are not explicitly provided. Subsequent to April 1995, survey data is given in X,Y,Z format, describing the eastings, northings and vertical elevation respectively.

Beach profiles have generally been surveyed from the top of the primary dune to approximately the -1 m MSL depth contour. The lower boundary varies between -0.5 m MSL and -2 m MSL, presumably due to tidal levels and wave conditions at the time the surveys were taken.

The following paragraphs summarize observations and conclusions made during the review of the beach profile surveys. It is noted that, for ease of reference, these trends are divided into the same sectors as discussed in Section 5, shown graphically on the map of Appendix E.

6.2.2 Port of Cape Town to Diep River Mouth

As shown on the fold-out map of Appendix E, four profile beacons are located between the Port of Cape Town and the Diep River mouth. Due to land reclamation performed together with the construction of the Ben Schoeman Container Terminal, the beacon locations for stations S03 to S05 are located a fair distance behind the current shoreline. The seaward movement of the cross-section is therefore not a resultant of natural shoreline accretion, but rather of land reclamation and subsequent shoreline hardening.

Profiles S03 and S04 have only been measured recently, since October 2005 and therefore do not contribute to the analysis of the long-term shoreline trends. Figure 6-1 below shows evidence of the revetment construction, with the recent near vertical slope between the 0 m MSL and +4 m MSL depth contour. In addition, significant variations in vertical beach level can be observed in front of the revetment.

Figure 6-1: Profile Station S05 – Cross Sections (May 1965 to February 2010)

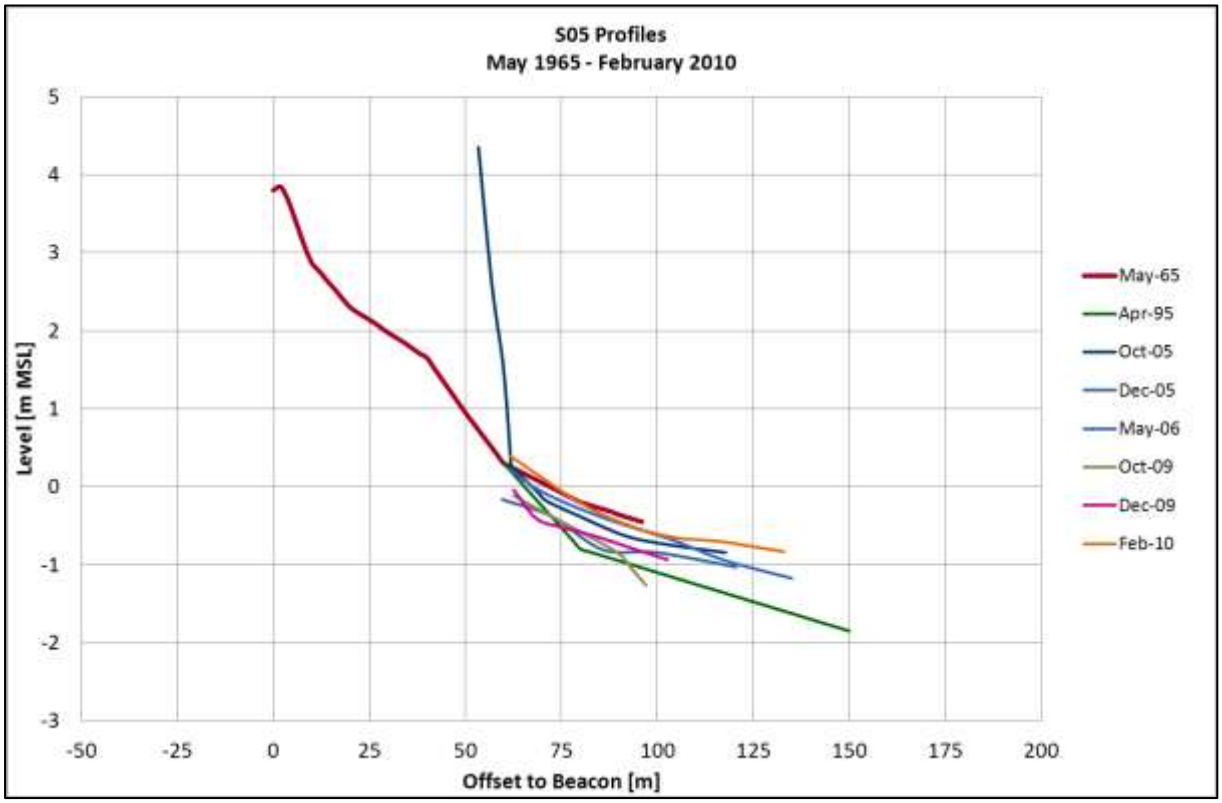

Figure 6-2 and Figure 6-3 show the excursions of the 0 m MSL, +1 m MSL, +2 m MSL and +3 m MSL contours at profile station S06 between 1965 and 2010, and between 2005 and 2010 respectively. These plots show the distance of the depth contours to the profile station beacon. A reduction in distance therefore indicates shoreline erosion, whilst an increased distance indicates shoreline accretion. Each point on the plot represents one survey, with the dashed line presenting a linear trend line fit for each of the four contours.

From Figure 6-2, shoreline erosion between 35 m and 45 m from the mid-1960's to February 2010 can be identified.

Figure 6-2: Profile Station S06 – Profile Excursions (May 1965 to February 2010)

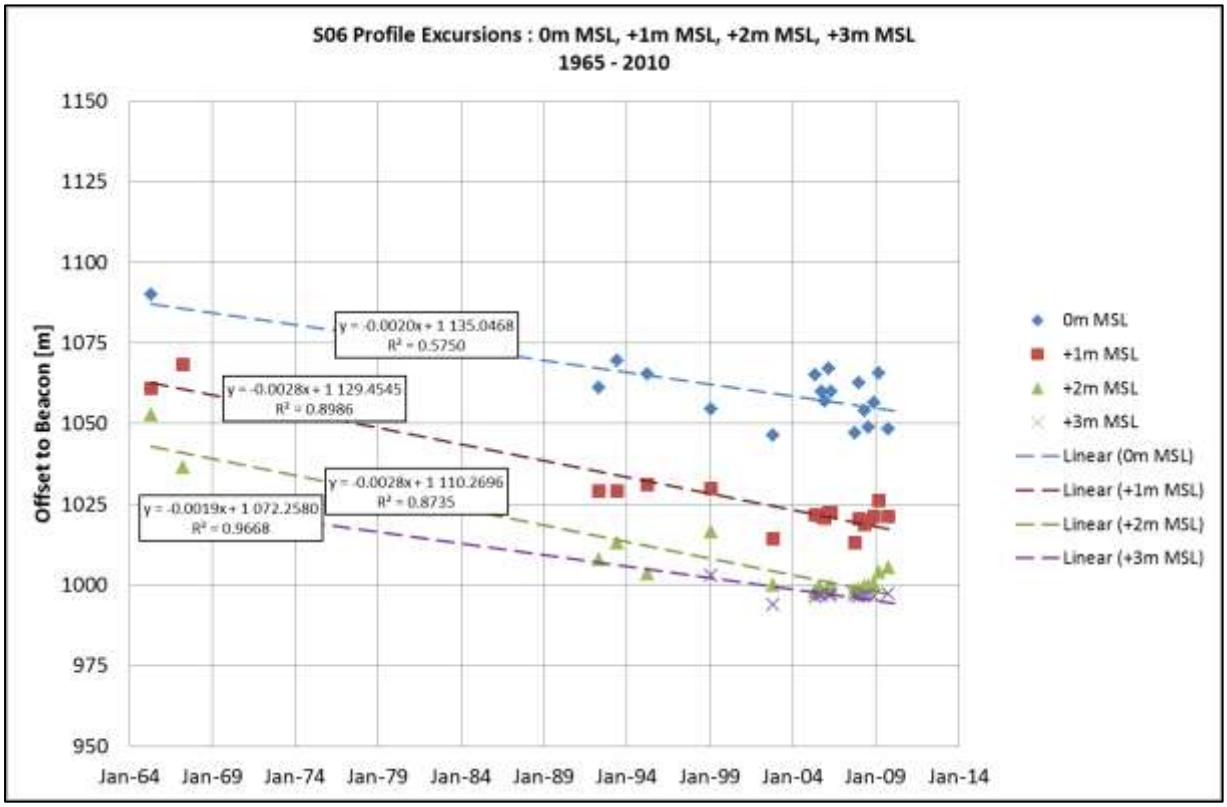

It could however be argued that the results of the beach surveys represented in these figures do not indicate long-term shoreline trends, but merely variations in beach levels due to episodic events such as storms. Referring to Figure 6-1, the vertical beach level variation at profile station S05 at an offset of 75 m from the profile beacon was approximately 0.5 m. If a beach slope of 0.02, which is the average beach slope at station S06, is applied to this 0.5 m vertical variation, a horizontal excursion of 25 m can be calculated. It can therefore be argued that beach contour excursions of within 25 m could be attributed to natural variations caused by episodic events. However, since shoreline erosion of up to 45 m is observed at profile station S06, it is concluded that these excursions fall outside the domain of natural short-term variability, thereby indicating long-term shoreline erosion.

Figure 6-3: Profile Station S06 – Profile Excursions (October 2005 to February 2010)

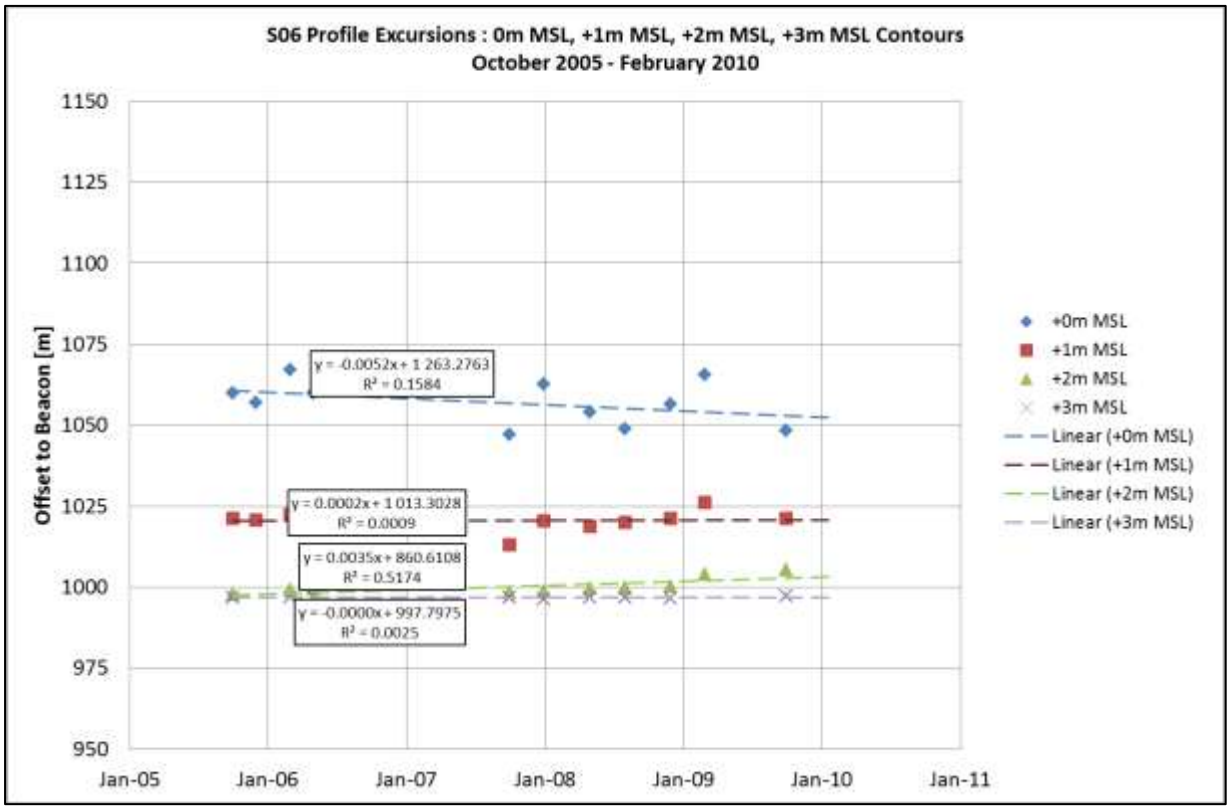

Furthermore, episodic events such as storms which result in shoreline erosion are usually balanced by periods of relatively calm conditions. Sediment which is transported offshore during storm events is brought back onto the beaches during calm conditions. It can therefore be assumed that, although significant variation in shoreline position can be expected in the short-term, over longer durations, episodic events such as storms are not thought to be significant (USACE, 2006a).

Table 6-4 shows the average annual excursion rates for profile station S06. These represent the gradients of the trend lines in Figure 6-2 and Figure 6-3, assuming a linear trend of erosion or accretion. Note that a negative value represents erosion.

Table 6-4: Excursion Rates – Station S06

Profile	Contour	May 1965 to February 2010		October 2005 to February 2010	
		Excursion Rate [m/year]	Total Excursion [m]	Excursion Rate [m/year]	Total Excursion [m]
S06	0 m MSL	-0.7	-32.7	-1.9	-8.2
	+1 m MSL	-1.0	-45.8	0.1	0.3
	+2 m MSL	-1.0	-45.8	1.3	5.5
	+3 m MSL	-0.7	-31.1	0.0	0.0

This table shows the extensive shoreline erosion since May 1965 at each of the four contours. However, it is equally clear that recently, the upper contours (+1m MSL to +3 m MSL) seem to have stabilized. This is presumably due to the dune stabilization project currently underway along the Lagoon Beach shoreline.

Figure 6-4: Evidence of Dune Stabilization near Lagoon Beach Hotel

Nevertheless, it can be argued that shoreline erosion is continuing, since the 0 m MSL contour, which is less likely to be influenced by the dune stabilization project, is continuing its landward movement. Furthermore, it is noted that the rate of erosion of this contour has more than doubled recently; possibly indicating that the stability of the upper contours is resulting in accelerated erosion of the lower profile, although the timeframe from October 2005 to February 2010 is too short to say this conclusively.

6.2.3 Woodbridge Island and Milnerton Golf Club Clubhouse

Each profile in this sector has been measured since May 1965, with the most regular measurements being taken since October 2005. All profiles show a trend of erosion, with the maximum shoreline retreat of approximately 55 m since May 1965 (+1 m MSL) being observed at station S10. Profile excursion rates for the period of May 1965 to February 2010 and October 2005 to February 2010 respectively are shown in Table 6-5 below.

Since October 2005, the shoreline at station S07 has accreted at a rate of between 0.3 m/year and 1.7 m/year at the +3 m MSL and +1 m MSL contours respectively. This is presumably due to the dune stabilization project being undertaken in the area, evidence of which is shown in Figure 6-5.

The mechanism by which this accretion occurs is thought to be one of progressive seaward movement, due to the continued capturing of wind-blown sediment by the dune vegetation. Wind-blown sand is trapped by the dune vegetation, resulting in the seaward growth of the dune.

Table 6-5: Excursion Rates – Stations S07 to S13

Profile	Contour	May 1965 to February 2010		October 2005 to February 2010	
		Excursion Rate [m/year]	Total Excursion [m]	Excursion Rate [m/year]	Total Excursion [m]
S07	0 m MSL	-0.6	-27.8	1.2	5.4
	+1 m MSL	-0.7	-32.7	1.7	7.3
	+2 m MSL	-0.8	-34.3	0.9	4.0
	+3 m MSL	-0.7	-32.7	0.3	1.4
S08	0 m MSL	-0.7	-29.4	-3.7	-16.0
	+1 m MSL	-0.7	-32.7	-0.7	-2.9
	+2 m MSL	-0.8	-34.3	0.6	2.5
	+3 m MSL	-0.6	-27.8	0.9	3.8
S09	0 m MSL	-0.1	-3.3	-2.5	-10.8
	+1 m MSL	-0.1	-3.3	-0.5	-2.2
	+2 m MSL	0.0	0.0	1.3	5.7
	+3 m MSL	0.0	-1.6	0.4	1.6
S10	0 m MSL	-1.9	-83.4*	-0.3	-1.4
	+1 m MSL	-1.2	-55.6	0.9	3.8
	+2 m MSL	-1.1	-47.4	1.8	7.9
	+3 m MSL	-1.1	-47.4	0.9	4.0
S11	0 m MSL	-1.1	-49.0	-2.7	-11.9
	+1 m MSL	-1.1	-47.4	0.4	1.7
	+2 m MSL	-1.0	-45.8	2.1	9.0
	+3 m MSL	-1.0	-45.8	0.7	3.2
S12	0 m MSL	-0.9	-42.5	-8.0	-34.5
	+1 m MSL	-1.0	-44.1	-4.3	-18.5
	+2 m MSL	-1.0	-45.8	-1.2	-5.1
	+3 m MSL	-1.0	-44.1	-1.5	-6.7
S13	0 m MSL	-0.2	-8.2	-0.4	-1.7
	+1 m MSL	-0.3	-13.1	0.9	4.1
	+2 m MSL	-0.3	-11.4	1.9	8.2
	+3 m MSL	-0.2	-8.2	1.0	4.3

* Note that profile measurements at station S10 did not extend to 0 m MSL during the May 1965 and April 1967 surveys. The excursion rate at the 0 m MSL contour is therefore extrapolated backwards using newer surveys. It is therefore likely that the total landward excursion of 83.4 m is an over-estimation. It is expected that all contours would have moved landward similar distances, which would mean a landward excursion of approximately 50 m of the 0 m MSL contour at station S10 since May 1965.

Excursion rates at stations S08, S09, S10, S11 and S13 indicate that since October 2005, the higher parts of the beach profiles, the +3 m MSL and +2 m MSL contours, have accreted slightly. However, the lower sections of the beach, the +1 m MSL and 0 m MSL contours, are continuing to erode. The beach is therefore becoming steeper in this area, indicating that shoreline erosion is continuing.

Figure 6-5: Fenced Off Dunes in Front of the Milnerton Golf Club Clubhouse

Erosion at station S12 has accelerated dramatically since October 2005, as shown in Table 6-5 above. This may be caused by flanking erosion resulting from shoreline protection structures (sandbag revetment – see Figure 6-5) at the Milnerton Golf Club clubhouse, and is therefore assumed to be a local effect. This assumption is confirmed by the absence of the accelerated erosion trend at station S13, situated 240 m north of stations S12.

In summary, this section of Table Bay has eroded between 10 m and 50 m since May 1965. This erosion is continuing, although not in the form of overall shoreline erosion, but rather as beach steepening.

6.2.4 Milnerton Golf Course and Sunset Beach

Referring to the fold-out map of Appendix E, this sector includes beach profile stations S14 to S24. Measurements at stations S14, S15, S16 and S22 have been performed since May 1965, whilst measurements at stations S18, S20 and S24 have only commenced in October 2005. Table 6-6 below summarizes the profile excursion rates within this sector.

Profiles measured since May 1965 indicate a trend of erosion in this portion of Table Bay, with the maximum shoreline retreat of approximately 35 m being observed at station S15. Shoreline erosion is significantly reduced at station S22, to approximately 15 m.

Profile stations S14 to S18 are located along the Milnerton Golf Course, whilst profile stations S22 and S24 are located along Sunset Beach. Considering this, it is clear that the shoreline along the Milnerton Golf Course is continuing to erode. Similar to previous observations, the top of the beach in this area (S14 to S18) seems to be relatively stable, with the lower portions of the beach continuing to erode.

Table 6-6: Excursion Rates – Stations S14 to S24

Profile	Contour	May 1965 to February 2010		October 2005 to February 2010	
		Excursion Rate [m/year]	Total Excursion [m]	Excursion Rate [m/year]	Total Excursion [m]
S14	0 m MSL	-0.6	-27.8	-1.6	-6.8
	+1 m MSL	-0.5	-22.9	-0.7	-3.2
	+2 m MSL	-0.4	-19.6	0.1	0.6
	+3 m MSL	-0.4	-18.0	0.2	0.8
S15	0 m MSL	-0.8	-34.3	-1.2	-5.1
	+1 m MSL	-0.8	-34.3	-0.5	-2.4
	+2 m MSL	-0.8	-34.3	0.0	0.0
	+3 m MSL	-0.6	-27.8	-0.3	-1.1
S16	0 m MSL	-0.5	-24.5	-1.8	-7.8
	+1 m MSL	-0.6	-27.8	-0.5	-2.1
	+2 m MSL	-0.6	-27.8	-0.2	-1.0
	+3 m MSL	-0.6	-26.2	-0.8	-3.5
S18	0 m MSL			-2.0	-8.9
	+1 m MSL			-0.2	-0.8
	+2 m MSL			0.1	0.5
	+3 m MSL			-0.3	-1.1
S20	0 m MSL			-2.6	-11.4
	+1 m MSL			-0.5	-2.1
	+2 m MSL			0.9	4.0
	+3 m MSL			-0.2	-1.0
S22	0 m MSL	-0.3	-13.1	-3.5	-15.2
	+1 m MSL	-0.3	-14.7	0.7	2.9
	+2 m MSL	-0.3	-13.1	1.4	6.2
	+3 m MSL	-0.4	-18.0	0.5	2.4
S24	0 m MSL			-0.7	-3.2
	+1 m MSL			-0.1	-0.6
	+2 m MSL			0.8	3.3
	+3 m MSL			0.5	2.4

The same observation can be made for the beaches fronting Sunset Beach (S20 to S22). However, whilst the top of the profiles along the golf course remain stable, the top of the profile along Sunset Beach is actively accreting. Additionally, the erosion rates of the lower portions of the profiles along Sunset Beach are relatively low.

The cause for the accretion and reduced beach steepening along Sunset Beach is likely to be the wide dune field, as well as the good health of the vegetation on the dunes. Wind-blown sand losses along this portion of coastline are expected to be minimal.

It can therefore be summarized that the shoreline along the Milnerton Golf Course is continuing to erode, with beach steepening being observed. The shoreline along Sunset Beach is stable, even accreting slightly. A slight measure of beach steepening can be observed along Sunset Beach.

6.2.5 Sunset Beach to Dolphin Beach

The fourth sector extends from profile station S28 to station S38, a distance of approximately 2 km. Four profile beacons are located along this piece of coastline, with only station S31 being measured since May 1965. Excursion rates are summarized in Table 6-7.

Measurements at station S31 indicate shoreline erosion of approximately 15 m of the upper section of the beach, whilst the 0 m MSL contour has moved backwards 31 m. This therefore indicates the continuation of the beach steepening trend observed further south.

Erosion rates at station S31 since October 2005 have not changed significantly compared to earlier records, indicating that erosional trends remain relatively unchanged since May 1965.

Referring to Table 6-7, it will be noticed that excursion rates observed at station S38 indicate accretion since October 2005, albeit fairly minimal. This relates to the active dune management system currently being implemented by the Dolphin Beach Body Corporate, as shown in Figure 6-6.

Table 6-7: Excursion Rates – Stations S28 to S38

Profile	Contour	May 1965 to February 2010		October 2005 to February 2010	
		Excursion Rate [m/year]	Total Excursion [m]	Excursion Rate [m/year]	Total Excursion [m]
S28	0 m MSL			0.1	0.6
	+1 m MSL			0.2	0.8
	+2 m MSL			-0.6	-2.7
	+3 m MSL			-1.8	-7.9
S31	0 m MSL	-0.7	-31.1	-0.7	-3.0
	+1 m MSL	-0.3	-14.7	-0.4	-1.6
	+2 m MSL	-0.3	-14.7	-0.6	-2.7
	+3 m MSL	-0.4	-16.3	-1.4	-5.9
S35	0 m MSL			-0.3	-1.1
	+1 m MSL			-0.4	-1.9
	+2 m MSL			-0.9	-4.1
	+3 m MSL			-1.5	-6.7
S38	0 m MSL			0.0	0.0
	+1 m MSL			0.4	1.7
	+2 m MSL			0.4	1.9
	+3 m MSL			0.3	1.3

Figure 6-6: Managed Dune Field at Dolphin Beach Hotel

Image: Google Earth (Google Inc., 2010)

6.2.6 Dolphin Beach to Blouberg Rocks

Four profile stations are located between Dolphin Beach and the rock outcrop at the northern end of the Blouberg beachfront, from stations S41 to S44. No data is available for station S43. Measurements at station S41 have been performed since May 1965, whilst stations S38, S42 and S44 have been measured since October 2005.

The Seli One shipwreck is located 500 m directly offshore of profile station S41. Referring to Figure 6-8, it is clear that the shipwreck has had a dramatic impact on local shoreline morphology, with rapid accretion in the order of 15 m having occurred.

It will be remembered that for the previous coastal sectors, excursion rates were given for the periods of May 1965 to February 2010 and from October 2005 to February 2010 respectively. This was done since the profile measurements have been most regularly taken at most profile stations since October 2005, allowing a detailed review of recent excursion rates.

However, since the wreck has had a prolific impact on the shoreline, and only arrived in September 2009, it was decided that for profile station S41, only the data pre- March 2009 was used to analyse the long-term trend. The short-term behaviour was analysed using only the post- March 2009 data. In doing this, the direct

impact of the shipwreck was investigated. It is noted that for stations S42 and S44, the categorization as used previously has been maintained.

Figure 6-7: Profile Excursions (May 1965 to March 2009)

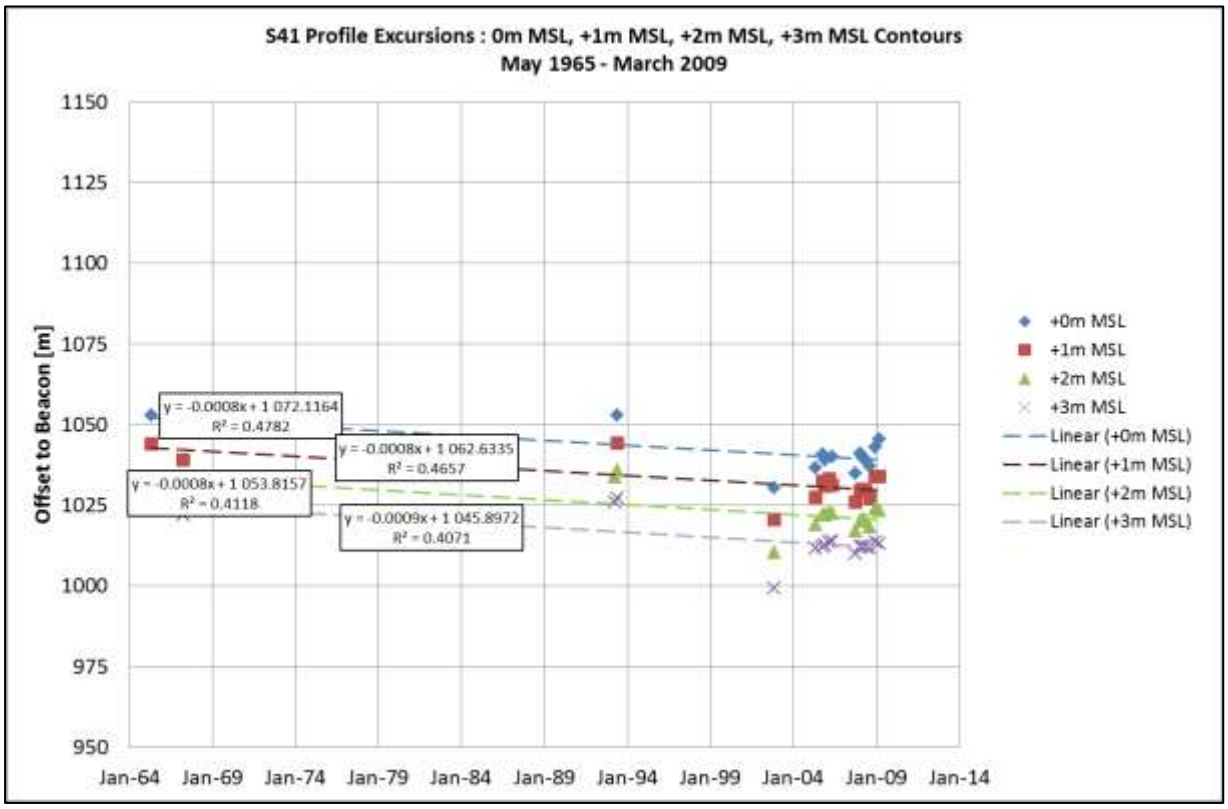

Figure 6-8: Profile Excursions – March 2009 to February 2010

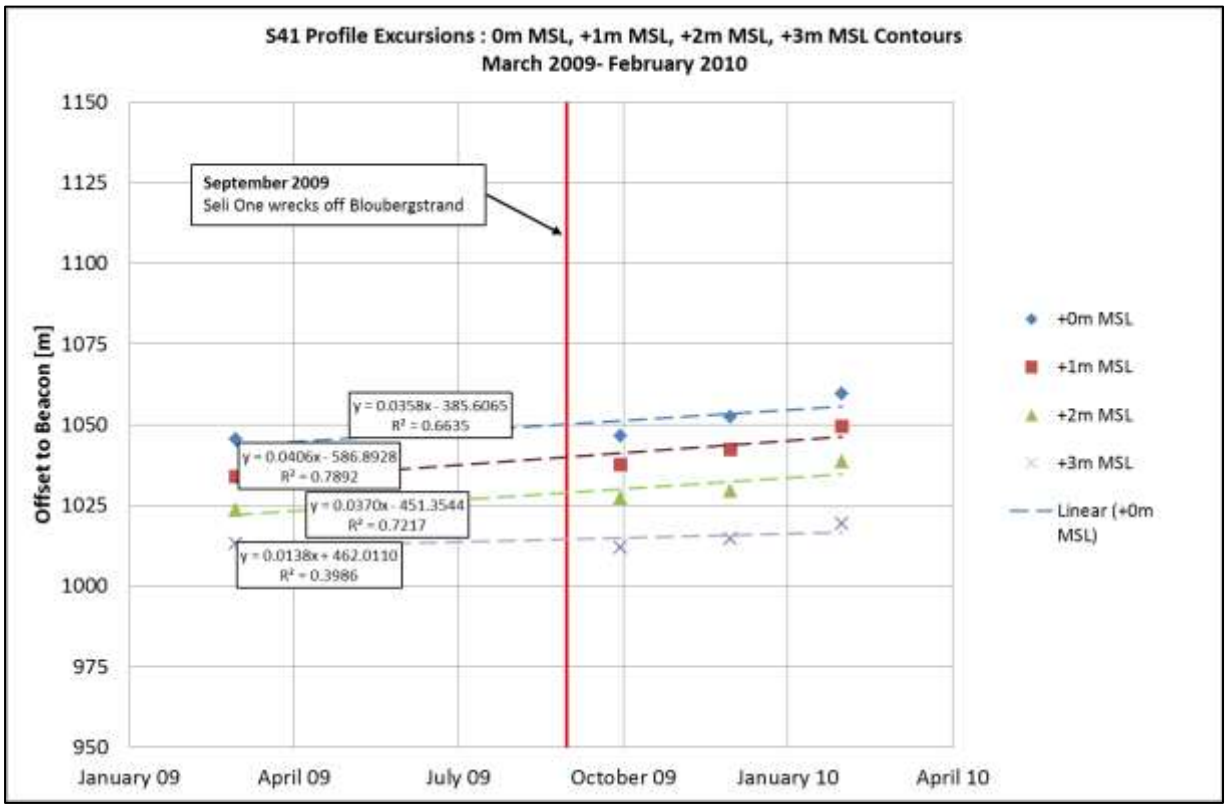

Figure 6-7 and Figure 6-8 represent the shoreline excursions at station S41 pre- and post- September 2009. From these plots, the impact of the wreck on the beach morphology becomes very visible. Referring to Table 6-8, before the wreck, the shoreline trend at station S41 was one of erosion, with the average rate of shoreline retreat being 0.3 m/year between 0 m MSL and +3 m MSL contours. Following the arrival of the wreck, this rate has reversed entirely, with the lower three contours having accreted at a rate of greater than 13 m/year.

Table 6-8: Excursion Rates – Station S41

Profile	Contour	May 1965 to March 2009		March 2009 to February 2010	
		Excursion Rate [m/year]	Total Excursion [m]	Excursion Rate [m/year]	Total Excursion [m]
S41	0 m MSL	-0.3	-12.8	13.1	12.1
	+1 m MSL	-0.3	-12.8	14.8	13.7
	+2 m MSL	-0.3	-12.8	13.5	12.5
	+3 m MSL	-0.3	-14.4	5.0	4.7

In addition to this, it is also clear that although the +3 mMSL is accreting, it is doing so at a much slower rate than the lower contours. This therefore indicates that significant beach flattening is taking place since the arrival of the shipwreck.

Table 6-9 indicates that the beach at profile stations S42 and S44 have remained stable since October 2005, suggesting that the dramatic accretion at station S41 is a local effect, due to the arrival of the Seli One shipwreck.

Table 6-9: Excursion Rates – Stations S42 and S44

Profile	Contour	May 1965 to October 2005		October 2005 to February 2010	
		Excursion Rate [m/year]	Total Excursion [m]	Excursion Rate [m/year]	Total Excursion [m]
S42	0 m MSL			0.1	0.5
	+1 m MSL			0.0	0.2
	+2 m MSL			-0.1	-0.5
	+3 m MSL			-0.2	-0.8
S44	0 m MSL			0.7	3.2
	+1 m MSL			0.4	1.9
	+2 m MSL			-1.2	-5.2
	+3 m MSL			-0.2	-0.8

6.2.7 Summary of Beach Profile Measurement Findings

Results of the beach profile measurements are summarized in Table 6-10 below. This table should be read by referring to the fold-out map of Appendix E.

From this table, it becomes clear that each area of Table Bay has undergone fairly significant erosion since the commencement of the beach survey campaign in May 1965. Erosion is most severe in the southern parts of Table Bay, especially along the Woodbridge Island coastline, where erosion has been observed to be as high as 55 m. In addition to this, it has been observed that, in general, the trend of erosion is continuing, albeit in the form of beach steepening compared to an overall landward movement of the entire cross-shore profile.

Table 6-10: Summary of Beach Profile Measurement Observations (1965 to 2010)

Sector	Long-Term Trend		Short-Term Trend
	Total Excursion	Rate of Excursion [m/year]	
Port of Cape Town to Diep River Mouth	Erosion: 30 m to 45 m	-0.7 to -1.0	Recent stabilization of upper profile Beach steepening continuing
Woodbridge Island and Milnerton Golf Club Clubhouse	Erosion: 25 m to 55 m	-0.5 to -1.0	Recent accretion of upper profile Beach steepening continuing
Milnerton Golf Course and Sunset Beach	Erosion: 20 m to 35 m	-0.3 to -0.8	Recent accretion of upper profile Beach steepening continuing
Sunset Beach to Dolphin Beach	Erosion: 15 m to 30 m	-0.3 to -0.7	Continued erosion Northern end of sector is stable
Dolphin Beach to Blouberg Rocks	Erosion: 10 m to 15 m	-0.3	Erosion of upper profile Accretion of lower profile i.e. beach flattening

6.3 Analysis of Aerial Photography

6.3.1 Analysis Methodology

6.3.1.1 Image Rectification

To enable the identification of historic shoreline trends, aerial images were rectified and imported into a GIS package. The rectification was performed by identifying fixed points with known coordinates on each of the images, performing a linear rectification process to geo-reference the images.

The older images, dating back to 1968, are not of sufficient resolution to be accurately rectified. It is estimated that the accuracy of the rectification is in the order of +-15 m, although this could be greater on the edges of the images. This means that shoreline excursions could not be quantified from aerial images in terms of exact distances.

Nevertheless, the photographs provided a useful tool to confirm, in an order of magnitude sense, the observations made from the beach profile analysis presented in Section 6.2, results of which are summarized in Table 6-10.

6.3.1.2 Wetted Line and Vegetation Line

The wetted line is defined as the boundary between wet and dry sand, where the wet sand can be identified as being slightly darker than the dry sand. The level at which this boundary occurs is dependent on tidal and wave run-up levels, and will therefore vary depending on the time at which the photograph was taken. It should however be considered that the sand below the high water mark remains fairly wet, even when the tide recedes. It is therefore thought that the position of the wetted line is approximately equal to the average wave run-up level during high tide, and remains fairly constant throughout the tidal cycle.

The vegetation line is defined as the seaward boundary of the vegetation along the coast. This line is therefore independent of tidal levels, and is more constant over time compared to the wetted line. Generally speaking,

the vegetation line is situated at the base of the primary dune, which has been assumed to be situated at a constant level of +3 m MSL along the entire Table Bay coastline. This assumption has been informed by analysing the cross-sectional shape of the beach profile measurements, discussed in the previous sections. Generally speaking, the gradient of the cross-sections flattens out below the +3 m MSL contour, indicating that this is the approximate location of the primary dune foot. This is illustrated graphically in Figure 6-9 below.

Figure 6-9: Profile Station S20 – Cross-Sections Indicating Flattening below +3 m MSL (May 1965 to February 2010)

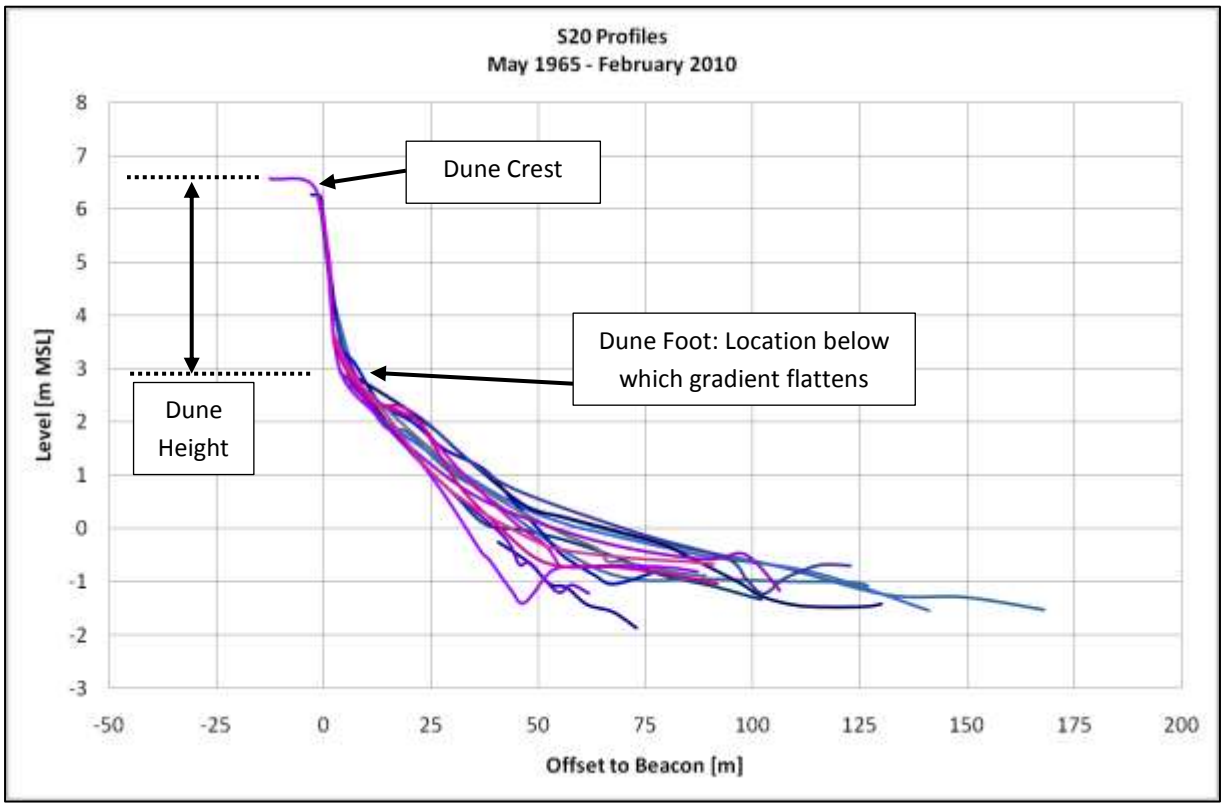

Considering the difficulties related to identifying the wetted line, it was decided to investigate the excursions of the vegetation line rather than the wetted line, and compare these movements to beach profile measurements. Referring to Figure 6-10, it is clear that it is virtually impossible to identify the boundary between wet and dry sand. However, the vegetation line can be clearly seen.

To verify the shoreline excursions observed by the beach profile measurements covered in Section 6.2, the excursions of the vegetation lines are analysed. A direct comparison of these two excursions can then be made, since the vegetation line is considered to be located at approximately the +3 m MSL depth contour.

For ease of reference, the analysis of the aerial photography was split into the same five coastal sectors as was done previously. The reader is referred to the fold-out map of these sectors, given in Appendix E.

Figure 6-10: Aerial Image of Woodbridge Island before Development in 1968

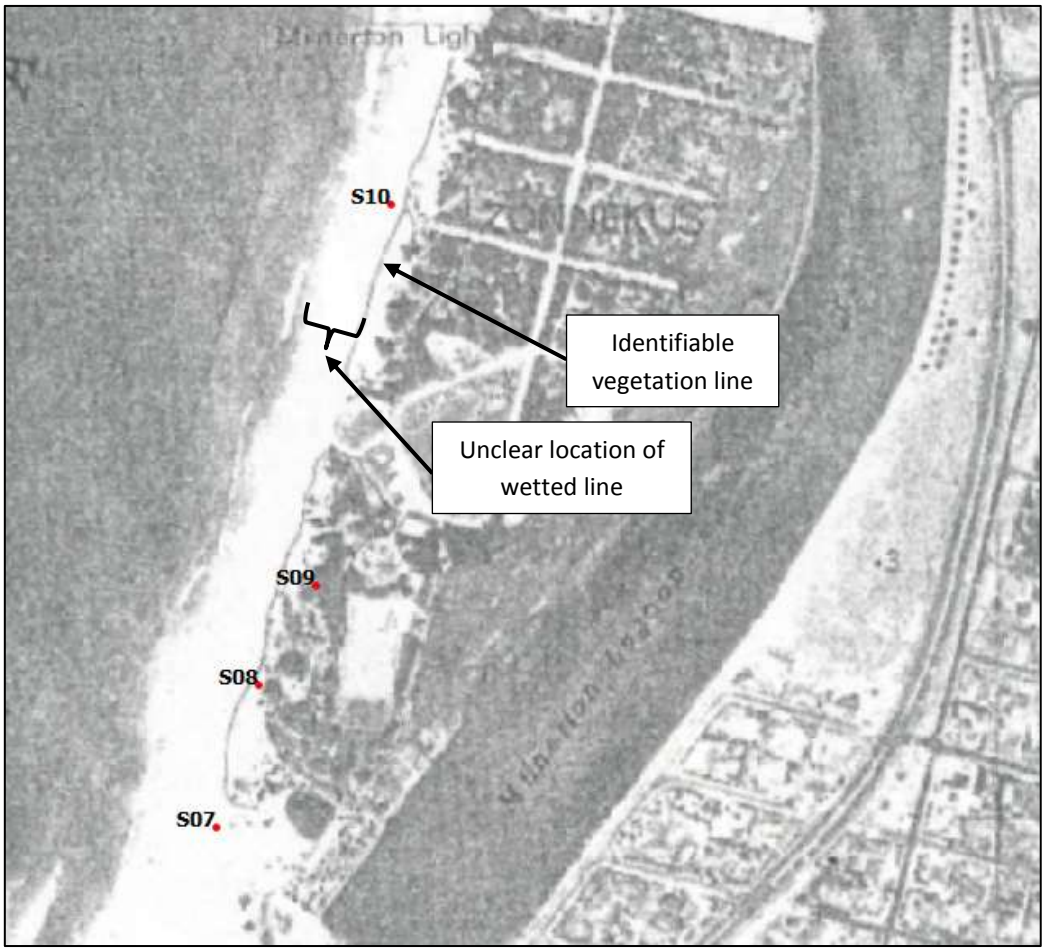

6.3.2 Port of Cape Town to Diep River Mouth

Figure 6-11 and Figure 6-12 show the vegetation lines between the Port of Cape Town and the Diep River mouth. Comparing these figures, it can be observed that the southern and central parts of this sector were historically sandy beaches. Furthermore, it can be seen that, with the construction of the concrete dolos revetment, the shoreline has been pushed seaward a distance of between 30 m and 50 m.

Between the northern end of the revetment and the Diep River mouth, beach profiles have indicated shoreline erosion of the +3 m MSL contour of between 30 m and 45 m. Comparing this to the excursion of the vegetation line in this area, given in Figure 6-13, a good correlation can be identified. This indicates that beach profile measurements accurately represent the historical shoreline behaviour at this location.

Figure 6-11: Vegetation Lines between the Port of Cape Town and the Diep River Mouth (Image 1968)

Figure 6-12: Vegetation Lines Between the Port of Cape Town and the Diep River Mouth (Image 2008)

Figure 6-13: Vegetation Line Excursions at Profile Station S06

6.3.3 Woodbridge Island and Milnerton Golf Course Clubhouse

Figure 6-14 and Figure 6-15 show the vegetation lines to the south and north of the Milnerton Golf Club clubhouse respectively. The landward movement of the vegetation line south of the clubhouse is in the order of 20 m to 30 m. This is reduced north of profile station S12 (which is situated 180 m north of the clubhouse), where the erosion is in the order of 10 m.

A further observation is the significant landward movement of the vegetation line between 1972 and 1977. Although the shoreline erosion continues between 1977 and 1987, the rate at which this occurs seems to be reduced compared to the previous period. Very little movement is observed after 1987.

Referring to Table 6-5, the profile excursions calculated from beach profile measurements has shown shoreline erosion between 25 m and 50 m at the +3 m MSL contour south of the clubhouse, whilst erosion has been determined to reduce to between 10 m and 15 m to the north of profile station S12.

A discrepancy between the observations between the beach profile measurements and aerial photography exists south of the Milnerton Golf Club clubhouse. However, this does not indicate incorrect data. The severe shoreline erosion occurring along the Woodbridge Island coastline has resulted in the formation of a dune scarp, as shown in Figure 5-8. Due to the steepness of this scarp, the vegetation line is no longer situated at the dune foot, but rather at the dune crest. This too can be observed in Figure 5-8.

It is thought that once the vegetation line moves from the dune foot to the dune crest across a dune scarp, the horizontal movement of the vegetation line is significantly reduced compared to the movement of the beach profile. This is because dune management projects, such as the initiatives being undertaken along the Woodbridge Island coastline, limit the landward movement of the dune vegetation.

As such, it is thought that once the vegetation line migrates to the top of the dune, it essentially stalls, whilst the erosion of the lower beach profile continues. This differential movement could therefore explain the discrepancy between excursions of the +3 m MSL contour as obtained from the beach profile measurements, compared to the excursion of the vegetation line, as obtained from aerial photography.

If one were to assume that the vegetation line is situated on the dune crest, assuming a dune crest elevation of +8 m MSL (based on beach profile measurements at profile station S10), the reduced erosion of the vegetation line indicates that beach steepening is occurring. This can be said since the lower portion of the cross-section is eroding faster than the upper sections of the profile.

The observation made during the beach profile analysis that the beach in this area is steepening due to on-going shoreline erosion is therefore confirmed by aerial photography. In addition, the accuracy and validity of beach profile measurements is confirmed.

Figure 6-14: Vegetation Line South of Milnerton Golf Club Clubhouse

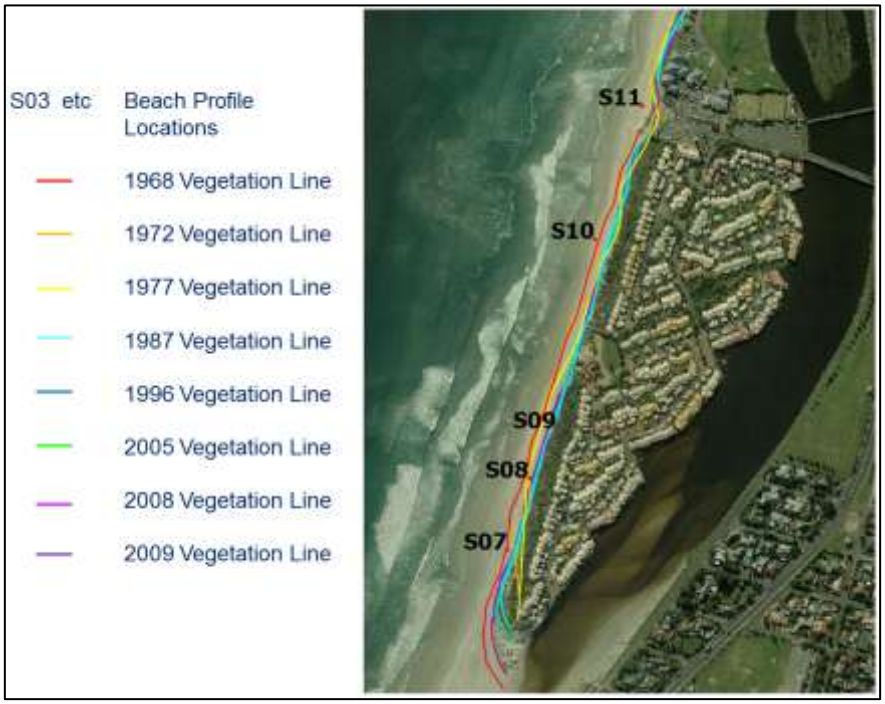

Figure 6-15: Vegetation Line North of Milnerton Golf Club Clubhouse

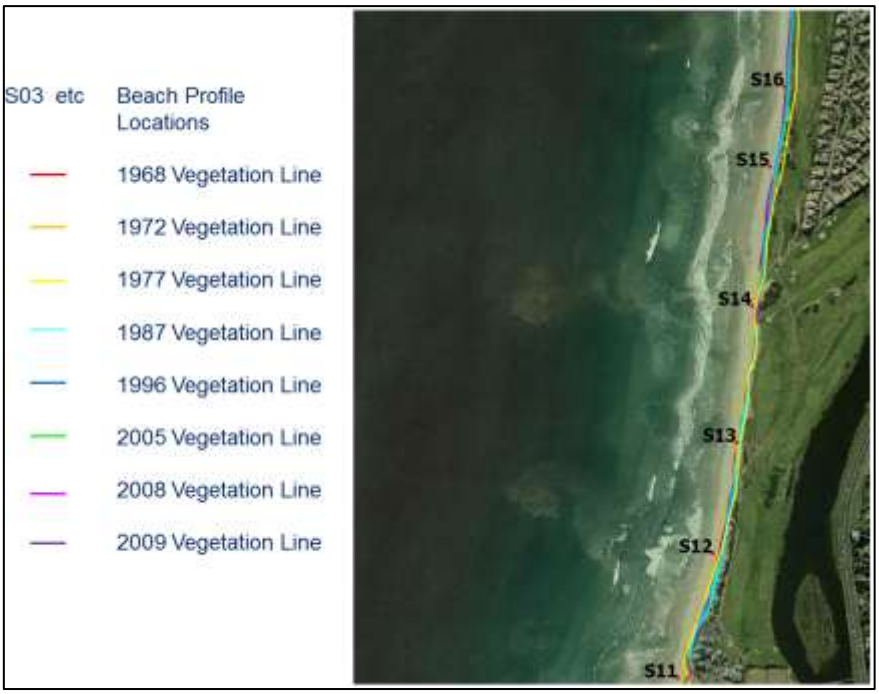

6.3.4 Milnerton Golf Course and Sunset Beach

The vegetation line along the Milnerton Golf Course and Sunset Beach indicates erosion to the order of approximately 10 m since 1977. This is compared to erosion of between 15 m and 25 m of the upper portions of the beach profiles (stations S14 to S24), determined from beach profile measurements, discussed in Section 5.4.3. Considering the level of accuracy of the aerial photographs, being within approximately 15 m, it is considered that the aerial images confirm, in an order of magnitude sense, observations made by the analysis of beach profile measurements in this sector.

6.3.5 Sunset Beach to Dolphin Beach

As shown in Figure 6-16, a significant seaward movement of the vegetation line is observed in the sector between Sunset Beach and Dolphin beach between 1977 and 1987, especially in the area where the Dolphin Beach Hotel is currently situated (near profile station S38 - see fold-out map of Appendix C). However, it is thought that this area has been artificially vegetated to stabilize the dune field in front of the hotel, to perform the dual function of both stabilizing the shoreline, as well as limiting the volumes of wind-blown sand entering the hotel area.

The seaward movement of the vegetation line does not necessarily indicate shoreline accretion, since it is likely that the artificially vegetated area was already at current levels, but was simply vegetated to ensure shoreline stability. However, since profile measurements at stations S35 and S38 have not been performed pre- 2005, this assumption remains unconfirmed.

Figure 6-16: Vegetation Lines Between Sunset Beach and Dolphin Beach

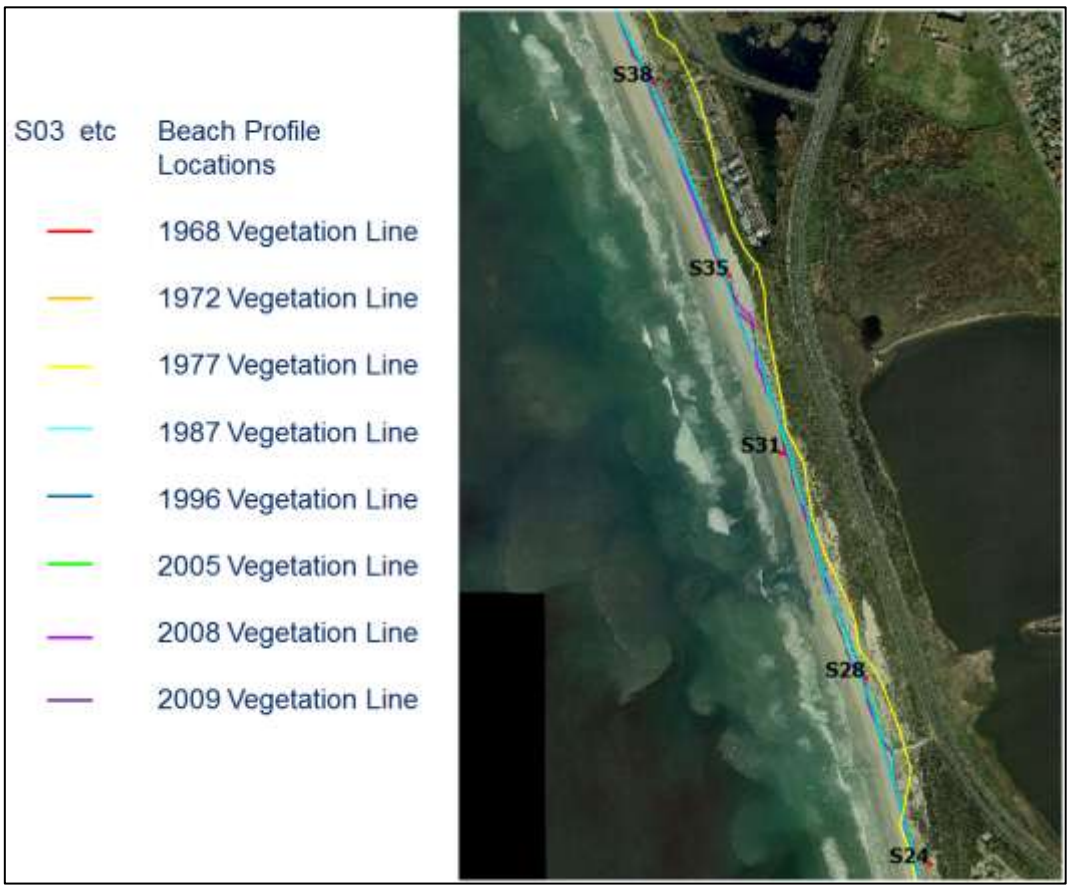

6.3.6 Dolphin Beach to Blouberg Rocks

As mentioned in the previous paragraph, a seaward migration of the vegetation line between 1977 and 1987 is noticed in the southern half of this sector, relating to the development of the Dolphin Beach Hotel, as well as the area between the intersection of Blouberg Road and Otto du Plessis Drive (see arrow in Figure 6-17) and the hotel. The vegetation line in the northern half of this sector has remained fairly stable, with an approximate variation of within 10 m being observed. This is compared to the shoreline erosion of approximately 15 m observed from beach profile measurements.

Similar to previous observations, the shoreline erosion in this area has resulted in the formation of a dune scarp, shown in Figure 6-18. From this figure it can also be seen that, due to the steep dune face, the vegetation line does not extend to the dune foot, but is located near the dune crest. It can therefore be said that the reduced excursion of the vegetation line compared to the +3 m MSL contour obtained from the beach profile measurements is caused by the elevated position of the vegetation line. This also leads to the conclusion that beach steepening is taking place, since the lower portion of the cross-section is moving landward faster than the upper sections of the beach.

Figure 6-17: Vegetation Lines Between Dolphin Beach and Blouberg Rocks

Figure 6-18: Dune Scarp along the Blouberg Beachfront (3rd July 2011)

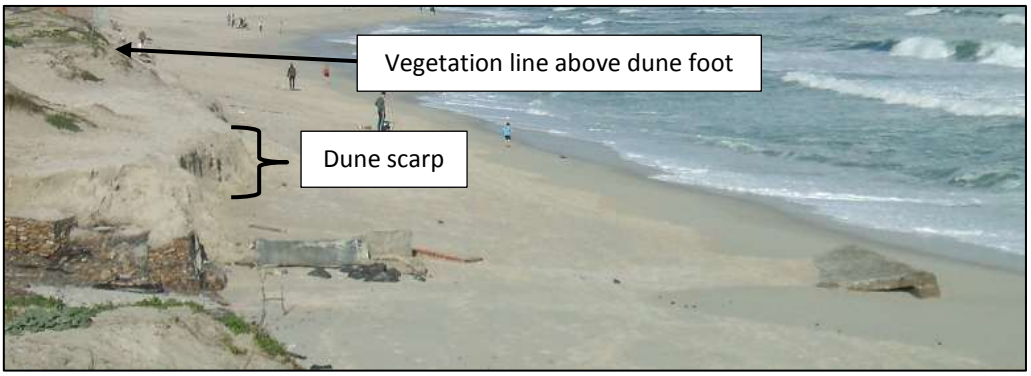

A review of aerial photographs has therefore confirmed, albeit in an order of magnitude sense, observations made from beach profile measurements along the Blouberg beachfront.

6.4 Summary and Conclusions

Beach profile measurements have been performed along the Table Bay coastline since the mid 1960's, with the most regular survey data being collected since 2005 and the most recent survey being performed in February 2010.

This data has been used to perform a shoreline stability analysis along the Table Bay coastline, determining the shoreline excursions since the mid-1960s. The results of this have shown that the Table Bay shoreline is eroding, with erosion being the most severe in the Woodbridge Island area, where erosion has been calculated to be between 30 m and 50 m since the mid-1960s. In addition to this, it has been discussed that, although the implementation of shoreline stabilization measures in the southern areas of Table Bay have reduced the rate of shoreline recession along the upper sections of the beaches, the underlying trend of coastal erosion is on-going, through the steepening of beach profiles. The shoreline in the northern areas of Table Bay has eroded to a lesser degree than in the south, in the order of between 10 m and 20 m. These results are graphically presented in Figure 6-19 below.

A beach profile station situated in the lee of the shipwreck has indicated that, since the arrival of the wreck in September 2009, approximately 15 m of shoreline accretion has been observed. It is noted that this survey, taken in February 2010, does not necessarily include the total extent of the final beach salient. In addition, from aerial photographs it is observed that shoreline erosion is occurring to the north of the vessel.

Observations and conclusions drawn from beach profile measurements have been validated using aerial photography of Table Bay.

Figure 6-19: Shoreline Erosion in Table Bay (May 1965 to February 2010)

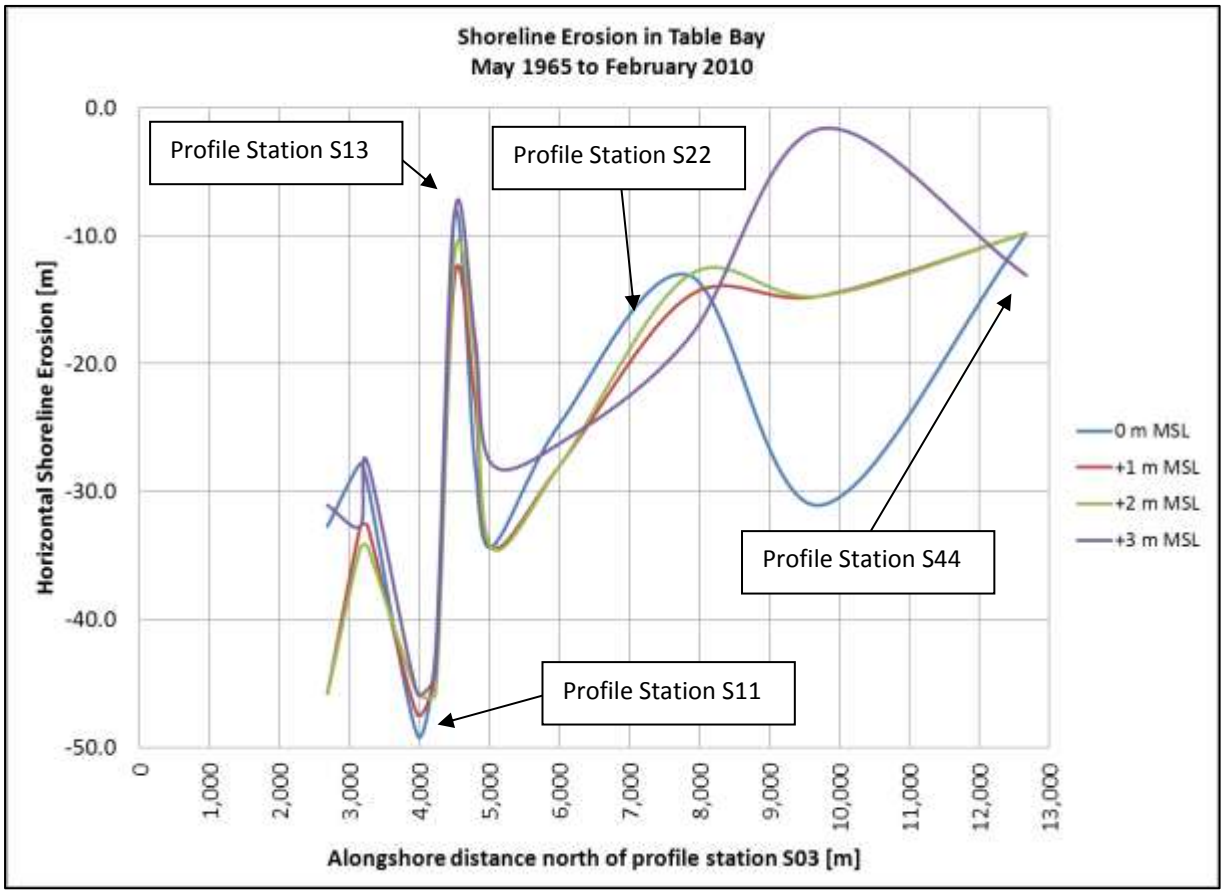

7. TABLE BAY SEDIMENT TRANSPORT SYSTEM

7.1 Introduction

As introduced previously, the Seli One shipwreck is located in the northern half of Table Bay. To be able to accurately analyse and simulate the impacts of the wreck on the sediment transport dynamics of the Blouberg beachfront, a sound understanding of the greater Table Bay sediment transport system is required. The understanding of this sediment transport system is based on observations of the beach profile measurements and aerial photography, discussed in Section 6.2 and 6.3 respectively.

The following sections describe the more pertinent aspects of this system.

7.2 Sediment Sources and Sinks

To analyse the Table Bay sediment transport system, all possible sediment sources and sinks have to be accurately identified and quantified. The following components were considered to be the dominant aspects of the Table Bay sediment transport system:

- Sediment transport in or out of Table Bay at the southern end of the bay, i.e. at the Port of Cape Town
- Sediment transport in or out of Table Bay at the northern end of the bay, i.e. at the Blouberg rock headland
- Fluvial sources and sinks (Salt- and Diep River)
- Wind-blown sediment sources and sinks
- Cross-shore sediment sources and sinks

The southern and northern ends referred to in the list above are shown on the fold-out map of Appendix E, with the southern end being the southern boundary to the “Port of Cape Town to Diep River Mouth” sector, and the northern end being the northern boundary of the “Dolphin Beach to Blouberg Rocks” sector.

It is noted that this initial discussion of sources and sinks does not include the sediment transport in or out of Table Bay at the northern end of the bay. It also does not include the potential sources and sinks resulting from cross-shore processes. This was done since both of these were quantified based on the results of a detailed sediment budget calculation. As such, these two components of the Table Bay sediment transport system are covered after the discussion of the sediment budget calculations.

7.2.1 Sediment Transport at Southern End of Table Bay

Following (CSIR, 2003), sediment travelling into or out of Table Bay was assumed to be minor, and therefore negligible. This was substantiated by the following arguments:

- The coastline to the south of the Port of Cape Town is predominantly rocky. There is therefore no significant sediment source available for northerly transport (CSIR, 2003).
- Bottom surveys extending 2.5 km offshore off Green Point indicate a largely rocky seafloor, with only limited sediment deposits visible. This indicates a limited sand supply from deeper waters (CSIR, 2003).
- If a significant sediment source was available to be transport into Table Bay, this sand would either accumulate to the west of the main breakwater of the Port of Cape Town, or be deposited in the

port's entrance channel. Neither of these two phenomena are evident from the surveys, thereby indicating the lack of offshore sediment sources feeding Table Bay (CSIR, 2003).

7.2.2 Fluvial Sources and Sinks

It was estimated that the Diep River discharges approximately 41 000 m^3 (bulk volume) of sediment into Table Bay annually (CSIR, 2003). However, the majority of this sediment consists of eroded Malmesbury shale, yielding very fine sediment. This portion of sediment is therefore lost to the system, as it is carried to deep water by the river current, waves and ocean currents. Since only the coarse fraction is likely to settle within the littoral zone, it was estimated that only approximately 5 000 m^3/year is added to the longshore sediment transport system from the Diep River discharges (CSIR, 2003).

Considering the extensive infrastructure development within the Diep River catchment, it is likely that the sediment load in the river has been reduced over time. However, this reduction in sediment load is thought to be relatively small, and has therefore not been included in the current study.

The Salt River run-off is significantly less than that of the Diep River (CSIR, 2003). Correspondingly, the sediment discharge of this river is equally insignificant, and was therefore not considered.

As mentioned previously, the Woodbridge Island development was constructed in the late 1980's. This included the dredging of approximately 30 000 m^3 of sand deposits within the river delta (CSIR, 2003). It can be argued that this volume of sand would have eventually been added to the Table Bay longshore sediment transport system. As such, the removal of this volume was considered to be a once-off removal of 30 000 m^3 sand from the system, during the late 1980's / early 1990's.

7.2.3 Wind-Blown Sediment Sources and Sinks

The predominant wind direction in the Cape Town area is south to south-east. This wind direction has the potential to transport sand from the Cape Flats area into the southern parts of Table Bay.

However, as discussed in HKS (1992), there is little evidence of sufficient sediment sources in the Cape Flats area which could be transported by south-easterly winds. Furthermore, it is clear from historical maps that the Cape Flats area was not devoid of vegetation, which would have limited the magnitude of wind-blown sand transport across this area (HKS, 1992). It is therefore unlikely that historically, a significant amount of sediment was added to the longshore sediment transport system through wind-blown sediment transport from the Cape Flats area, and that this has not changed recently.

As will be shown in later sections of this report, during the summer, autumn and spring months, the predominant wind direction is south to south-east, whilst during the winter months, the south-easterly and westerly winds are more or less balanced. During the summer, autumn and spring months, the south and south-easterly breezes are significantly stronger than winds from other directions, whilst in winter, the strongest winds have a north-westerly direction.

Referring to the fold-out map of Appendix E, a strong southerly or westerly wind may be able to remove sand from the northern part of Table Bay, blowing it landward and out of the longshore sediment transport system. This phenomenon has been experienced first-hand by the author on numerous occasions, as shown in Figure 7-1. This photograph shows sand accumulating on the landward side of the coastal road running along the Blouberg beachfront, taken on 29th March 2012.

Figure 7-1: Evidence of Wind-Blown Sand Loss Along Blouberg Beachfront

In addition to this, numerous wind "blow-outs" can be observed from aerial photographs along the northern half of Table Bay. These blow-outs are created when fine sediment is picked up from the beach face and is blown onto the dune. This sand then settles on the dune due to the obstruction of the dune vegetation. Over time, the dune vegetation is covered by sand, as can be seen in Figure 7-2.

Blow-outs are useful in identifying in which areas sediment is being lost due to wind. Along Table Bay, blow-outs occur in the northern part of the bay, indicating that sediment is being lost along this piece of coast.

Figure 7-2: Wind "Blow-Out" in northern Table Bay

It has been estimated that prior to man-made influences, this sediment sink could have been in the order of 10 000m^3/year (CSIR, 2003). However, the primary dune field in this area has since been vegetated and stabilized, reducing the wind-blown sediment transport capacity. For purposes of this study, it has been estimated that the annual wind-blown onshore sand losses along the Blouberg beachfront are in the order of 5 000m^3/year.

7.3 Sediment Characteristics in the Longshore Zone

7.3.1 Table Bay Grain Size Distribution

A detailed analysis of beach sediment along the Table Bay beaches was performed by John Rogers of the Department of Geological Sciences of the University of Cape Town (Rogers, 2006). Beach sediments were sampled at ten locations, coinciding with existing beach profile stations, discussed previously. Referring to the fold-out map of Appendix C, these locations are:

- S03, S05, S06, S07, S12, S16, S22, S31, S41, S44

Additional samples were taken north of the Blouberg headland, at the following locations (see fold-out map of Appendix D):

- N21, N18, N13, N07, N02

Samples were taken at three levels along the beach at each of the 15 locations, one below the waterline, one at the waterline and one above the waterline. The result of this investigation yielded the following curve of grain size between the Port of Cape Town and Melkbosstrand. The gap in the curves represents the rock headland at Blouberg.

Figure 7-3: Grain Size North of the Port of Cape Town

Based on (Rogers, 2006)

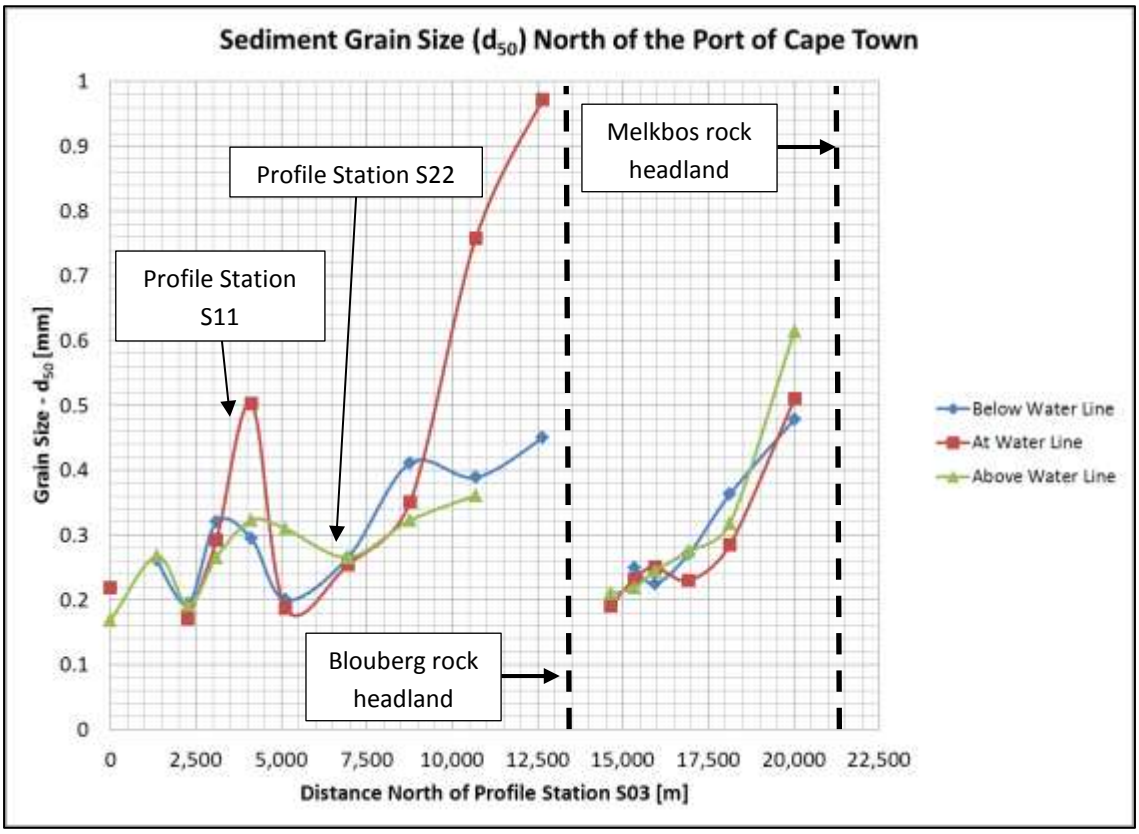

This figure indicates a clear coarsening trend of the median grain size (d_{50}) from the southern to the northern end of Table Bay, with the d_{50} of around 0.2 mm near the Port of Cape Town increasing to approximately 0.5 mm south of the Blouberg rock headland. It is further visible that immediately south of the Blouberg rock

headland, the d_{50} at the water line spikes to approximately 1 mm, which may be an outlier in the measurements.

Figure 7-3 also clearly identifies a discontinuity in the d_{50} between the southern and northern side of the Blouberg rock headland. On the southern side, the d_{50} is approximately 0.5 mm whilst immediately north of the headland the d_{50} reduces to approximately 0.2 mm. Northwards of the headland, a coarsening trend is once again observed, with the d_{50} increasing from 0.2 mm to 0.5 mm between the Blouberg and Melkbos headlands respectively.

An additional study was performed by Soltau (2009) to investigate the cross-shore distribution of sediment grain diameters within the longshore transport zone. During this study, six sets of grab samples were taken along four lines (Figure 7-4) at varying depths within the littoral zone in an attempt to identify any grain size trends. The result of this analysis is shown in Table 7-1.

Figure 7-4: Sediment Sampling Locations in Table Bay (Soltau, 2009)

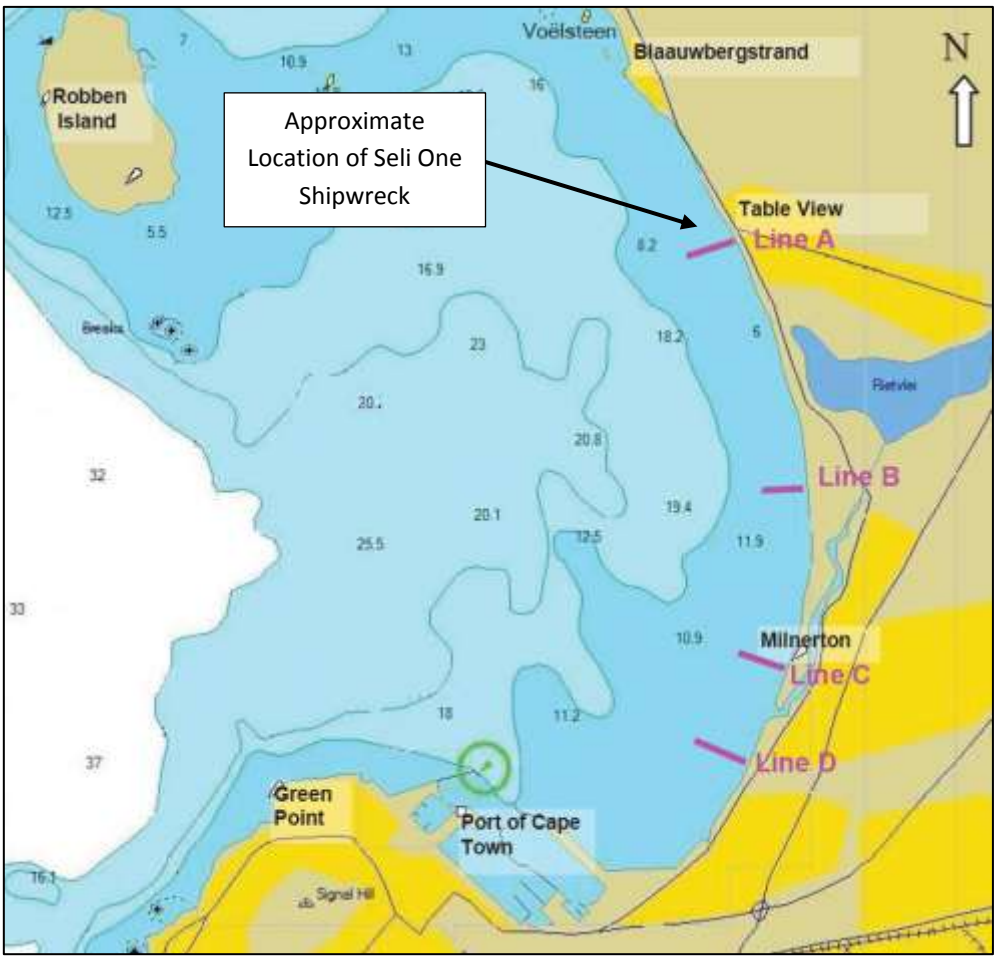

Table 7-1 and Figure 7-5 make reference to the following description of the sampling locations (Soltau, 2009):

Mid-Tide	A location approximately midway between high- and low tide
Inner-surf	A location approximately midway between the offshore boundary of the breaker zone and the mid-tide position
Trough	Landward of the offshore boundary of the breaker zone
Bar	Along the offshore breaker zone boundary
Nearshore	Seaward of the offshore breaker zone boundary

Table 7-1: Grain Sizes (D_{50} [mm]) in the Longshore Transport Zone in Table Bay (Soltau, 2009)

Cross-Shore Location	Line A	Line B	Line C	Line D
Mid-Tide	0.469	0.273	0.175	0.155
Inner-surf	0.175	0.253	0.171	0.159
Trough	0.177	0.186	0.179	0.173
Bar	0.157	0.162	0.172	-
Nearshore	0.145	0.156	0.170	0.165
Average of Longshore Transport Zone	**0.225**	**0.206**	**0.173**	**0.163**

Figure 7-5: Indication of Typical cross-Shore Sampling Locations

Based on (Soltau, 2009)

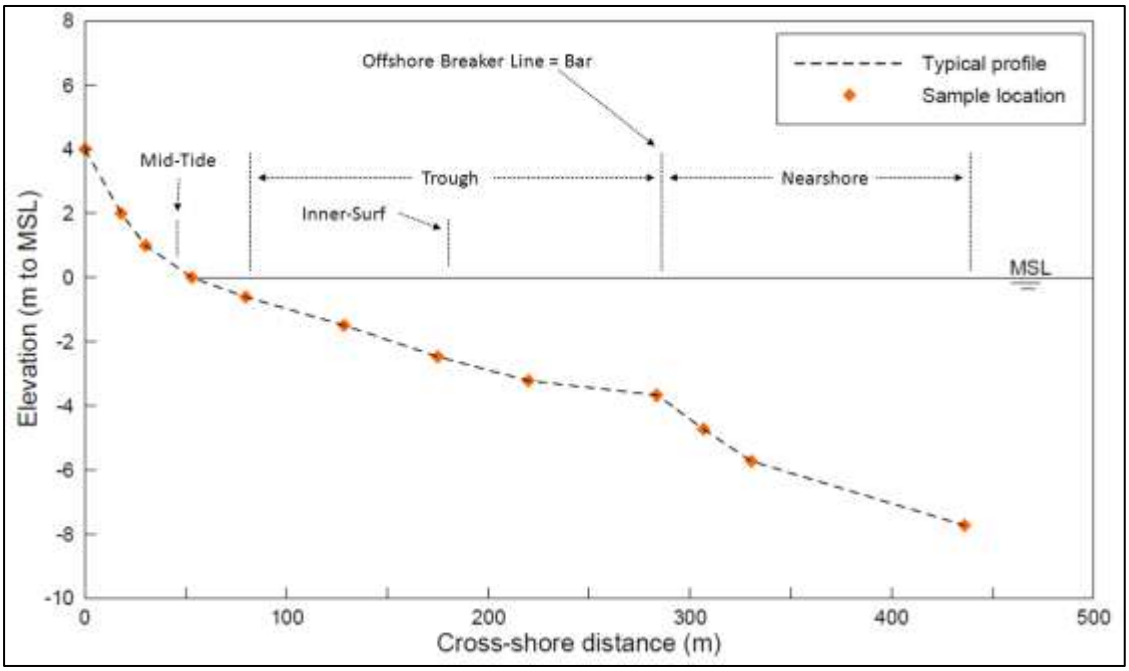

If the median grain sizes of the mid-tide area of Soltau (2009) are compared to the samples of Rogers (2006), a strong correlation can be observed. Whilst the earlier study determined a coarsening from 0.2 mm at the port to 0.45 mm at the Blouberg rock headland, Soltau (2009) identifies this coarsening to range from 0.155 mm to 0.469 mm.

However, referring to Table 7-1, if one were to analyse the median grain diameters of the lower portions of the cross-shore profile, excluding the mid-tide zone, no clear alongshore grain size trend can be identified. The coarsening of the grain size of the average longshore transport zone is therefore a function of the coarsening of the mid-tide zone only.

This leads to the conclusion that although a grain coarsening of beach sediment can be observed from south to north in Table Bay, this trend does not extend across the entire cross-shore profile and can therefore not be seen as representative of the entire littoral zone.

Referring to Figure 7-3, since the grain size on the beach face does not necessarily represent the entire cross-shore profile, the discontinuity on the upper beach observed between the southern and northern end of the Blouberg headland does not necessarily indicate a discontinuity across the entire profile. This does therefore not necessarily indicate a discontinuity in the longshore sediment transport between the southern and northern end of the Blouberg headland.

7.3.2 Cause for Beach Sediment Coarsening

The cause for the coarsening of the grain diameter along the upper beach from south to north in Table Bay is likely to be the increase in wave energy from the south to the north of Table Bay. The increased turbulence of the larger waves results in finer sediment to be washed away in the north, whereas in the south, the finer sediment portion remains on the beach.

This wave energy gradient is caused by the reduced sheltering effect of the Green Point headland in the north compared to in the south of Table Bay. This is shown graphically in Figure 7-6, which is an output of the wave transformation simulations performed specifically for the current study. This shows clearly an increase in significant wave height from approximately 1.0 m in the south to approximately 1.4 m in the north.

Figure 7-6: Increase in Wave Energy in the north of Table Bay

(Boundary Wave: H_{mo}=4m, Dir=220°, T_p=12s)

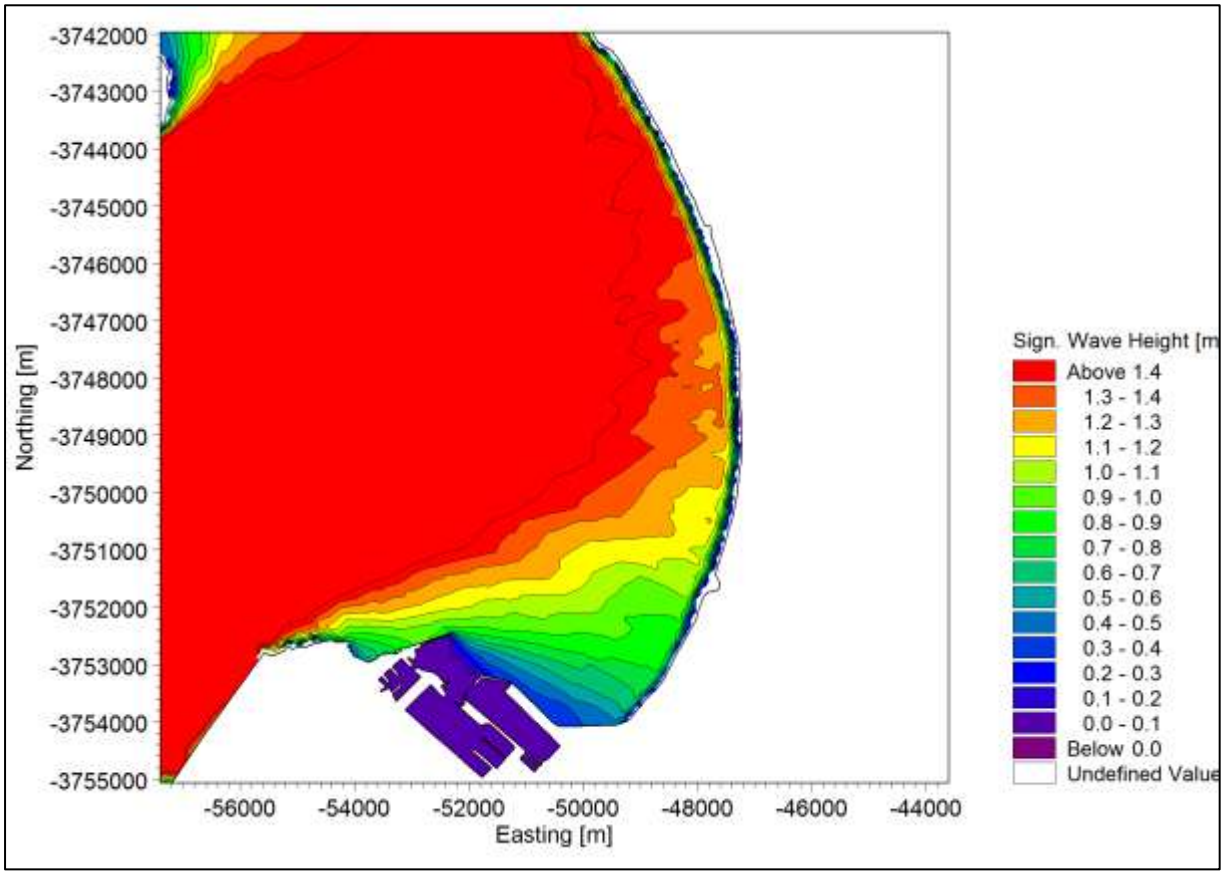

7.4 Table Bay Sediment Budget

7.4.1 Introduction

To enable the determination of the longshore sediment transport capacity at the northern end of Table Bay, as well as the determination of potential cross-shore sediment losses, a detailed sediment budget calculation is required. It has been shown that no sediment is able to enter or exit Table Bay at the southern end of the bay. Therefore, if there is a net loss of sediment from the bay, this sand has to exit the bay either via longshore transport north out of the bay, or via cross-shore transport to deeper water or by onshore wind-blown sand losses. If, for example, the system shows zero net sediment movement, i.e. no sediment is lost out of Table Bay over time, the sum of all sources and sinks have to equate to zero.

The beach profile measurements covered in Section 6.2 are used to perform a beach volume analysis, to determine the volumes of sand moving in or out of Table Bay.

It is clear that beach profile measurements, which generally extend to the 0 m MSL contour, do not extend to the depth of closure, and therefore do not incorporate the entire littoral zone. Beach surveys by themselves are therefore insufficient to determine the net longshore transport rates. Through implementation of numerical modelling software, it was possible to determine the distribution of longshore sediment transport along the cross-shore profile, and to accurately identify the depth of closure along Table Bay. Using this depth, together with assumptions relating the behaviour of the profile below 0 m MSL (which is not surveyed during beach profile measurements) to the behaviour of the profile above 0 m MSL, the volume of sediment moving in or out of the bay was calculated.

7.4.2 Depth of Closure Determination

To be able to perform a sediment budget calculation, the extent of the active littoral zone needs to be identified. The lower boundary of the active littoral zone, the depth of closure, is determined by using Equation 3.24 (USACE, 2006a), discussed during the literature review(repeated here for ease of reference). To determine the variability of this parameter along Table Bay, the depth of closure was calculated at 500 m alongshore intervals, using wave climates extracted from the wave transformation model described in Appendix A. Wave climates were extracted at the -10 m MSL depth contour, as shown in Figure 7-7.

$$h_c = 2.28H_e - 68.5\left(\frac{{H_e}^2}{g{T_e}^2}\right) \qquad \text{Equation 3-24}$$

Where

H_e Effective significant wave height, which is exceeded only 12 hours per year

T_e Effective peak period, which is exceeded only 12 hours per year

Figure 7-7: Wave Climates Extracted at 500 m Alongshore Intervals at -10 m MSL Depth Contour

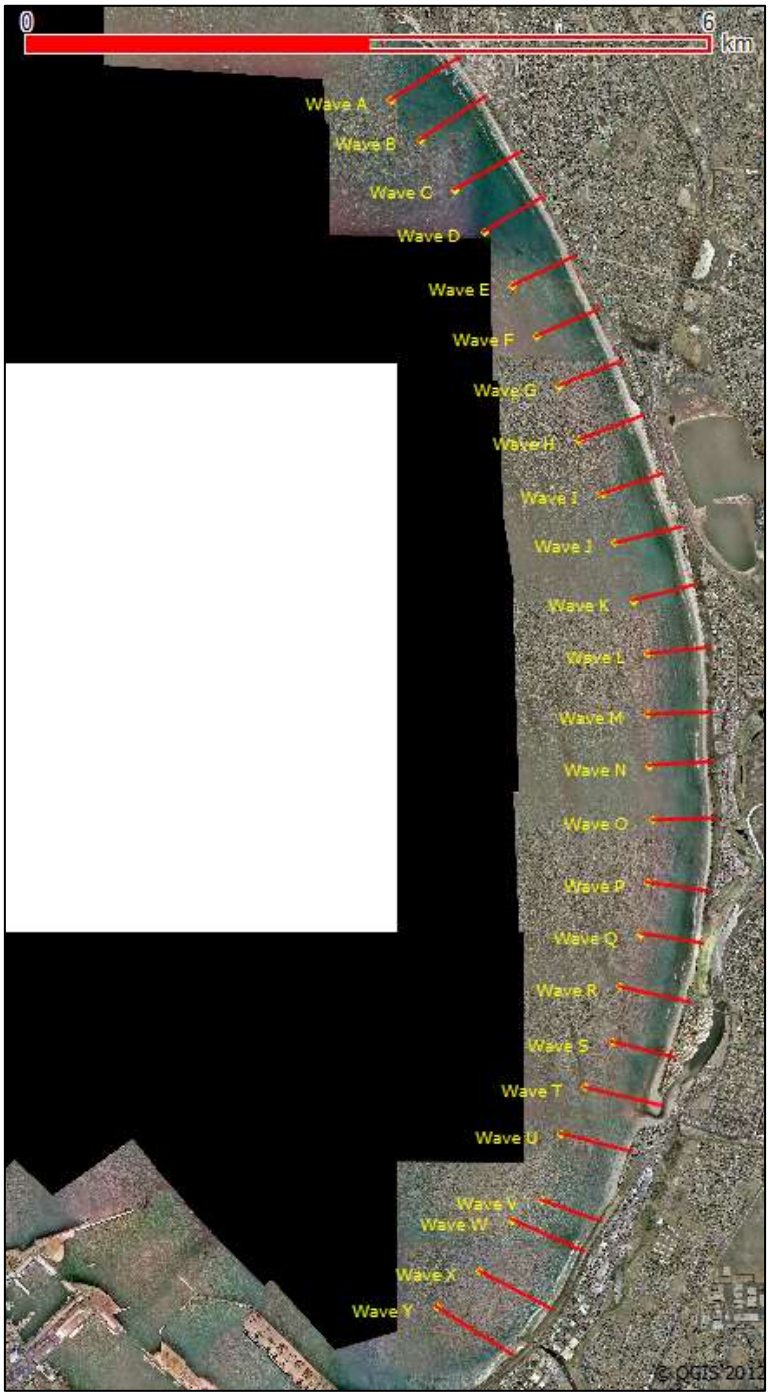

Results of this analysis are given in Table 7-2 below, which are graphically presented in Figure 7-8.

Table 7-2: Effective Wave Height, Effective Wave Period and Depth of Closure along Table Bay

Wave Station	H_e [m]	T_e [m]	Depth of Closure [m MSL]
A	2.92	16.28	-6.44
B	2.99	16.31	-6.57
C	2.93	16.29	-6.45
D	2.98	16.38	-6.57
E	2.93	16.40	-6.47
F	2.91	16.40	-6.42
G	2.88	16.44	-6.36
H	2.88	16.48	-6.36
I	2.78	16.52	-6.13
J	2.83	16.59	-6.24
K	2.79	16.65	-6.16
L	2.72	16.70	-6.02
M	2.78	16.82	-6.15
N	2.75	16.89	-6.09
O	2.76	17.00	-6.11
P	2.69	17.09	-5.95
Q	2.58	17.19	-5.72
R	2.64	17.24	-5.85
S	2.53	17.31	-5.62
T	2.43	17.40	-5.39
U	2.23	17.42	-4.97
V	2.09	17.51	-4.66
W	2.15	17.59	-4.79
X	1.99	17.71	-4.45
Y	1.80	17.80	-4.03

From Figure 7-8, the interdependency of the depth of closure and the effective wave height becomes evident; the larger the wave height, the deeper the depth of closure. In the southern parts of Table Bay, the wave heights remain relatively small due to the sheltering effect of the Green Point headland. Because of this, the depth of closure remains relatively shallow, above -5 m MSL in the southern 2.5 km of the bay. With increasing wave heights, the depth of closure increases to approximately -6.5 m MSL along the Blouberg beachfront.

Figure 7-8: Depth of Closure and Effective Wave Height along Table Bay

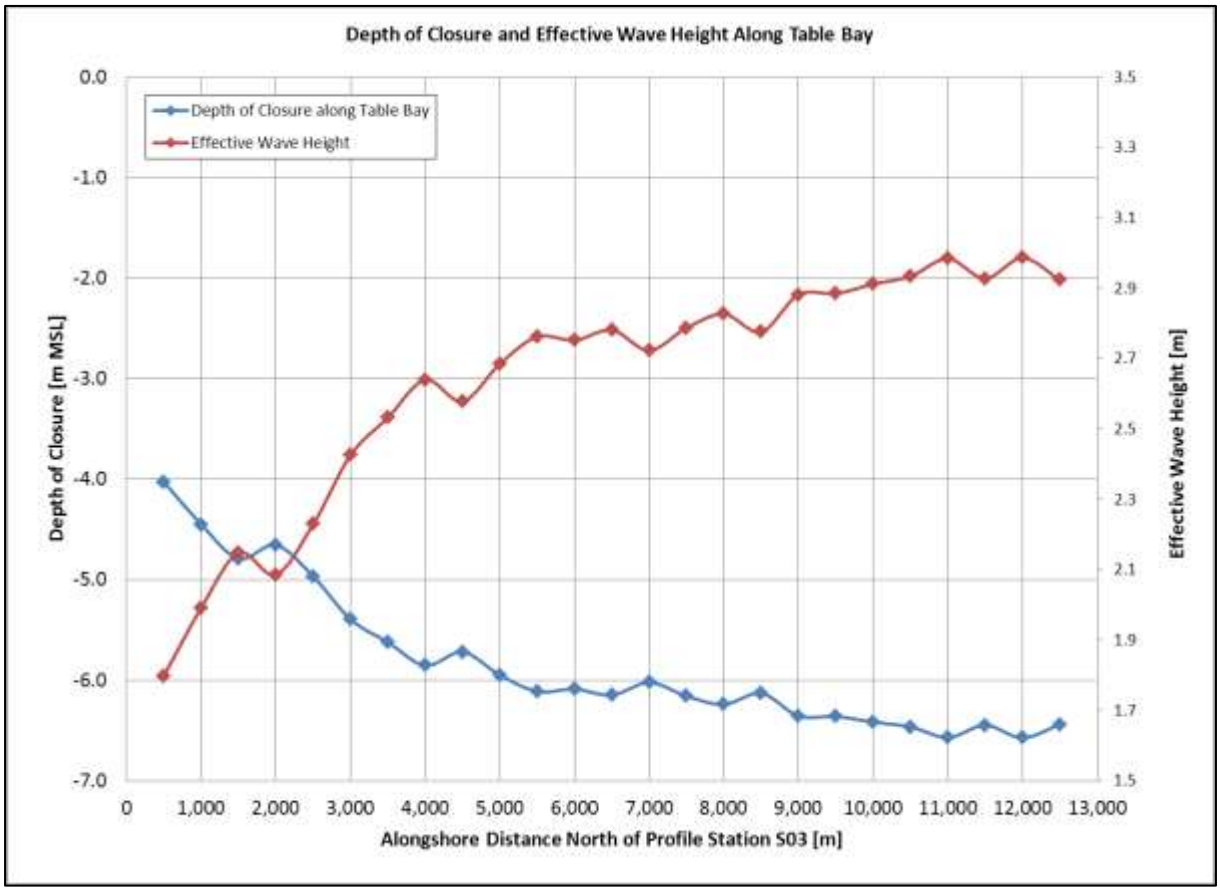

7.4.3 Calculation of Beach Volume Gains and Losses

As mentioned previously, beach profile measurements were used to perform a beach volume analysis. This was done by analysing the movement of various depth contours between the first beach surveys performed in May 1965 to the measurements performed in October 2005. The latter date was chosen as this was used as the end of the shoreline model calibration period, with the period between October 2005 and February 2010 used as validation period. This will however be discussed in more detail in later sections of this report.

Generally, when shorelines erode they do so only up to the depth of closure since no net longshore transport occurs below this depth (see Section 3.3.1.4). This is schematically shown in Figure 7-9. The extent of profile erosion, i.e. the magnitude of the landward excursion, reduces with increased depth, up to the depth of closure where the erosion is equal to zero.

As pointed out previously, the Table Bay beach profile measurements do not extend to the depth of closure, but only to approximately 0 m MSL. The time-based behaviour of the lower part of the active littoral zone is therefore not explicitly available. Since the majority of longshore sediment transport occurs below the water line and can therefore not be excluded from a beach volume analysis, certain assumptions have to be made to incorporate this volume into the analysis.

Figure 7-9: Schematic of Original and Typical Eroded Shoreline

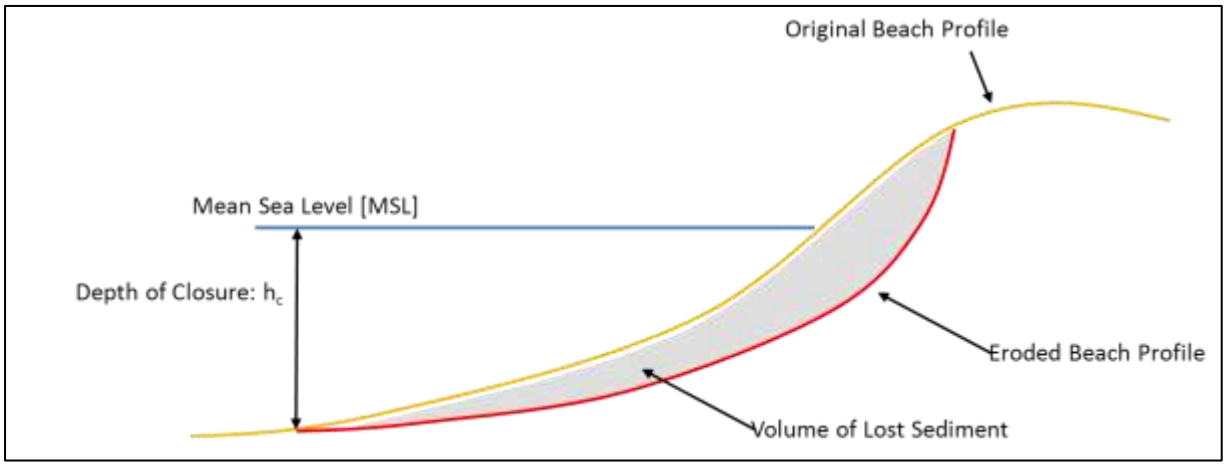

The first method which can be used to determine the total volume of sediment lost from a cross-section is to shift the entire profile based on the landward excursion of the upper profile. The assumption here is that the slope near the depth of closure is near horizontal, meaning that a landward movement of this position does not result in a vertical variation of the seabed. This concept is shown in Figure 7-10. Here, the original beach profile is shifted landward, maintaining the vertical position. No sediment is lost below the depth of closure, since the seabed slope is near horizontal at that location. Comparing Figure 7-9 and Figure 7-10, it can be argued that this method provides a relatively accurate approximation of the total volume of sediment lost from a cross-section, based on the observed shoreline excursions of the upper cross-section.

Figure 7-10: Schematic of Method to Determine Sediment Loss on Lower Cross-Shore Profile

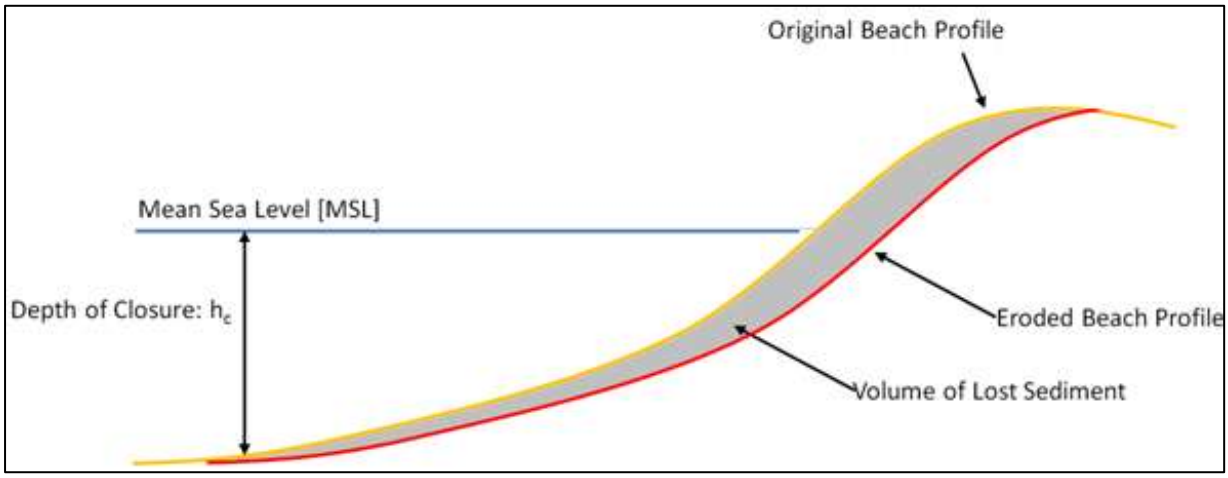

However, applying this method in reality is not necessarily as accurate as the schematics would indicate. Figure 7-11 shows this method applied to profile station S11. The blue line, which shows the recent cross-shore profile, was generated using a combination of the beach profile measurements performed in October 2005, as well as the offshore bathymetry measured during an offshore bathymetric survey performed in October 2006. Based on historic profile measurements discussed in Section 6.2, the shoreline in this area has eroded approximately 45 m since May 1965. To obtain an approximation of the cross-shore profile for May 1965, the modern profile was shifted seaward by 45 m (red line).

Figure 7-11: Profile Station S11 – Recent and Shifted Cross-Shore Profile

Eroded Profile in October 2005 (measured) and Original Profile in 1965 (shifted)

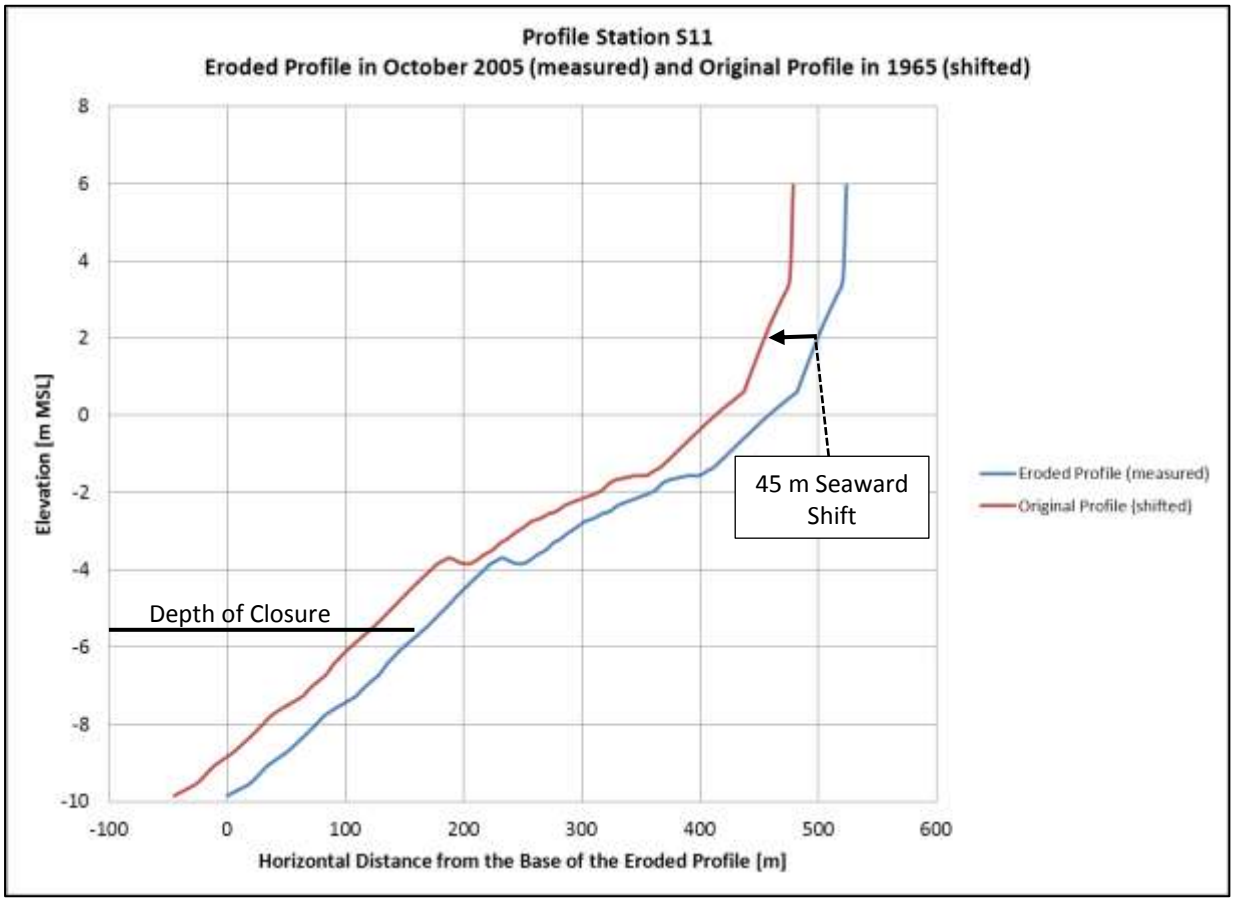

The depth of closure at profile stations S11 is approximately -5.6 m MSL (Table 7-2 - wave station S). From the figure above, it is clear that, due to the fact that the seabed slope at the depth of closure is not near horizontal, this method would not result in the accurate determination of the volume of sediment lost from this cross-section. The method of shifting the recent profile based on observed shoreline excursions above the water line would result in a significant overestimation of the volume of sediment lost from the cross-shore profile. This method could therefore not be used to estimate the total volume of sediment lost from the Table Bay littoral zone.

An alternative method was therefore developed for the current study. As shown in Table 7-3, the depth contours between +3 m MSL and 0 m MSL were analysed at 0.25 m intervals. The distance between the depth contour and the profile beacon during the May 1965 and October 2005 surveys were then compared to determine a depth contour excursion. Note that a negative excursion denotes shoreline erosion. This distance was then multiplied by 0.25 m, being the vertical interval between the contours, to determine the net area lost or gained within this vertical domain. These areas were then summed to determine the total volume of sand gained or lost from the beach profile between 0 m MSL and +3 m MSL between the two survey dates.

The assumption with regards to the profile between 0 m MSL and the depth of closure is that this area accretes or erodes in the same way as the 0 m MSL contour, i.e. the excursion of the 0 m MSL contour is multiplied by the depth of closure. This is clearly an overestimation of the volume of sediment that is lost from the lower cross-shore profile, since it has been established that the seabed at the depth of closure does not move.

Table 7-3: Station S11 Beach Volume Analysis

Depth Contour [m MSL]	Distance from Profile Beacon to Depth Contour [m]		Depth Contour Excursion [m]	Gain / Loss of Beach Volume [m^3/m]
	May 1965	October 2005		
3	1031.3	989.3	-42.1	-10.5
2.75	1035.7	991.0	-44.7	-11.2
2.5	1040.0	993.7	-46.3	-11.6
2.25	1042.8	999.1	-43.7	-10.9
2	1045.6	1003.5	-42.0	-10.5
1.75	1048.3	1007.8	-40.5	-10.1
1.5	1051.7	1010.8	-40.9	-10.2
1.25	1055.8	1014.3	-41.5	-10.4
1	1060.0	1017.8	-42.2	-10.6
0.75	1066.3	1021.4	-44.8	-11.2
0.5	1072.5	1026.0	-46.5	-11.6
0.25	1078.8	1030.6	-48.2	-12.0
0	1085.3	1038.5	-46.8	-11.7
-5.6	*N/A*	*N/A*	*-46.8*	*-262.1*
Total gain / loss of beach volume above 0 m MSL [m^3/m]				-142.6
Total gain / loss of beach volume below 0 m MSL [m^3/m]				*-262.1*
TOTAL GAIN / LOSS OF BEACH VOLUME [m^3/m]				**-404.7**

* Items in italics are extrapolated from the 0 m MSL contour to the depth of closure

This overestimation is compensated for by the exclusion of the volume of sediment that is lost above the +3 m MSL contour. Referring to Figure 7-12, which shows the measured beach profile at station S11 in May 1965 and October 2005, it is clear that significant volumes of sediment has been lost above the +3 m MSL contour. It is postulated that this excluded volume is approximately equal to the overestimated volume of the lower cross-section.

It is estimated that the method discussed above is accurate to within approximately 5% of the real volume of sediment lost from the Table Bay littoral zone. This estimate is based on a trial calculation at profile station S15. Here, it was assumed that the erosion of the profile between 0 m MSL and the depth of closure tapers off linearly. The volume of sediment having been lost above the +3 m MSL contour has been included to provide a more accurate estimate.

Using the method of over-estimating the losses below 0 m MSL and compensating for this by excluding the volume above +3 m MSL, an average loss of 1 637 m^3/year was calculated for profile station S15. Using the method of assuming that the erosion between 0 m MSL and the depth of closure tapers off linear and including the losses above +3 m MSL, an average loss of 1 564 m^3/year was determined for profile station S15. These two values are within approximately 5% of each other.

It is recommended that additional surveys be performed, extending from the depth of closure to landward of the primary dune, to verify the above-mentioned calculation method.

The calculation procedure discussed during the preceding paragraphs was performed at each of the beach profile stations which have been surveyed since May 1965, results of which are summarized in Table 7-4. These calculations indicate that between May 1965 and October 2005, approximately 1.6 million m^3 of

sediment has been lost from the Table Bay littoral zone. Note that the accreted volume at profile station S05 has not been included in this calculation. This accretion was caused by the construction of the concrete dolos revetment and corresponding land reclamation works performed during the development of the Port of Cape Town, and was therefore not caused by any long-term longshore processes.

If the sediment loss of 1.6 million m^3 is averaged evenly over the interval between the two survey dates, 48 230 m^3 of sediment has been lost from the littoral zone annually since May 1965.

Figure 7-12: Station S11 Beach Volume Analysis

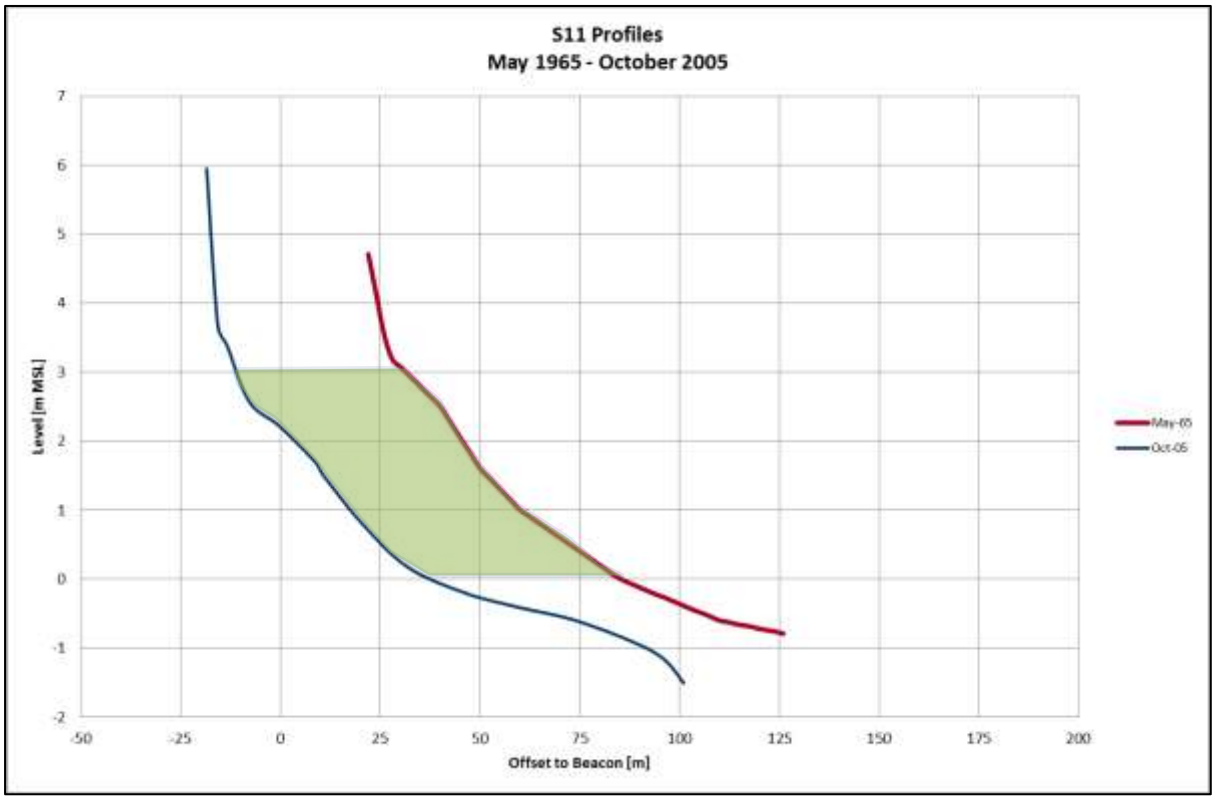

Table 7-4: Table Bay Beach Volume Analysis

Profile Station	Gain / Loss of Beach Volume [m^3/m]	Applicable Alongshore Length [m]	Gain / Loss of Beach Volume for Alongshore Length [m^3]	Annual average gain / loss of beach volume for alongshore length [m^3/year]
S05	42.7	1 805	77 074	1 736
S06	-291.8	879	-256 492	-6 339
S07	-363.6	472	-171 619	-4 240
S08	-318.8	103	-32 836	-812
S09	34.6	200	6 920	171
S10	-646.9	268	-173 369	-4 281
S11	-404.7	243	-98 342	-2 399
S12	-212.3	260	-55 198	-1 364
S13	-212.3	275	-58 383	-1 445
S14	-225.6	290	-65 424	-1 616
S15	-288.5	230	-66 355	-1 637
S16	-190.3	1 001	-190 490	-4 711
S22	-147.0	1 826	-268 422	-6 637
S31	-117.3	1 875	-219 938	-5 436
S41	-102.9	2 942	-302 732	-7 482
TOTALS		**12 667**		**-48 230**

7.4.4 Table Bay Net Longshore Transport

The next task is to convert the average annual beach volume losses for each of the coastal sectors given in Table 7-4 into an annual average longshore sediment transport rate along the Table Bay coastline.

As discussed in Section 3.3.2, it was assumed that cross-shore sediment transport is in equilibrium over a long period of time. This leads to the assumption that the 1.6 million m^3 loss of sediment from the Table Bay littoral system occurs via longshore transport. The net transport direction is northwards, from the Port of Cape Town towards the rock outcrop at Blouberg Rocks. This is substantiated by the fact that the shoreline south of the Port of Cape Town is predominantly rocky, and is therefore not fed by a southern longshore transport direction. In addition to this, considering the dominant wave direction in the southern part of Table Bay, it is not possible for sediment to exit the bay past the Port of Cape Town and the Green Point headland in a southerly direction.

This means that the southern end of Table Bay is the southern boundary of a closed littoral cell, with no sediment entering or leaving Table Bay at this location, i.e. the net longshore transport is equal to zero.

The transport volumes shown in Table 7-4 are the volumes gained or lost within each of the longshore sectors along Table Bay, not considering the movement of sediment in adjacent sectors. To determine the net longshore transport rates, these volumes were accumulated from the southern to northern end of Table Bay, taking into account that the net transport rate at the southern end of the bay, taken to be profile station S03, is equal to zero.

Table 7-5: Calculated Table Bay Longshore Transport Rates

Sector	Annual average gain / loss of beach volume for sector [m^3/year]	Sediment Source or Sink [m^3/year]	Net longshore transport rate [m^3/year]
S03 to S06	-6 339	0	6 339
S06 to S07	-4 240	5 000	15 579
S07 to S08	-812	0	16 392
S08 to S09	171	0	16 221
S09 to S10	-4 281	0	20 502
S10 to S11	-2 399	0	22 901
S11 to S12	-1 364	0	24 265
S12 to S13	-1 445	0	25 710
S13 to S14	-1 616	0	27 326
S14 to S15	-1 637	0	28 964
S15 to S16	-4 711	0	33 675
S16 to S22	-6 637	0	40 312
S22 to S31	-5 436	0	45 748
S31 to S41	-7 482	-5 000	48 230

Figure 7-13: Sediment Budget Calculations in Sector S06 to S07

Figure 7-13 shows a schematic of the sediment budget calculation performed for the coastal sector from profile station S06 to station S07. The volume lost from the sector S03 to S06 is 6 339 m^3/year, and functions as a source for the cell currently under discussion. In addition, sediment discharged from the Diep River is added to this cell as a fluvial source. Finally, according to the beach volume analysis introduced in Section 7.4.3, 4 240 m^3/year of sediment is lost along the shoreline between profile station S06 and S07. Due to the net northern longshore transport direction at profile station S06, the net transport rate at station S06, the fluvial source of the Diep River and the volume of sediment lost along this coastal stretch are added together to determine the net transport rate at station S07, equalling 15 579 m^3/year.

The wind-blown sediment loss along the Table View beaches was included in the final sector, as shown in Figure 7-14. Since this is a loss of sediment, the net northern transport rate past station S41 was reduced by 5 000 m^3/year.

Figure 7-14 shows the net northern longshore transport rate along Table Bay. On this figure it is clear that in the south of the bay, the net longshore transport is equal to zero, gradually increasing to almost 50 000 m^3/year at the northern boundary of the bay.

Figure 7-14: Table Bay Net Longshore Sediment Transport Regime

7.4.5 Evaluation of Net Longshore Transport Rate and Direction

Longshore sediment transport calculations generally require a fair amount of engineering judgement. As such, it is useful to take a step back following the detailed beach volume analysis, and to evaluate the results discussed above in a more regional sense.

In summary, it has been determined that, to satisfy beach profile measurements, a net volume of approximately 50 000m^3 of sediment has to exit Table Bay annually. It has further been argued that these losses occur as a longshore process, rather than a cross-shore process, and that the longshore transport direction is northwards. This means that approximately 48 000 m^3/year of sediment is transported northwards past the rock outcrop at Blouberg, which is shown in Figure 7-15.

Figure 7-15: Blouberg Rock Headland at Northern End of Table Bay

The question that arises now is whether it is possible for this volume of sediment to move past this rock outcrop, considering the rocky shoreline and the two detached rock outcrops, as shown in Figure 7-15. To evaluate this, numerous aspects of the littoral transport system are evaluated, summarized in the following paragraphs.

Referring to Section 7.3, it has been pointed out that a discontinuity in sediment characteristics exists between the southern and northern side of the Blouberg rock outcrop, with the sediment north of the outcrop being significantly finer than the sediment to the south. At first, this would therefore suggest that sediment does not bypass the rock outcrop, and that it represents the boundary to the littoral cell.

However, it has also been discussed that if the sediment above the mid-tide zone is excluded from the sediment grain size analysis, no trends with regards to coarsening from south to north of Table Bay can be identified. The discontinuity in sediment grading above the mid-tide zone between the south and north of the rocky headland at Blouberg does therefore not necessarily indicate a discontinuity in longshore transport, since the grain characteristics below the mid-tide zone could be similar on either side of the headland.

Furthermore, it has been determined that the net longshore transport direction immediately north of the Blouberg rock outcrop is northwards. This has been determined by performing an additional LITDRIFT simulation, at the position shown in Figure 7-16 below. It is also interesting to note the angle between the beach and the wave north of the rock outcrop, resulting in a northern longshore transport at the time the photograph was taken.

Figure 7-16: Location of LITDRFIT Simulation North of Blouberg Rock Outcrop

If sand was not bypassing the rocky headland, shoreline erosion would take place along the beaches immediately north of the headland. Since this is not happening, it can be concluded that sand has to move from the southern to the northern side of the headland.

Nevertheless, the transport capacity past the Blouberg rock outcrop should be confirmed and quantified using a coupled two-dimensional hydrodynamic, wave and sediment transport model. During the current study, it has been assumed that the transport volumes suggested in Table 7-5 are accurate.

7.5 Summary and Conclusions

To summarize and conclude this section, a detailed investigation of the Table Bay sediment transport system was performed, including an analysis of all possible sediment sources and sinks in and out of the bay. This has shown that the southern end of Table Bay, which is essentially the Port of Cape Town, is the southern boundary of a closed littoral cell. This means that no sediment is able to enter or exit the bay at this location. In addition, it has been discussed that the Diep River discharges approximately 5 000 m^3/year of sediment into the bay, whilst the same volume is estimated to exit the bay along the Blouberg beach front via aeolian transport. This transport is thought to occur mostly during the summer months, when strong south-easterly winds are prevalent in the area.

The sediment characteristics have been analysed, which have shown that beach sediment coarsens from south to north along the Table Bay beaches, but that this coarsening is not evident below the mid-tide line. Mean grain diameters range between approximately 0.15 mm (lower profile) and 0.5 mm (upper profile).

Furthermore, a detailed sediment budget calculation has been performed in an attempt to quantify the net longshore sediment transport rates in Table Bay. This has been performed using results of the beach profile measurements, analysing the volume of sand that has been lost from each beach cross-section since the mid-1960s. Naturally, the beach profiles do not extend to the depth of closure, thereby necessitating an assumption relating the volume of beach sand lost versus the volume of sand lost from the lower areas of the cross-section. To this end, it has been assumed that the cross-shore profile between the 0 m MSL contour and the depth of closure behaves identically to the 0 m MSL contour. This results in an overestimation of the volume of sediment which is lost along the lower cross-shore profile. This is compensated for by excluding the volume lost above the +3 m MSL depth contour. Additional surveyed data is required, specifically of the lower cross-shore profile, to perform an accurate beach volume analysis and evaluate the accuracy of the above assumption.

This analysis has shown that approximately 1.6 million m^3 has been lost from the Table Bay littoral system since the mid-1960s. If this loss of sediment is distributed evenly across the period under consideration, being May 1965 to February 2010, it was calculated that approximately 48 230 m^3 of sand has been lost annually.

The net sediment transport direction has been identified as being northerly, with the annual loss of sediment exiting Table Bay via the northern boundary of the bay. The transport capacity past the Blouberg headland has been introduced. From this, it has been concluded that although it seems likely that sediment bypasses this headland, additional investigations are required to confirm this assumption.

8. BAY-WIDE SHORELINE MODELLING

8.1 Introduction

As mentioned previously, the bay-wide shoreline model included the coastline from the Port of Cape Town to the rock headland at Blouberg, thereby including the entire Table Bay. The simulation was categorized into two periods, being the calibration and validation periods. The calibration period was used to setup the model, changing key parameters to obtain the correct results. The validation period followed on from the calibration period, and was run over timeframes within which additional measured data was available.

The calibration period for the bay-wide shoreline model was from May 1977 to May 2005, a period of 28 years. This starting date was chosen since the earliest aerial imagery covering the entire Table Bay was taken at this time. Since aerial imagery was required to develop the model's starting shoreline, this was the earliest date which could be modelled. The end date for the calibration period was chosen arbitrarily, prior to the end of the available beach profile data.

The model validation period started at the end of the calibration period, in May 2005. The end of the validation period was the 8th September 2009, the day before the Seli One ran aground. The local shoreline model was used to simulate the shoreline morphology from the 9th September 2009 onwards.

8.2 Mapping Approach

The one-dimensional LITLINE shoreline model has numerous limitations, summarized in Section 4.3.5.2. As mentioned during this discussion, the model assumes a straight, semi-infinite coastline, which means that shoreline excursions are calculated based on the assumption that the angle between the baseline and the shoreline is small, and therefore negligible. Excursions are therefore simulated as an increase or reduction in the distance between the baseline and the shoreline, as shown in Figure 8-1.

Figure 8-1: Calculation of Shoreline Excursion in LITLINE

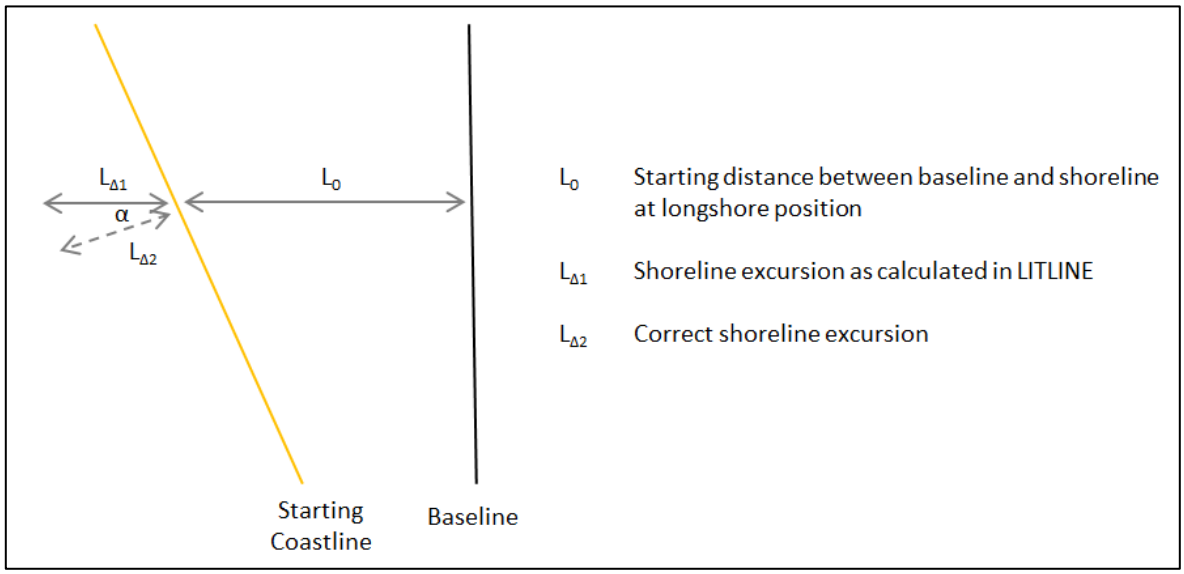

The curvature of Table Bay results in the angle between the baseline and the shoreline at the northern end of the bay being approximately 30^o. If LITLINE was applied without correction, a 15% (cos 30^o) error would have therefore been made in the prediction of the shoreline position in this area.

A so-called mapping approach has been adopted to compensate for this error. In this approach, the shoreline was mapped onto a straight coastline, by rotating the shore-normal to become perpendicular to the baseline. In the figure above, the rotation would be equal to the angle α in a clockwise direction.

To ensure consistency between the coastline and the nearshore wave climate, the wave directions have been rotated by the same angle as the shoreline. This meant that the relative angle between the coastline and the wave climate was kept consistent. In doing so, the longshore processes were not altered, which meant that the longshore current and corresponding longshore sediment transport remained unchanged between the actual and mapped conditions.

The shoreline accretion or erosion at each alongshore position were then determined by comparing the starting and final shoreline positions of the mapped simulation. To determine the final unmapped shoreline position, the shoreline excursions were applied perpendicularly to the actual starting shoreline.

8.3 Model Setup

8.3.1 Starting Shoreline Parameters

The shoreline in a LITLINE model is described by using two input files, being the “coastline” and “profile” files. The coastline file describes the parameters which change in an alongshore direction, and is made up by a user-chosen number of nodes. During the current study, the 12.65 km long Table Bay coastline was split into 5 m sectors, each described by one node. This meant that coastline file of the bay-wide shoreline model was made up of 2 530 nodes, each described by the following information.

- Distance from baseline to shoreline at alongshore node
- Distance from baseline to dune at alongshore node
- Height of dune at alongshore node
- Cross-shore profile number applicable at alongshore node (Section 8.3.2)
- Depth of closure at alongshore node

The starting shoreline used for the bay-wide shoreline evolution model has been taken from aerial imagery of 1977. The “shoreline” referred to in this context is the wetted beach line. Although the identification of the wetted line remains a fairly subjective choice, as discussed in Section 6.3, and cannot be described as scientifically accurate, it was thought that the wetted line was a more representative shoreline position for numerical modelling purposes compared to the vegetation line. Furthermore, it was thought that inaccuracies with regards to the choice of the wetted line would be smoothed out by the simulation fairly quickly, since the simulation, if calibrated correctly, would emulate reality. Since an inaccurate choice of wetted line would not be realistic, it was thought that the model would correct this inaccuracy fairly quickly.

Since simulated shoreline excursions were compared to the beach profile measurements covered in Section 0, the shoreline had to be related to a specific vertical datum. Referring to Section 8.3.4, the average high water level is in the order of +1 m MSL. As such, the shoreline being simulated by the LITLINE model is assumed to be equivalent to the +1 m MSL contour along Table Bay.

The shoreline position during the 1977 aerial imaging campaign, serving as the starting shoreline for the bay-wide shoreline evolution model, is shown in Figure 8-2. This shoreline is described by nodes spaced at even 5 m alongshore intervals.

Because of the mapping approach used for the bay-wide shoreline modelling, the shoreline shown in Figure 8-2 was modelled by being stretched out into a straight line. The shoreline excursions calculated by the

numerical model were then applied in a perpendicular direction to the real shoreline at the respective alongshore positions, to reverse the mapping approach and determine the actual modelled shoreline position.

Figure 8-2: Table Bay Shoreline Position in 1977 (Image: June 1977)

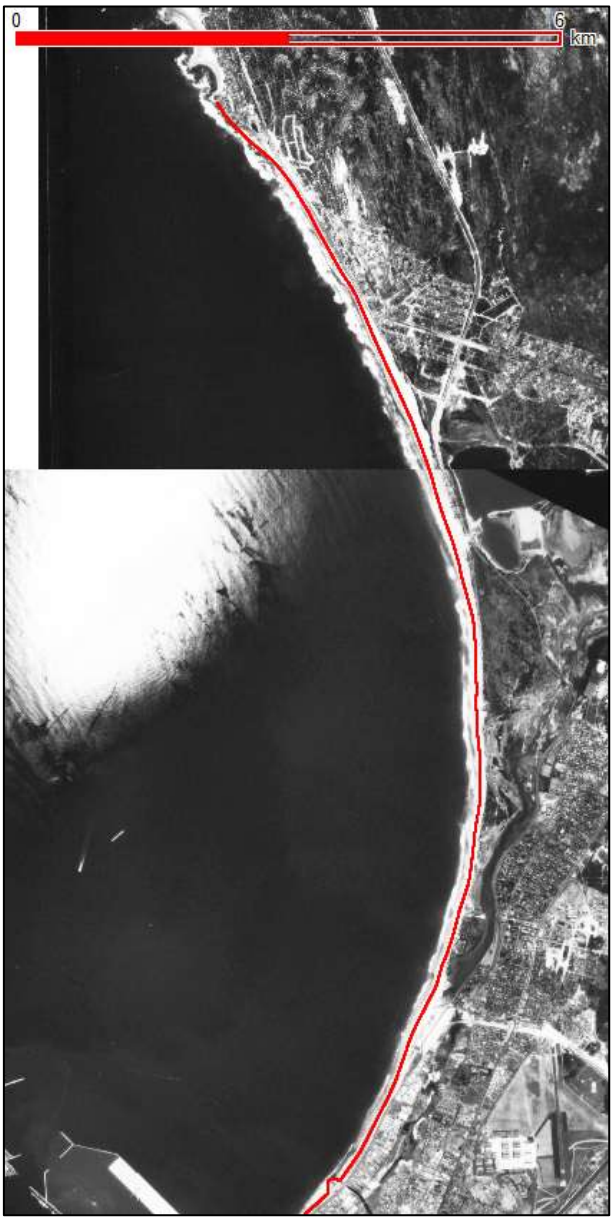

The position of the primary dune relative to the shoreline was determined from aerial photography, assuming that the vegetation line represented the position of the dune foot. The active depth (or closure depth) was discussed previously, given in Table 7-2. A further input parameter into the shoreline evolution model is the height of the active beach, being the distance from 0 m MSL to the elevation above which no longshore sediment transport occurs. This parameter has been used as calibration parameter, and will be introduced in later sections of this report.

8.3.2 Cross-Shore Parameters

The cross-shore parameters in a LITLINE model must be described by a maximum of five discrete profile files. The information contained in each of these files includes:

- Cross-shore bathymetry [m]
- Cross-shore bed roughness [m]
- Cross-shore distribution of mean grain diameters [mm]

The first task in describing these parameters was categorizing the shoreline of Table Bay into five sectors, each of which to be described by one of the five profile files. This discretization was done according to changes in the cross-shore bathymetry along the bay, with areas of similar cross-shore bathymetry being described by the same profile file. Figure 8-3 shows the coastal discretization, whilst Figure 8-4 shows the bathymetry used for each of the five sectors. The cross-shore bathymetry for each of the sectors was chosen to represent an approximate average bathymetry of the area encompassed within the sector.

Figure 8-3: Alongshore Categorization of Cross-Shore Parameters

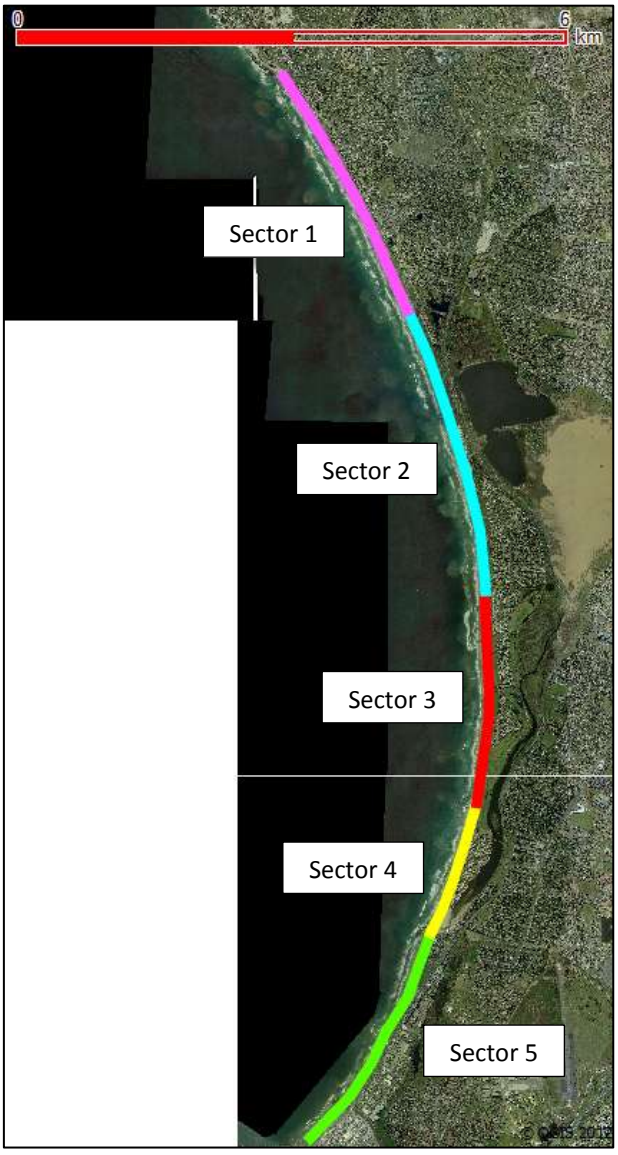

As can be seen in Figure 8-4, all profiles extended to the -10 m MSL depth contour, to ensure the inclusion of the entire littoral zone. In addition, this location was chosen to coincide with the extraction depths for the nearshore wave climates.

The cross-shore distribution of the median grain diameters has been based on the findings of the study performed by Soltau (2009), results of which are summarized in Table 7-1.

Figure 8-4: Discretized Nearshore Bathymetry

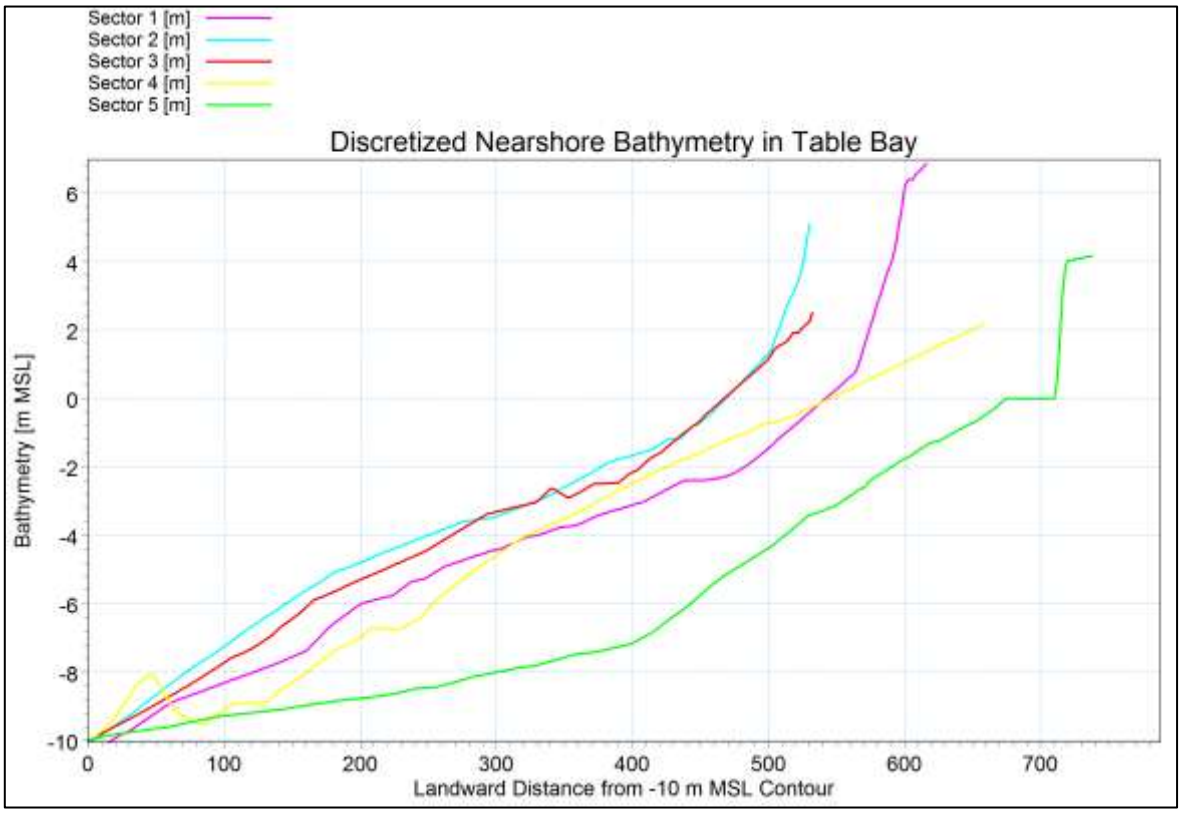

8.3.3 Wave Climates

A detailed analysis of the Table Bay wave climate was performed as part of this study, by developing a wave transformation model using MIKE21 SW. The domain of the wave transformation model included the coastline from Cape Point to Saldanha Bay, with the model's mesh being the most refined within Table Bay. To ensure the model's accuracy, calibration was performed by comparing simulated nearshore wave conditions to measured nearshore wave conditions. Two sets of measured wave data were available for use during the current study, the first being measured near the Koeberg Power Station north of the Melkbos rock headland, and the second data set being measured near the entrance channel of the Port of Cape Town. Details of the Table Bay wave climate analysis are included in Appendix A.

Twenty-five nearshore wave climates were extracted from the calibrated wave transformation model at 500 m intervals along the -10 m MSL depth contour, numbered "Wave A" to "Wave Y" from north to south, as shown in Figure 8-5. Wave roses are included on this figure, to highlight trends with regards to the nearshore wave climate along Table Bay.

Figure 8-5: Nearshore Wave Climates for Bay-Wide Shoreline Evolution Model

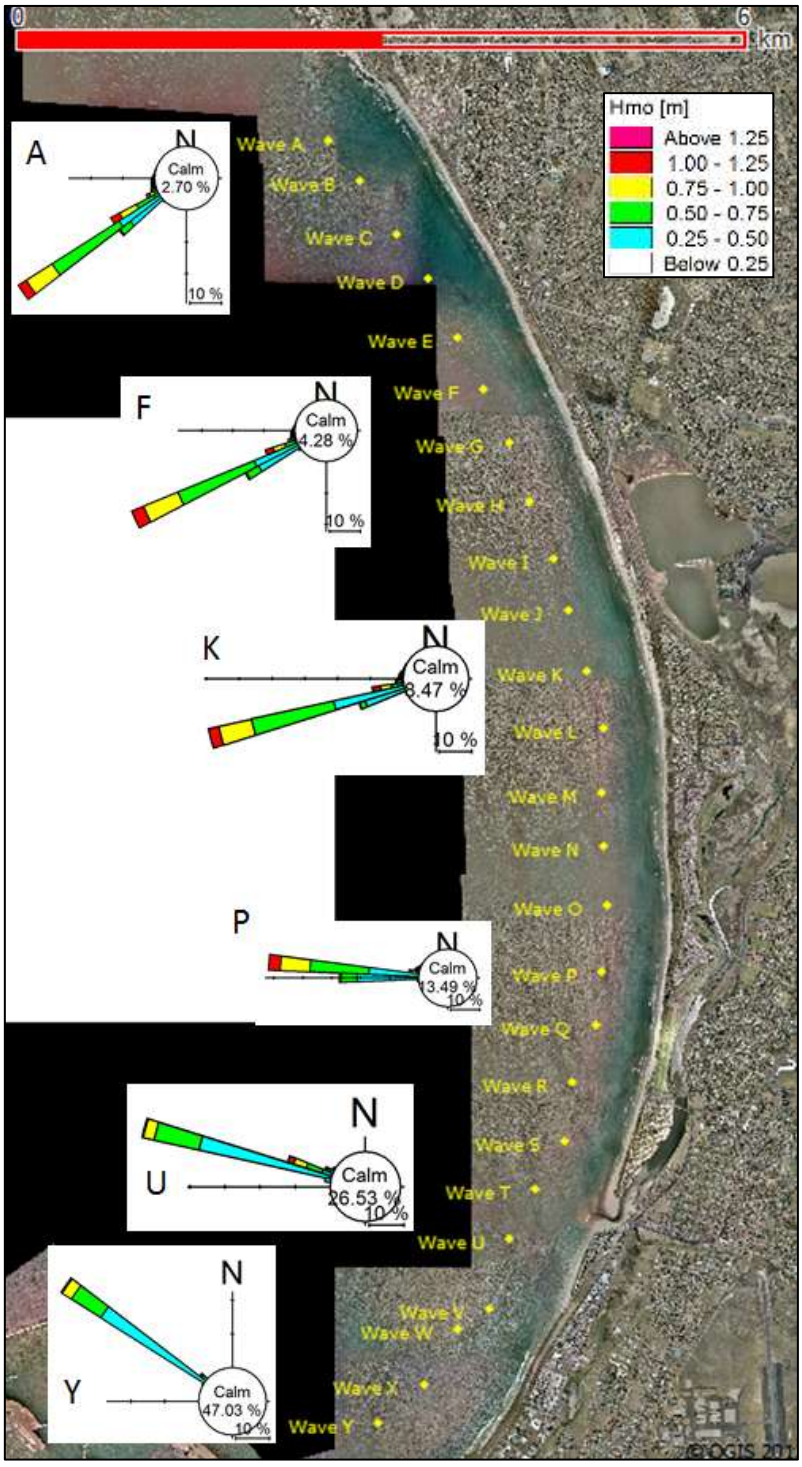

From this figure, the clockwise rotation of the mean wave direction from north to south in Table Bay is evident. In addition to this, the reduction in wave height in the southern parts of the bay is clear, with 47.03% of all waves being "calm" at wave station Y (significant height of smaller than 0.25 m). Both of these phenomena are caused by the increased sheltering effect of refraction and diffraction in the southern parts of Table Bay compared to the northern sectors.

To maintain the relative angle between the coastline and the wave climate, the wave direction needed to be rotated through the same angle as the shoreline orientation. Initially, this rotation was performed by

inspection, by rotating the wave climate through an approximate angle and determining the resulting net longshore transport rate. It was soon determined that the net longshore transport rate was extremely sensitive to the rotation angle, with a relative change in mean wave direction of 1° resulting in a change in net longshore transport rate of tens of thousands of cubic metres annually.

A more systematic approach was therefore adopted following the first trial rotations. This included the calculation of the net longshore transport rate by implementing the Kamphuis equation, discussed in Section 3.3.1.1. The wave conditions at the -10 m MSL depth contour at each of the wave stations shown in Figure 8-5 were used to calculate the breaking wave conditions, assuming linear wave theory. These conditions were then applied to the Kamphuis equation, together with the shoreline orientation, average beach slope and median grain diameter for each specific wave station. By repeating this calculation for each time step in the wave record, an annual average net longshore transport rate could be determined.

Through an automated iterative approach, changing the shoreline orientation by a fraction of a degree, the shore-normal orientation required to satisfy the target net longshore transport rate at each of the 25 wave stations was determined. The results of these calculations are summarized in Table 8-1.

The mapped shoreline used in the shoreline evolution modelling was arbitrarily given an orientation of 270°. Each of the wave climates were therefore rotated by an angle of the shoreline orientation at the respective wave station, subtracted from 270°.

Table 8-1: Wave Climate Rotations Following Kamphuis Equation

Wave Station	Target Net Longshore Transport Rate [m3/year]	Shore-Normal Orientation [deg]	Required rotation for mapped coastline [deg]
A	47 857	239.98	30.02
B	47 585	241.50	28.50
C	47 310	242.84	27.16
D	47 046	245.52	24.48
E	46 734	248.62	21.38
F	46 469	248.21	21.79
G	46 190	251.00	19.00
H	45 910	251.30	18.70
I	45 155	254.59	15.41
J	44 030	256.58	13.42
K	42 734	258.10	11.90
L	41 447	264.29	5.71
M	39 557	267.57	2.43
N	37 953	267.39	2.61
O	36 188	269.63	0.37
P	29 502	275.70	-5.70
Q	27 990	278.33	-8.33
R	23 471	281.10	-11.10
S	17 911	283.83	-13.83
T	9 208	288.57	-18.57
U	14 091	288.23	-18.23
V	5 991	292.36	-22.36
W	4 854	297.94	-27.94
X	2 873	301.96	-31.96
Y	966	305.93	-35.93

* A positive rotation represents a clockwise rotation of the wave directions

8.3.4 Water Levels and Ocean Currents

Water level variations were included in the bay-wide shoreline evolution model by incorporating the predicted tidal level for Table Bay. A time series of predicted tidal levels covering the period from 1977 to 2030 was obtained from the MIKE C-MAP database (DHI, 2011h). Chart datum is used as reference level in this database, and, since the wave modelling and beach profile measurements were performed to mean sea level, a correction of 0.825 m was incorporated in the water level data to correct for the differing reference levels.

It should be noted that these water levels do not include storm surge. It was thought that, considering the timeframe over which the shoreline models are run, being years rather than hours, the impact of storm surge would be smoothed out and would ultimately not have a significant impact on the simulated shoreline position (based on (SANHO, 2012)).

Figure 8-6: Predicted Tides for Table Bay – January 1977

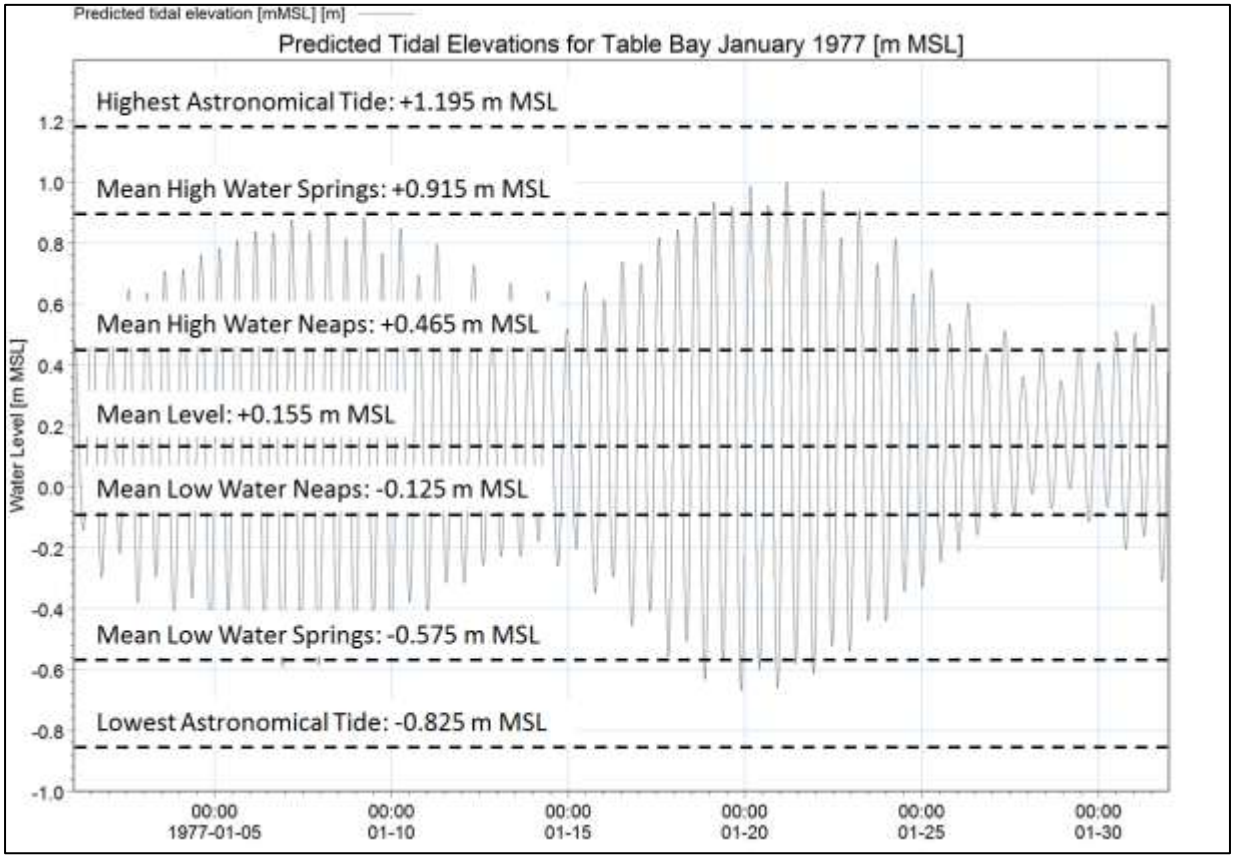

The time-series of water levels shown in Figure 8-6 were scrutinized through a comparison with the tidal levels for the Port of Cape Town, as obtained from South African Tide Tables (SANHO, 2012), shown in Table 8-2. This comparison yielded a good correlation, indicating that the predicted tidal levels obtained from the MIKE C-MAP database were accurate.

It should be noted that sea level rise was not included in any of the simulations performed during this study. This was done since the main objective of this study was to determine the relative impact of the Seli One shipwreck on the Table Bay beaches. Since sea level rise will occur with or without the wreck, the inclusion would not alter the relative impact of the vessel.

Table 8-2: Tidal Levels for the Port of Cape Town (SANHO, 2012)

Tidal Level	Acronym	Water Level [m CD]	Water Level [m MSL]
Lowest Astronomical Tide	LAT	0.00	-0.825
Mean Low Water Springs	MLWS	0.25	-0.575
Mean Low Water Neaps	MLWN	0.70	-0.125
Mean Level*	ML	0.98	0.155
Mean High Water Neaps	MHWN	1.29	0.465
Mean High Water Springs	MHWS	1.74	0.915
Highest Astronomical Tide	HAT	2.02	1.195

*Note that the Mean Level given in the table above is the mean of the heights of MHWS, MHWN, MLWS and MLWN, and is not equal to the Mean Sea Level. Mean Sea Level is equal to Land Levelling Datum.

LITLINE gives the user the opportunity to include a so-called ocean current in the simulation. An ocean current is defined as a current which is not generated by the local wave field. Through a review of navigation guides for the Port of Cape Town, including the African Pilot (UKHO, 2002), it was determined that no significant ocean current exists in Table Bay. In addition, wind driven flow may play a small role, but wave driven currents dominate. It is therefore concluded that all longshore sediment transport in Table Bay is carried by wave driven currents.

8.3.5 Structures

The concrete dolos revetment lining the southern 2.9 km of Table Bay has been included in the shoreline evolution model as a revetment in the LITLINE model, being one of the standard structures which is included in the LITLINE software. Although there are numerous other structures located in Table Bay which may influence the longshore transport characteristics, such as the managed dune field fronting the Dolphin Beach Hotel, these were not included in the simulation. This has been done since it is thought that although these structures may slow down shoreline erosion to a certain extent, it is unlikely that they will prohibit shoreline retreat in the long-term.

8.3.6 Sources and Sinks

Sources and sinks have been included in the shoreline evolution model as per the discussion in Section 7.2, and include a sediment source of 5 000 m^3/year from the Diep River, as well as a loss of 5 000 m^3/year as a result of wind-blown sand along the Blouberg beachfront.

Since Cape Town's wet season is during winter, it is likely that the majority of the sediment discharge from the river into the littoral zone occurs during winter months. Similarly, the strongest winds in Cape Town occur during the summer months, resulting in the majority of wind-blown sediment losses occurring during that time. Both of these aspects have been incorporated in the simulation by generating a time-series of the sediment sources and sinks, as shown in Figure 8-7. Note that this figure shows the sediment sources and sinks for only two arbitrarily chosen years, from January 1980 to December 1981. An identical time series has been generated for the entire simulation period.

Figure 8-7: Table Bay Sediment Sources and Sinks (1980 to 1981)

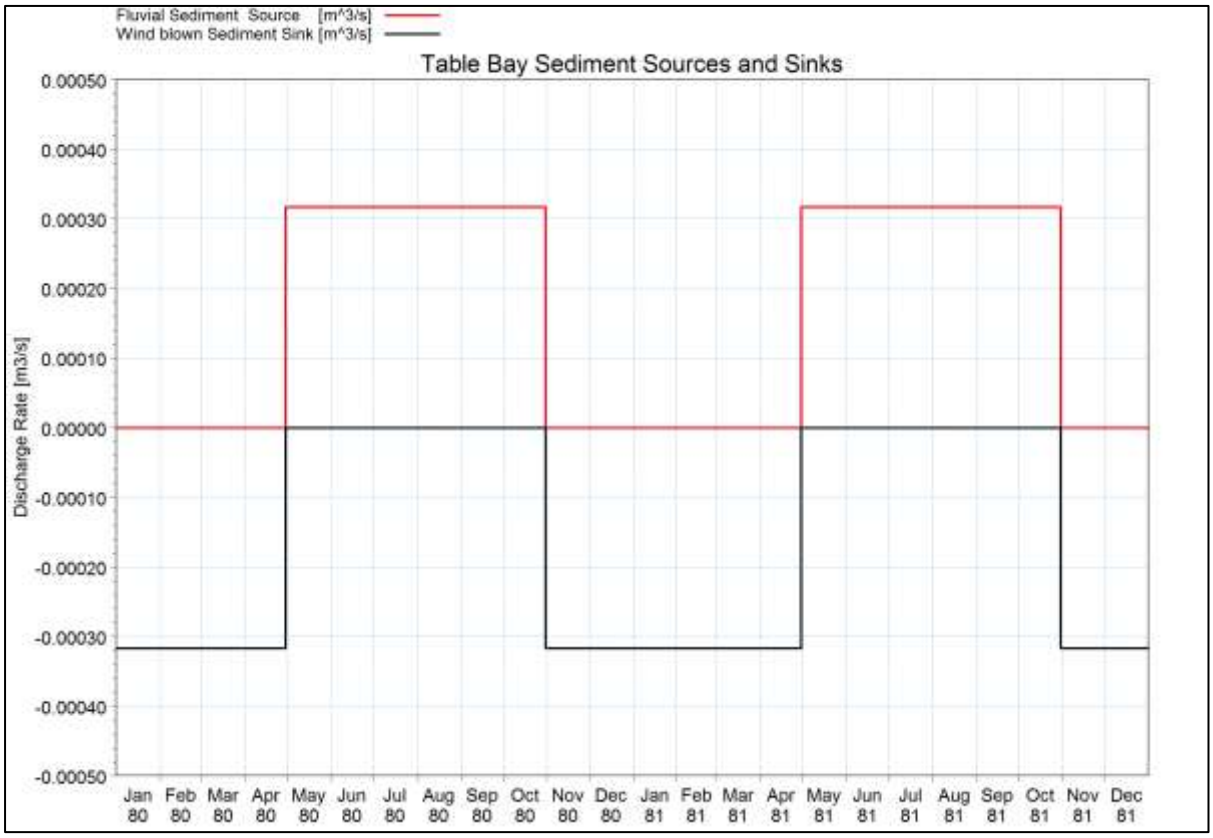

8.3.7 Boundary Conditions

The correct representation of the boundary conditions is arguably the most important and most challenging aspect of shoreline evolution modelling, since the conditions at the boundary control the volume of sediment entering and exiting the model. As discussed in Section 7.2.1, the southern boundary represents the southern boundary of a closed littoral cell. As such, no sediment should enter or leave the model at this location. The northern boundary represents an open boundary, with approximately 50 000 m^3 of sand exiting the bay annually, as calculated in Section 7.

A virtual groyne structure was used to simulate the closed southern boundary. Usually, a physical groyne has the combined effect of both blocking longshore sediment transport as well as changing local wave and current characteristics. Clearly, the second effect is undesired in the current shoreline model, since this would alter the longshore sediment transport behaviour in the south of Table Bay.

To overcome this unwanted effect, the so-called 'groyne length' and 'apparent groyne length' parameters in LITLINE were used. The 'groyne length' is defined as the physical groyne length simulated by the model. This therefore has the combined effect of blocking sediment transport as well as impacting the wave and current climate (DHI, 2011d). The 'apparent groyne length' is a virtual length up to which longshore sediment transport is blocked, but which does not have an impact on the wave and current patterns (DHI, 2011d). The 'apparent groyne length' cannot be shorter than the 'groyne length'. If, for example the 'groyne length' is defined as 1 000 m, whilst the 'apparent groyne length' is defined as 2 000 m, the physical groyne impacting hydrodynamic conditions is 1 000 m long. However, sediment is transport is blocked up to 2 000 m from the model's baseline.

During the current study, this function was applied by defining the 'groyne length' as 0 m, with the 'apparent groyne length' extending 10 000 m from the model's baseline. This high distance was chosen to ensure than no sediment entered the simulation from the south. In this way, sediment that would otherwise have entered from the south was blocked without affecting the wave and current patterns in the south of Table Bay.

The northern boundary of the bay-wide shoreline evolution model was simulated as an open boundary, with the shoreline position not being pinned and no prescribed transports being applied.

8.3.8 Wave Climate Categorization and Wave Theory

As with any numerical model, certain assumptions are made during the shoreline evolution model in an attempt to reduce the computational effort, whilst maintaining the simulation's accuracy and realism. In LITLINE, one of these simplifications is the categorization of individual wave conditions into typical events. This has the advantage of allowing the software to pre-calculate longshore sediment transport rates for each of the events, depending on site specific information such as cross-shore bathymetry and sediment grain distributions, and applying the appropriate transport rate to the wave condition as and when this occurs. This means that the longshore sediment transport rate is not re-calculated for each time step, but rather calculated once-off in the beginning of the simulation and referred to for every hydrodynamic event corresponding to that specific event. Naturally, not every single event is pre-calculated. The transport rate for an event which does not coincide with one of the pre-calculated events is determined through linear interpolation between adjacent events.

This simulation methodology requires an understanding of all potential wave events which may occur during the simulation. After a review of all 25 nearshore wave climates, the binning scheme shown in Table 8-3 was used. Note that the wave direction refers to the relative angle between the wave crest and shoreline.

Table 8-3: Binning of Nearshore Wave Conditions for LITLINE Simulations

Parameter	Minimum Value	Maximum Value	No of Values	Bin Width
Wave direction	-89°	89°	25	7.5°
Wave period	4 s	20 s	9	2 s
Wave height (H_{rms})	0 m	2 m	15	0.14 m
Water level	-1 m MSL	+1.4 m MSL	25	0.1 m

8.3.9 Sediment Properties

The sediment properties were chosen according to the LITLINE user manual (DHI, 2011d), since no additional data was available to suggest otherwise. These values are summarized as follows:

Relative sediment density: 2.65
Critical Shields Parameter: 0.045 Pa
Sediment Porosity: 0.4

8.4 Model Calibration

8.4.1 Calibration Approach

There are essentially two parameters which need to be evaluated when calibrating a shoreline evolution model, being the net longshore sediment transport rate and the shoreline changes occurring as a result of this transport rate. During the current study, calibration was performed by first adjusting the model to obtain the correct transport rates, as summarized in Table 7-5. This was followed by making slight additional changes to the model to obtain the correct shoreline changes, without affecting the net longshore sediment transport characteristics of the model.

The first calibration step was performed by altering the relative angle between the mean wave direction and the shoreline orientation at each of the 25 wave climate input locations. Although this may seem to be a change which results in the model no longer accurately representing the environmental conditions of the bay, it should be considered that a previous rotation has already been performed to straighten the coastline from the real curved coastline to the mapped straightened coastline. It will be recalled that this rotation has been performed according to the Kamphuis Equation, which, being an empirical relationship, cannot be seen to be accurate to within more than, say, 1°. In addition, the un-rotated wave angles determined from the bay-wide wave transformation model cannot be said to be accurate to within more than approximately 1°. As such, an additional change of a few decimal points would not result in the model misrepresenting the environmental conditions of Table Bay.

Once the correct net longshore sediment transport rate was obtained, the active beach height parameter in LITLINE was altered to obtain the correct shoreline excursions. As will be discussed later, the active beach height which resulted in a good correlation was +3 m MSL.

8.4.2 Calibration Results

8.4.2.1 Net Longshore Sediment Transport Rate

The calibration process of the bay-wide simulation model turned out to be an arduous process, due to both the sensitivity of the model to the relative angle between the wave direction and shoreline orientation, as well as due to the large number of wave climates used as model forcing. It was found that changing the relative wave direction at one location had a knock-on effect over the entire model domain. It was therefore not a matter of changing the relative wave angle progressively from one end of the model to the other, but rather a process of educated trial and error until the correct net longshore transport rate was obtained.

The calculated and simulated net longshore transport rates, as well as the difference as a percentage value, are shown in Figure 8-8. From this figure it is clear that, as expected, the simulated net longshore sediment transport rate agrees well with the calculated rate. It is noted that the model under-predicts the net longshore transport rate in the southern 2.5 km of Table Bay, which corresponds to the stretch of coastline being protected by the concrete dolos revetment. It is further clear that the model results in a less irregular curve, with a smoother alongshore gradient in transport rate being observed.

Figure 8-8: Calculated and Simulated Longshore Drift in Table Bay (Calibration)

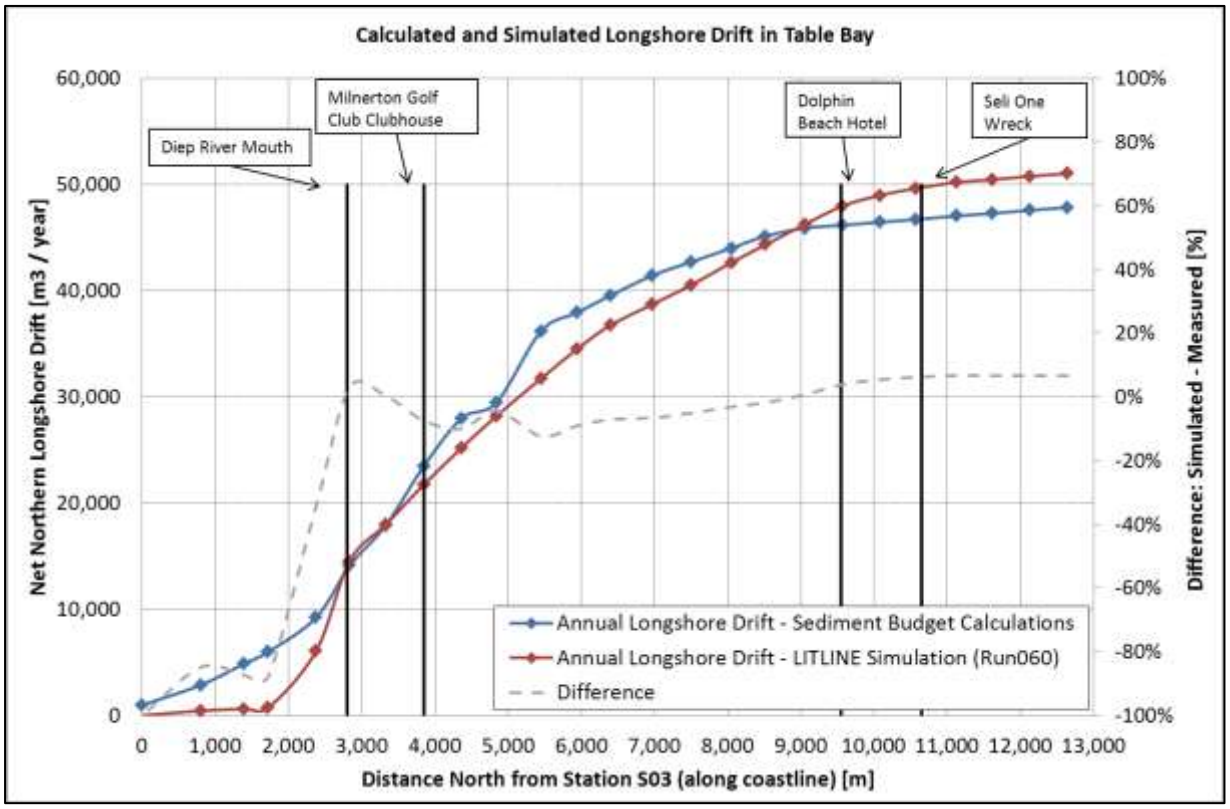

The difference between the calculated and simulated net longshore transport rates in the southern 2.5 km is not thought to be an under-prediction on the model's part, but rather a product of the sediment budget analysis methodology. Referring to Section 7, the long-term sediment budget calculations were based on those beach profile stations which have been measured since the mid 1960's. The most southern profile station satisfying this requirement is station S06, situated 2.3 km north of the southern model boundary. The net longshore transport rate of the southern 2.3 km is therefore based on a linear interpolation between the closed southern boundary, i.e. zero net transport, and the net transport rate for profile station S06. The near zero net longshore transport rate of the model in the southern 1.8 km is considered to be a more accurate representation compared to the calculated rates. The revetment hinders any shoreline erosion of the upper beach. This means that since the beach levels in front of the revetment have not dropped significantly since the construction of the revetment, the longshore sediment transport gradient along this stretch of coastline has to be near zero. Since the net longshore transport rate at the southern end of the revetment, being the southern boundary of the Table Bay littoral cell, is equal to zero, for the sediment transport gradient to remain zero, the net transport rate along the revetment is required to remain near-zero. It is therefore thought that this process is represented more accurately by the model than by the sediment budget calculations.

As expected, the remainder of the calculated and modelled net longshore transport rates agree well, remaining within approximately 8% of each other. This expectation is due to the fact that, as discussed previously, the model was forced to replicate the net longshore transport rates at discrete locations along Table Bay based on the Kamphuis equation.

8.4.2.2 Shoreline Changes

Once it had been determined that the bay-wide LITLINE model accurately replicated the net longshore sediment transport rate along Table Bay, the next step in ensuring model accuracy was to compare the

measured and simulated shoreline excursions. Adjustments were made to the active beach height parameter to obtain an accurate representation of the measured shoreline morphology. An active beach height of +3 m MSL over the entire bay yielded a satisfactory comparison.

Table 8-4 summarizes the comparison between the calculated and simulated shoreline excursions at each of the beach profile stations which have been surveyed since the mid 1960's. These results are shown graphically in Figure 8-9.

Table 8-4: Calculated and Simulated Shoreline Excursions in Table Bay (Calibration)

Profile Station	Distance from Profile Station S03	Shoreline accretion/erosion May 1977 to May 2005		Difference	
	[m]	Measured [m]	Simulated [m]	[m]	[%]
S06	2 263	-28.6	-26.9	1.7	-6%
S07	3 096	-20.2	-20.9	-0.7	3%
S11	3 839	-29.5	-21.7	7.8	-26%
S16	5 109	-17.6	-17.5	0.1	-1%
S22	6 950	-9.0	-9.6	-0.6	7%
S31	8 749	-10.3	-10.7	-0.4	4%
S41	10 667	-8.5	-8.4	0.1	-1%

From these, it is clear that the model accurately simulates shoreline excursions to within 7% at all except one beach profile station, being station S11. From Figure 8-9 it is evident that the shoreline erosion experienced at station S11 is greater than along the surrounding beaches, and may therefore be caused by a local effect.

Referring to Figure 8-10, a sandbag revetment has been constructed, which protrudes further seaward than adjacent infrastructure, and is in close proximity to profile station S11. It is thought that this structure, by prohibiting shoreline erosion in this area, is resulting in accelerated shoreline erosion on either side of the structure. This structure has, however, not been included in the bay-wide shoreline evolution model, and does therefore not include this effect.

Furthermore, Figure 8-10 shows a staircase which leads from a public parking lot down to the beach immediately landward of beach profile station S11. It is therefore possible that shoreline erosion is exacerbated in this area when higher waves result in local scouring effects in front of the stairs. In addition, it is thought that large amounts of foot traffic near the stairs potentially loosen the beach sand, making it easier for this material to be picked up and carried away by natural processes. These processes are not included in the bay-wide shoreline evolution model.

With this being said, it is not expected that the LITLINE model is inaccurate in this area, but only excludes the local effect of the flanking erosion resulting from the sandbag revetment, and the local erosion caused by large amounts of foot traffic. The long-term longshore processes are expected to be accurately included in the model, especially considering the accurate representation of the shoreline excursions at profile stations S07 and S12.

Figure 8-9: Calculated and Simulated Shoreline Excursions in Table Bay (Calibration)

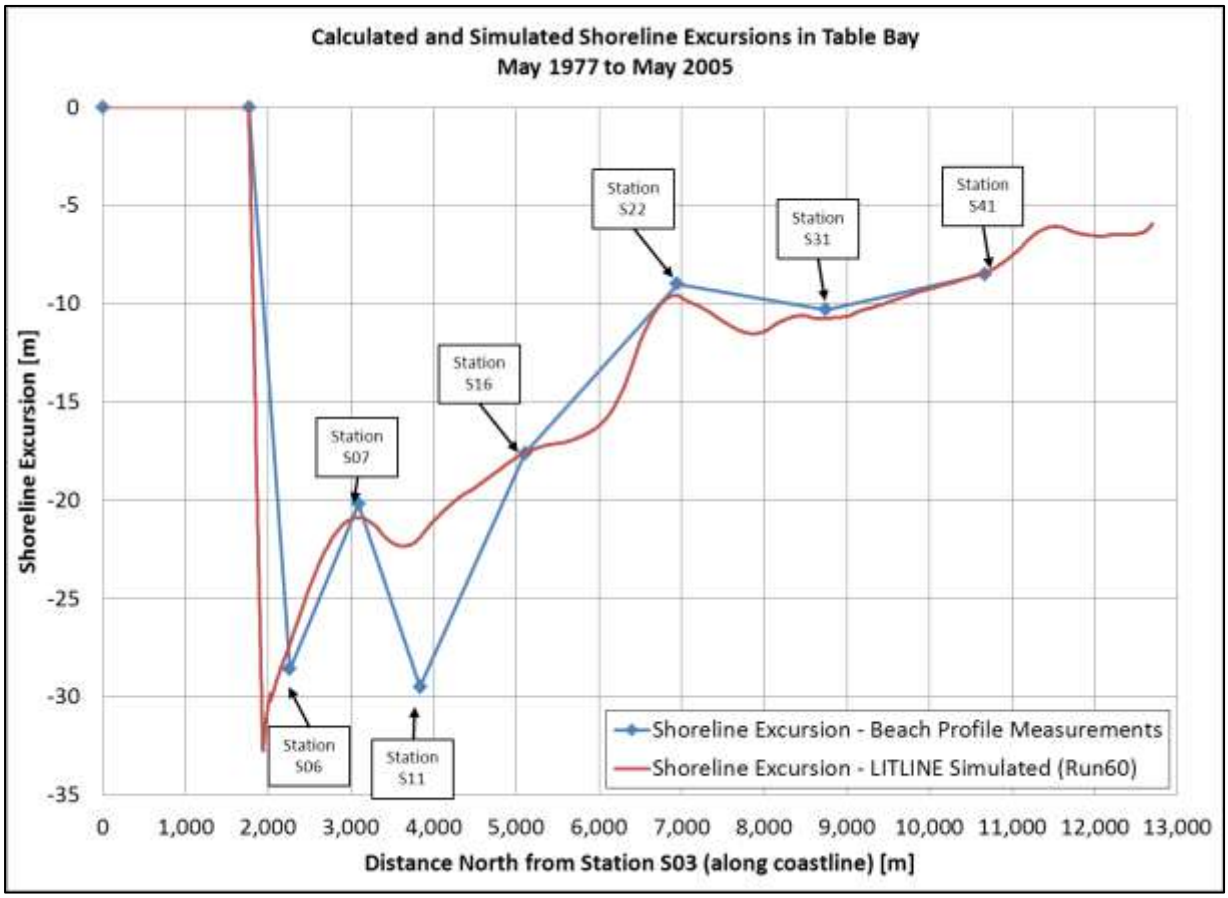

Figure 8-10: 1977 and 2005 Shoreline Positions near Milnerton Golf Club Clubhouse

In addition to comparing the total calculated and simulated shoreline excursions, i.e. the shoreline positions at the beginning and end of the simulation, it is useful to compare the measured and simulated shoreline position as a function of time. This determines the accuracy of the simulation to the time-dependant shoreline morphology.Figure 8-11 through Figure 8-14 show the temporal variability of the shoreline position at four representative locations in Table Bay.

The figures show the shoreline position during each individual survey, as well as the linearly interpolated shoreline position as a function of time. The simulated shoreline position through the course of the simulation is superimposed onto this.

These figures show a strong correlation between the linearly interpolated and simulated shoreline morphology. It is clear that the measured shoreline shows a significantly greater temporal variability than the simulated shoreline. This relates to the simplification of the coastal processes in the LITLINE model, such as the exclusion of certain cross-shore processes. However, since these processes cancel each other out over time, the LITLINE model remains accurate. The more gradual shoreline changes of the simulation compared to shoreline measurements was therefore expected, and the temporal shoreline variability shown inFigure 8-11 to Figure 8-14 is deemed as an accurate representation of the long-term Table Bay shoreline behaviour.

Figure 8-11: Profile Station S07 – Measured vs Simulated Shoreline Morphology (Calibration)

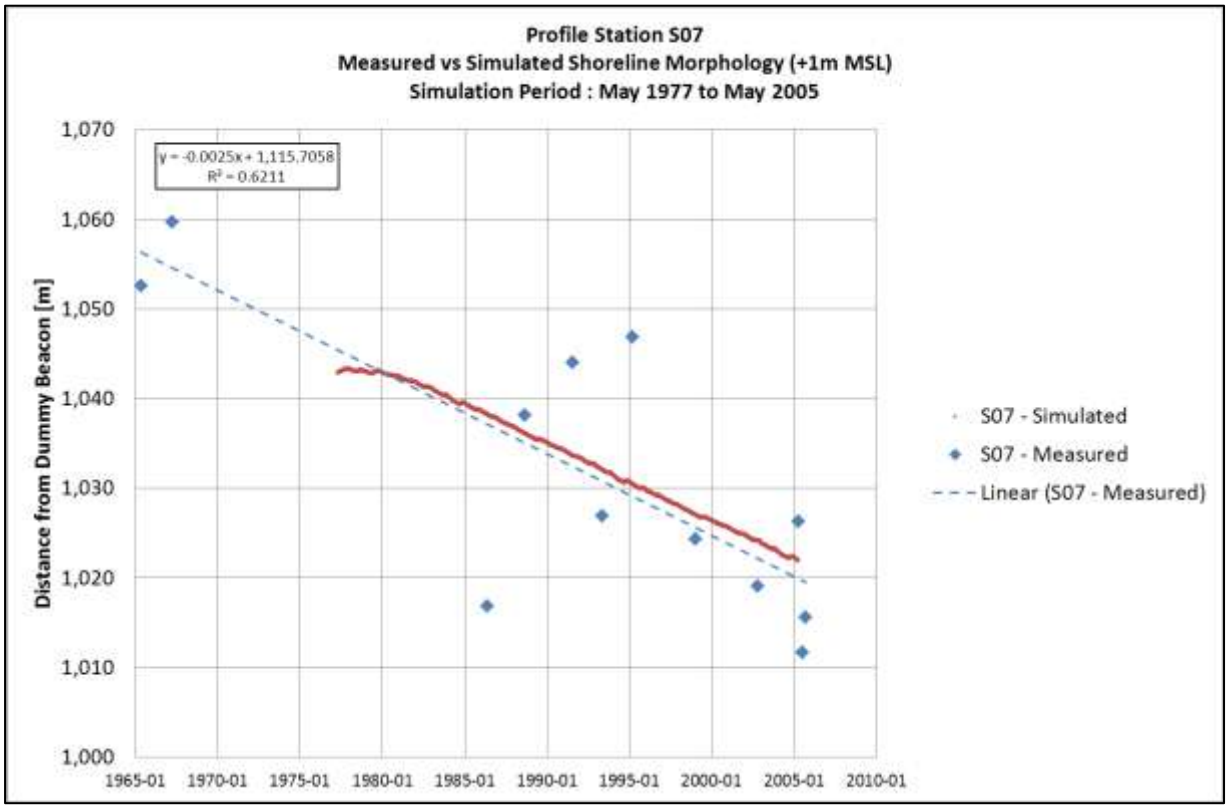

Figure 8-12: Profile Station S14 – Measured vs Simulated Shoreline Morphology (Calibration)

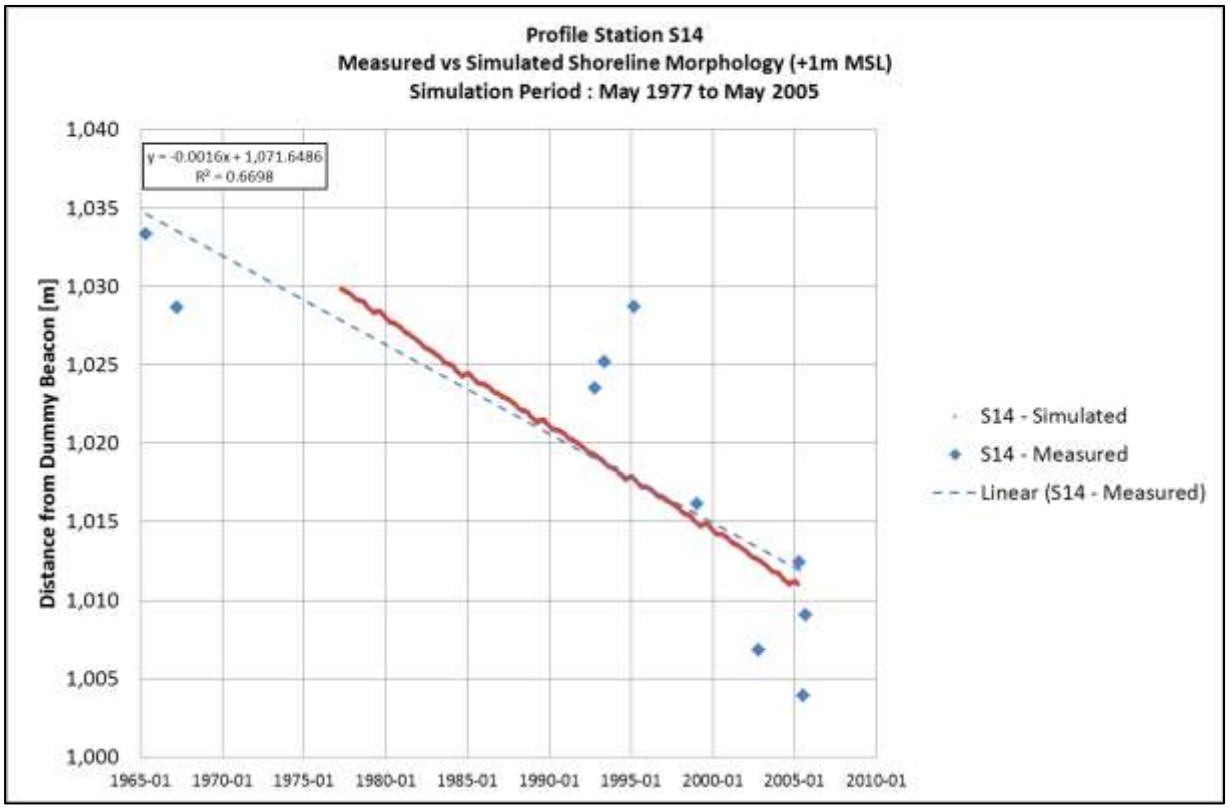

Figure 8-13: Profile Station S31 – Measured vs Simulated Shoreline Morphology (Calibration)

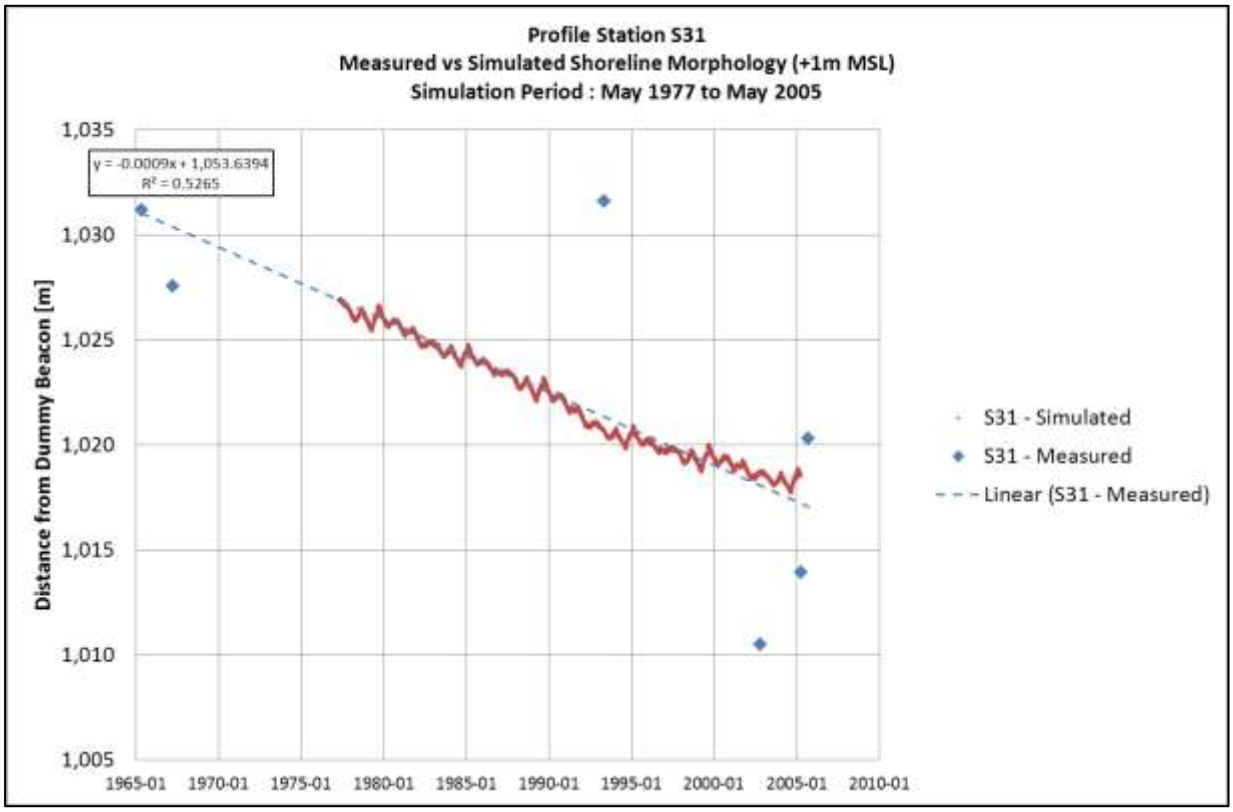

Figure 8-14: Profile Station S41 – Measured vs Simulated Shoreline Morphology (Calibration)

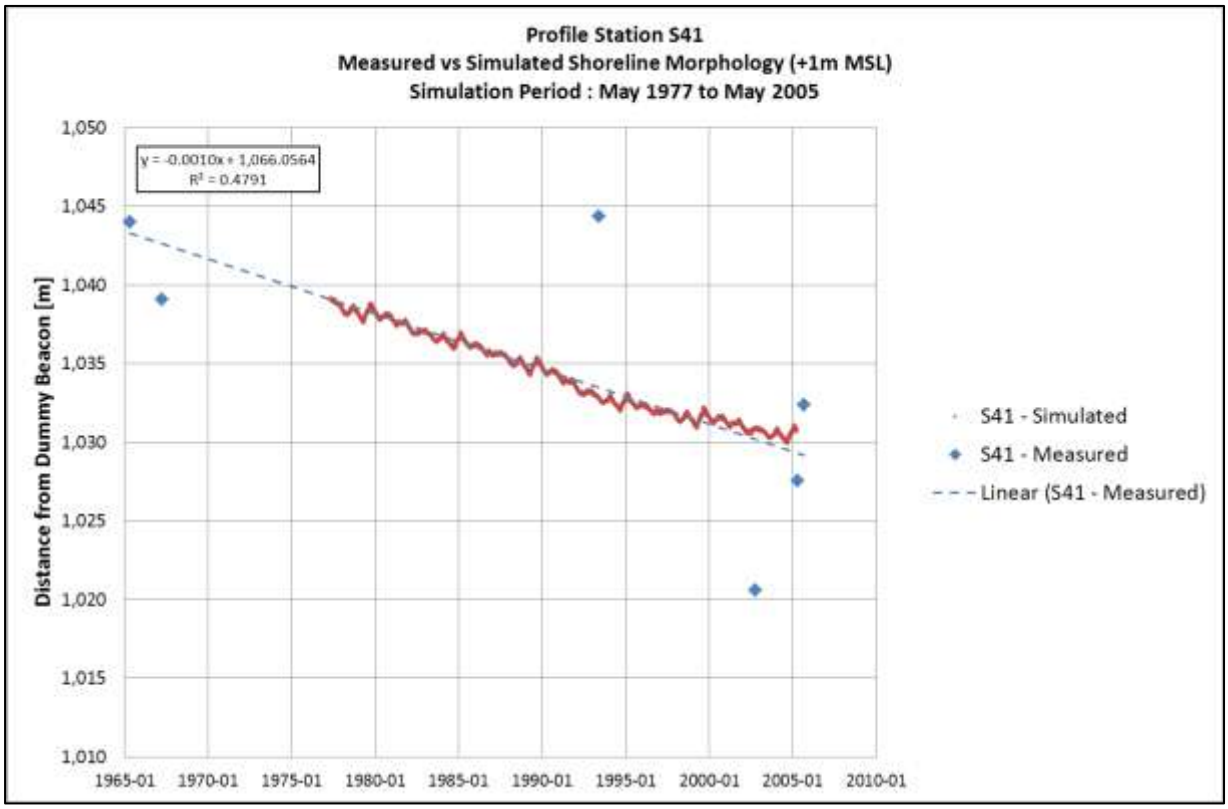

8.4.2.3 Temporal Variability of Net Longshore Sediment Transport Rate

In Section 3.3.1.3, the variability of longshore sediment transport was introduced. Although this discussion focussed on the difference between net and gross longshore transport, it highlighted an important aspect of longshore sediment transport, being the variability thereof, both in a spatial and a temporal sense. To gain a better understanding of the Table Bay sediment transport system, a review of the temporal variability of the net longshore sediment transport volumes was conducted. To aid this, the net longshore sediment transport rates at beach profile station S22 were analysed, results of which are shown in Figure 8-15.

This figure shows the annual net longshore transport volumes during the calibration period, as well as the average net longshore transport rate over the entire simulation. This indicates the significant variability of the experienced longshore transport versus the average transport. The lowest net annual transport volume was approximately 24 000 m^3 in the year 2000, whilst the largest was 49 000 m^3, in 1979.

The high temporal variability in net longshore transport rate highlights the sensitivity of shoreline assessments to the timeframe under consideration. If a different timeframe is chosen to that being considered during the current investigation, it is possible that the average net transport rate is determined to be a value different than what has been determined during this investigation, which may affect the overall results. As a general guideline, it is therefore advisable to use all available data during shoreline evolution assessments, to describe the longest possible duration.

Figure 8-15: Temporal Variability of Net Longshore Sediment Transport Rate at Beach Profile Station S22

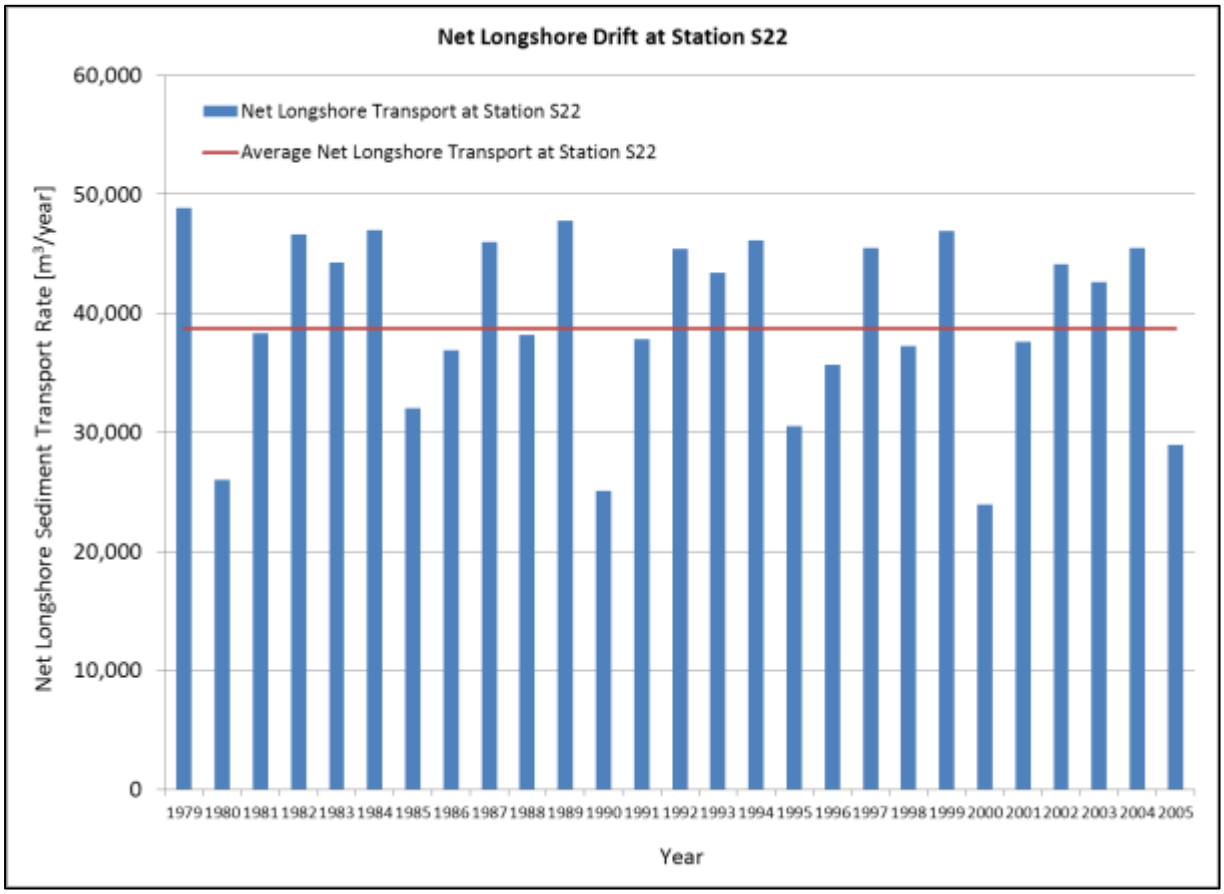

8.5 Model Validation

8.5.1 Net Longshore Transport Rate

As an initial confidence check, the simulated net longshore transport rate of the validation period was compared to that observed previously during the calibration period, shown in Figure 8-16. The intention of this initial check was to confirm that the bay-wide model functions correctly in general, before performing the more detailed model validation, which is based on simulated shoreline changes and will be discussed in Section 8.5.2. In general, it can be said that the results of the two simulations are similar, with the same general trend being observed. This trend is a zero net longshore transport rate at the southern boundary to the Table Bay littoral cell, which increases gradually to approximately 50 000 m^3/year net northerly at the northern boundary. It is however equally clear that differences exist, most noticeably that the net transport rate during the validation period peaks at about 45 000 m^3/year approximately 3 km south of the rock outcrop at Blouberg, before reducing to approximately 38 000 m^3/year at the northern model boundary.

Although this may initially seem to be a cause for concern, reference is made to the previous discussion regarding the temporal variability of longshore sediment transport. It is likely that, due to the short duration of the validation simulation compared to the calibration simulation, short-term environmental conditions play a more significant role.

Figure 8-16: Simulated Net Longshore Transport (Calibration vs Validation)

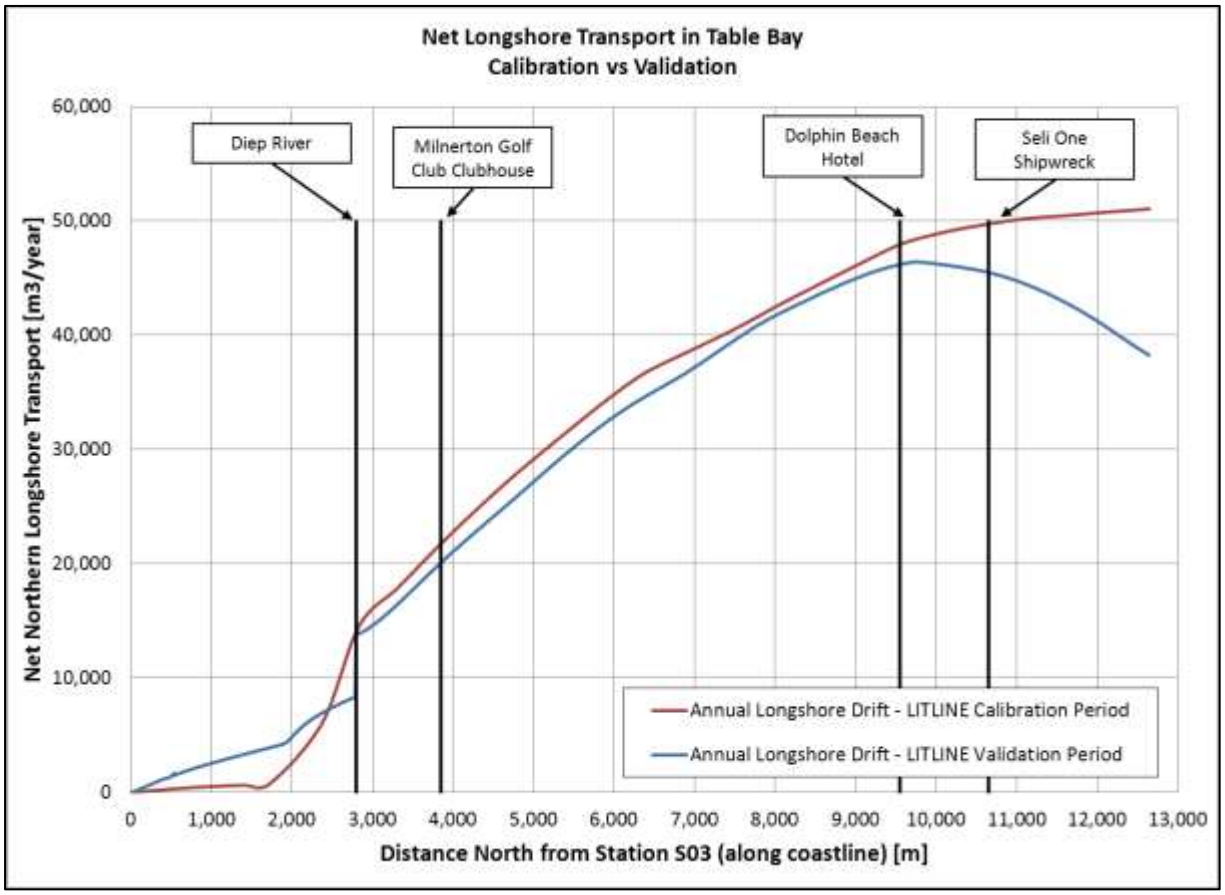

The discrepancy between the net northern longshore transport rate observed during the calibration and validation simulations prompted a review of the wave conditions used during each of the simulations, with the intention of this being to identify the causes for the difference in simulated longshore transport rates. The median relative wave direction was interrogated, being the angle between the wave ray and the shore-normal. This was done at each of the wave stations along the Table Bay shoreline. The results of this interrogation are shown in Table 8-5 below. Note that a positive difference in median relative wave direction means that the wave crest becomes more shore-parallel, which would result in a reduction of longshore transport.

From this table, it is clear that there are subtle changes in the median relative wave angle between the calibration and validation timeframes. These differences are present along the entire bay, but are most significant along the northern Table Bay beaches. Here, the reduction in the relative median wave angle (from calibration to validation) is approximately 0.06°.

Following this, an empirical equation, vis. the Kamphuis equation, was used to determine the reduction in net northern longshore transport that could result through a clockwise rotation of the median wave angle by 0.06°. This calculation was performed at Wave Station A, where the difference between the transport rates of the calibration and validation simulations is in the order of 12 000 m^3/year. This reduction potential was calculated to be in the order of 10 000 m^3/year, similar to the observed difference of 12 000 m^3/year.

From this, it is concluded that the difference in simulated net northern longshore transport rate between the calibration and validation simulations is caused by differences in the nearshore wave characteristics of the two timeframes.

Table 8-5: Comparison of Median Relative Wave Direction of Calibration and Validation Simulations

Wave Station	Distance north from profile Station S03	Median Relative Wave Direction [deg]		
		Calibration	Validation	Difference
Wave A	12 645	5.624	5.562	0.062
Wave B	12 130	5.368	5.309	0.059
Wave C	11 618	5.000	4.936	0.064
Wave D	11 125	4.634	4.580	0.054
Wave E	10 571	4.651	4.594	0.057
Wave F	10 083	4.554	4.493	0.061
Wave G	9 574	4.724	4.667	0.057
Wave H	9 059	4.79	4.7355	0.055
Wave I	8 517	4.656	4.606	0.050
Wave J	8 052	4.656	4.608	0.048
Wave K	7 505	4.295	4.248	0.047
Wave L	6 971	3.769	3.733	0.036
Wave M	6 397	4.627	4.597	0.030
Wave N	5 943	4.06	4.025	0.035
Wave O	5 449	3.556	3.532	0.024
Wave P	4 843	3.514	3.494	0.020
Wave Q	4 364	3.534	3.5165	0.017
Wave R	3 847	3.408	3.394	0.014
Wave S	3 328	2.454	2.445	0.009
Wave T	2 833	2.685	2.682	0.003
Wave U	2 375	3.331	3.3265	0.005
Wave V	1 722	3.066	3.064	0.002
Wave W	1 389	2.773	2.778	-0.005
Wave X	801	2.572	2.58	-0.008
Wave Y	0	2.243	2.256	-0.013

A question that may arise now is what environmental conditions would result in the median wave direction along the northern Table Bay shoreline to rotate by 0.06°, but would not cause the same rotation in the southern part of the bay. It is postulated that the cause for this is the impact of Robben Island on the nearshore wave climate. Westerly waves could possibly diffract southward around the northern end of the island, resulting in a slight clockwise rotation of the waves along the northern Table Bay shoreline. This effect would not extend to the southern part of the bay, since the diffraction effects of the island would not extend to this area.

It is therefore concluded that, although discrepancies between the net longshore sediment transport rates simulated during the calibration and validation period exist, the bay-wide shoreline evolution model accurately represents the Table Bay sediment transport system.

8.5.2 Shoreline Changes

Similar to the calibration result evaluation, the shoreline changes need to be assessed in conjunction with the net longshore transport rates to assess the total model functioning. A comparison of the measured and simulated shoreline excursions are summarized in Table 8-6, shown graphically in Figure 8-17. The slight shoreline accretion being observed in the northern part of Table Bay referred to previously is identified in Table 8-6.

Table 8-6: Measured and Simulated Shoreline Excursions in Table Bay (Validation)

Profile Station	Measured Shoreline Excursion [m]	Simulated Shoreline Excursion [m]	Difference [m]
S06	0.2	-2.0	-2.2
S07	6.0	-2.7	-8.7
S08	-2.4	-2.9	-0.5
S09	-1.8	-3.0	-1.2
S10	3.1	-3.1	-6.3
S11	1.5	-3.0	-4.5
S12	-15.3	-2.9	12.4
S13	3.5	-2.8	-6.3
S14	-2.6	-2.8	-0.2
S15	-2.0	-2.9	-0.9
S16	-1.8	-2.8	-1.1
S18	-0.7	-2.5	-1.8
S20	-1.6	-1.9	-0.3
S22	-1.2	-2.1	-1.0
S24	-0.5	-2.0	-1.5
S28	0.6	-1.5	-2.2
S31	-1.3	-1.4	-0.1
S35	-1.5	-1.1	0.4
S38	1.4	-0.5	-1.8
S41	-0.9	0.3	1.2

Figure 8-17: Measured and Simulated Shoreline Excursions in Table Bay (Validation)

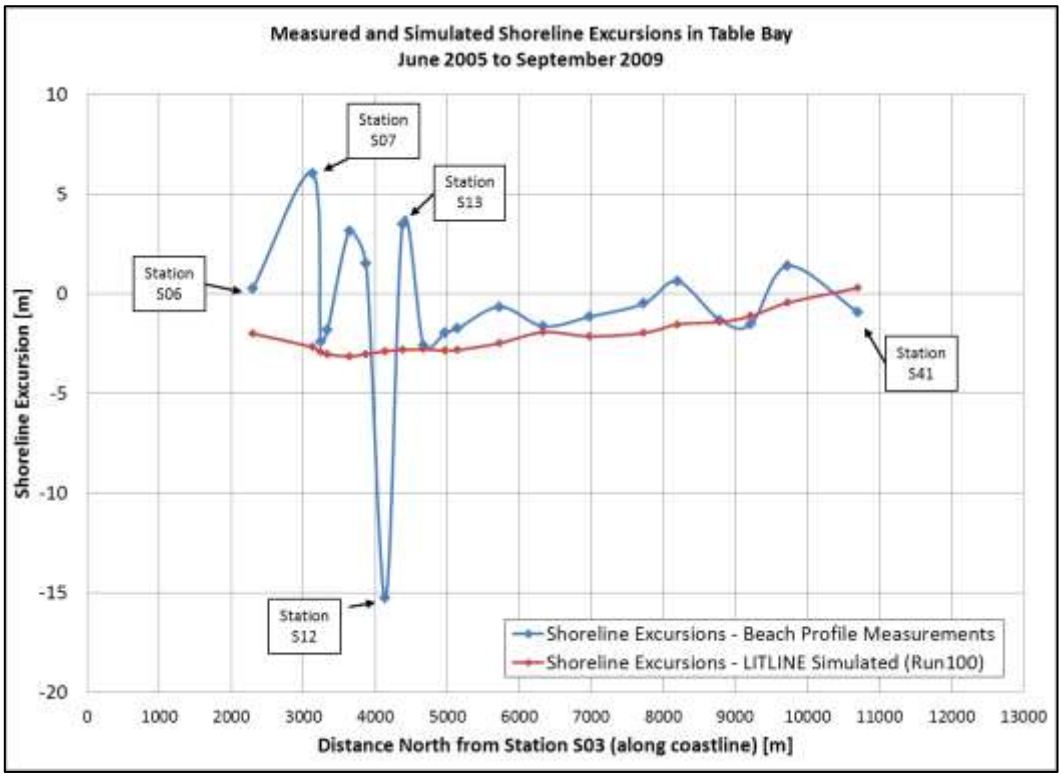

As can be seen from the figure, discrepancies between measured and simulated shoreline excursions exist in the southern third of the model domain, which can be described as the model slightly over-predicting the shoreline erosion. In the northern two-thirds, the model seems to accurately replicate the observed shoreline excursions.

It should be considered that not all physical characteristic of the Table Bay shoreline can be included in the LITLINE shoreline model. Aspects such as dune stabilization and/or dune trampling, which can have a significant impact on shoreline behaviour, cannot be included in the model. Simulation results therefore require a fair amount of judgement before being accepted as a true representation of the coastal processes.

It should further be considered that the bay-wide shoreline model has been setup using long-term shoreline trends, whereas during the validation period, it is attempted to replicate short-term shoreline trends. The short-term behaviour of shorelines is however unlikely to be limited to longshore events, but may be significantly impacted by short-term cross-shore events such as storm erosion. As such, differences between the measured and simulated shoreline are expected due to the relatively short validation period.

Public and private developments which are thought to interact with the littoral zone were introduced in Section 5.4. A large number of these developments are located within the southern half of Table Bay, in the areas wherein the shoreline excursions do not seem to have been accurately replicated by the bay-wide shoreline evolution model. It has further been discussed that since many of these developments are under threat due to shoreline erosion, public and private shoreline stabilization schemes have been implemented. These schemes include the fencing off of dunes, coupled with irrigation systems to promote dune vegetation, as well as the placement of sand bags to prevent further dune erosion.

Furthermore, it has been pointed out in Section 6 that continued beach steepening is being observed in the southern half of Table Bay, which indicates continued erosion in this area. It is therefore thought that the erosion being simulated and the erosion actually occurring on site are similar, but that these are occurring through different mechanisms. The model predicts a general landward movement of the profile, whereas the real erosion is occurring as profile steepening.

A further aspect which is noticeable in Figure 8-17 is the excessive erosion being observed at profile station S12. As indicated in Section 6.2.3, this is presumably caused by flanking erosion of the shore protection measures fronting the Milnerton Golf Club clubhouse. Since this effect is not included in the bay-wide shoreline evolution model, the discrepancy between measured and simulated shoreline at this location does therefore not suggest that the model is not functioning correctly, but rather that a local effect has not been included. This is confirmed by the fact that the shoreline is accurately predicted approximately 1 km north of profile station S12, at which point the flanking erosion effect of the shore protection measures of the Milnerton Golf Club would no longer have an effect.

In summary, it is concluded that although discrepancies exist between the measured and simulated shoreline positions, these can be explained by considering site specific conditions such as shoreline stabilization measures which are not included in the shoreline model, as well as the increased significance of short-term cross-shore sediment transport events which play a more prominent role during the relatively short simulation. Furthermore, considering that the Seli One is located in the northern half of Table Bay, in the area where the bay-wide model accurately predicts the short-term shoreline changes, the bay-wide shoreline evolution model is considered to be accurate for the current application.

8.6 Summary and Conclusion

The Table Bay longshore sediment transport system has been modelled by implementing the one-dimensional shoreline evolution model LITLINE by DHI. Due to the curved nature of Table Bay, a mapping approach was developed during which the curved coastline was mapped onto a straight coastline, to align with assumptions made by the software. In doing so, the relative angle between the coastline and the incident wave had to be kept constant, to retain the characteristics of the coastal processes of the bay.

It was concluded that through the implementation of the mapping approach, the longshore transport regime of Table Bay could be accurately replicated, both in terms of net longshore sediment transport and shoreline morphology. It was determined that local effects, such as the impacts of a short sandbag revetment along the Milnerton Golf Club clubhouse, potential local scouring effects near a staircase leading down to the beach, as well as the potential loosening of sand through large amounts of foot traffic, could not be included in the simulation, which meant that the measured and simulated shoreline morphology were often not the same. As such, significant engineering judgement was required when qualifying whether simulations results as being either accurate or inaccurate.

Furthermore, the temporal variability of longshore sediment transport rates has been highlighted. The net longshore transport rates have been observed to range between 24 000 m^3/year and 49 000 m^3/year at a representative location in Table Bay. It was therefore determined, that in general, when performing shoreline stability assessments, the longest possible duration needs to be analysed, incorporating all available data. If analysis periods are kept short, short-term variations such as cross-shore sediment transport processes may be falsely categorized as longshore processes, resulting in errors.

It has further been observed that in general, the shoreline excursions predicted by the one-dimensional shoreline model are smoother and less sporadic than shoreline measurements. This is related to the exclusion of short-term cross-shore processes from the model.

To conclude, the one-dimensional shoreline model LITLINE has been evaluated, through modifications relating to the curved nature of the bay, as being able to replicate the longshore sediment transport system of Table Bay.

9. LOCAL SHORELINE MODELLING – SELI ONE WRECK

9.1 Introduction

Two of the main study objectives discussed in Section 1.3 are the determination of the short-term and long-term impact of the Seli One shipwreck on the local sediment transport regime and the associated shoreline changes on the Table Bay beaches.

The short-term impact is defined as the impact prior to the 3rd July 2011. This date has been chosen since it coincides with the day on which a beach survey was performed by the author as part of this study. During this survey, the author measured beach cross-sections at regular intervals near the wreck to identify the altered shoreline position. Details of this survey campaign are included in Appendix B.

Following the evaluation of the accuracy of the local shoreline model in determining the impact of the Seli One shipwreck, an assessment of the long-term potential impact of the Seli One was made. The assumption during this assessment was that the vessel does not undergo any further breaking up, and remains in its current configuration indefinitely.

9.2 The Seli One as Detached Offshore Breakwater

Prior to commencing with the investigation of the impacts of the Seli One shipwreck, it was considered to be useful to attempt to classify the extent of the changes that were expected to be seen. The design procedures for offshore breakwaters covered in Section 3.4.2 were used to do this.

The length of the vessel is 178 m, whilst the distance offshore is in the order of 510 m. The relationship between the structure length and distance offshore of 0.35, the Seli One would result in a *subdued salient.*

The beach response index, I_s, of 4.84, also indicates the Seli One resulting in the formation of a *subdued salient*.

Both design methods therefore indicate that, although the Seli One is expected to result in the formation of a salient, the extent of this salient is expected to be limited. A tombolo is therefore not expected to form between the shoreline and the shipwreck, both in the short- and long-term.

9.3 Model Setup

9.3.1 Model Domain and Starting Shoreline

The domain of the local shoreline evolution model was significantly reduced compared to the bay-wide model discussed in Section 8. The southern boundary of the model was situated at approximately the southern end of the Dolphin Beach Hotel, whilst the northern boundary was approximately 600 m south of the rock outcrop at Blouberg. This represents an alongshore length of 2.75 km.

The starting shoreline for the local shoreline evolution model has been obtained from the results of the bay-wide shoreline model. It will be remembered that the validation period of the bay-wide model concluded on the 8th September 2009, immediately prior to the arrival of the Seli One wreck. The resulting shoreline position of the bay-wide model could therefore be used to generate the starting shoreline for the local shoreline model.

Due to the relatively small model domain, the shoreline encompassed within this model was fairly straight, with only a small change in shoreline orientation between the southern and northern ends being observed. This resulted in the shoreline mapping approach used for the bay-wide shoreline modelling not being necessary during this application. The simulated shoreline was therefore the real shoreline as shown in Figure 9-1, with the wave climate rotation not being necessary.

Similar to the bay-wide model, the shoreline of the local model was split into 5 m alongshore sections.

Figure 9-1: Starting Shoreline for Local Shoreline Evolution Model

Showing Wave Extraction Locations

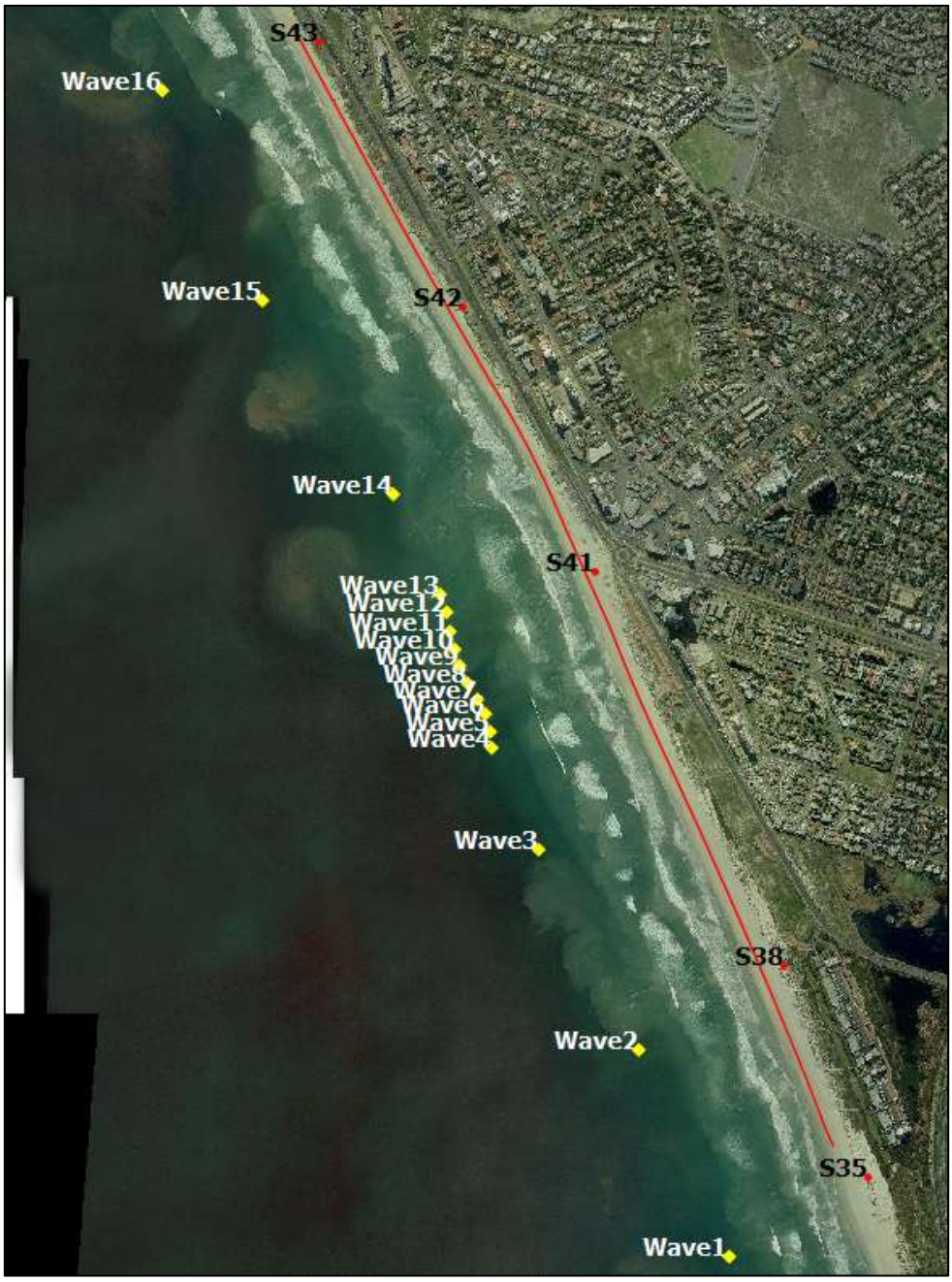

9.3.2 General Setup

Many of the model parameters used for the local shoreline model were similar to those of the bay-wide model, and will therefore not be discussed in as much detail here. For more detail, the reader is referred to Section 8.3.

The alongshore variation of cross-shore parameters was split into two sectors, the one being for the shoreline south of the traffic circle shown in Figure 9-1, whilst the second was for the section north of the traffic circle. This boundary was chosen since the beach slope south of the boundary is relatively flat, whilst this steepens north of the traffic circle.

Similar to the bay-wide model, no ocean currents were incorporated in the local shoreline model. Water level variations were obtained from the MIKE C-MAP database (DHI, 2011h). Although the parking lot along the Blouberg beachfront is thought to impact the shoreline behaviour somewhat, this structure was not incorporated in the model. Results were however interpreted to comment on the possible impact of the parking lot on the shoreline changes.

9.3.3 Wave Climates

One of the structures which can be incorporated in a LITLINE shoreline model is an offshore breakwater (see Section 4.3.5.2). During initial trial simulations, it was therefore thought that this structure could be used to describe the impact of the wreck on the local wave climate. The intention was therefore to determine the unaffected wave conditions offshore of the shipwreck using MIKE21 SW, apply these conditions to the offshore boundary of the LITLINE model, and let LITLINE calculate the impact of the wreck on the nearshore wave and current conditions. However, a model limitation relating to the way in which LITLINE calculates wave diffraction, based on simple wave diffraction diagrams (see Section 3.2.2) meant that this approach could not be used.

It has been indicated that if the offshore distance of a breakwater is short compared to its length, the diffraction effects at either end of the structure do not interact in the structure's lee, since there is insufficient distance between the structure and the coast for them to develop sufficiently. In the case of the Seli One however, this relationship does not hold, since the offshore distance is approximately three times as large as the length of the vessel. In this case therefore, diffraction effects do have sufficient space in the lee of the vessel to develop fully. Diffracted waves originating from either end of the wreck therefore interact with each other in the lee of the vessel, which is not accounted for in LITLINE. LITLINE is therefore unable to accurately replicate the nearshore wave climate in the lee of the Seli One wreck.

The impact of the wreck on the nearshore wave field was therefore calculated using the bay-wide wave transformation model, introduced in Appendix A. Slight changes had to be made to this model to incorporate the impact of the wreck, which was modelled as a solid structure, with a reflection coefficient of 1.0 (Figure 9-2). The remainder of the model setup was kept identical to that used for the bay-wide wave transformation modelling, to maintain the accurate calibration.

Figure 9-2: Nearshore Bathymetry showing Intact Seli One Shipwreck Prior to 4th September 2011

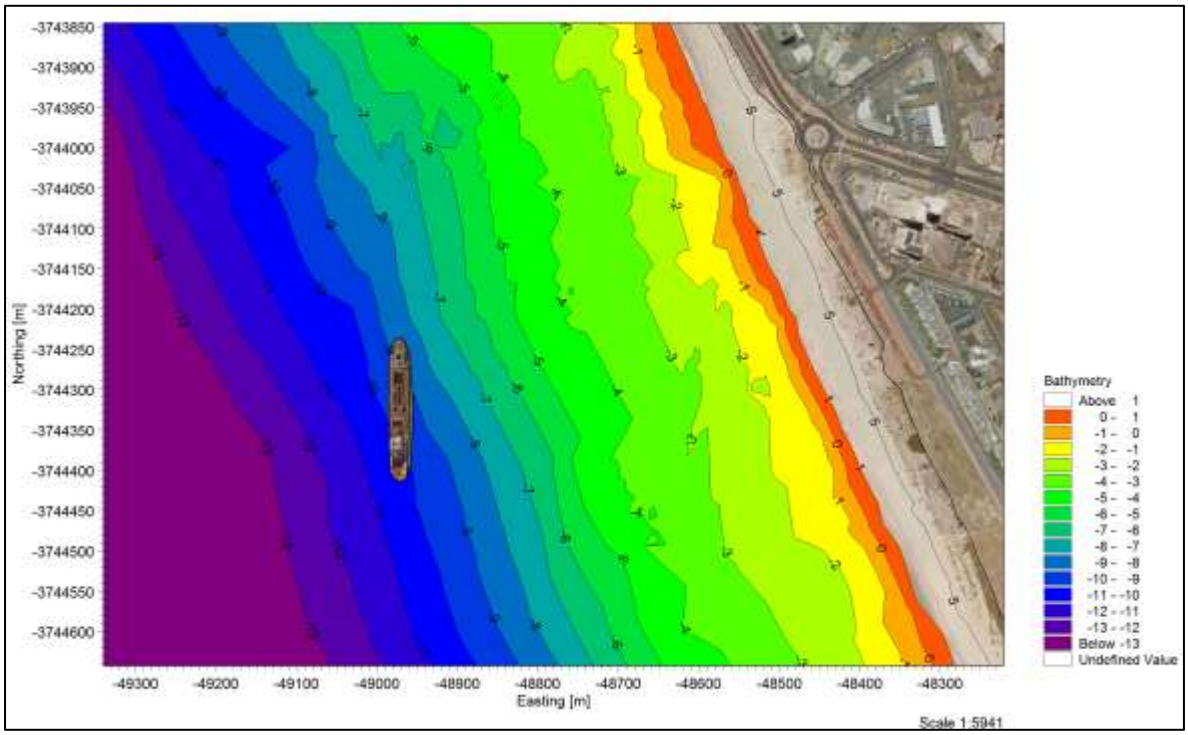

As introduced in earlier sections of the thesis, the Seli One shipwreck broke up during a large storm on the 4th September 2011. The broken up vessel was modelled as shown in Figure 9-3, with each of the three sections being a separate structure with a reflection coefficient of 1.0. This modelling methodology included the assumption that the vessel has broken up all the way to the seabed, not just above the water surface.

Figure 9-3: Nearshore Bathymetry showing Broken Seli One Shipwreck After 4th September 2011

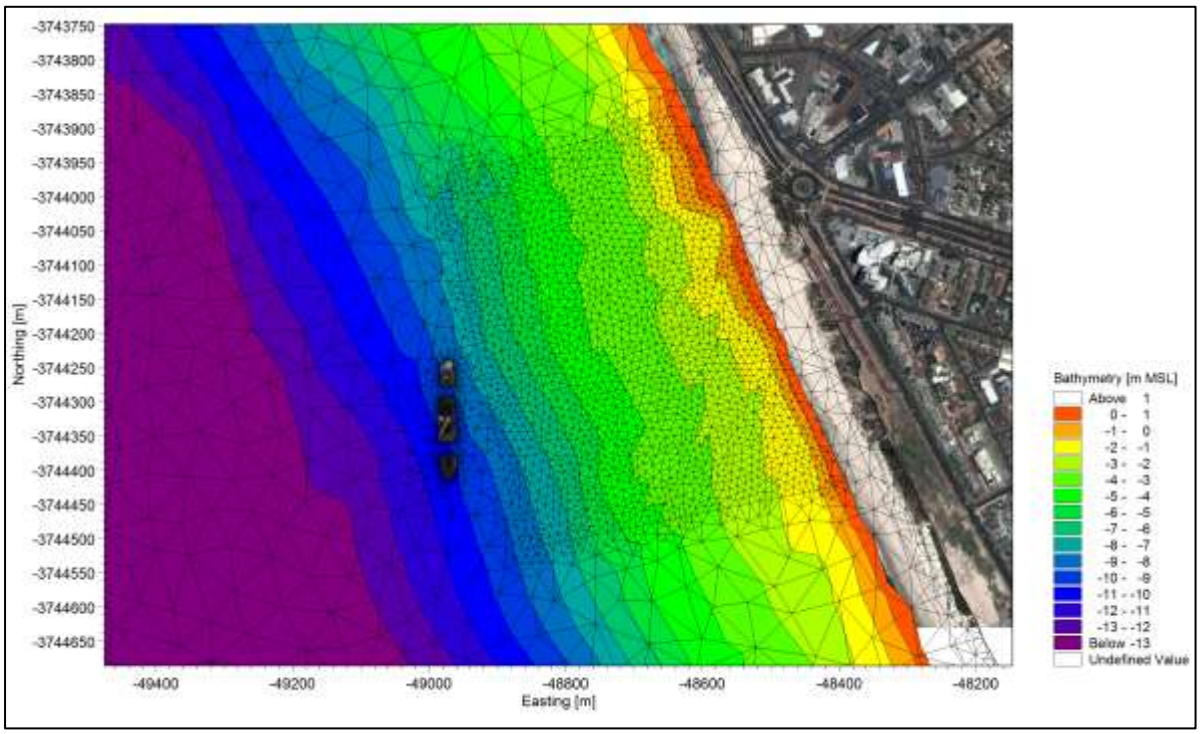

The wave transformation model's mesh was sufficiently refined around the shipwreck to resolve the gaps between the three pieces accurately. This is shown graphically in the figure above.

Naturally, for the influenced nearshore wave climate to be incorporated in the LITLINE shoreline evolution model, the wave extraction points needed to be inshore of the shipwreck. For the bay-wide shoreline model, wave climates were extracted at 500 m centres along the -10 m MSL depth contour. If this was repeated for the local shoreline model, the impact of the wreck would not be incorporated in the shoreline evolution analysis since the wreck has settled at a depth of between -8.5 m MSL and -10.5 m MSL. As such, for the local shoreline evolution model, wave climates were extracted at the -6 m MSL depth contour, as shown in Figure 9-1.

The impact of the Seli One shipwreck on the average wave height (H_{rms}) along the model domain is shown in Figure 9-4. From this figure, it is clear that this impact is fairly localized, within approximately 250 m either side of the shipwreck. The average wave height is drastically reduced, from approximately 0.65 m to 0.25 m. It is noted that the difference in wave height between the intact and broken vessel are fairly minimal, with the waves resulting from the broken vessel being slightly larger. Finally, it is observed that the impact of the wreck is situated off-centre relative to the ship. This may be due to the slightly oblique wave attack, with the most predominant wave direction being slightly more northwards than the shoreline orientation.

Figure 9-5 shows the impact of the intact and broken shipwreck on the average wave direction along the local shoreline model domain. It is noted that on the southern side of the wreck, the effect is an anti-clockwise rotation of the waves, caused by diffraction into the lee of the vessel. Conversely, the effect at the northern side of the wreck is a clockwise rotation of the mean wave direction. It is noted that the clockwise rotation at the northern side of the wreck is larger than the anti-clockwise rotation at the southern side of the vessel. This is caused by the relative orientation of the vessel to the mean wave direction.

Figure 9-4: Impact of Seli One Shipwreck on Nearshore Wave Height (H_{rms})

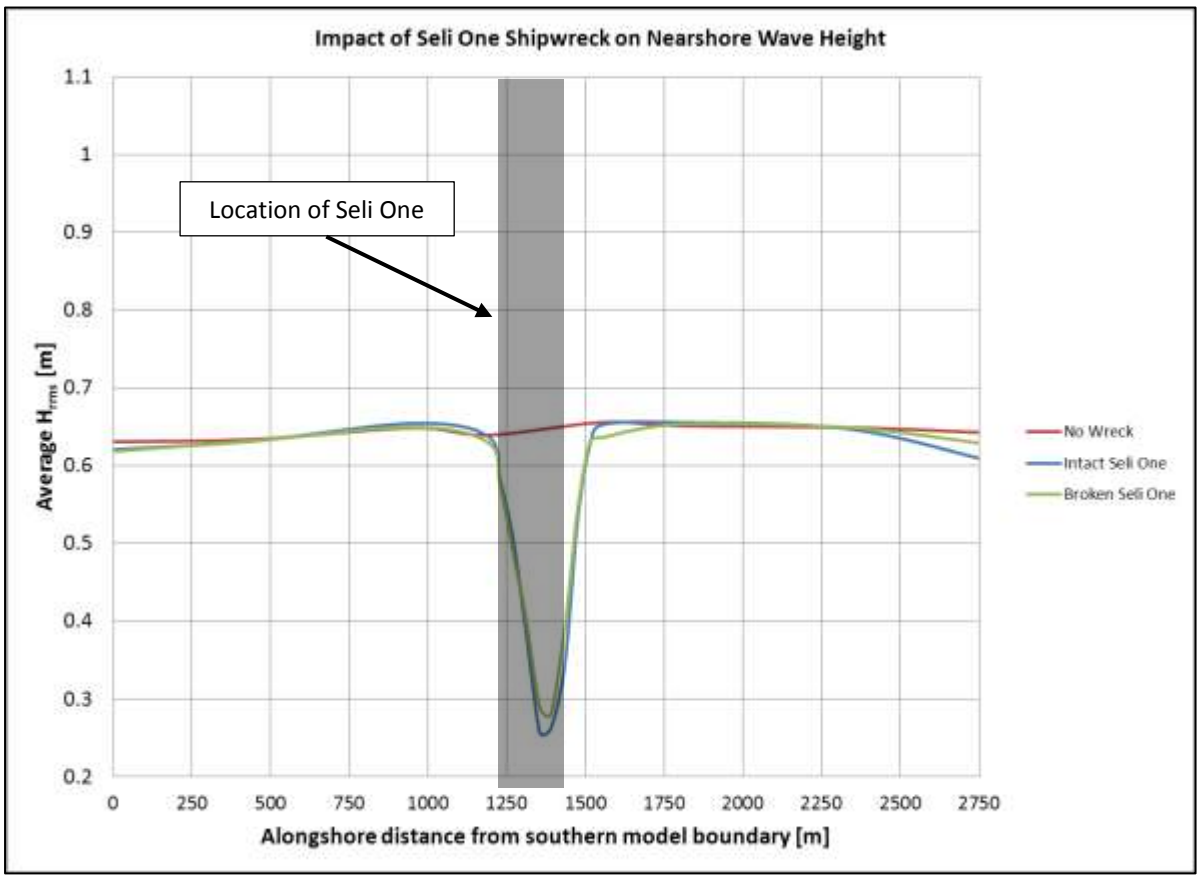

Figure 9-5: Impact of Seli One Shipwreck on Nearshore Wave Direction (D_p)

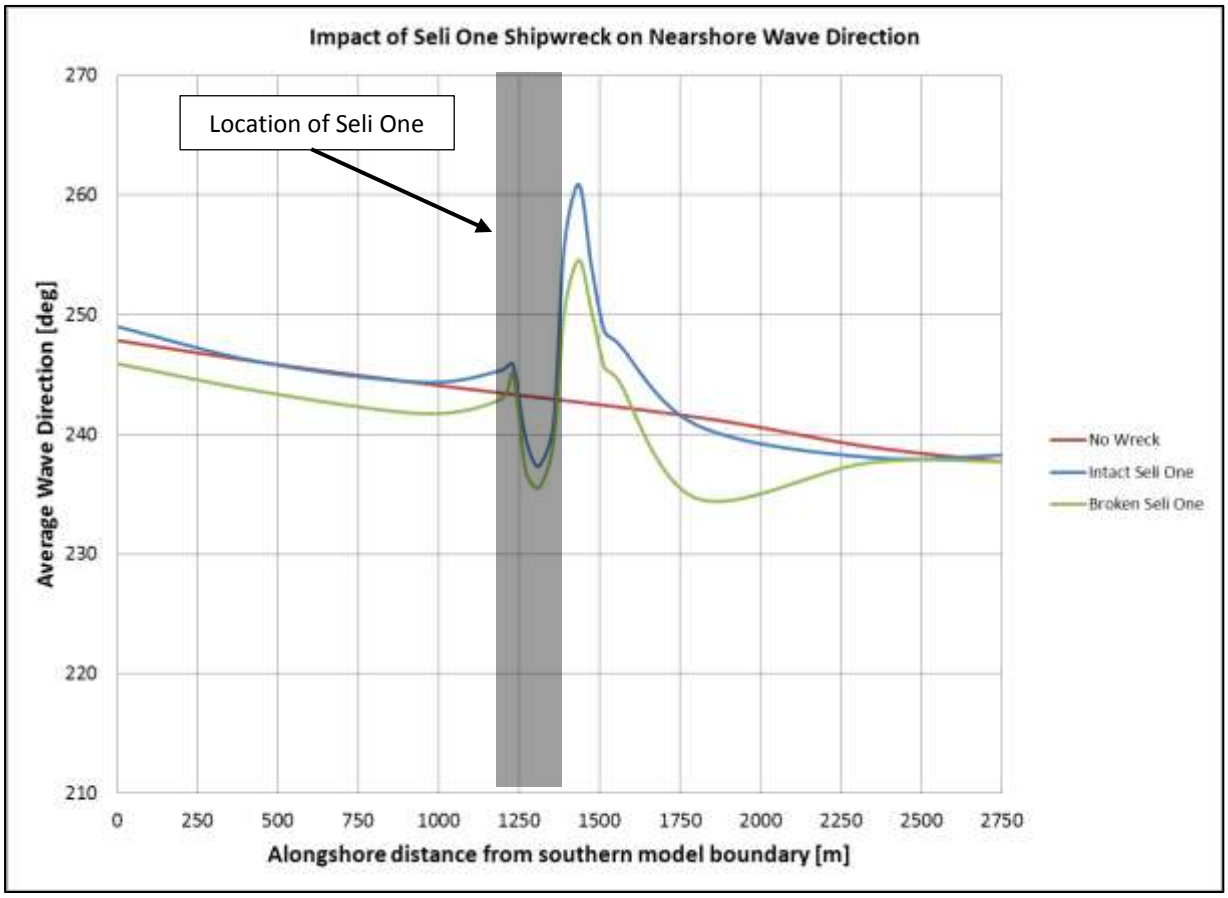

Furthermore, it is noted that the impact of the shipwreck on the average annual wave direction stretches over a longer alongshore distance than the effect on the average wave height.

9.3.4 Boundary Conditions

Boundary conditions for the local shoreline model, in terms of inbound and outbound sediment transport volumes, were obtained from the results of the bay-wide model. The boundaries of the local model were therefore simulated as closed boundaries, with a sediment source and sink being placed at the southern and northern model ends respectively. The magnitude of this source/sink was equivalent to the net longshore transport rate at the appropriate position in the bay-wide model.

9.4 Model Validation

Calibration of the local shoreline model as such was not necessary, since the input information and model settings were already calibrated during the bay-wide shoreline modelling part of this study. Validation was however still necessary to ensure that the net longshore transport rate calculated by this local shoreline model was representative of the site and similar to the rates obtained from the bay-wide model.

As mentioned previously, the annual net longshore transport rates vary significantly over time. To avoid a scenario in which the local shoreline model is validated against fairly short-term environmental conditions, the validation period of the local model was chosen to be equal to the calibration period of the bay-wide model,

being from May 1977 to May 2005. The thinking here was that the longer the validation period, the greater the confidence that can be attributed to the correct functioning of the model.

The resulting net northerly longshore sediment transport rates of the two models are shown in Figure 9-6. From this figure, it is clear that both models show a similar transport rate, with the local model giving slightly higher values compared to the bay-wide model. These differences are however limited to approximately 2 000 m^3/year, and therefore not thought to make a noticeable difference in terms of shoreline evolution.

Figure 9-6: Net Longshore Transport Rates of Bay-Wide and Local Shoreline Models

May 1977 to May 2005

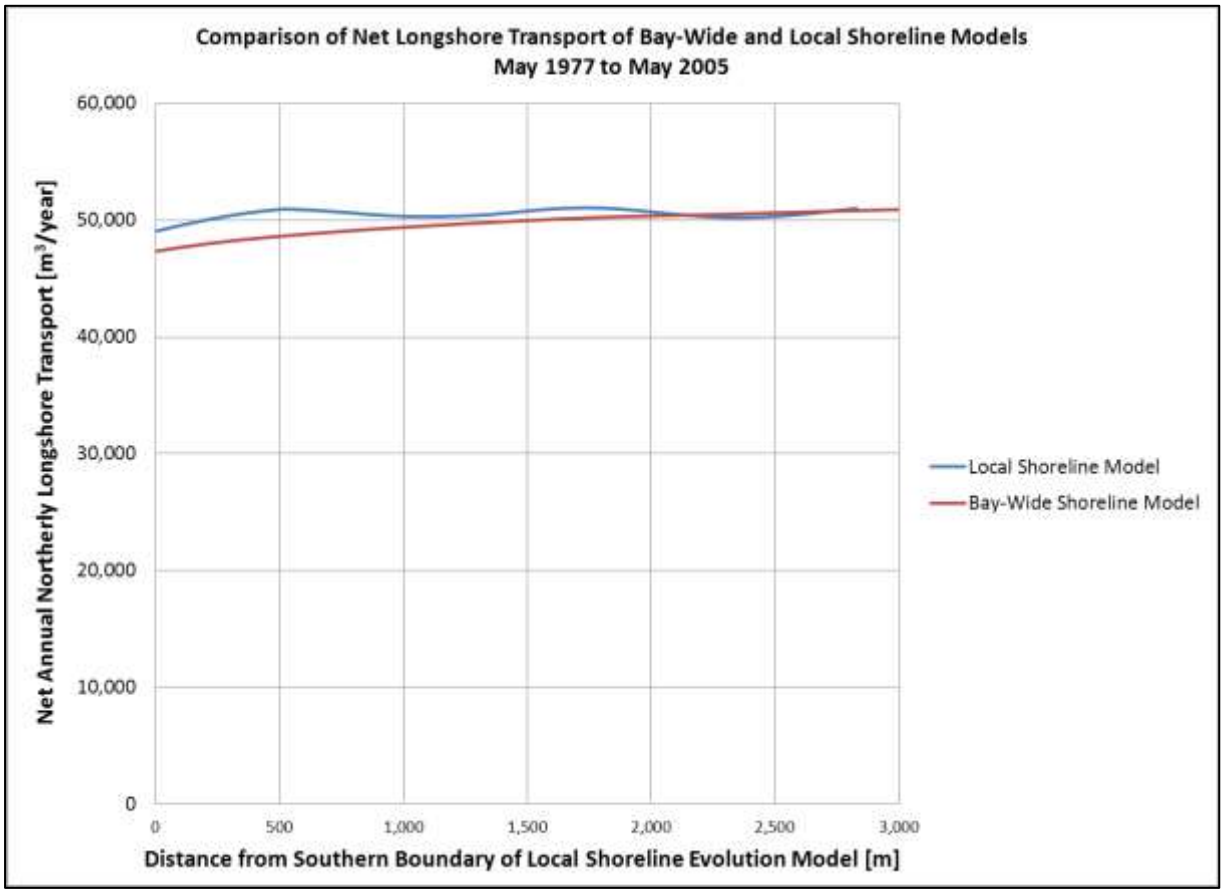

9.5 Model Results: Short-Term Impact of Seli One Shipwreck

The impact of the Seli One shipwreck on the net longshore sediment transport between the 9th September 2009 and the 3rd July 2011 is shown in Figure 9-7. From this figure it can be seen that in the lee of the shipwreck, the net northern longshore transport is reduced by approximately 37 500 m^3/year, with this effect decreasing exponentially with distance away from the wreck. The impact is effectively zero at a distance of approximately 1.5 km either side of the vessel.

Considering the initial average net longshore transport rate in the area of the Seli One wreck, being in the order of 50 000 m^3/year, a reduction as shown in Figure 9-7 suggests that the shipwreck does not result in the complete blockage of longshore sediment transport within this initial 21 month period. It can be calculated that approximately 12 500 m^3/year of sediment is still transported northwards in the lee of the shipwreck.

Figure 9-7: Impact of Seli One Shipwreck on Net Longshore Sediment Transport [m^3/year]

9^{th} September 2009 to 3^{rd} July 2011

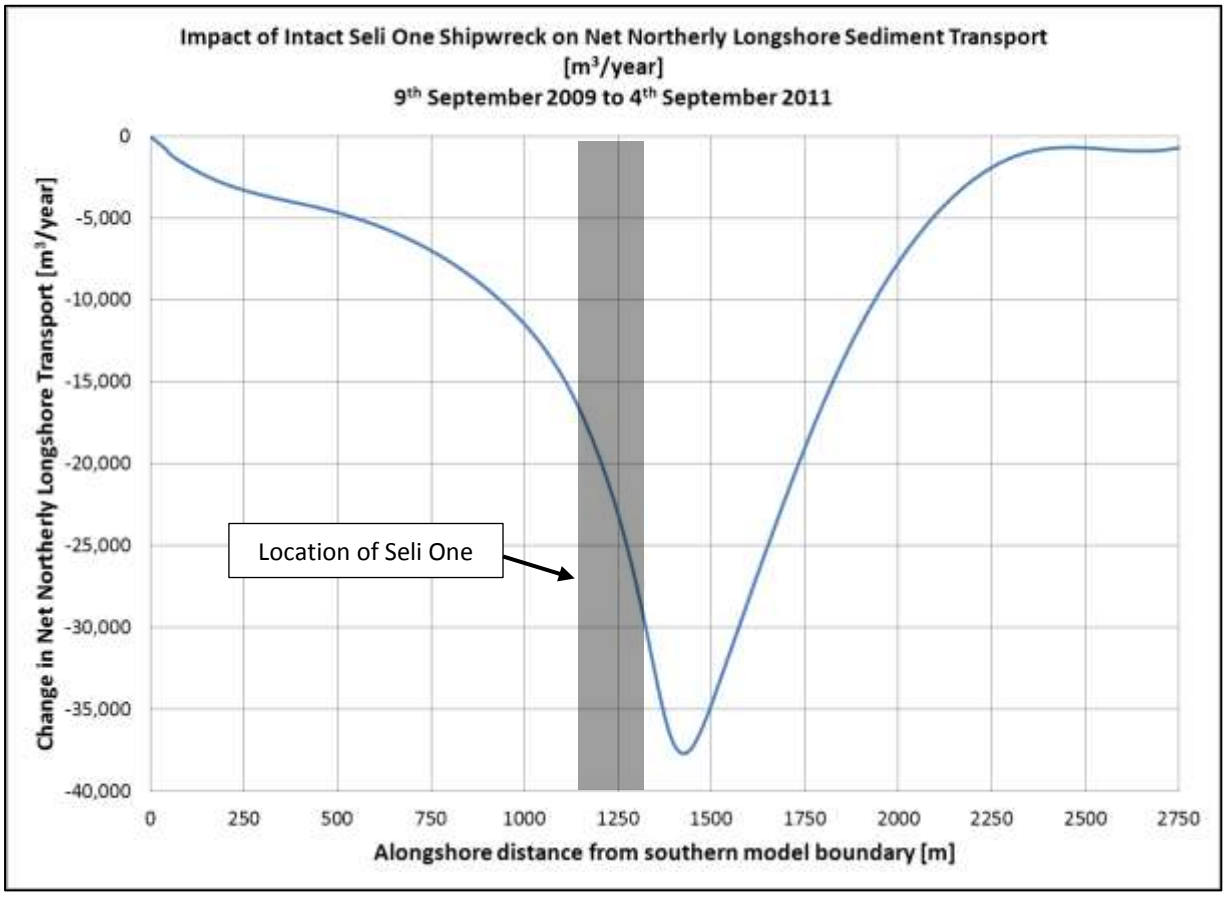

The coastal processes surrounding a detached breakwater were discussed in Section 3.4.1. During this discussion, it was pointed out that the differential alongshore wave height distribution resulting from the effects of a shipwreck creates opposing currents from either end of the wreck. The fact that the longshore sediment transport is not completely blocked by the Seli One suggests that the southward longshore current, caused by the wave height differential between the lee of the vessel and the area to the north of the vessel, is sometimes reversed to become a northern current. In this way, the current direction becomes uniformly northwards, allowing sediment to pass through the lee of the shipwreck.

For this to occur, the wave attack is required to be quite oblique from the south. In this way, the sheltering effect of the wreck will not be as effective as during a normal wave attack, which may be sufficient to overcome the southward longshore current created by the differential wave heights. It is further thought that this condition occurs during the summer months, during which strong south-easterly winds predominate.

Figure 9-8 shows three curves, the blue and red being the simulated shoreline positions on the 3^{rd} July 2011 excluding and including the effect of the Seli One respectively. The green line shows the direct impact of the Seli One, from which the background shoreline behaviour has been removed. From this figure it can be seen that the maximum shoreline accretion resulting as a direct result of the Seli One shipwreck is approximately 27.5 m in the lee of the vessel, with shoreline erosion to the extent of 15 m being observed to the north of the vessel. It is further clear that at a distance of approximately 1.3 km north of the wreck, no impact on the shoreline can be observed. The impact of the vessel on the shoreline approximately 1.3 km south of the wreck is minimal, less than approximately 1 m.

Figure 9-8: Impact of Seli One Shipwreck on Shoreline Morphology

9th September 2009 to 3rd July 2011

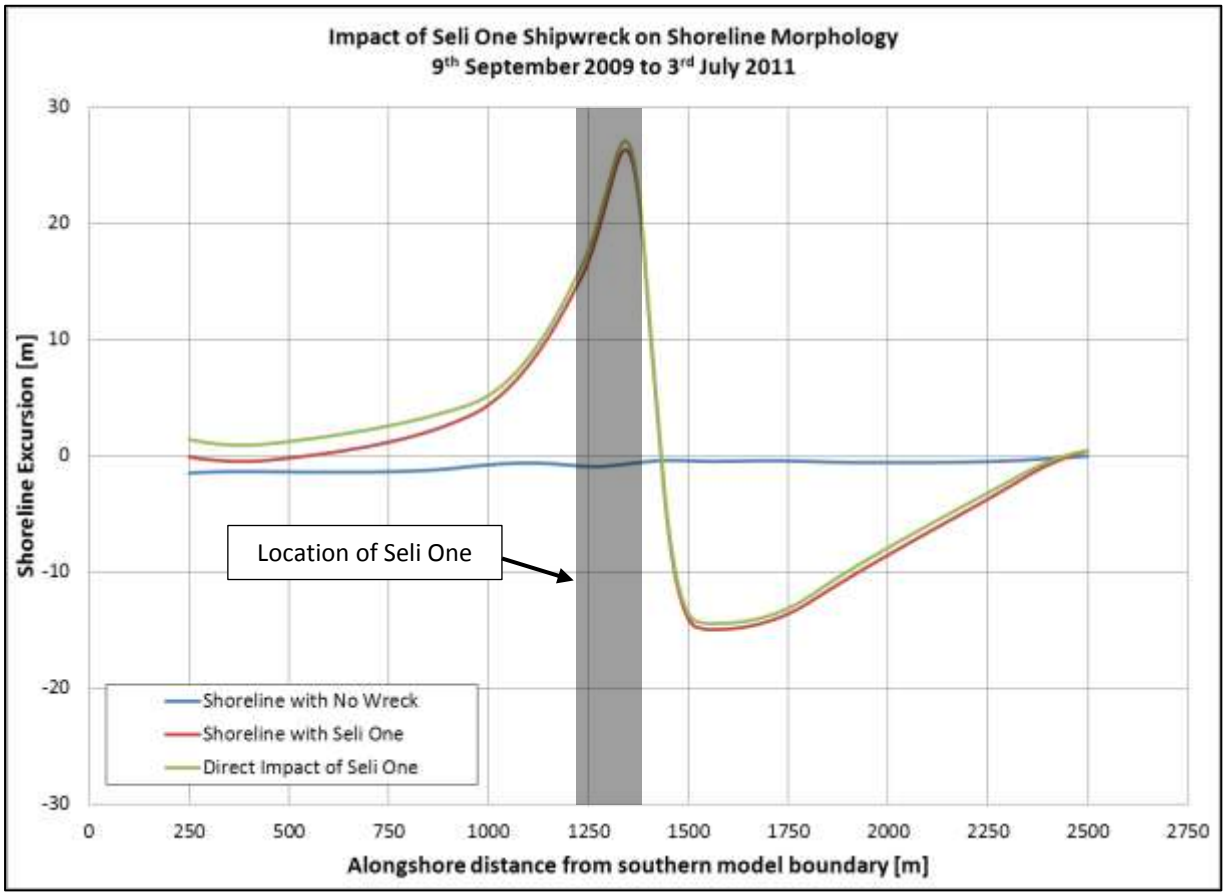

Reference is made to Section 6.2.6, in which it is stated that the impact of the Seli One is accretion to the extent of approximately 15 m, rather than the 27.5 m stated here. Two aspects should be considered relating to this. The first aspect is that the beach profile measurements used to determine the 15 m excursions were taken in March 2009 and February 2010, whereas the 27.5 m is related to the period between the 9th September 2009 and the 3rd July 2011. These are clearly two different periods, which would have resulted in different shoreline excursions being observed. Secondly, as will be shown in later sections, in February 2010, the beach salient in the lee of the wreck had not yet fully developed. This means that the impact of the wreck, as identified by the beach profile measurements, would not have included the entire extent of the accretion, thereby being less than the salient as identified by the numerical model.

Comparing Figure 9-7 and Figure 9-8, it may be noticed that the peak of the accreted shoreline is situated southwards of the peak of the reduction in longshore sediment transport rate. This is considered to be an accurate representation of the coastal process, since for the transport rate reduction to be maximized, the sediment would have had to be deposited before this location. If the net transport direction is northwards, the shoreline accretion would have to be offset to the south compared to the change in net longshore transport rate.

Figure 9-9 shows the simulated and measured shorelines on the 3rd July 2011 including the impact of the Seli One shipwreck. A comparison of these reveals a strong correlation, with the extent of the simulated salient being very similar to the measured salient.

It may further be observed that the model generally over-predicts the shoreline erosion to the north of the vessel. It may also be observed that the measured salient shape is more gradual, being spread out over a longer alongshore distance compared to the simulated salient, which is a shorter feature.

The over-prediction of the erosion to the north of the Seli One is thought to be related to the effect of the parking lot along this coastal stretch. Although this is not thought to have the same impact as, say, a revetment, the parking lot is expected to hold the top of the beach profile in position to a certain extent. The effect of this is that shoreline erosion in reality occurs more as profile steepening process, compared to a general retreat of the shoreline. The over-prediction of the modelled shoreline erosion is therefore not thought to be an incorrect description of the coastal process, but rather a discrepancy in the mechanism in which erosion has occurred and is being modelled in this area.

Figure 9-9: Surveyed and Simulated Shoreline Position during Beach Survey on 3rd July 2011

Regarding the time-based behaviour of the shoreline morphology in the lee of the wreck, Figure 9-10 shows the total shoreline movement, the shoreline movement per day as well as the average rate of the shoreline

movement from the 9th September 2009 to the 3rd July 2011. It should be noted that this represents only one alongshore location in the lee of the Seli One, and does therefore not necessarily represent the entire shoreline behaviour.

This figure shows a rapid initial shoreline movement, with the average accretion rate of approximately 0.5 m/day being observed for the first two months. The shoreline accreted 20 m during this period, representing 75% of the total accretion until the 3rd July 2011.

Following the initial rapid accretion, mild additional accretion is observed from November 2009 until May 2010, following which little shoreline accretion is observed. This therefore indicates that a new equilibrium shoreline was reached at the beach salient within approximately nine months of the arrival of the Seli One. If the vessel would not have broken up during a storm in September 2011, it could be argued that minimal additional shoreline changes would have occurred in the lee of the shipwreck.

Figure 9-10: Maximum Shoreline Accretion due to Seli One Shipwreck

And Corresponding Rate of Shoreline Movement from 9th September '09 to 3rd July '11

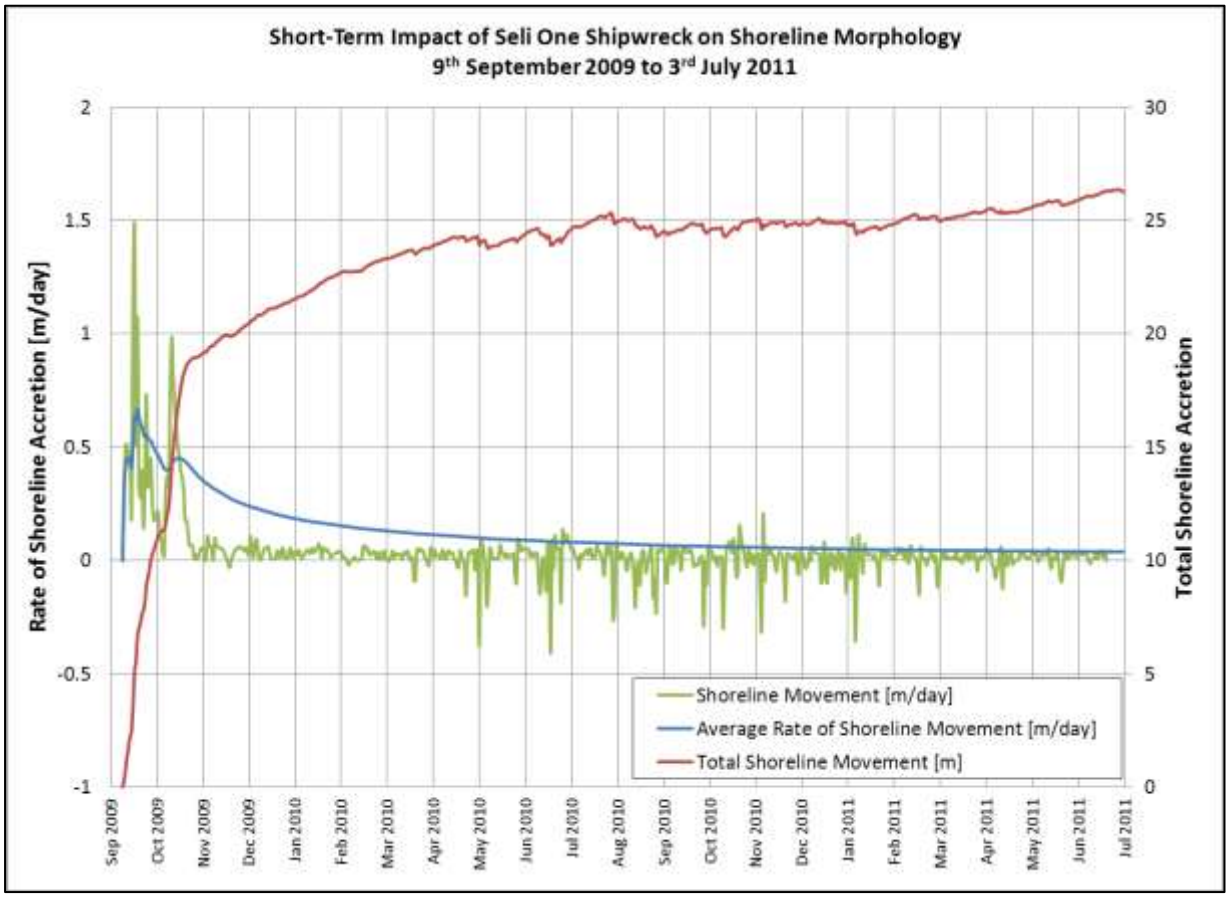

9.6 Model Results: Long-Term Potential Impact of Seli One Shipwreck

The long-term potential impact of the Seli One shipwreck was calculated by extending the simulation investigating the short-term impact of vessel to the 31st December 2024. The resulting shoreline of the short-term model was used as the starting shoreline for the extended model, with the input wave climate now being changed to that resulting of the broken up vessel. In doing so, the time-based change of the wreck configuration was included in the investigation into the long-term potential of the Seli One wreck.

Figure 9-11 shows the temporal average impact of the shipwreck on the net northerly longshore sediment transport rate between the 9th September and the 31st December 2024. Comparing this to Figure 9-7, it is clear that this impact is significantly reduced, to a reduction of approximately 7 500 m^3/year. This effect decreases linearly to become a non-impact at a distance of approximately 1.5 km either side of the vessel.

This therefore suggests that more sediment is able to bypass in the lee of the broken up Seli One compared to the intact Seli One. This is related to two facts. Firstly, and most importantly, more wave energy is able to get to the lee of the broken shipwreck, due to the gaps in the structure. In this way, the difference in wave height between the lee and the areas adjacent to the wreck is reduced, which means that the longshore current generated due to the wave height differential is reduced. More importantly, this means that the southward current on the northern side of the wreck is weakened, resulting in more frequent wave events being able to reverse this current. This results in an increase in the frequency of sediment bypassing through the lee of the wreck, which results in the reduction in the net longshore sediment transport resulting from the broken shipwreck to be reduced compared to the intact shipwreck. Secondly, the fact that this simulation is run for a longer duration means that any changes in terms of net longshore transport are divided by a longer duration, resulting in a lower average rate of reduction.

Figure 9-11: Impact of Seli One Shipwreck on Net Longshore Sediment Transport [m^3/year]

9th September 2009 to 31st December 2024

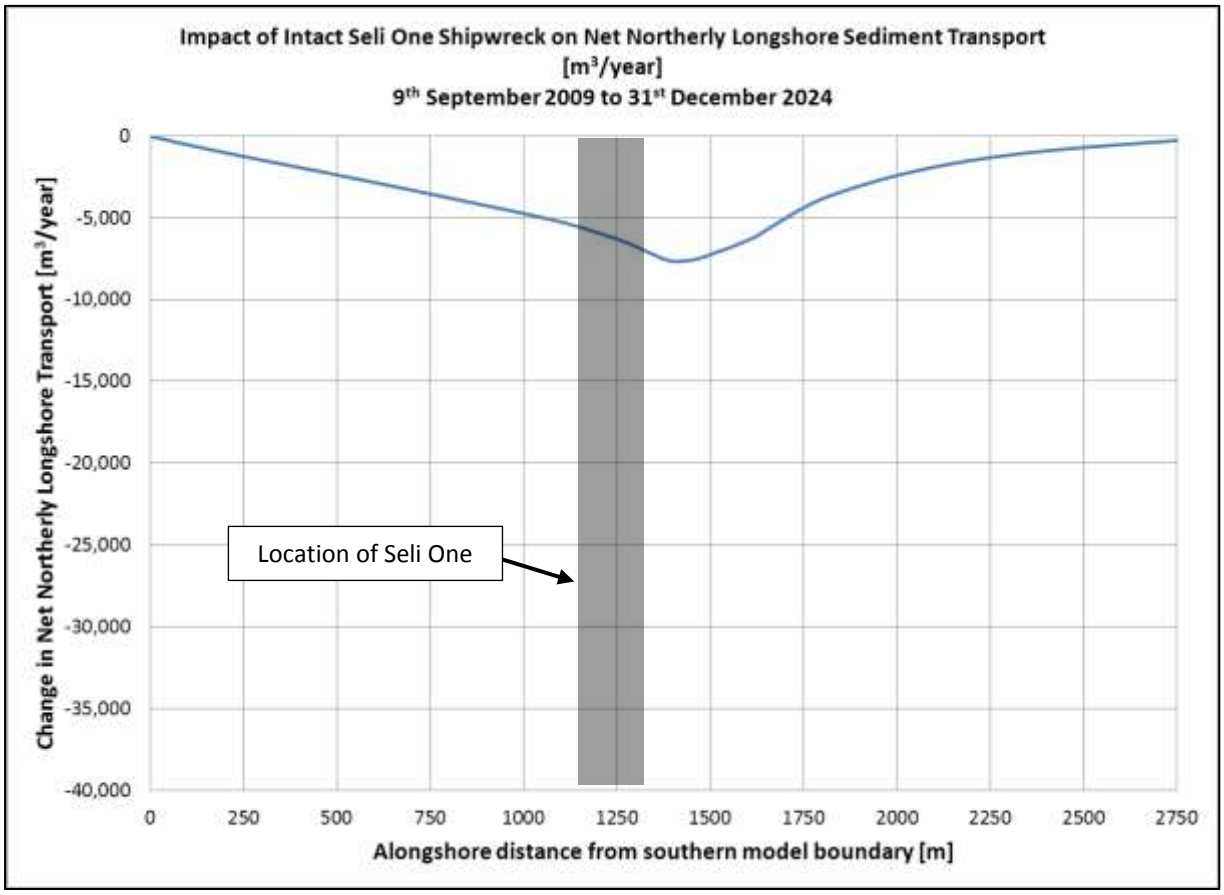

Figure 9-12 shows the long-term potential impact of the wreck on the shoreline positions, showing the fictive shoreline position excluding the impact of the wreck, the shoreline resulting from the wreck, as well as the direct impact of the wreck. Comparing this figure to Figure 9-8, the salient excursion has reduced from approximately 27 m at the intact wreck to approximately 15 m due to the combined intact and broken up vessel. This 12 m reduction relates to the reduced impact of the broken up vessel on the nearshore wave dynamics in the lee of the vessel.

Furthermore, it is clear that the updrift accretion resulting from the wreck has increased to approximately 8 m, which extends to the southern model boundary, indicating that this effect extends further south than the model domain. This shows that, although it has been shown that the salient in the lee of the vessel had reached an equilibrium shape within a few months of the vessel's arrival, the shoreline adjacent to the salient had not reached equilibrium within the same time period. This is thought to be related to continued sediment deposition between the vessel and the beach (i.e. not on the beach), thereby resulting in a blockage of the sediment transport occurring lower down the cross-shore profile. This phenomenon will be discussed in more detailed in Section 11.

Figure 9-13 shows the modelled shoreline positions excluding and including the impact of the Seli One on the 31st December 2024. It should be noted that the shoreline resulting from the Seli One wreck includes the background shoreline behaviour. The accretion and erosion on the updrift and downdrift sides of the wreck respectively are evident. The erosion of up to 25 m within the first 1 km north of the wreck may result in the damage of public infrastructure, referring especially to the public parking lots and the coastal road situated immediately behind the parking lots.

Figure 9-12: Impact of Seli One Shipwreck on Shoreline Movements

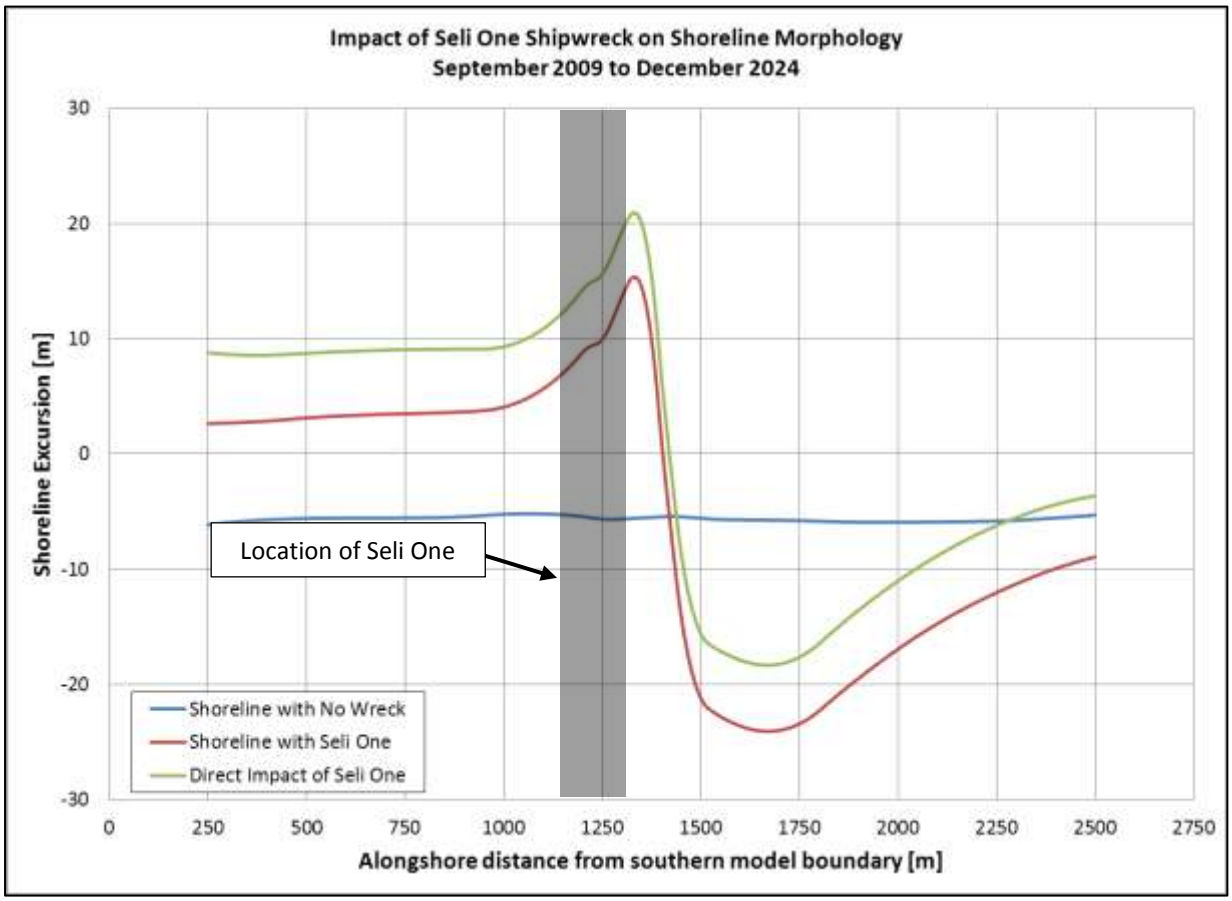

Figure 9-13: Long-Term Potential Impact of Seli One Shipwreck – 31st December 2024

Figure 9-14 summarizes the time-based shoreline behaviour of the salient over the duration of the long-term simulation. Similar trends as observed previously can be identified here. The rapid accretion following the arrival of the wreck can be observed, as well as the levelling off of this accretion during the subsequent months. In addition to this, it can be observed that following the breaking up of the vessel in September 2011,

a rapid retreat of the salient can be identified, to the extent of approximately 12 m. The duration of this retreat is approximately three months.

Furthermore, it can be observed that following the rapid erosion of the salient following the break-up of the wreck, the salient seems to reach a new dynamic equilibrium. The gradual erosion of the salient is thought to be related to the background shoreline erosion, not the erosion of only the salient.

The seasonal variability of the shoreline position becomes evident from Figure 9-14, with accretion occurring during the summer months, and erosion occurring during the winter months. These short-term shoreline variations however cancel each other out in the long-term.

Figure 9-14: Maximum Shoreline Accretion due to Intact and Broken-Up Seli One Shipwreck And Corresponding Rate of Shoreline Movement from September 2009 to September 2024

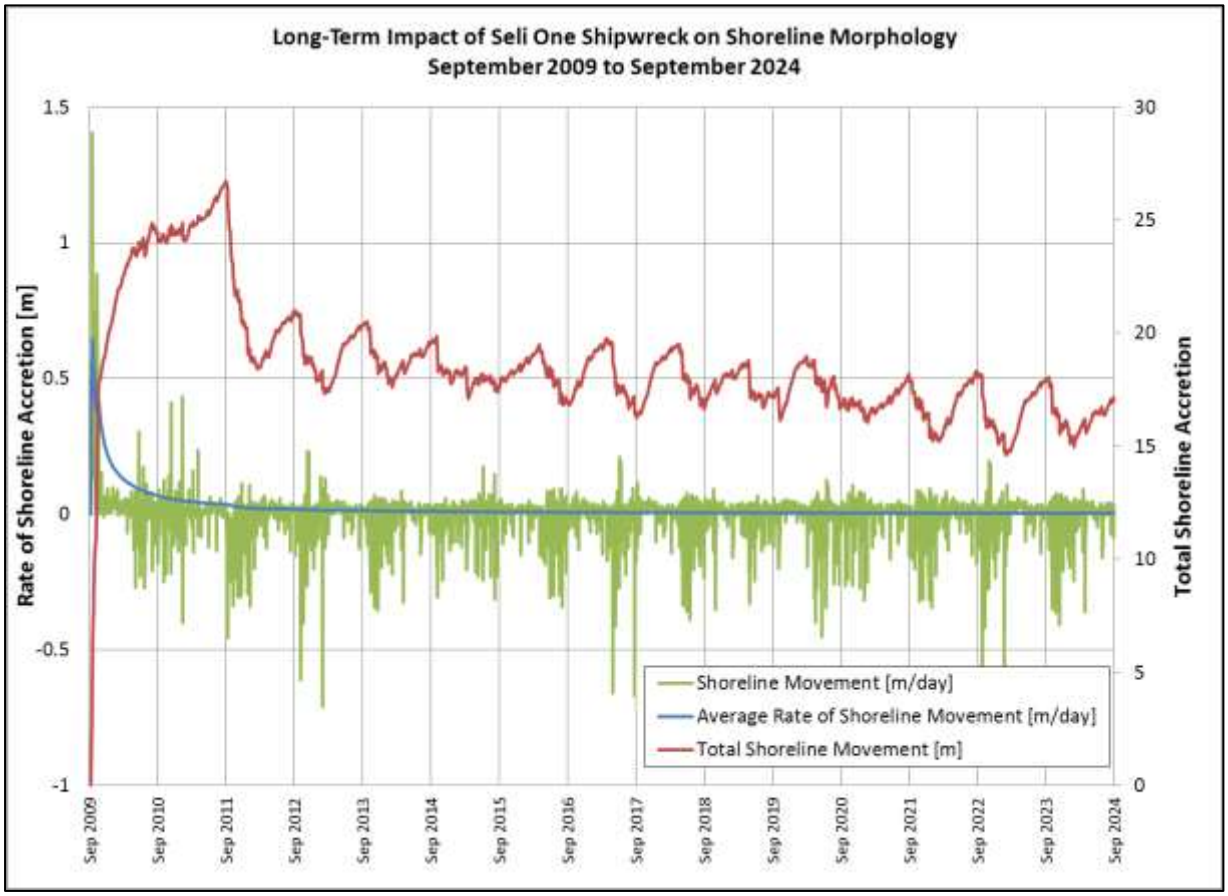

9.7 Summary and Conclusions

The one-dimensional shoreline evolution model LITLINE by DHI has been used to assess the impact of the Seli One on the local Blouberg shoreline behaviour. This investigation was split into a short-term study, from the 9th September 2009 to the 3rd July 2011, and a long-term study, from the 3rd July 2011 to the 31st December 2024, to investigate the long-term potential of the Seli One shipwreck.

Prior to the commencement of the modelling work, the impact of the Seli One on the local shoreline was classified as being a subdued salient, i.e. not resulting in the ultimate formation of a tombolo, utilizing existing

empirical relationships. This meant that it was expected, that the longshore sediment transport is not blocked off completely, and that the ultimate formation of a tombolo was unlikely.

It was determined that the LITLINE model did not simulate the wave diffraction effects in the lee of the vessel correctly, caused by assumptions made of the length of the vessel relative to her distance offshore. The wave diffraction effects were subsequently calculated using a wave transformation model, with the resulting wave climate in the lee of the vessel being applied to the LITLINE model. The shipwreck, as such, was therefore not applied directly in the shoreline model.

Results of this wave modelling exercise have shown that the wave heights in the lee of the vessel are significantly reduced compared to the no-wreck situation. It has further been shown that the effect of the broken up vessel in terms of wave heights is fairly insignificant compared to the intact vessel. Changes in wave directions due to the arrival of the shipwreck have also been determined, which has indicated a clockwise rotation at the northern end of the vessel, and a southern rotation at the southern end of the Seli One.

The approach of determining the wave conditions inshore of the wreck through a wave transformation model, and applying these conditions to the shoreline evolution model, has produced excellent results. It has been shown that, as expected, the shipwreck has resulted in a significant reduction the net longshore sediment transport rate in the lee of the vessel, but that this reduction has not been a complete blockage of longshore transport. It has further been shown, by comparing the simulated shoreline with the measured shoreline on the 3rd July 2011, that the model accurately replicates the extent of the beach salient.

Furthermore, it has been shown that approximately 75% of the salient accretion occurred within the first two months of the vessel's arrival.

The long-term potential of the Seli One shipwreck, in its current broken up configuration, has been modelled and discussed. This has shown that the salient width resulting from the shipwreck is reduced to approximately 20 m, compared to the initial 27 m. However, due to the continued deposition of sediment between the vessel and the beach, moderate amounts of additional accretion are expected along the southern beaches, whilst some additional erosion is expected along the northern beach.

It can be concluded that the shoreline changes occurring in the lee of the Seli One are, in fact, occurring as a direct result of the shipwreck on the local wave and current conditions.

In addition, it can be concluded that LITLINE is able to reasonably replicate and predict the impact of the Seli One shipwreck on local shoreline morphology. It is further concluded that, in general, depending on the length of the vessel relative to her distance offshore, the altered wave climate needs to be determined in a separate wave transformation model to be subsequently applied to the shoreline model.

It is further concluded, that shipwrecks have the potential to significantly alter local shoreline morphology in general. Depending on local conditions, this may pose significant risks to seaside infrastructure. Considering the rapid rate at which the initial shoreline changes occur, a limited window of opportunity exists to remove the shipwreck from the coast to prevent damage to seaside infrastructure due to rapid shoreline erosion.

Considering a scenario where a vessel runs aground near the Milnerton Golf Club clubhouse for example, erosion to the extent of 15 m within two months in front of the clubhouse would result in serious undermining risks for this building.

10. LOCAL SHORELINE MODELLING – WORST CASE GROUNDING SCENARIOS

10.1 Introduction

As mentioned during the discussion of the study aims and objectives in Section1.3, two worst-case vessel grounding scenarios were investigated in addition to the Seli One. These scenarios can broadly be described as the worst-case parallel and perpendicular grounding scenarios.

The intention during these investigations was to simulate the impact of the largest possible shipwreck likely to occur in the waters of Table Bay. Since most vessel traffic in Table Bay is generated by the Port of Cape Town, this vessel was chosen to be the largest vessel that can call at the port, which was determined to be a 6 000 TEU container ship (Ruthenavelu, 2011). The dimensions of this vessel are summarized in Table 10-1 (Ruthenavelu, 2011).

Table 10-1: Characteristics of 6 000 TEU Container Ship (Ruthenavelu, 2011)

Length Overall	Beam	Loaded Draft	Ballast Draft
350 m	45 m	14 m	9 m

10.1.1 Worst-Case Parallel Grounding Scenario Characterization

The worst possible impact caused by a shipwreck orientated parallel to the shoreline is likely to be caused by a vessel which is close to or within the surfzone. The position at which a vessel comes to rest when running aground is dependent on numerous factors, most importantly the water level and draft of the vessel. By combining these parameters, the worst possible grounding scenario for a vessel could be identified.

As shown in Table 8-2, the highest astronomical tide for Table Bay is +1.195 m MSL. Including a storm surge allowance of 0.75 m, the highest possible water level for Table Bay is in the order of +1.95 m MSL. Considering a ballast draft of 9 m, it is likely that the closest a 6 000 TEU vessel can get to the shoreline is the -7 m MSL depth contour.

The worst-case parallel scenario was therefore taken as the grounding of a 350 m long vessel, located along the -7 m MSL depth contour. To be able to compare these results to those obtained during the Seli One investigation, this larger vessel was simulated to have run aground in the same alongshore location as the Seli One.

10.1.2 Worst-Case Perpendicular Grounding Scenario Characterization

Although it may seem unlikely that a vessel remains in a perpendicular orientation relative to a shoreline after running aground, depending on water levels and the speed of the vessel, it may have gotten sufficiently high up on the beach to remain in that orientation. Examples of such events are available, one of which is shown in Figure 10-1. Here a fishing trawler ran aground at Clifton near Cape Town during low visibility conditions.

The vessel used during this investigation was the same 6 000 TEU vessel introduced in the previous section. Since the vessel approaches the shoreline head-on during this scenario, it was thought that it is able to run higher up onto the beach than the -7 m MSL depth contour discussed earlier. During this application, it was therefore assumed that the vessel is able to reach the surfzone, thereby blocking all longshore sediment transport. The position of the wreck in this scenario was chosen to be at beach profile station S41, which is approximately the projected centre point of the Seli One wreck.

Figure 10-1: Fishing Trawler Running on Clifton Beach, South Africa

(Anon, 2012)

10.2 Model Setup

The validated local shoreline evolution model used for the assessment of the impact of the Seli One shipwreck was used to simulate the effect of the two worst-case vessel grounding scenarios. Model settings and parameters were kept unchanged, which meant that model calibration and validation was not necessary prior to this application.

The nearshore wave climate resulting from the parallel shipwreck was calculated using the bay-wide wave transformation model introduced earlier. The 6 000 TEU container ship was modelled as a 350 m long, 45 m wide obstruction along the -7 m MSL contour, with a reflection coefficient of 1.0. This is shown graphically in Figure 10-2. Wave climates were extracted at the same locations as for the Seli One shoreline model, along the -6 m MSL depth contour.

The perpendicular wreck was modelled as a groyne structure, blocking all longshore sediment transport. The length of the "groyne" was taken to be 350 m, equal to the length of the 6 000 TEU container ship.

The effect of groynes is accurately simulated by the LITLINE model. It was therefore not necessary to determine the impact of the perpendicular wreck in the wave transformation model. As such, the wave climates used as input for this shoreline model were unaffected waves, as they were prior to any shipwrecks. These were extracted at the same locations as was done for the Seli One and worst-case parallel wreck shoreline models discussed previously.

Figure 10-2: Nearshore Bathymetry, Showing Worst-Case Parallel Wreck

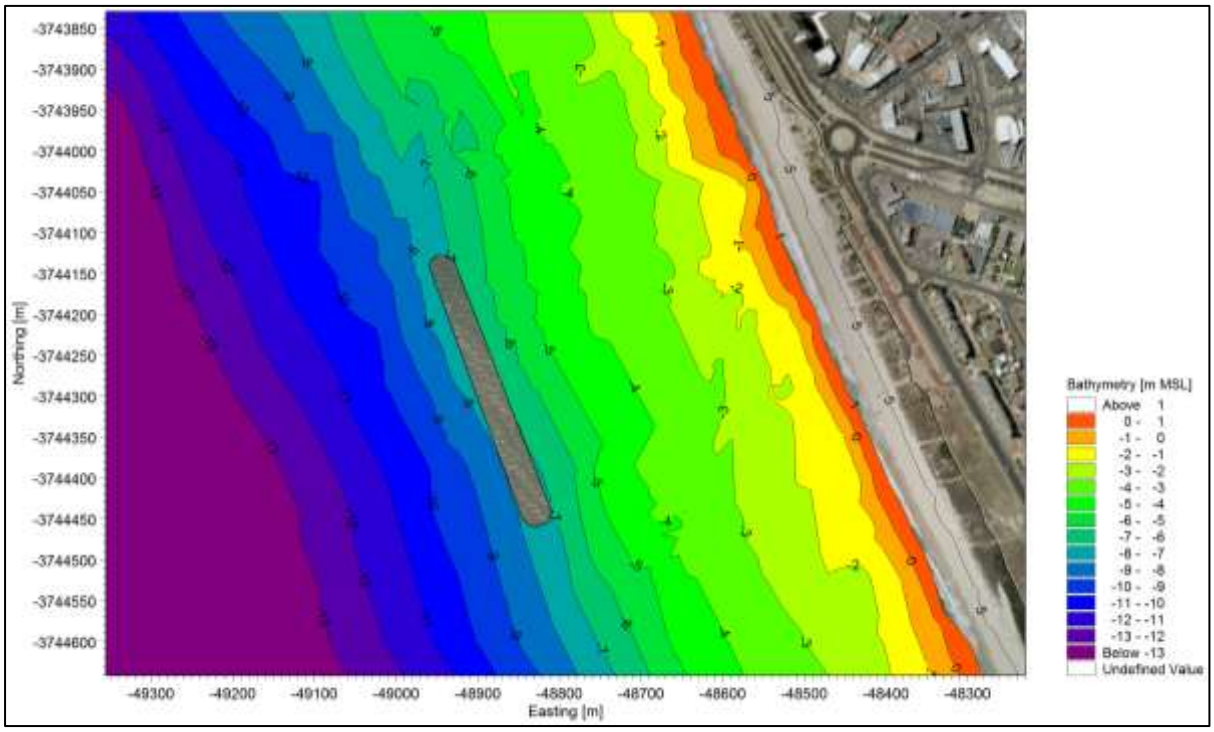

10.3 Model Results: Impact of a Worst-Case Parallel Grounding Event

The impact of the worst-case parallel shipwreck on the net northerly longshore sediment transport rate is shown in Figure 10-3. From this figure it is clear that since the original net northerly longshore transport rate was in the order of 50 000 m^3/year, this shipwreck results in the complete blockage of longshore sediment transport in the lee of the vessel. This impact reduces linearly to a reduction of approximately -10 000 m^3/year at the model boundaries.

The extended length of the 6 000 TEU container ship has the effect that even oblique southerly waves, which result in the reversal of the southerly longshore current at the northern side of the Seli One, are unable to do the same here. This means that there is no mechanism for sediment to get through the lee of the parallel wreck, resulting in the complete blockage of longshore sediment transport.

The impact of the parallel shipwreck on the shoreline morphology is summarized in Figure 10-4. Comparing this figure to the one showing the long-term potential impact of the Seli One shipwreck (Figure 9-12), it is clear that the worst-case parallel shipwreck results in significantly greater shoreline changes, with the simulated shoreline accretion being in the order of 120 m. The erosion observed to the north of the parallel wreck is simulated to be approximately 60 m.

Both of these observations are caused by the complete blockage of the longshore sediment transport in the lee of the parallel wreck, compared to the partial blockage at the Seli One.

Figure 10-3: Impact of Worst-Case Parallel Shipwreck on Net Longshore Sediment Transport

9th September 2009 to 31st December 2024

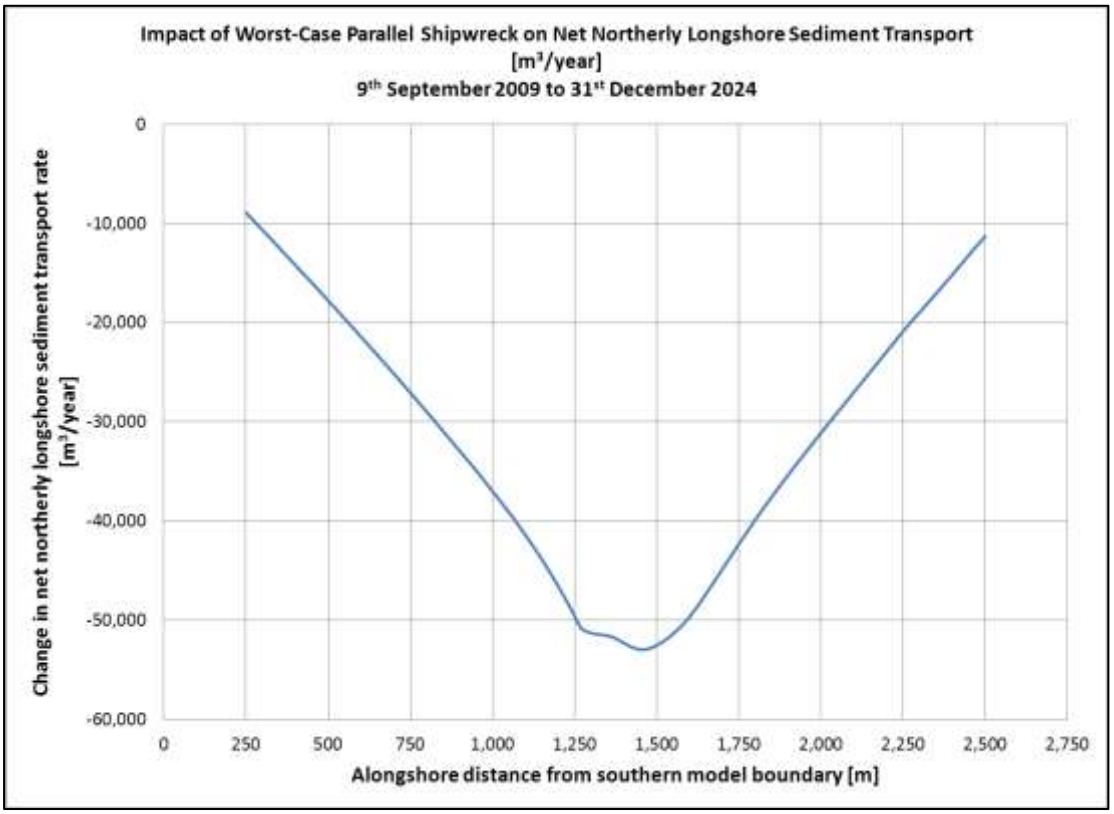

Figure 10-4: Impact of Worst-Case Parallel Shipwreck on Shoreline Morphology

9th September 2009 to 31st December 2024

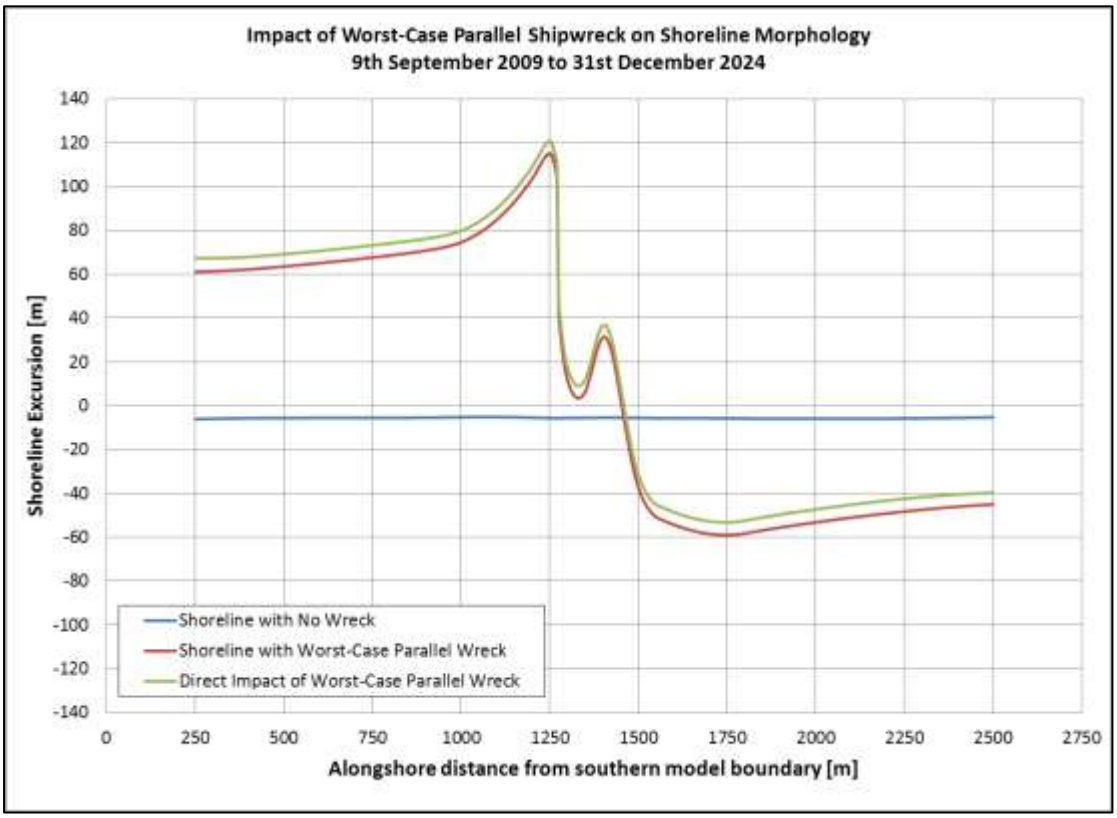

Referring to Figure 10-4, it can be seen that the parallel wreck results in the formation of a double salient. This is caused by the longer alongshore length of calm wave and current conditions compared to the Seli One. Sediment being transport northwards is deposited on the southern side of the wreck. This is caused due to the reduction in the northward longshore current speed moving further into the lee of the wreck. Conversely, sediment which is transported in a southerly direction is deposited on the northern side of the wreck, caused by the progressive reduction in the southward longshore current speed moving further into the lee of the wreck.

The cause for the southern salient being larger than the northern salient is that the net longshore sediment transport direction is northwards, which means that more sediment is transported in a northerly direction.

Figure 10-5: Impact of Worst-Case Parallel Shipwreck – 31st December 2024

The potential impact of the parallel wreck on the nearshore infrastructure can be seen in Figure 10-5. From this figure it is clear that, if such a grounding scenario would occur at the same location as the Seli One, and if this wreck would remain intact for an extended period, severe damage would occur to public and private infrastructure. This refers especially to the coastal road running parallel to the coast south of the rock headland at Blouberg. In addition to this, the widening of the southern beaches by more than 100 m may also be an unwanted result of the worst-case shore-parallel shipwreck.

10.4 Model Results: Impact of a Worst-Case Perpendicular Grounding Event

The impact of the worst-case perpendicular grounding event on the net longshore sediment transport is shown in Figure 10-6. It is clear that since this shipwreck is essentially a 350 m groyne extending perpendicularly from the shoreline, it results in the complete blockage of longshore sediment transport. Comparing Figure 10-3 and Figure 10-6, it will be observed that the impacts of the two worst-case scenarios in terms of net longshore sediment transport are essentially the same.

Figure 10-6: Impact of Worst-Case Perpendicular Shipwreck on Net Longshore Sediment Transport 9th September 2009 to 31st December 2024

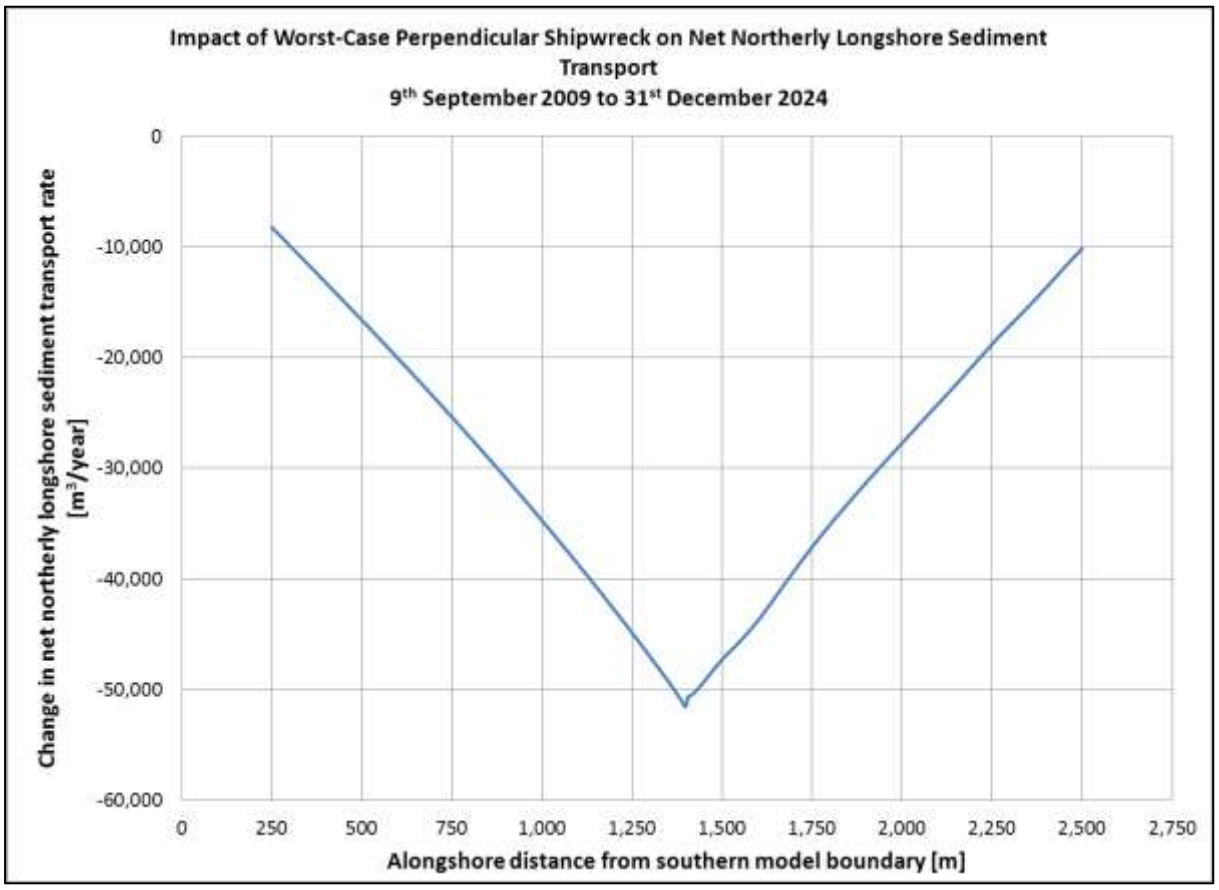

It should however be noted that the causes for the reductions of the net northern longshore transport rates for the two scenarios are quite different. The parallel wreck resulted in the formation of a large wave shadow, resulting in the formation of opposing longshore currents on either end of the wreck, causing sand to be deposited. The perpendicular wreck however, is simply a cross-shore “wall”, blocking all longshore sediment movement. Although the perpendicular wreck does result in some alterations to the nearshore wave and current climate, it does not cause the formation of a large calm area, in which sediment naturally settles out.

This results in the fairly simple shoreline behaviour shown in Figure 10-7, with sediment piling up against the shipwreck in the south, and being eroded away in the north. Nevertheless, considering that both wrecks are having a similar effect on the net longshore sediment transport rate, being the complete blockage thereof, the extents of shoreline accretion and erosion observed on either side of the vessels are similar. As such, the potential impact of the perpendicular wreck on public and private infrastructure is essentially the same as the parallel wreck, as shown in Figure 10-5.

It is noted that, as discussed previously, the model does not accurately include diffraction effects around coastal structures. As such, the diffraction effects which are expected to generate a sand fillet on the northern side of the perpendicular wreck are not included. This means that, referring to Figure 10-7, it is expected that a small sand filled would form immediately to the north of the perpendicular wreck.

Figure 10-7: Impact of Worst-Case Perpendicular Shipwreck on Shoreline Morphology

9th September 2009 to 31st December 2024

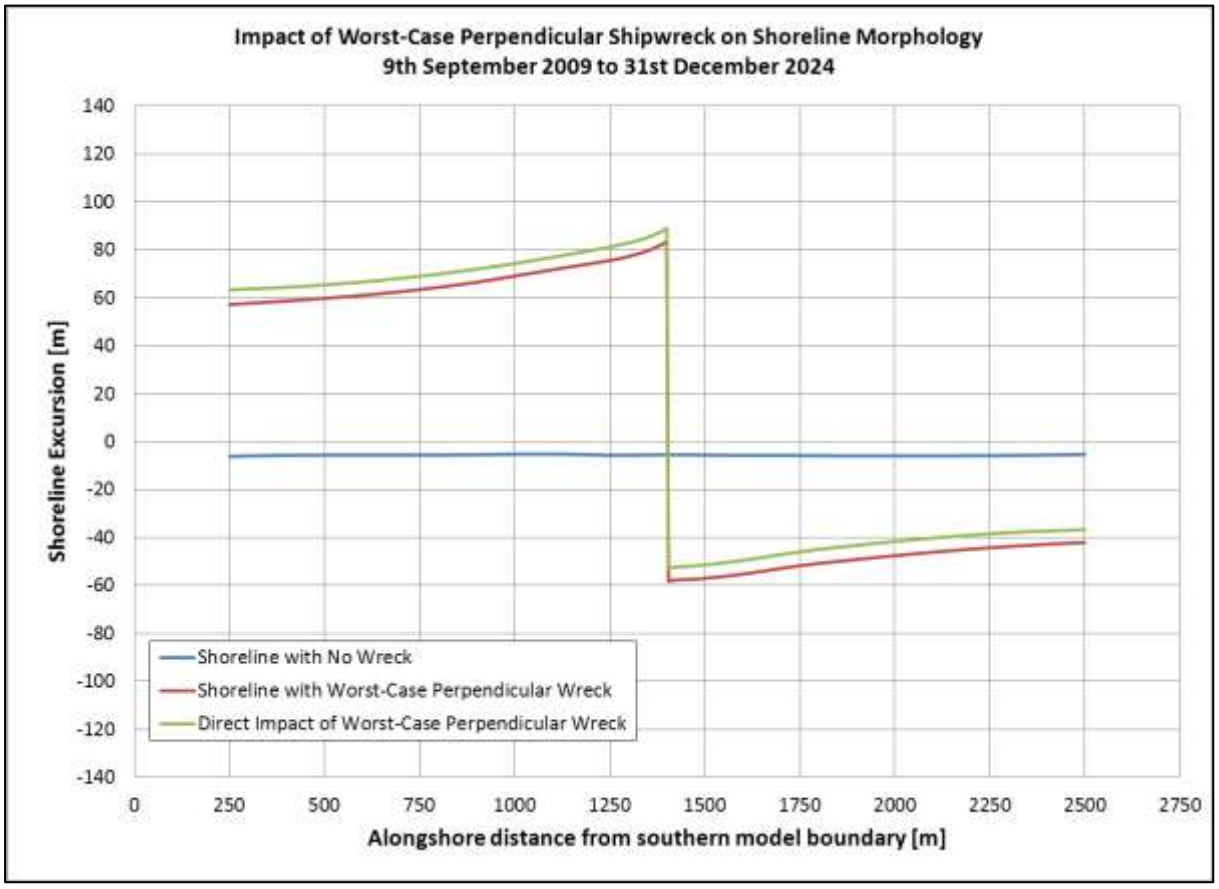

Similar to the parallel wreck, the accretion and erosion shown in Figure 10-7 is expected to continue until the accreted shoreline has reach the end of the perpendicular wreck, at which point, sediment bypassing will recommence.

10.5 Summary and Conclusion

Two worst-case vessel grounding scenarios were investigated using the one-dimensional shoreline evolution model LITLINE. During these scenarios, the largest vessel currently able to call at the Port of Cape Town, being

a 6 000 TEU container vessel, was simulated to run aground along the Blouberg beachfront in a parallel and perpendicular fashion.

It has been determined that both scenarios result in the complete blockage of longshore sediment transport. This results in the long-term effects of these scenarios to be significantly greater than the Seli One. At the Seli One, the long-term impact was not as significant, since, following the formation of the beach salient, sediment was able to partially bypass in the lee of the vessel. This meant that the beaches to the north of the Seli One were still fed with certain volumes of sand, limiting the extent of erosion.

However, during these scenarios, the complete blockage of longshore transport results in the continued sedimentation updrift of the vessel, and corresponding continued erosion on the downdrift side of the vessel.

The extent of downdrift erosion has been discussed to be a function time. It was shown that for the simulation performed for the current study, the erosion was modelled to be approximately 60 m between September 2009 and December 2024.

It can therefore be concluded that the potential exists for shipwrecks to result in major shoreline erosion in Table Bay, highlighting the need to salvage shipwrecks as soon as possible to avoid such impacts.

11. TWO-DIMENSIONALNEARSHORE SEDIMENT TRANSPORT MODELLING

11.1 Introduction

A coupled two-dimensional wave, hydrodynamic and sediment transport model was applied to investigate the apparent sediment accretion between the Seli One shipwreck and the shoreline. It should be noted that the intention of this model was to investigate the offshore sedimentation, not the shoreline changes which were discussed in Section 9. Two models were required to perform this investigation; the first excluding the shipwreck and the second including the vessel.

The significant computational requirements of such a coupled model results in the run-times being days or weeks, rather than hours. The simulation period used during the shoreline modelling, being from the 9th September 2009 to the 31st December 2024, could therefore not be repeated here. The simulation period used here was from the 9th September 2009 to the 15th November 2010, a period of approximately 14 months. The latter date was chosen to coincide with an aerial image of the wreck.

11.2 Model Setup

11.2.1 Domain, Bathymetry and Modelling Approach

The model domain and bathymetry used for the two-dimensional model is shown in Figure 11-1. The figure also shows the mesh used for each of the models.

The bathymetry used for the two-dimensional model was a simplified, straightened bathymetry. Referring to Figure 11-1, the shore-parallel contours become evident, together with the straightened coastline. This bathymetry was setup by replicating a single cross-shore profile in an alongshore direction. The profile chosen for this was taken perpendicularly to the shoreline, running through the centre of the shipwreck, thereby being representative of the area of interest.

There were numerous reasons for incorporating the simplified bathymetry, all of which related to the reduction in complexity of the two-dimensional model. If, for example, the real bathymetry was used, together with the real shoreline, numerous offshore wave climates would have been required to describe the changing conditions along the offshore boundary. For the simplified model however, only one wave condition was required. By making the alongshore characteristics of the model the same, the resulting alongshore hydrodynamics (excluding the shipwreck) were kept the same, which made the identification of model inaccuracies a significantly simpler task.

It could be argued that the simplified model does not replicate reality, and this is in fact correct. However, as will be introduced in Section 11.3, no measured data was available for the calibration and validation of this model. This meant that even if the model domain was setup to replicate the real situation more accurately, no greater confidence could be given to the corresponding results compared to the simplified model, since neither had gone through a rigorous calibration process.

The intention of the development of the coupled two-dimensional sediment transport model was to identify, in principal, that sediment is in fact being deposited in the lee of the shipwreck, and that this is caused as a direct result of the impact of the shipwreck on the coastal processes. Considering this, together with the lack of detailed calibration data, the simplified model was considered to be a representative tool to identify the changes in coastal processes, as well as the sedimentation characteristics.

Figure 11-1: Model Domain and Bathymetry

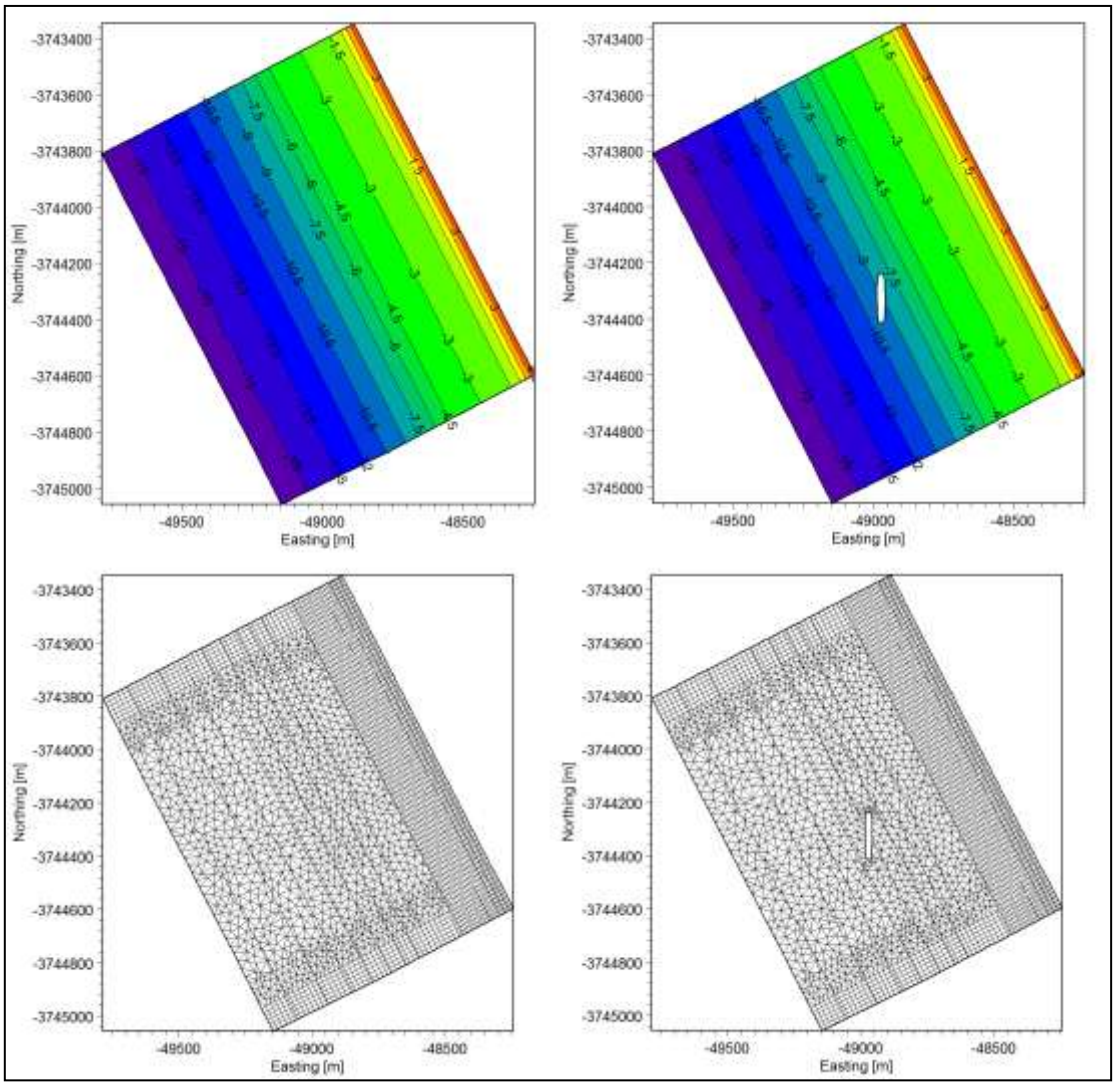

A combination of rectangular and triangular mesh elements were used during the generation of the bathymetry, as shown in Figure 11-1. Rectangular elements were generally used on the model boundaries, in an attempt to make these more regular and uniform, thereby reducing boundary errors. Triangular mesh elements were used in the central area of the domain. This was required since the triangular elements are flexible in terms of size and orientation, thereby being able to adjust to suit the location and size of the shipwreck.

Element sizes along the eastern, southern and northern boundaries were kept small at approximately 20 m by 20 m. This high density is required due to the high variability of the hydrodynamic conditions in the littoral zone.

11.2.2 Sources and Sinks

Referring to previous discussions, the two main sources and sinks in Table Bay is the fluvial source of the Diep River, as well as the wind-blown sediment sink along the Blouberg beachfront. Naturally, the fluvial source is not included in this model, since it falls outside the domain of the model. Although the wind-blown sediment sink is located within this model domain, it has also been excluded from the simulation. This has been done

since it was thought that sediment losses along the upper beach would not have a significant impact on the sedimentation between the vessel and the coastline.

11.2.3 Boundary Conditions

The coupled sediment transport model under investigation has three coastal boundaries, being the southern, western and northern boundary. Each of these boundaries is setup for the hydrodynamic, wave and sediment transport conditions, as discussed below.

Regarding hydrodynamic conditions, all three boundaries were described by a time-varying water level. These water levels were obtained from the MIKE C-MAP data (DHI, 2011h), described earlier in Section 8.3.4.

The wave forcing was applied to the western model boundary. These wave conditions were obtained from the bay-wide wave transformation model, discussed in Appendix A. The location at which this climate was extracted was at the offshore end of the cross-shore profile used to generate the simplified model bathymetry. The northern and southern wave boundaries were described by so-called lateral boundaries. At these boundaries, the model performs a process of linear wave refraction from the offshore to the inshore ends. The reduction in wave height and rotation of wave direction were therefore accounted for along these boundaries.

All three sediment transport boundaries were simulated to be open flux boundaries. This meant that sediment was able to enter or exit the model depending on the wave and hydrodynamic conditions near the model boundaries.

11.3 Model Verification

To accurately calibrate a coupled two-dimensional model would require substantial amounts of measured data. Ideally, one would require measurements of the impacted wave and current conditions in the lee of the vessel, as well as a survey of the altered bathymetry. During the current investigation however, none of this data was available. This meant that the two-dimensional model could not be calibrated or validated.

Results were however tested for correctness by comparing the simulated changes in the bathymetry to the observed wave refraction patterns in the lee of the shipwreck. Wave refraction theory states that a wave will change direction in order to become aligned with the bottom contours, with the wave direction becoming progressively parallel to the seabed slope (USACE, 2002). As such, if a change in wave direction is observed from an aerial image, it can be inferred that a corresponding change in seabed slope exists.

Figure 11-2 shows an aerial image of the Seli One shipwreck taken on the 15th November 2010 obtained from Google Earth (Google Inc., 2010). Waves in the northern half of the shipwreck's lee are rotated in a clockwise direction, whilst waves in the southern half of the shipwreck's lee are rotated in an anti-clockwise direction. It is clear that these effects are due to the combined effects of refraction and diffraction. This made a direct comparison between the wave crests and bottom contours more difficult, since the wave patterns are not exclusively linked to the bottom contours. Furthermore, it should be noted that the wave pattern shown in Figure 11-2 depicts only one instant, and can therefore not necessarily be regarded as being representative of all situations. Nevertheless, in the absence of any additional data, this method gave a first impression of the accuracy of the modelled sediment transport dynamics in the lee of the Seli One shipwreck.

As mentioned previously, the end of the model simulation was chosen to coincide with the day on which the aerial image of Figure 11-2 was taken, allowing a time-related comparison of the observed wave pattern and simulated bathymetry. In doing so, a good correlation could be identified. From Figure 11-2, it seems as though the wave rotation is lagging behind the bathymetry. It may therefore be argued that the simulated sedimentation is greater than the actual sedimentation. However, considering the lack of measured data, the model results shown in the figure below confirm, in principal, the correct model functioning.

Figure 11-2: Comparison of Bathymetry and Wave Refraction Pattern In the Lee of the Seli One Shipwreck

Furthermore, the location of the submerged salient in the lee of the shipwreck seems to be modelled correctly, since this coincides well with the line along which the northward and southward wave trains collide. Since this collision is likely to cause low currents, sediment deposition is likely to be maximized in this area, thereby resulting in more rapid salient accretion.

11.4 Model Results

The influence of the shipwreck on the nearshore wave conditions was analysed by investigating the coastal processes before and after the arrival of the Seli One. During the following discussion, these processes are described using plots of the impact on the significant wave height, water surface elevation and the nearshore current field. It should be noted that these plots show only one specific time step, and therefore do not necessarily describe all possible coastal processes which may occur at the site. Images have however been chosen to aid the description of the most common coastal processes resulting due to the arrival of the vessel. The discussion of the model results is concluded with the review of the sediment transport dynamics which result from the wave and current field near the Seli One shipwreck.

The impact of the Seli One shipwreck on the nearshore wave height is shown in Figure 11-3 and Figure 11-4. The first figure shows two plots of the wave conditions at one specific time step, excluding and including the shipwreck.

Figure 11-3: Significant Wave Height before and after the arrival of the Seli One Shipwreck

Boundary Wave: H_s = 1.0 m, Dir = 241°

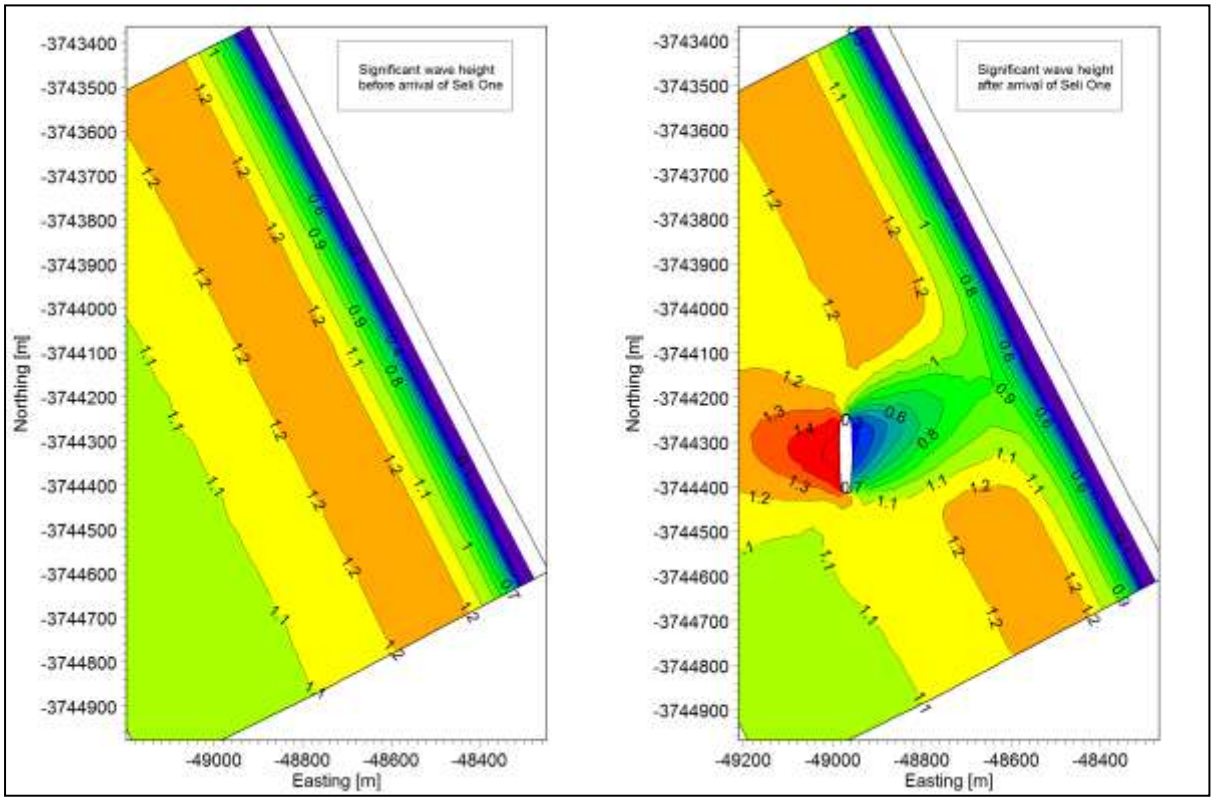

Figure 11-4 shows a difference plot of the two snapshots shown in Figure 11-3, which is the wave height including the Seli One subtracted from the original wave height. This plot therefore shows the increase or reduction of the wave height as a result of the shipwreck.

From this figure, the wave reduction is highest in the immediate lee of the vessel, reducing towards the shoreline. The reduction in wave height near the shoreline is limited to only 0.1 m, noting that the offshore significant wave height for this particular time step is 1.0 m. The reduction of the sheltering effect is caused by diffracted waves moving around the vessel, progressively into the sheltered zone. Furthermore, the reflected wave is dissipated offshore, reducing in height with increased distance. It is noted that, considering an offshore wave height of 1.0 m, an increase of 0.5 m approximately 50 m to the west of the vessel is substantial.

The impact of the vessel on the wave direction is shown in Figure 11-5, which is a difference plot of the wave direction before and after the arrival of the Seli One. From this, the clockwise rotation caused by wave diffraction is visible at the northern end of the vessel. The anti-clockwise rotation from the southern end of the vessel is also visible. The anti-clockwise rotation in the offshore region is caused by the reflected wave. For this particular time step, the offshore wave direction is 241°, which is therefore reflected in a north-westerly direction off the wreck. Since the wave condition offshore of the wreck is now a combination of the inbound and outbound wave, the north-westerly component results in an anti-clockwise rotation of the total wave direction.

Figure 11-4: Impact of Seli One Shipwreck on Significant Wave Height

Boundary Wave: H_s = 1.0 m, Dir = 241°

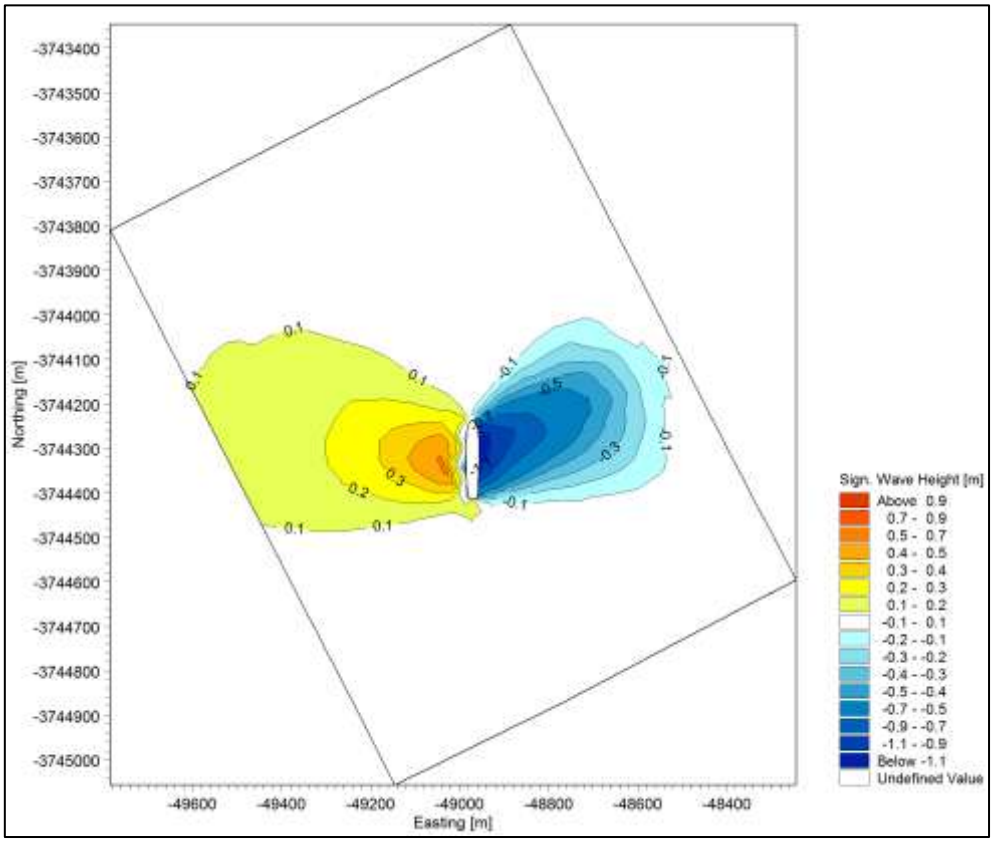

Figure 11-5: Impact of Seli One Shipwreck on Wave Direction

Boundary Wave: H_s = 1.0 m, Dir = 241°

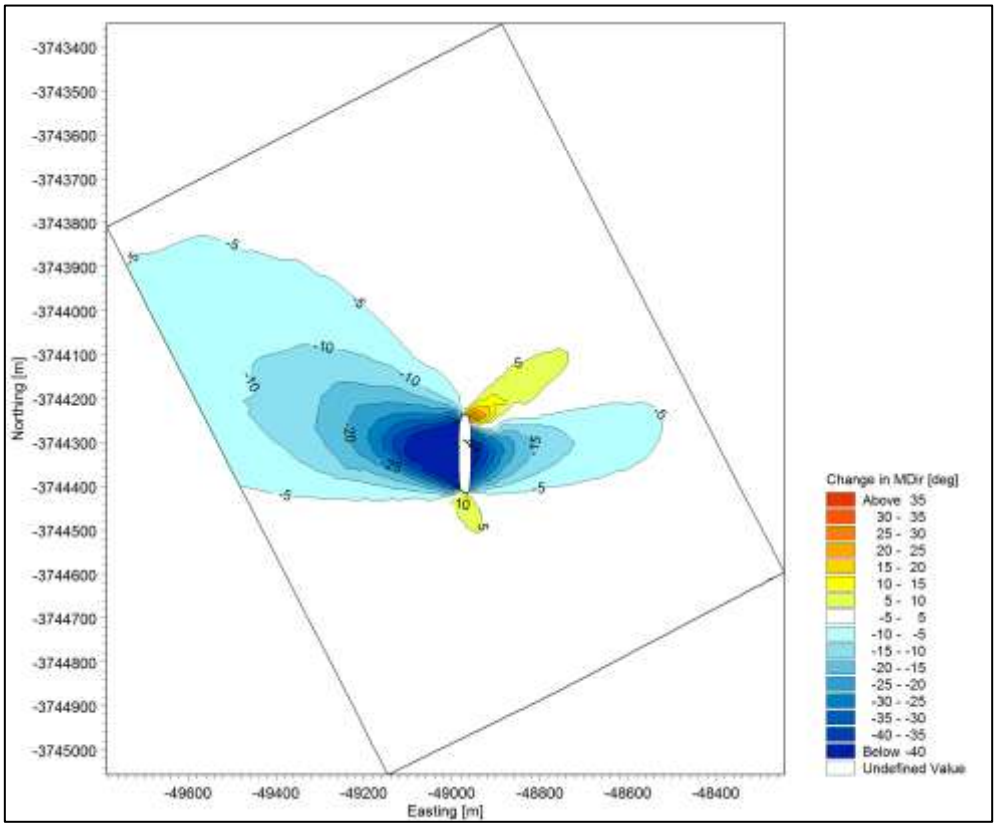

Referring to Section 3.2.3, it was discussed that nearshore waves result in wave setup, which is the increase of the water level landward of the wave breaking point (Figure 3-4). It was further pointed out that the magnitude of this setup is directly related to the wave height, with a higher wave generating a large wave setup.

The reduction in wave height in the lee of the vessel therefore results in the reduction of the mean water level in the lee of the ship. This is confirmed through the coupled two-dimensional wave and current model, as shown in Figure 11-6. These results indicate a maximum reduction of the water surface occurring as a direct result of the Seli One of approximately 0.5 m. The increase in the water level of approximately 0.01 m immediately seaward of the reduced water level is essentially a reduction in the wave set-down of the pre- and post- wreck situation.

Figure 11-6: Impact of Seli One Shipwreck on Water Surface Elevation

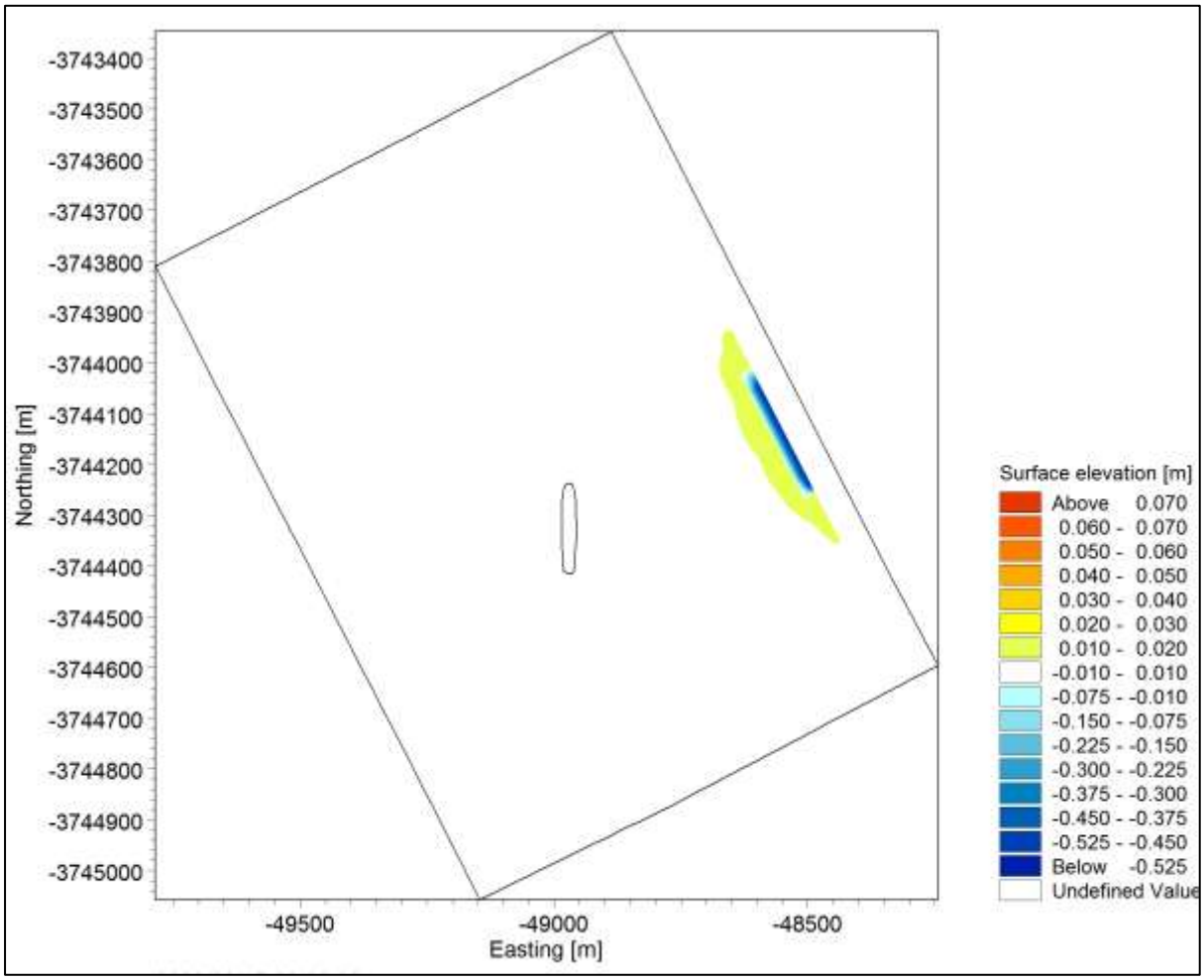

Although this water level variation may seem small and therefore negligible, it results in the generation of significant longshore currents, which ultimately lead to the complete reconfiguration of the alongshore sediment transport characteristics in the area.

Figure 11-7 shows the pre- and post- wreck current field. It is clear from this figure that significant changes have resulted due to the fairly minimal changes in average water level. Referring firstly to the original current field excluding the Seli One, it can be seen that a northerly current is present, which is slightly stronger in the nearshore area compared to the deeper areas of the model. It can further be seen that in the very shallow areas of the model, the currents turn to become onshore. This is thought to be caused by the run up of water onto the beach.

Referring now to the plot including the effect of the shipwreck, it can be seen that the longshore current immediately to the north of the vessel now reversed towards the lee of the vessel. This is caused by the head difference between the area north of the vessel and the lee of the ship, shown in Figure 11-6.

The opposing current on the northern and southern side of the vessel collide in the lee of the ship, resulting in the formation of a rip current. This current initially heads towards the wreck, to become deflected southward further near the vessel.

Comparing the current speeds of the pre- and post- wreck situation, a general acceleration of the currents near the shipwreck can be observed. The northern current on the southern side of the vessel is increased from the original speed of approximately 0.05 m/s to around 0.3 m/s, a six-fold increase. The rip current has a speed of approximately 0.25 m/s, whilst the current on the northern side of the vessel has a speed of around 0.2 m/s.

Figure 11-7: Longshore Current Pattern before and after the arrival of the Seli One Shipwreck

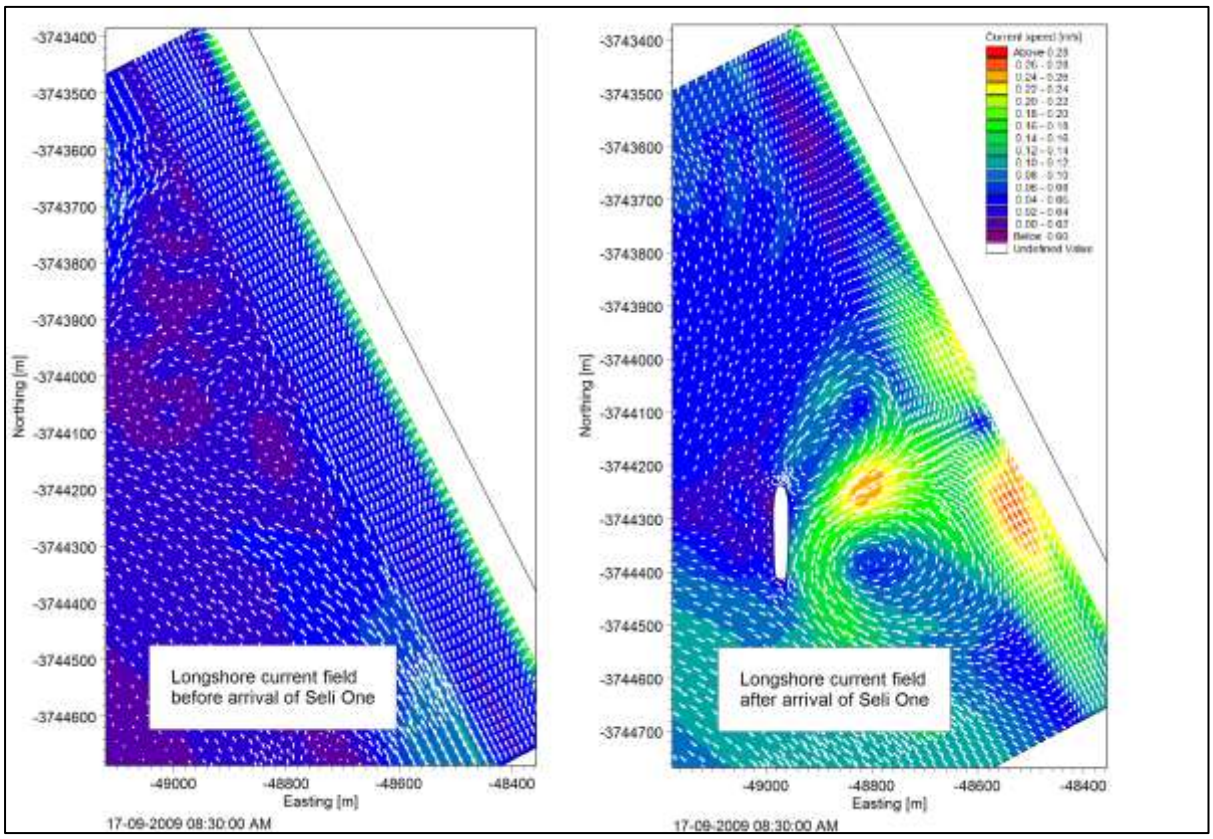

The sediment transport characteristics resulting from the above discussed wave and current climates are described in Figure 11-8 and Figure 11-9.

The resulting bathymetry in the lee of the shipwreck seems to be modelled fairly accurately. Figure 11-8 shows the simulated bathymetry over the entire model domain, with the salient being clearly visible. The direct impact of the shipwreck is shown on the difference plot in Figure 11-9. This plot shows the simulated bathymetry excluding the shipwreck subtracted from the bathymetry including the shipwreck. It is clear from the latter figure that the shipwreck results in the formation of a salient in her lee, with significant amounts of sediment being deposited there due to the calm hydrodynamic conditions.

However, referring to Figure 11-9, it is clear that the sediment transport model does not simulate the bathymetric changes correctly over the entire model domain. It can be observed that near the shoreline at the

northern model boundary, significant accretion as a result of the shipwreck has been simulated. In addition, seabed erosion has been simulated in relatively deep water on either side of the salient. Both of these observations are not thought to be a realistic impact of the Seli One shipwreck.

Figure 11-8: Simulated Nearshore Bathymetry by 15th November 2010

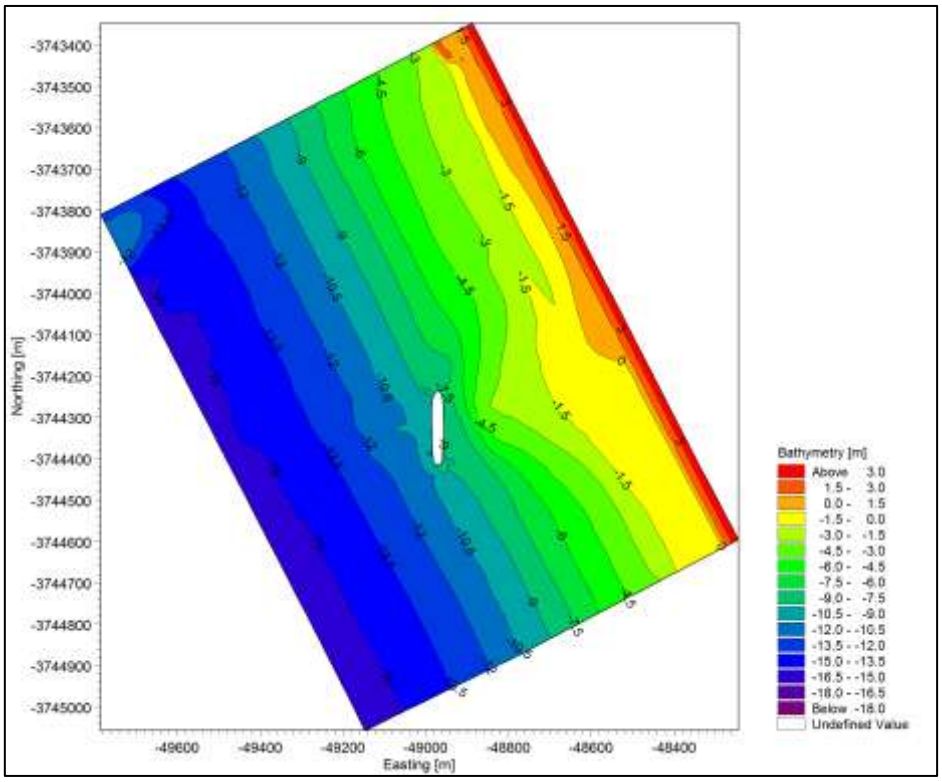

Figure 11-9: Impact of Seli One Shipwreck on Nearshore Bathymetry by 15th November 2010

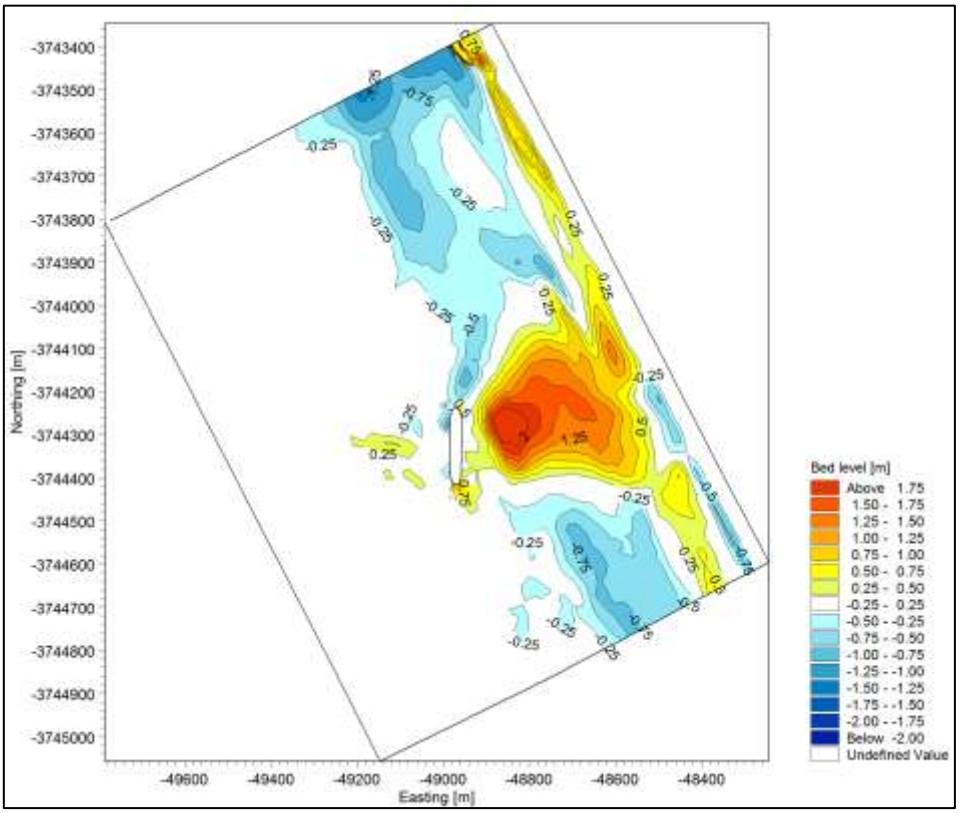

The cause for the inaccuracy of the sediment transport calculations is thought to be the proximity of the area of interest to the model boundaries. Referring to Figure 11-4 to Figure 11-7, it is clear that the impacts of the vessel on wave and hydrodynamic conditions reach the model boundary for all but one of the parameters. This is especially of relevance for the current speed, since this is the mechanism for sediment transport. An incorrect current along the model boundary would therefore result in incorrect volumes of sediment entering and/or exiting the model, which could lead to a sediment imbalance over the model domain.

Since it is thought that boundary errors are the most likely cause for the incorrect sediment transport simulation, a possible solution to the problem would be to increase the model domain. The extent of this increase would be to ensure that the impacts of the vessel do not come near any boundaries, and that these have sufficient area to develop fully without impacting the wave, current and sediment transport conditions of the boundary. In this way, the sediment balance of the base model, being the model excluding the shipwreck, could be maintained.

The original intention of the two-dimensional sediment transport modelling exercise was the identification of the postulated submerged salient, as well as the confirmation of the Seli One being the sole cause for the formation of this salient. Considering the above discussion, the two-dimensional nearshore sediment transport model can be said to have correctly simulated the seabed change between the wreck and the shoreline.

11.5 Summary and Conclusions

A two-dimensional wave, current, hydrodynamic and sediment transport model was developed to investigate the apparent sediment deposition between the Seli One and the Blouberg beachfront. Due to computational requirements, the domain of this model was limited to an area of approximately 1.5 km by 1.0 km.

It has been pointed out that no measured data was available to calibrate or validate this model. As such, model validation was limited to a comparison between wave refraction pattern and the modelled bathymetry, the argument being that the two should be approximately parallel due to refraction processes. This initial review showed a good correlation, indicating the correct functioning of the coupled two-dimensional sediment transport model.

The impacts of the wreck on the local wave conditions were analysed, comparing both wave height and wave direction pre- and post-wreck. This analysis has shown that, as expected, the wreck results in a reduction in the wave height in her lee. In addition, the vessel results in an increase in the wave height on the western side of the vessel, related to wave reflection off the vessel's hull.

It has further been shown that the average water level in the lee of the wreck is reduced compared to the surrounding area. This is caused by the wave height differential in the area, resulting in differences in the wave setup and set-down. The changes in the longshore current field resulting from the water level variations have been discussed. This discussion has shown that the northern current, originally fairly uniform along the Blouberg beachfront, has been reversed on the north side of the wreck. In addition, dramatic current acceleration has been observed to the south of the Seli One.

Finally, it has been shown that the opposing currents from the northern and southern sides of the vessel generate a rip current. This current has been observed to head towards the vessel, to be deflected southwards due to the orientation of the vessel.

The sediment transport characteristics resulting from the altered wave and current characteristics have been simulated. It has been shown that two-dimensional sediment transport model developed during the current

study does not accurately replicate the sediment transport behaviour across the entire model domain. This inaccuracy was caused by the proximity of the Seli One to the model boundaries.

Nevertheless, it has been argued that, although this model cannot be seen to be entirely accurate, it has identified that the Seli One is, in fact, causing sedimentation between the shipwreck and the beach. The objective relating to the two-dimensional sediment transport modelling has therefore, in principal, been accomplished.

It can therefore be concluded that shipwrecks have the potential of causing sedimentation between the vessel and the beach, in addition to the morphological shoreline changes discussed previously.

It is further concluded that shipwrecks have the potential of creating dangerous conditions in their lee, due to the formation of strong rip currents. These may result in swimmers and other ocean users to be pulled out to sea, increasing the risk of drowning's.

Although the sediment transport dynamics were not modelled entirely accurately during the current study, the capability of the model to perform such an analysis has been confirmed. This statement can be made since the model accurately identifies the coastal processes which govern the sedimentation processes in the lee of the shipwreck. The model domain should be increased substantially, to ensure that the impacts of the vessel in terms of waves and hydrodynamics do not reach the model boundaries.

12. CONCLUSIONS AND RECOMMENDATIONS

12.1 Conclusions

Details of conclusions made during each of the sub-investigations performed during this study are included in the each of the respective chapters, and are therefore not repeated in detail here. The discussion below therefore represents a summary of the conclusions discussed previously.

The running aground of the Seli One shipwreck on the Blouberg coastline is not an isolated incident of a vessel entering the littoral zone along a sandy coastline. Understanding what impact a shipwreck has on the nearby coastal processes is therefore valuable information for coastal engineers and decision makers alike. This thesis therefore adds to the understanding of the risks related to shipwrecks, and is therefore considered to be of benefit to the field of coastal engineering.

A review of existing literature has indicated a lack of empirical or deterministic relationships to quantify the impacts of detached offshore breakwaters or shipwrecks on nearby coastal processes. Diffraction diagrams can be used to identify the impacts on inshore wave patterns, but even these make assumptions making them unsuitable for this purpose. The empirical equations available to quantify the impacts of shipwrecks on local shoreline morphology are limited to the classification thereof as being either a salient or tombolo, rather than quantifying specific lengths and widths.

Furthermore, the literature review has indicated numerous methods to determine net longshore sediment transport rates. Although these relationships are useful to attain a first understanding of the sediment transport characteristics of a site, they can only be used to determine the potential longshore transport, and as such, cannot be used to quantify the impacts of shipwrecks on the local sediment transport regime.

The literature review has further indicated that coastal processes in the lee of structures, whether an offshore breakwater or shipwreck, are generally too complex to be quantified using simple empirical methods. As such, numerical sediment transport models are often employed to perform these investigations.

An assessment of historic beach profile measurements have indicated that since the mid-1960s, approximately 1.6 million m^3 of sediment has been lost from the Table Bay littoral zone, at a rate of approximately 50 000 m^3/year. It has further been determined that the net longshore sediment transport direction in Table Bay is northwards, with sediment moving past the Blouberg rock headland each year. In addition to this, it has been shown that no sediment enters or exits the bay near the Port of Cape Town.

A wave transformation model has been developed to determine the nearshore wave climate in Table Bay.

The bay-wide shoreline evolution modelling was performed using LITLINE by DHI. From this, it was determined that, through modifications relating to the curved nature of Table Bay, the longshore sediment transport system could be accurately replicated, both in terms of longshore sediment transport rates and shoreline excursions. Even with large amounts of calibration and validation data, significant engineering judgement is required when analysing simulation results.

Field investigations, in the form of a beach survey, were performed on the 3rd July 2011. This survey confirmed the existence of a beach salient in the lee of the shipwreck.

The near-field shoreline modelling was performed using LITLINE by DHI. This investigation has shown that LITLINE was unable to accurately determine the diffracted wave climate in the lee of the Seli One. This is caused by the manner in which LITLINE performs diffraction calculations, being through the implementation of simple diffraction diagrams rather than calculating wave parameters deterministically. This error was circumnavigated by determining the diffracted wave climate using the wave transformation model, and

applying this to the shoreline evolution model. Implementing this approach delivered excellent results in terms of simulated shoreline excursions.

Through the analysis of simulation results, it was concluded that, as expected, the shipwreck has resulted in a significant reduction in the net longshore sediment transport rate in her lee, but that this reduction does not represent a complete blockage of longshore sediment transport. The simulated accretion of approximately 27 m in the lee of the shipwreck agrees well with the measured salient characteristics. Furthermore, it has been shown that approximately 75% of the salient accretion occurred within the first two months of the vessel's arrival. This indicates that following the arrival of the Seli One, beach sedimentation occurred rapidly at first, but that an equilibrium salient shape was reached fairly rapidly.

Furthermore, shoreline erosion on the northern side of the salient resulting directly from the shipwreck has been shown to be approximately 15 m. This too occurs relatively rapidly, within approximately two months of the vessels arrival.

It has been determined that the breaking up of the Seli One into three pieces has resulted in the reduction of the salient from the initial 27 m to approximately 20 m, and that this 20 m wide salient is in dynamic equilibrium. Furthermore, due to continued deposition between the shipwreck and the beach, a slight continuation of beach accretion and erosion is expected along the southern and northern shoreline respectively, to the extent of approximately 5 m respectively until December 2024.

It has been concluded that, by determining the altered wave climate resulting of the Seli One shipwreck by a wave transformation model, LITLINE was able to accurately replicate and predict the impact of the Seli One shipwreck on the local longshore sediment transport system, both in terms of transportation rates and shoreline morphology.

The investigation of the two worst-case vessel grounding scenarios have shown that, potentially, a shipwreck could result in severe shoreline erosion, resulting in significant damage to public and private infrastructure.

A two-dimensional coupled wave, current and sediment transport model has been developed to identify the sedimentation occurring between the vessel and the beach. This investigation has identified the coastal processes which are generally encountered at offshore breakwaters, being the reduction of wave energy in the lee of the vessel, the reduction of the average water level in the lee of the vessel due to the wave height differential adjacent to- and in the lee of the vessel, as well as the corresponding longshore current generated by the water level variations.

It has been shown that two-dimensional sediment transport model does not accurately replicate the sediment transport behaviour across the entire model domain. This inaccuracy was caused by the proximity of the Seli One to the model boundaries. It has however been argued that, although the model developed during the current study cannot be seen to be entirely accurate, it has accurately identified the governing coastal processes in the lee of the Seli One. With an increase in model domain size, it is therefore thought that the coupled wave, current and sediment transport model will be able to accurately simulate the sedimentation occurring in the lee of the shipwreck.

It can be concluded that the shoreline changes occurring in the lee of the Seli One can be reasonably reproduced using shoreline (one dimensional) and two-dimensional sediment transport models, thereby enabling the long-term prediction of a shipwreck on the coast.

It is further concluded that shipwrecks have the potential of significantly altering local longshore sediment transport characteristics in general. Depending on local conditions, this may pose significant risks to seaside infrastructure. Considering the rapid rate at which the initial shoreline changes occur, a limited window of

opportunity exists to remove the shipwreck from the coast to prevent damage to seaside infrastructure due to rapid shoreline erosion.

Furthermore, it can be concluded that shipwrecks have the potential of creating dangerous conditions in their lee, due to the formation of strong rip currents. These may result in swimmers and other beach users to be pulled out to sea, increasing the risk of drowning's.

12.2 Recommendations

Through the review of existing literature, it has been shown that no empirical methods are currently available that could be used to quantify the impacts of offshore breakwaters or shipwreck on local shoreline morphology. Although guidelines are available to categorize the impact of an offshore structure, in terms of being a salient or tombolo, these cannot be used to estimate the corresponding shoreline erosion occurring adjacent to the salient. As such, no methods are available to estimate the combined effect of a structure, in terms of shoreline accretion and corresponding shoreline erosion.

Considering the rapidness of shoreline changes resulting from a vessel running aground, and the corresponding limited time that decision makers have to evaluate the risks associated with the shipwreck, it is recommended to develop a method which can be used to quickly identify the extent of shoreline changes which may occur as a result of the altered nearshore coastal processes. This could be done by performing a number of numerical simulations to quantify the shoreline changes resulting from a range of different shipwreck scenarios. The results of these simulations could be used to develop an empirical relationship. This could be used to evaluate whether seaside infrastructure is in immediate danger of shoreline erosion.

Regarding the Table Bay sediment budget analysis performed during the current study, one of the remaining uncertainties is the behaviour of the beach cross-section below the water line, i.e. between the mid-tide zone and the depth of closure. It is therefore recommended that beach profile measurements be continued, and that these measurements include the submerged portion of the profile extending to the depth of closure. This will allow a more robust beach volume analysis to be performed, which will indicate the precise volume of sediment which has been lost out of the Table Bay littoral zone.

LITLINE does not accurately simulate wave diffraction in the lee of offshore breakwaters or shipwrecks. It is therefore recommended that the software be amended so that this calculation is not based on simple wave diffraction diagrams, but rather on deterministic wave diffraction equations. In this way, the interim step of simulating the nearshore wave climate with a wave transformation model, and applying this climate to the shoreline evolution model, can be eliminated.

Considering the impact that a shipwreck can have on local shoreline changes, with special regard to the rate at which these shoreline changes can occur, it is recommended that the results obtained from the current study be used to estimate the impact of potential future shipwreck scenarios in Table Bay.

13. REFERENCES

AMSA, 2009. *Response to Pasha Bulker Grounding - Report of the Incident Analysis Team,* Australia: Australian Maritime Safety Authority.

Anon, 2012. *SA-People.* [Online] Available at: http://www.sa-people.com/2012/05/17/clifton-beach-shipwreck-photographs/[Accessed 25 07 2012].

Anonomous, 2009. *Shipwrecks of South Africa.* [Online] Available at: www.sashipwrecks.com[Accessed 19 08 2012].

Battjes, 1974. *Surf Similarity.* Copenhagen, Denmark, American Society for Civil Engineers, pp. 466-480.

CERC, 1984. *Shore Protection Manual, Volume I and II,* s.l.: Coastal Engineering Research Centre.

Chasten, M., Rosati, J. & McCormick, J., 1993. *Engineering Design Guidance for Detached Breakwaters as Shoreline Stabilization Structures.* s.l.:s.n.

CSIR, 1983. *Assessment of Zonnekus Development, Milnerton,* Stellenbosch, South Africa: Council for Scientific Research.

CSIR, 1989. *Stability Analysis and Management Options for the Table View Coastline,* Stellenbosch, South Africa: Council for Scientific Research.

CSIR, 1996. *Coastline Stability and Erosion Problems at Milnerton,* Stellenbosch, South Africa: Council for Scientific Research.

CSIR, 1999. *The Effect of Proposed Harbour Extensions on the Milnerton Shoreline,* Stellenbosch, South Africa: Council for Scientific Research.

CSIR, 2003. *Port of Cape Town Strategic Environmental Assessment: Specialist Study on Shoreline Stability,* Stellenbosch, South Africa: Council for Scientific Research.

CSIR, 2006. *Wave and Current Measurements in Table Bay,* Stellenbosch, South Africa: Council for Scientific Research.

DHI, 2006. *Stockton Beach Coastal Processes Study, Final Report, Stage 1 Sediment Transport Analysis and Description of on-going Processes,* Copenhagen, Denmark: Danish Hydraulics Institute.

DHI, 2011a. *MIKE Spectral Waves FM, User Guide.* Copenhagen, Denmark: Danish Hydraulics Institute.

DHI, 2011b. *MIKE by DHI, LITDRIFT, Longshore Current and Littoral Drift, LITDRFIT User Guide.* Copenhagen, Denmark: Danish Hydraulics Institute.

DHI, 2011c. *MIKE by DHI, LITSTP, Non-cohesive Sediment Transport in Currents and Waves, LTSTP User Guide.* Copenhagen, Denmark: Danish Hydraulics Institute.

DHI, 2011d. *MIKE by DHI, LITLINE, Coastal Evolution, LITLINE User Guide.* Copenhagen, Denmark: Danish Hydraulics Institute.

DHI, 2011e. *MIKE by DHI, MIKE21 Flow Model FM, Hydrodynamic Flow Module, User Guide.* Copenhagen, Denmark: Danish Hydraulics Institute.

DHI, 2011f. *MIKE by DHI, MIKE21 Flow Model FM, Sand Transport Module, User Guide.* Copenhagen, Denmark: Danish Hydraulics Institute.

DHI, 2011g. *MIKE by DHI, MIKE21/3 Coupled Model FM, User Guide.* Copenhagen, Denmark: Danish Hydraulics Institute.

DHI, 2011h. *MIKE C-MAP, Extraction of World Wide Bathymetry Data and Tidal Information, User Guide,* Copenhagen, Denmark: Danish Hydraulics Institute.

DHI, 2012. *Cape Town Container Terminal Expansion, Coastal Engineering Study,* Copenhagen, Denmark: Danish Hydraulics Institute.

Entech, 1995. *Milnerton Lagoongate Development: Proposal for Coastal Protection Measures and their Effect on adjacent Beaches,* Cape Town, South Africa: Entech Consultants (Pty) Ltd.

Google Inc., 2010. *Google Earth (Version 6) [Computer Program],* Washington, USA: Google Inc..

Harris, L. B., 1993. *The Seaport, Table Bay - An Archeological and Historical Perspective,* Carolina, USA: East Carolina University.

HKS, 1992. *Milnerton Coastal Erosion,* Cape Town: Hill Kaplan Scott Inc Consulting Engineers.

Holthuijsen, L. H., 2007. *Waves in Oceanic and Coastal Waters.* Holland: Delft University of Technology and UNESCO-IHE.

Joubert, J., 2008. *An Investigation of the Wave Energy Resource on the South African Coast, Focusing on the Spatial Distribution of the South West Coast,* Stellenbosch, South Africa: Department of Civil Engineering, University of Stellenbosch.

Kalnay, E. & et al, 1996. The NCEP/NCAR Reanalysis 40-Year Project. *Bulletin of the American Meteorological Society,* I(1), pp. 437-471.

Kamphuis, J., Davies, M., Nairn, R. & Savao, O., 1985. *Calculation of Littoral Sand Transport Rate,* Canada: Department of Civil Engineering Queen's University.

Longuet-Higgins, M. S., 1970. *Longshore Currents Generated by Obliquely Incident Sea Waves, 1,* Corvallis: Oregon State University.

Main, D., 2003. *Sealand Express Salvage Operation,* Cape Town, South Africa: s.n.

Mangor, K., 2004. *Shoreline Management Guidelines.* Copenhagen, Denmark: Danish Hydraulics Institute.

McCowan, J., 1983. On the Solitary Wave. *Philosophical Magazine,* 36(5th Series), pp. 430-437.

PRDW, 2009. *Nuclear Sites Safety Report, Coastal Engineering Investigations, Duynefontein, Report No 1010/4/102,* Cape Town, South Africa: Prestedge Retief Dresner Wijnberg.

Preston, G. L., Gilbert, R. D., McCoy, M. A. & Murrell, E. R., 1997. *Ship Groundings in the Pacific Islands Regions - Issues and Guidelines,* s.l.: s.n.

Rogers, J., 2006. *Report on Particle-Size Analyses of Beach Sediments from the Coast of Table Bay between Paarden Eiland and Melkbosstrand,* Cape Town, South Africa: Department of Geological Sciences, University of Cape Town.

Ruthenavelu, M., 2011. *Port Engineering Course, Stellenbosch, Expansion of the Cape Town Container Terminal,* Cape Town, South Africa: Transnet National Port Authority.

SANHO, 2011. *2011 South African Tide Tables,* Simonstown, South Africa: South African Hydrographic Office, SA Navy.

SANHO, 2012. *2012 South African Tide Tables,* Simonstown, South Africa: South African Hydrographic Office, SA Navy.

Seifart, H., 2009. *The Jolly Kitesurfer.* [Art] (Private).

Soltau, C., 2009. *The Cross-Shore Distribution of Grain Size in the Longshore Transport Zone,* Stellenbosch, South Africa: Department of Civil Engineering, University of Stellenbosch.

Tritan Survey CC, 2006. *Report on Bathymetric Survey of Table Bay,* Cape Town, South Africa: Tritan Survey CC.

UKHO, 2002. *Admiralty Sailing Directions, Africa Pilot, Volume II,* United Kingdom: United Kingdom Hydrographic Office.

USACE, 2002. *Coastal Engineering Manual, Part II, Chapter 3, Estimation of Nearshore Waves.* Washington, USA: United States Army Corps of Engineers.

USACE, 2002. *Coastal Engineering Manual, Part III, Chapter 2, Longshore Sediment Transport.* Washington, USA: United States Army Corps of Engineers.

USACE, 2003. *Coastal Engineering Manual, Part II, Chapter 4, Surfzone Hydrodynamics.* Washington, USA: United States Army Corps of Engineers.

USACE, 2006a. *Coastal Engineering Manual, Part III, Chapter 3, Cross-Shore Sediment Transport.* Washington, USA: United States Army Corps of Engineers.

USACE, 2006b. *Coastal Engineering Manual, Part V, Chapter 3, Shore Protection Structures.* Washington, USA: United States Army Corps of Engineers.

USACE, 2006c. *Coastal Engineering Manual, Part II, Chapter 7, Harbour Hydrodynamics.* Washington, USA: United States Army Corps of Engineers.

APPENDIX A – TABLE BAY WAVE CLIMATE ANALYSIS

A.1 Introduction

One of the study tasks identified in Section 1.3 was the assessment of the Table Bay wave climate using the identified numerical wave transformation model. This information was required to determine the nearshore wave climate which was required as input information to the sediment transport analysis.

This was performed by performing an in-depth review of the available offshore wave data at the Slangkop and Cape Point wave measuring stations.

As introduced during the literature review, this model is the MIKE21 Spectral Waves Flexible Mesh Model (DHI, 2011a). The wave modelling was preceded by an in-depth review of available offshore wave data

A.2 Data

A.2.1 Offshore Wind Climate

Information regarding the local wind patterns was obtained from the National Centre for Environmental Prediction, or NCEP (Kalnay & et al, 1996). The coordinates at the location where the data was extracted from the online database are shown below. The water depth at this location is approximately 220 m.

Southing 34.00°

Easting 17.40°

Although the information obtained from the NCEP database include hindcast wave data, this was not utilized since measured wave data at the Cape Point and Slangkop stations was available. Only the wind data of the NCEP database was therefore utilized.

A.2.2 Offshore Wave Climate

Two sets of offshore wave measurements were made available for this investigation, namely the Slangkop and Cape Point waverider measurements. The Slangkop buoy was situated approximately 13 km directly off Kommetjie in approximately 170 m of water, and was in operation from 1978 to 1993. In 1994, the Slangkop buoy was moved to the current Cape Point location, approximately 7 km offshore and in 70 m of water (Joubert, 2008).

Figure A - 1: Location of Slangkop and Cape Point Wave Measuring Buoys (Joubert, 2008)

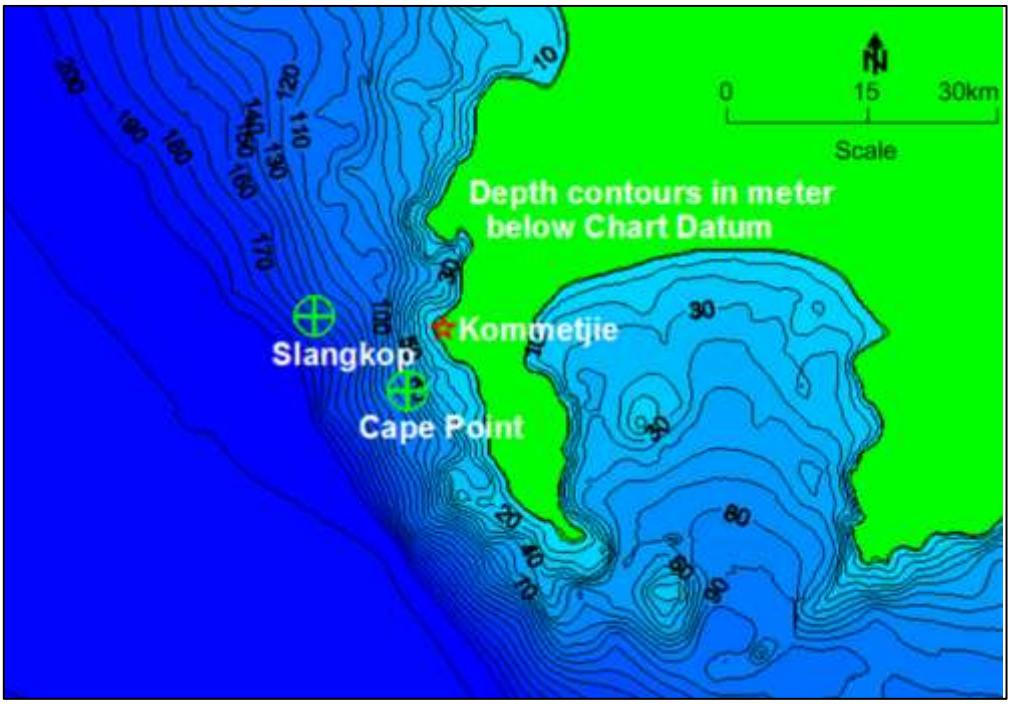

Table A - 1: Slangkop and Cape Point Wave Measuring Stations (Joubert, 2008)

Station	Position – WG 19		Water depth [m CD]	Operational time	Measurement Interval
	X [m]	Y [m]			
Slangkop	-76 055.55	3 765 076.33	-170	3 October 1978 – 14 May 1993	6 hourly initially, later 3 hourly
Cape Point	-65 744.04	3 786 445.73	-70	7 June 1994 – Current	3 hourly initially, later 30 mins

The Slangkop waverider buoy measured a one-dimensional spectrum, including the wave energy as a function of wave frequency. The frequencies were split into 35 bins, with the highest being 0.338 hertz, and the lowest being 0.006 hertz. The bin width was approximately 0.01 hertz.

Table A - 2 shows a typical measurement taken at the Slangkop buoy. It will be noticed that these measurements include only the wave energy at the respective frequencies. No directional data was available.

Initially, the Cape Point measurements also did not include directional information, with only the wave frequencies and corresponding wave energies being measured. From the 22nd October 1998 however, the peak wave direction, as well as the wave spreading were included in the measurements. This data was also divided into frequency bins, as shown in Table A-3.

Table A - 2: Extract from Slangkop Wave Measurements (3rd October 1978, 12h00)

Wave frequency [hertz]	Wave period [seconds]	Wave Energy [m^2/Hz]
0.006	166.7	0.070
0.016	62.5	0.057
0.025	40.0	0.084
0.035	28.6	0.112
0.045	22.2	0.168
0.055	18.2	0.110
0.064	15.6	0.083
0.074	13.5	0.146
0.084	11.9	0.073
0.094	10.6	0.195
0.104	9.6	0.402
0.113	8.8	0.118
0.123	8.1	0.205
0.133	7.5	0.538
0.143	7.0	0.489
0.152	6.6	0.838
0.162	6.2	0.666
0.172	5.8	0.400
0.182	5.5	0.988
0.191	5.2	1.636
0.201	5.0	1.824
0.211	4.7	2.995
0.221	4.5	4.176
0.230	4.3	3.403
0.240	4.2	7.317
0.250	4.0	12.402
0.260	3.8	12.671
0.270	3.7	21.887
0.279	3.6	4.250
0.289	3.5	0.155
0.299	3.3	0.019
0.309	3.2	0.017
0.318	3.1	0.006
0.328	3.0	0.009
0.338	3.0	0.004

Table A - 3: Extract from Cape Point Wave Measurements (22nd October 1998, 07h55)

Wave frequency [hertz]	Wave period [seconds]	Wave Energy [m^2/Hz]	Peak Direction [deg]	Spreading [deg]
0.006	166.7	0.092	188.300	32.120
0.016	62.5	0.114	194.100	28.880
0.025	40.0	0.068	194.900	32.300
0.035	28.6	0.135	197.300	19.430
0.045	22.2	0.141	192.800	21.450
0.055	18.2	0.120	187.000	21.020
0.064	15.6	0.083	191.000	19.620
0.074	13.5	0.120	176.300	20.040
0.084	11.9	0.064	189.700	22.840
0.094	10.6	0.128	177.800	22.170
0.104	9.6	0.158	178.500	27.430
0.113	8.8	0.118	182.400	18.980
0.123	8.1	0.116	173.100	25.820
0.133	7.5	0.114	171.900	38.920
0.143	7.0	0.162	190.100	32.320
0.152	6.6	0.353	202.800	26.620
0.162	6.2	0.500	193.400	22.130
0.172	5.8	0.249	184.400	31.540
0.182	5.5	0.388	186.900	34.660
0.191	5.2	0.511	191.800	30.420
0.201	5.0	0.373	206.900	42.480
0.211	4.7	0.985	214.400	21.550
0.221	4.5	1.324	198.400	24.550
0.230	4.3	2.652	206.900	26.360
0.240	4.2	2.079	219.800	32.180
0.250	4.0	7.373	221.500	26.330
0.260	3.8	6.782	207.800	27.620
0.270	3.7	1.603	217.600	34.270
0.279	3.6	0.117	251.000	42.100
0.289	3.5	0.030	216.800	35.110
0.299	3.3	0.292	226.900	34.930
0.309	3.2	0.009	199.400	25.300
0.318	3.1	0.005	201.100	23.810
0.328	3.0	0.003	168.400	25.240
0.338	3.0	0.008	227.900	37.640

It should be noted that the wave energy shown in the table above is the total energy for a specific frequency bin. For the given spectrum, the total wave energy of waves with frequencies between 0.104 and 0.113 hertz is equal to 0.158 m^2/Hz.

The peak direction shown in the table is the direction at which the highest amount of energy is recorded within the corresponding frequency bin. If one were to parameterize the one-dimensional spectrum, the direction could be described as the peak direction at the peak period. The mean wave direction cannot be calculated from the above information.

A.2.3 Bathymetry

The bathymetric survey was performed in October 2006 by Tritan Survey, and has been made available for use during the current study by PRDW.

The survey was performed using an echo sounder mounted on a survey vessel. This echo sounder was used to measure the water depth, which included corrections for tidal elevations at the time of measurement. A global positioning system (GPS) was used to determine the lateral location of the survey vessel at the exact time when the echo sounder measured the water depth. The bathymetric survey covered an area from False Bay to Saldanha Bay (Tritan Survey CC, 2006).

A.2.4 Nearshore Wave Measurements for Model Calibration

To ensure the accuracy of the wave refraction simulations, the model was calibrated following the initial set up. The measured and simulated wave climates were then compared, and adjustments made to the numerical model in an attempt to reduce the error between the two climates.

Two sets of measured nearshore wave climates were made available for use in this study, the locations of which are shown in Table A - 4 below.

Table A - 4: Wave Simulation Calibration Data

Description	Oceanographic parameters measured	Water depth	Position – WG19	Data Range
Koeberg data set	Waves, currents, seawater temperature, salinity	- 30 m CD	X = -56 587 m Y = -3 727 857 m	11 July 2008 to 18 September 2010
Port of Cape Town entrance data set	Waves, currents	– 17 m CD	X = - 51 422.7 m Y = -3 751 913.9 m	27 August 2006 to 27 September 2006

The wave measurements outside the entrance to the Port of Cape Town were taken using a Seapac wave gauge. The wave gauge was deployed on the 27th August 2006 and collected on the 27th September 2006. One month of wave data was therefore collected for the calibration of the numerical model (CSIR, 2006).

Since the dataset at the Port of Cape Town only represents one month of wave measurements, the Koeberg data set was used as primary calibration point, with the data measured at the Port of Cape Town being as secondary verification point.

Figure A - 2: Location of Calibration Data received from PRDW

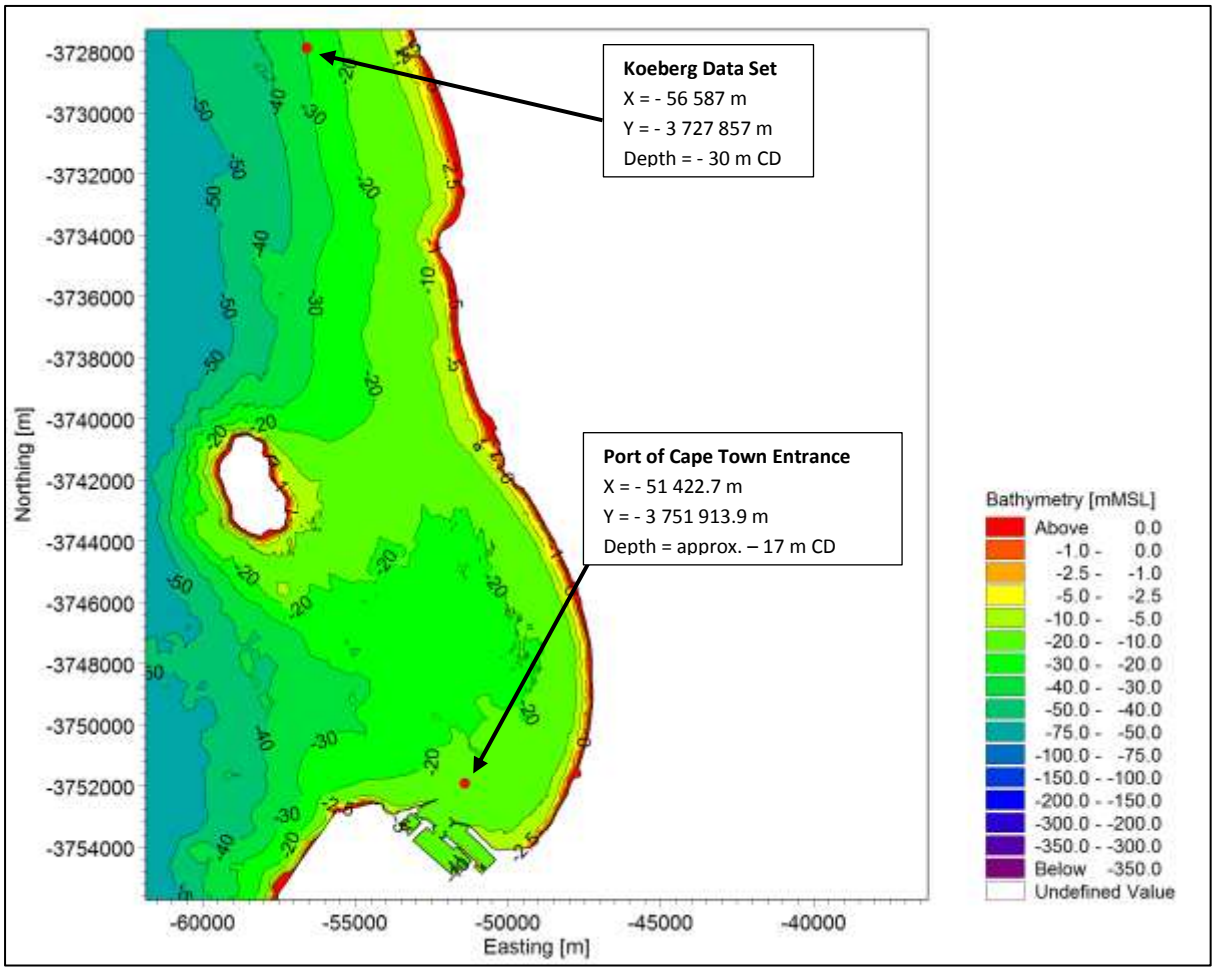

A.3 Analysis of Offshore Wave and Wind Climate

A.3.1 Offshore Wind Climate

The sea-state along the south-western coast of South Africa is dominated by large, long-period swells being generated thousands of kilometres away during storms in the South-Atlantic Ocean. Further to these swells, strong local winds generate short period waves which superimpose onto the long-period swells (CSIR, 1999).

Figure A-3 below shows the annual wind rose and wind exceedence curve for the south-western coast. It will be noticed from this figure that the wind direction is predominantly from the south-east, as well as from the north-west. Although south-westerly winds are also common, they are generally less strong. North-easterly winds are very rare, with generally very slow speeds.

Figure A - 4 shows the wind climate divided into the four seasons, which are categorized into the following months:

Summer	1st December – 28th (29th) February
Autumn	1st March – 31st May
Winter	1st June – 31st August
Spring	1st September – 30th November

Figure A - 3: Annual Wind Rose and Exceedence Histogram (NCEP, 17.50° East, 34.00° South)

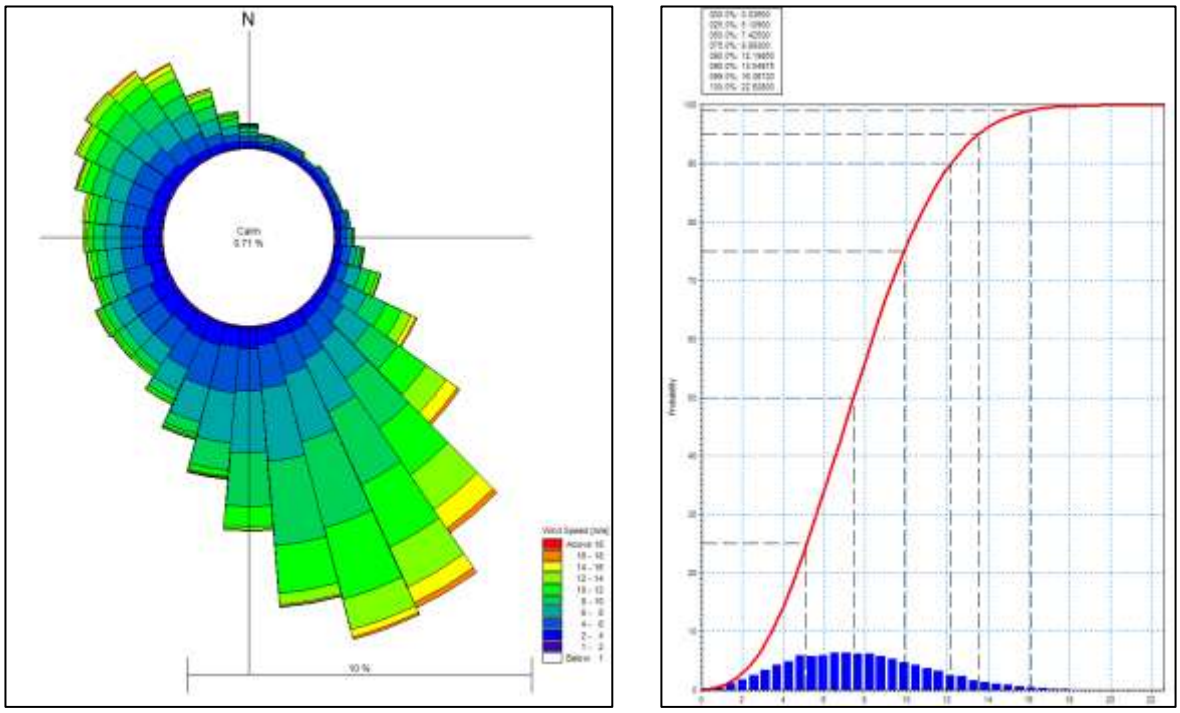

It will be observed from Figure A - 4 that during the summer months, strong south-easterlies dominate the wind fields, reaching speeds of up to 20 m/s (approximately 40 knots). During winter months, the wind direction swings around to the north-west, with the wind speeds generally being slightly weaker than during the summer. During autumn and spring, the wind direction varies between south-east and north-west, with speeds generally being quite mild.

A further observation which can be made, is that the percentage of “calm conditions”, which is taken to be a wind speed of less than 1 m/s, is significantly lower during the spring and summer months compared to the autumn and winter months. This indicates that the spring and summer months are “windier” than the autumn and winter months.

Figure A - 4: Seasonal Wind Roses (NCEP, 17.50° East, 34.00° South)

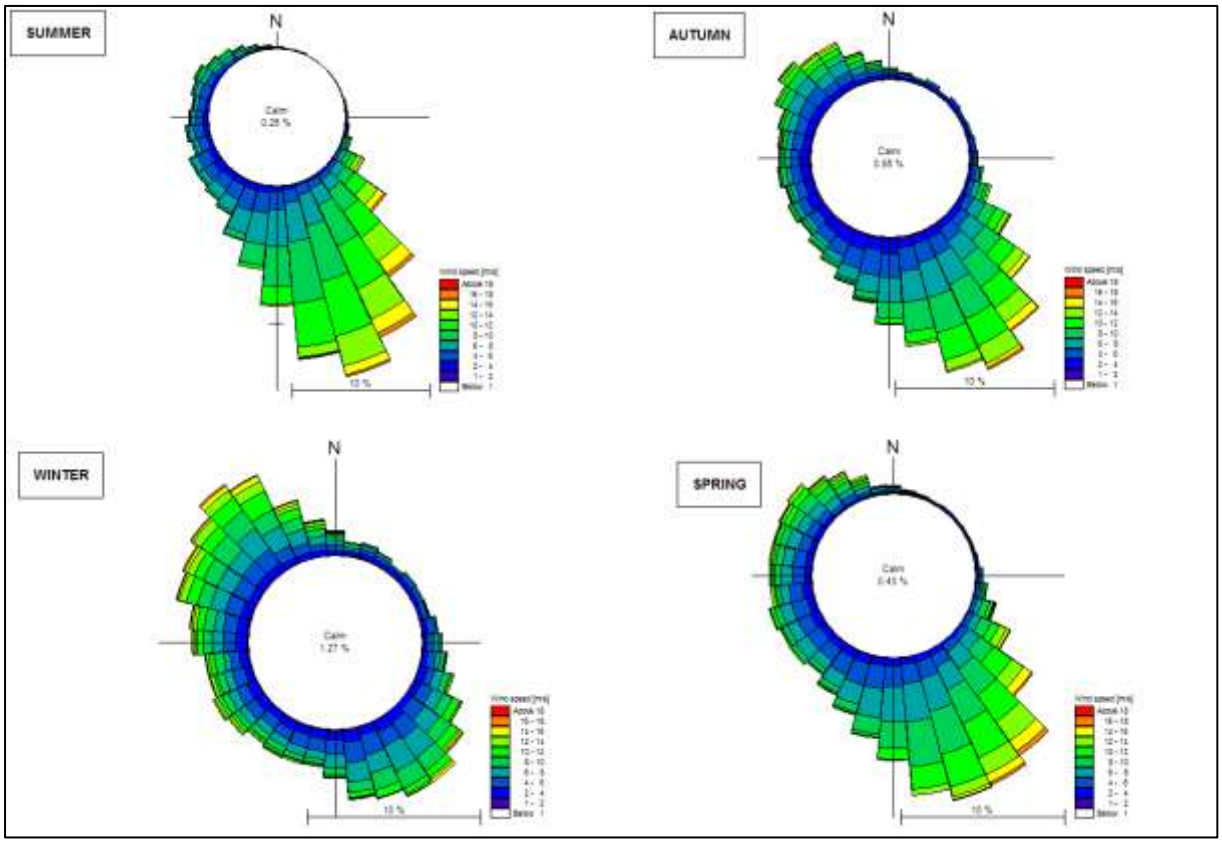

A.3.2 Offshore Wave Climate

Since the Slangkop one-dimensional wave spectra do not include directional information, the Cape Point measurements formed the focus of the offshore wave climate analysis. As mentioned previously, the wave spectra at the Cape Point measuring station include the wave energy, peak direction and peak spreading as a function of wave frequency. Since this spectrum is one-dimensional, in the sense that the measurements have already been integrated over the directional domain, a fully spectral analysis was not possible. Instead, a parametric analysis and wave modelling approach was adopted.

It was discussed in the previous section, that the winds in Cape Town regularly exceed 20 m/s, thereby generating large wind waves. By being generated in the near-field, these waves have fairly short periods. Since the peak direction of the long-period swell is often not the same as the peak direction of the local wind-waves, a componential wave analysis approach is required. This aims at dividing the total offshore climate into sea (local wind-waves) and swell components.

Consider the following example: A large swell, with a peak period of, say, 16 seconds, is approaching the model domain from the south-west. Concurrently, a strong north-westerly wind is blowing, generating fairly large wind-waves, with peak period of, say, 6 seconds. If one were to parameterize the total sea-state, the peak period would be equal to the peak period of the swell component of 16 seconds, since the swell component generates more energy than the sea-component.

In addition to this, the peak direction would be equal to the peak direction of the swell component with the total energy being the sum of the two components.

This results in an error. According to the wave parameters, the entire wave energy, inclusive of both the sea and swell components, approach from the south-west, with a peak period 16 seconds. It is therefore clear that, in general, by parameterizing the entire sea-state into one set of wave parameters, the sea component is often lumped into the same direction and period as the dominating swell, which may lead to inaccuracies.

Considering now the study area at hand, it will be clear that local wind-waves generated by strong south-easterly winds would not refract into Table Bay, since they are heading offshore. An approach which does not consider the sea and swell as two separate components would combine the sea-energy to the swell energy, thereby overestimating the wave energy which enters Table Bay. This could result in the overestimation of wave heights in Table Bay.

The boundary between the sea and swell component was taken to be a cut-off period, below which the energy is taken to be locally generated (sea-component) and above which, the energy is taken to be swell driven. This boundary was determined by iteration, choosing the cut-off period at six, eight and ten seconds respectively.

The resulting sea climate was then compared to the local wind fields (Figure A - 3); with the argument being that the locally generated wind waves having similar directions as the local winds. Figure A - 5, Figure A - 6 and Figure A - 7 present the resulting sea climate of the three cut-off periods.

In doing this comparison, it was noticed that by taking the peak period cut-off at six seconds, the resulting sea climate closely resembled the wind fields. Furthermore, it was observed that by taking the cut-off at ten seconds, a large amount of south-westerly energy was included. The eight second cut-off climate was a compromise between the six and ten second climates.

Figure A - 5: Sea Wave Climate – Cut-off T_p = 6 seconds

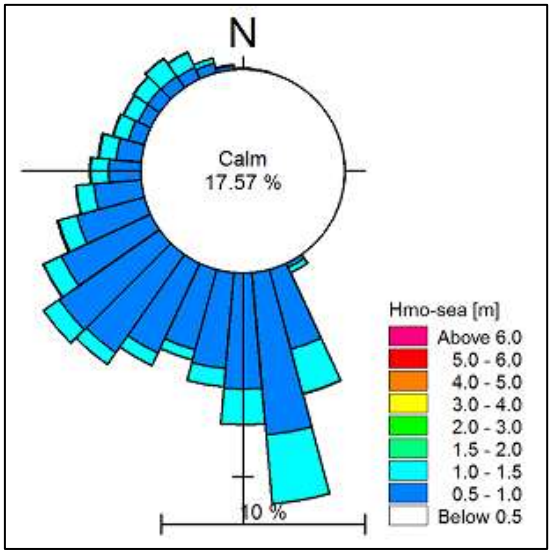

Figure A - 6: Sea Wave Climate – Cut-off T_p = 8 seconds

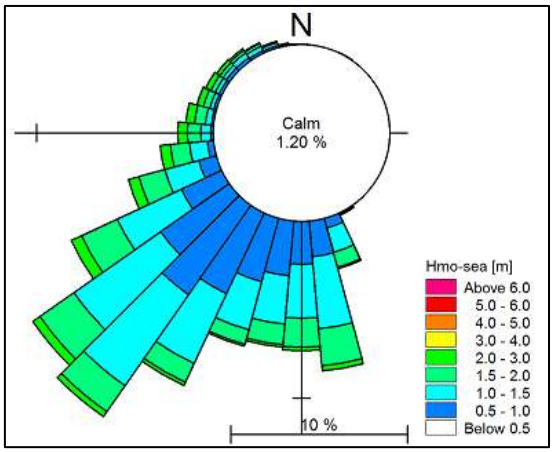

Figure A - 7: Sea Wave Climate – Cut-off T_p = 10 seconds

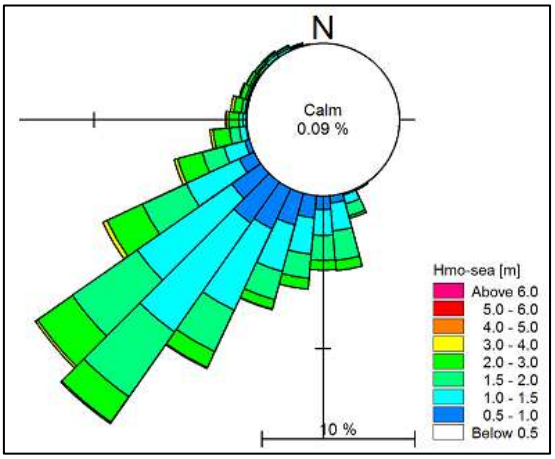

Figure A - 8: Wave Roses and Cape Point Wave Measurements – Sea, Swell and Total

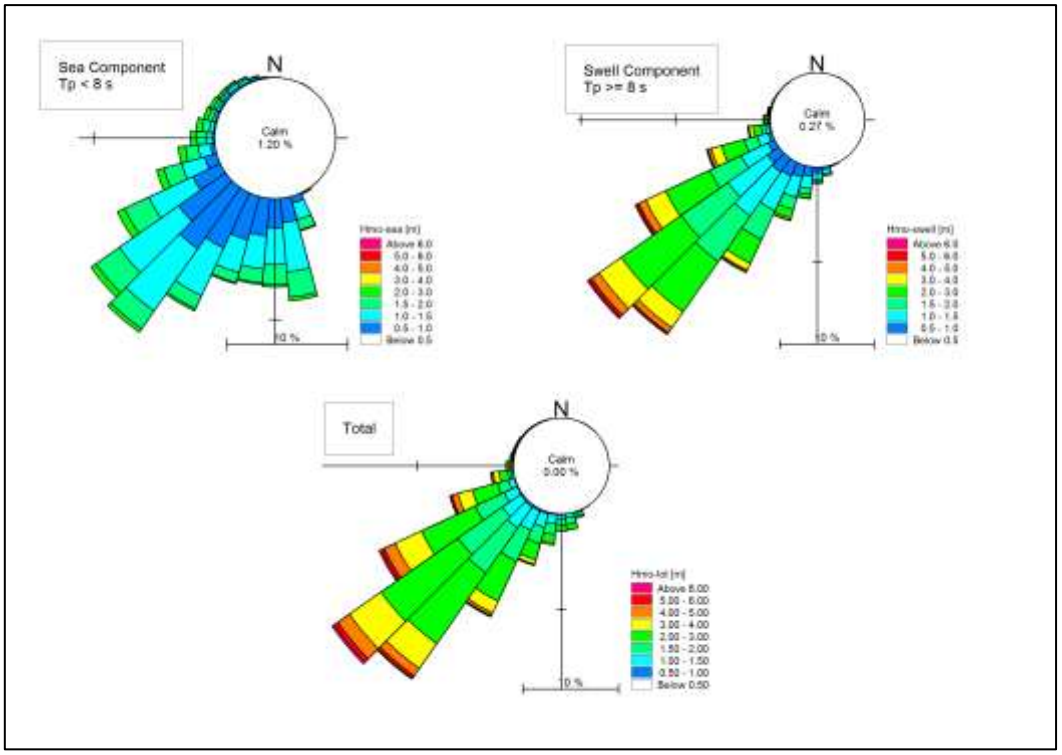

At first glance, one would assume that the six second cut-off climate would describe the real sea-state the most accurately. However, by inspecting Figure A - 5 more closely, it can be observed that the wave heights with a peak period of below six seconds do not exceed a significant height of 1.5 m.

It will however be determined, by performing fetch limited wave growth calculations, that the significant wave height with a fetch of approximately 15 km and wind speed of 40 knots is in excess of 1.5 m. It can therefore be concluded that a cut-off period of six seconds is too low to describe the sea component accurately. A cut-off peak period of eight seconds was therefore chosen as the boundary between the sea and swell components.

Figure A - 8 above shows the sea and swell components, as well as the total sea-state at the offshore Cape Point measuring station. The total sea-state represents the wave parameters if the split between sea and swell components is not taken into consideration.

It will be noticed that the swell component and total sea-state wave roses resemble each other closely, which confirms the argument that the sea-component is mostly overshadowed by the high-energy swell component.

A.4 Modelling Approach

As with any type of numerical simulation, it is of utmost importance to calibrate the model with actual measurements to ensure its accuracy. As mentioned earlier, wave measurements within Table Bay were used to calibrate the wave refraction model. The offshore wave conditions used as the model boundary were measured at the Cape Point measuring station. Model calibration was performed by comparing simulated parameters (H_{mo}, T_p and D_p) to measured parameters at the same location. The primary calibration location was off the Koeberg Power Station.

To limit computational requirements during the wave refraction exercise, the “look-up table” modelling approach was used. This approach is used to determine the refraction coefficients over the entire model domain for specific wave conditions applied at the offshore boundary. The refraction coefficients are then applied to the time series of the offshore wave climate to determine the nearshore wave conditions at the point of interest.

Consider the case of a wave with significant height of 1.0 m, peak period of four seconds and direction of 200˚ entering the model domain: The simulation is performed to determine the resulting wave height, period and direction of this wave over the entire model domain. From these results, the refraction coefficient at a certain location can be determined, say 0.5. This process is repeated for all possible waves that may occur during the offshore time series (this implies the requirement to review the offshore wave climate to ensure that all wave conditions are in fact refracted).

Once all wave cases have been simulated, the time series is analysed by applying the already calculated refraction coefficients. Each offshore wave which has a peak period of four seconds and direction of 200˚ can now be refracted simply by multiplying the parameters by the refraction coefficient of 0.5.

The advantage of using this approach compared to simulating the entire offshore time series is a significant saving in computational demand, resulting in a time saving. This is since each wave condition is only simulated once, irrespective of how many times it occurs in the actual offshore time series.

A.5 MIKE21 SW Setup and Calibration

A.5.1 Model Boundaries

A.5.1.1. Land Boundary

The domain for the numerical wave refraction model was chosen to extend from Cape Point to slightly southward of Saldanha Bay. Both False Bay and Saldanha Bay were excluded from the simulation, as it was thought that they do not have a significant effect on the wave climate near the Seli One shipwreck.

The land boundary was generated by following the shoreline on the aerial imagery. For dissipative beaches, the boundary of the model was generally chosen at the crest of the primary dune. This was done to ensure that the level of the land boundary was higher than the highest wave run-up level.

Other boundaries, such as the outlines of the Port of Cape Town, the Koeberg Power Station breakwaters and the Robben Island Harbour structures were also traced from aerial images.

All boundaries within the numerical model, with the exception of the breakwaters and quay walls of the Port of Cape Town, were assumed to be fully absorptive, which means that none of the incoming wave energy is reflected back into the model. The main breakwater of the Port of Cape Town is constructed of concrete caissons, resulting in significant amounts of energy being reflected back into Table Bay. This is especially pronounced for the north-easterly to north-westerly wave directions.

One of the two measurement points used to calibrate the numerical model is located fairly close to the entrance of the Port of Cape Town. It can be assumed that the wave climate in this area is significantly affected by reflected waves off the main and secondary breakwaters. A reflection coefficient of 0.8 applied to the breakwaters and quay walls of the port was therefore incorporated in the simulation in order to allow accurate calibration of the numerical model.

A.5.1.2 Offshore Boundary

The model domain stretches from Cape Point to the southern end of Saldanha Bay. The offshore model boundary was created in a semi-circular shape between these two positions.

The reasoning behind choosing the semi-circular offshore boundary was to minimize the extent of the model domain, whilst also ensuring that the model boundaries remain far away from the point of interest. Furthermore, it is thought that creating a model domain with corners would result in computational errors along the boundaries.

Figure A - 9: Spectral Wave Model Domain and Bathymetry

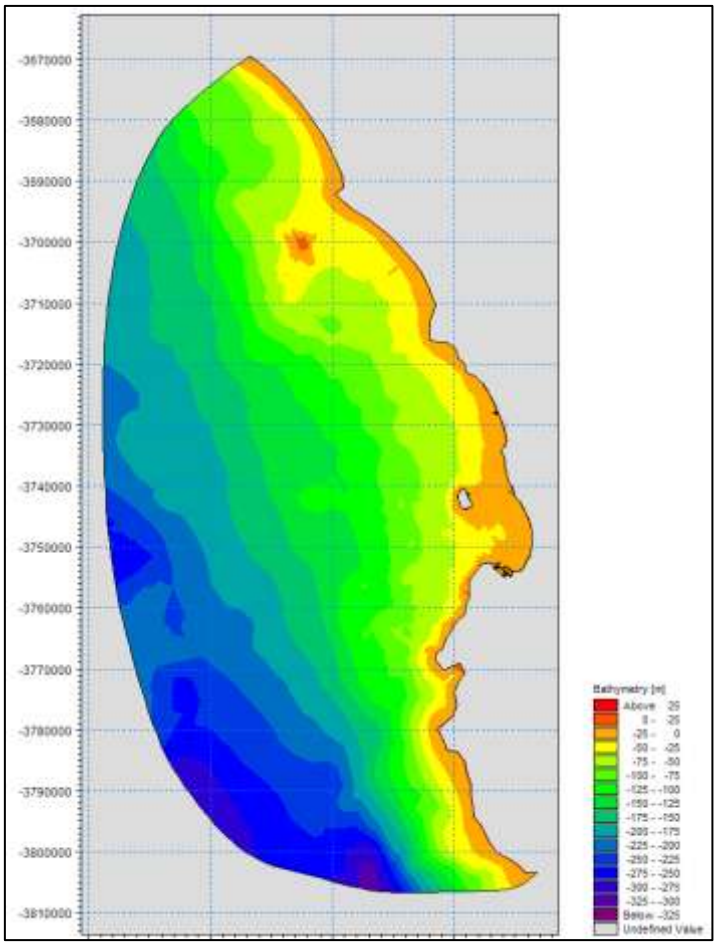

A.5.2 Bathymetry and Nested Grids

A.5.2.1 Bathymetry

The offshore wave climate, discussed in Section A-3 of this report, was measured at the Cape Point measuring station. This waverrider buoy is located in approximately 70 m of water (Figure A - 1). As shown in Figure A - 9, the depth along the offshore boundary of the wave model is significantly larger than this.

To accurately describe the wave climate within Table Bay, the offshore depth was limited to -70 m MSL. This means that all depths greater than -70 m MSL were fictionally made -70 m MSL (see Figure A - 10).

This approach includes an important assumption, namely that all waves along the -70 m MSL contour are equal, in height, period and direction.

During the simulation, a wave that enters the model domain at the boundary remains un-refracted until it reaches the -70 m MSL contour, from where it starts changing as it propagates towards the shoreline.

Although being an unconventional wave simulation approach, it will be shown in later sections of this report that the results obtained are sufficiently accurate to describe the nearshore wave climate.

Figure A - 10: Fictional Bathymetry and Nested Grid Approach

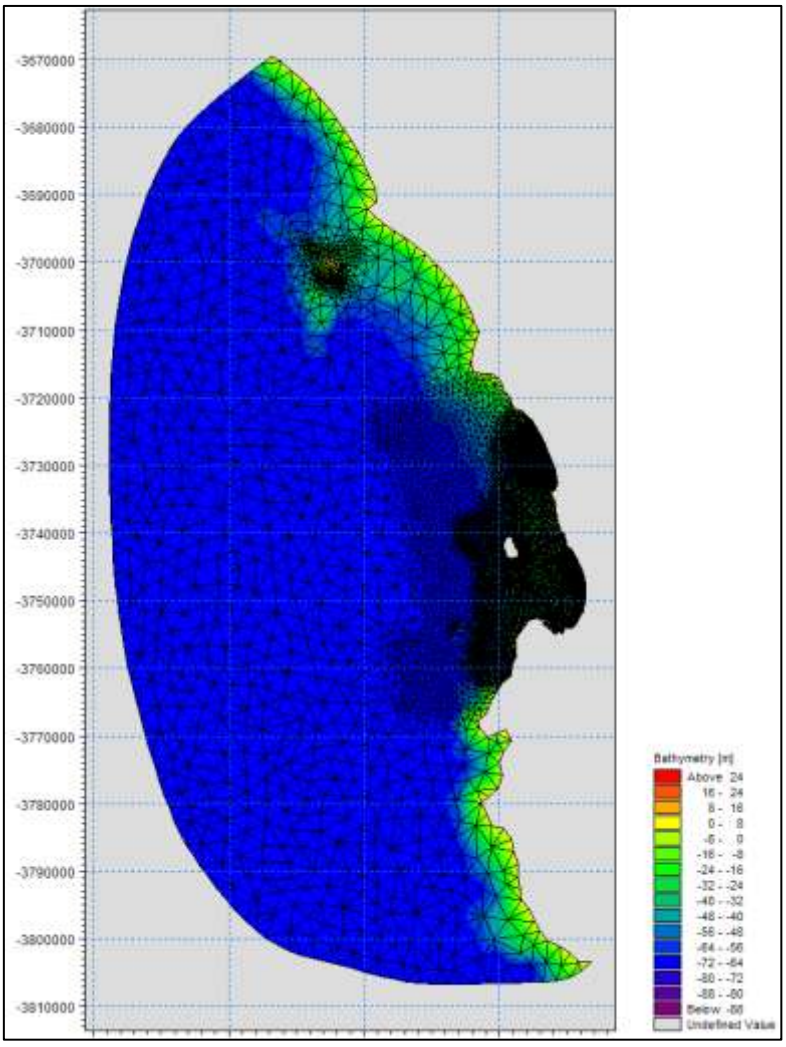

A.5.2.2. Nested Grids

A nested triangular mesh approach was used to describe the bathymetry. This approach makes use of varying mesh element sizes, in order to determine the sea-bottom accurately, whilst also attempting to minimize the computational effort required when performing the simulation.

As will be seen in Figure A - 10 and Figure A - 11, a coarse mesh was utilized for the offshore regions, as well as areas of non-interest towards the far northern and far southern parts of the model domain, becoming more refined approaching the shoreline. This was done for two main reasons: Firstly, it is less important to describe the bathymetry in detail in deep water areas, since small inaccuracies will have a negligible impact on wave refraction results in the nearshore, and secondly, the extent of bathymetric information is significantly denser closer to the shoreline compared to the offshore regions. It is therefore unnecessary to refine the mesh in deeper water, since there is insufficient data to enhance the resolution of the bottom contours.

Figure A - 11 depicts the nearshore area of the model domain, which shows five general areas in which the mesh is refined. The first of these areas is around the Koeberg Power Station. This area needs to be accurately described to facilitate the model calibration. The refinement around Robben Island has been included since the bathymetry in this area is fairly steep, which has a significant effect on the wave patterns in

the lee of the island. The refinement at the entrance to the Port of Cape Town has been included to accurately describe the bathymetry at the secondary calibration point.

Figure A - 11: Local Nested Grids

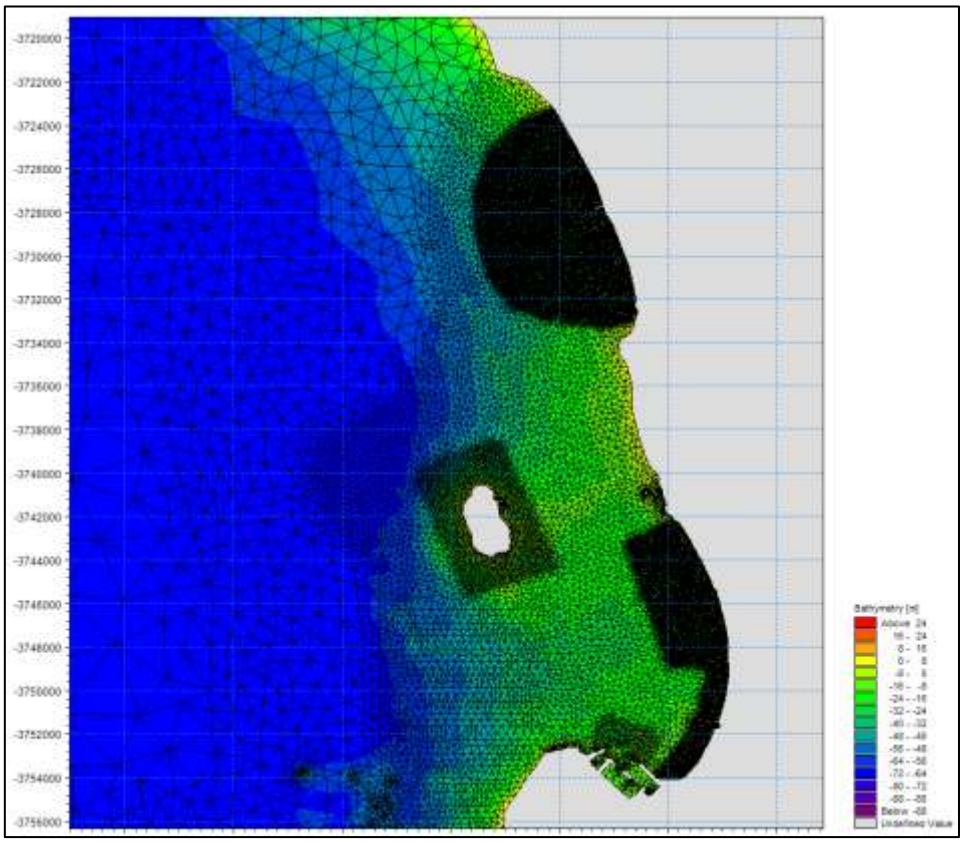

The refinement along the Table Bay shoreline, as well as the Seli One shipwreck has been included to accurately determine the wave climates in these areas, as these will be used as input in the sediment transport simulations.

A.5.3 Spectral Wave Model Setup

The wave action balance equation is used to describe wave propagation in the spectral wave model. Two different formulations are available in the MIKE21 SW model, namely the 'Directionally decoupled parametric formulation', as well as the 'Fully spectral formulation' (DHI, 2011a). As discussed previously, the boundary condition is a parametric wave climate, thereby necessitating the use of the parametric wave propagation formulation.

The wave directions within the model are described by discrete directional bins. Although the input waves were limited to ranging between 120˚ and 360˚, the entire 360˚ directional rose, binned into 10˚ sectors, was included in the directional description. This was because although the offshore waves are limited in a directional sense, the refracted nearshore waves are not necessarily limited to the same directions as the offshore waves.

Furthermore, the spectral wave model did not include water level variations, current conditions, wind forcing, ice coverage, diffraction effects, or any structures within the model domain. The initial condition of the model domain was a 'zero spectra', meaning that the water surface was flat and no waves were present in the model. The assumption with regards to wind forcing was that the offshore wave climate, used as input information

into the bay-wide wave transformation model, already included the effect of the wind, which therefore did not need to be included once more.

Depth-induced wave breaking was included in the simulation, and is based on the formulation of Battjes and Janssen (USACE, 2003). The gamma value of 0.8 is constant over the entire model domain.

The bottom friction was used as calibration parameter, varied until satisfactory results were obtained. Details of this parameter will be discussed later.

A.6 Model Calibration

A.6.1 Calibration Parameters

As pointed out earlier, the bottom friction was used as calibration parameter for the spectral wave model. Four different formulations are available in MIKE21 SW to describe the bottom friction (DHI, 2011a), namely the

- Friction coefficient, C_{fw}
- Friction factor, f_w
- Nikuradse roughness, k_N
- Sand grain size, d_{50}

The sand grain size description was not considered as a viable parameter, since the bottom conditions in Table Bay are predominantly rocky (CSIR, 1999). Although it would be possible to calibrate the model to accurately represent the wave climate at the two calibration locations, the model would not be reliable to accurately describe the wave climate over the entire model domain.

The Nikuradse roughness was not considered since, according to the MIKE21 SW User Manual, this description is most often used for offshore applications using the fully spectral formulation, but is usually too high for nearshore applications (DHI, 2011a).

The remaining two descriptions, the friction factor and friction coefficient, were both investigated to determine the most accurate for the current investigation. From preliminary trial runs, it was determined that the friction factor was the most accurate, and was therefore used further during the model calibration exercise.

A.6.2 Post Processing

The spectral wave simulation was followed by an extensive post-processing exercise. The first of these tasks was to combine the sea- and swell components, refracted to the calibration position separately. The significant wave heights and peak periods were combined using Equation A-1 and A-2 respectively.

$$H_{mo-total} = \sqrt{(H_{mo-sea})^2 + (H_{mo-swell})^2} \qquad \text{Equation A-1}$$

$$T_{p-total} = \frac{T_{p-sea} * (H_{mo-sea})^2 + T_{p-swell} * (H_{mo-swell})^2}{(H_{mo-sea})^2 + (H_{mo-swell})^2} \qquad \text{Equation A-2}$$

The peak direction was calculated using a vector approach, considering the wave height of each of the two components together with their respective peak direction. Each of the components was split up into vector

components, with the x-axis being positive east and the y-axis being positive north. The two vector components (x and y) of the sea- and swell components were then added linearly, and the combined peak direction calculated. See Figure A - 12, Figure A - 13 and Figure A - 14 below for a graphic representation of this approach.

The combined wave climate was then compared to the measured wave climate, in order to determine the accuracy of the simulation model. This was done by comparing the time series of the measured and simulated H_{mo}, T_p and D_p. Visual inspections of certain sections of the time series were also made to determine the causes for possible inaccuracies.

Figure A - 12: Vector Discretization of D_p, Sea Component

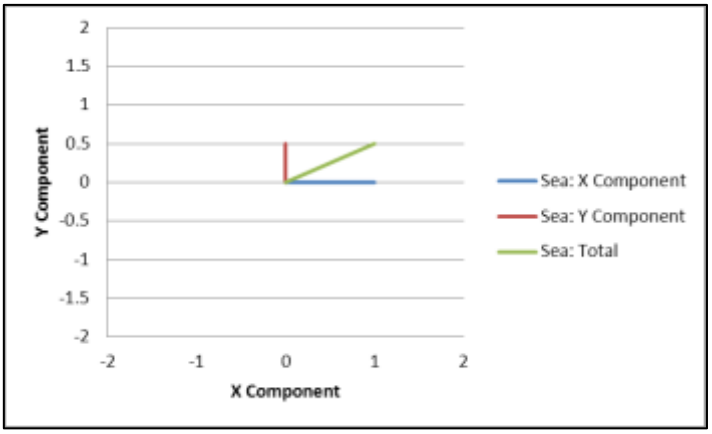

Figure A - 13: Vector Discretization of D_p, Swell Component

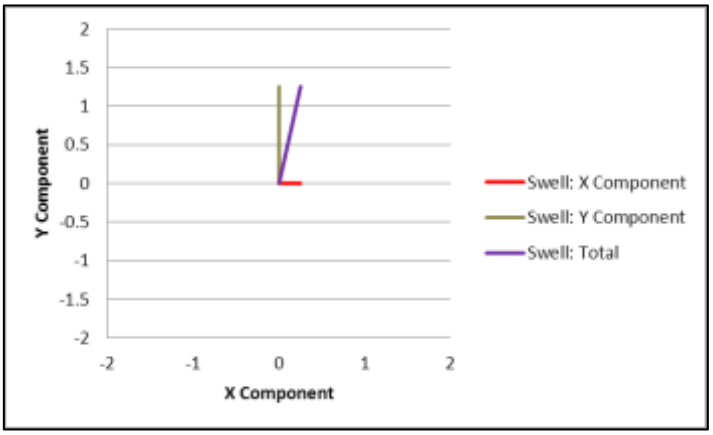

Figure A - 14: Vector Discretization of D_p, Total

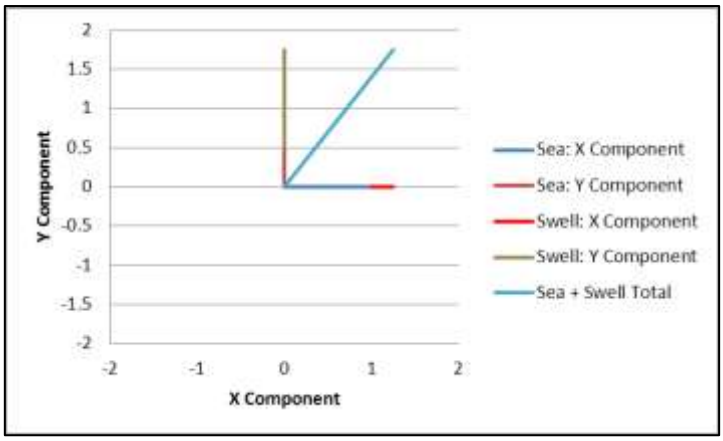

A.6.3 First Simulation Run

The first simulation run was performed using the default friction factor value recommended by the DHI User Manual (DHI, 2011a). This value is a friction factor of 0.0212.

Figure A - 15 below shows a comparison of the simulation and measured significant wave heights. This graph also shows a line representing a perfect correlation between the simulation and measurements (red line).

It will be observed from Figure A - 15 that the simulated wave heights are approximately 30% larger than the measured wave heights. This means that the amount of energy which arrives at the calibration location is too high, which indirectly means that the level of energy dissipation as the waves travel from the offshore boundary to the nearshore is insufficient. To increase this energy dissipation, the friction factor was increased during subsequent runs.

Figure A - 15: Default Friction Factor, Koeberg Calibration Position, H_{mo} Comparison

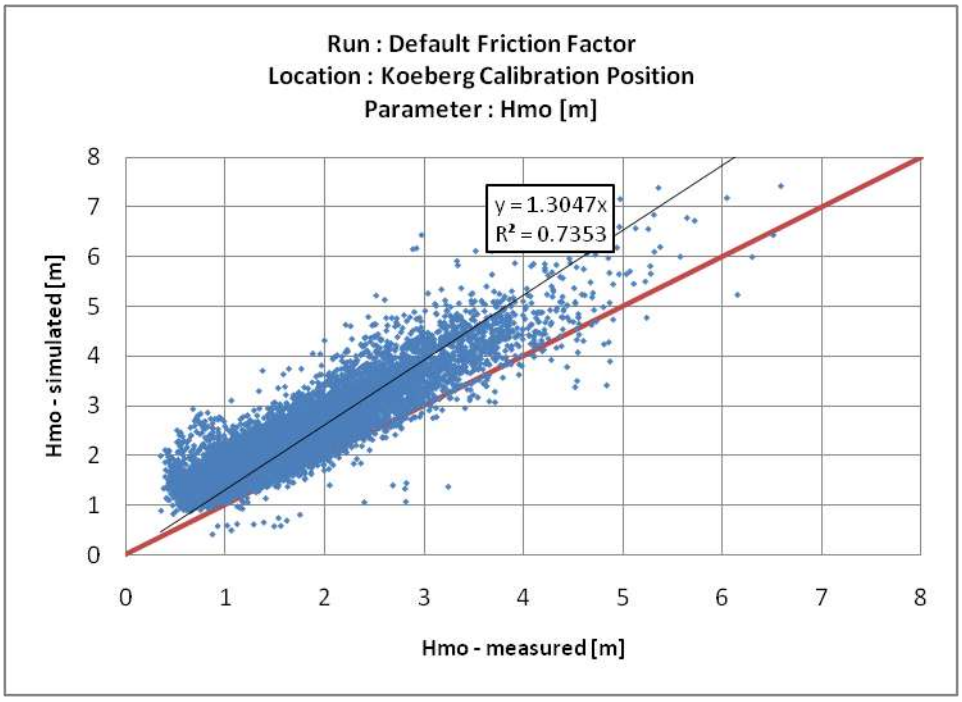

Referring now to Figure A - 16, the simulated and measured wave directions are densely situated between 180˚ and 315˚. It will also be observed that the simulated wave directions tend to be lower than the measured directions.

Basic wave refraction theory states that waves turn such that the wave ray is perpendicular to the shoreline. A wave ray at the Koeberg Power Station therefore has an orientation of between 225˚ and 270˚, shown graphically in Figure A - 16.

Investigating the simulated wave directions, it will be noticed that they lie predominantly between 180˚ and 270˚, thereby being lower than the measured directions. This means that the simulated waves have not turned as much compared to the measured waves.

Figure A - 16: Default Friction Factor, Koeberg Calibration Position, D_p Comparison

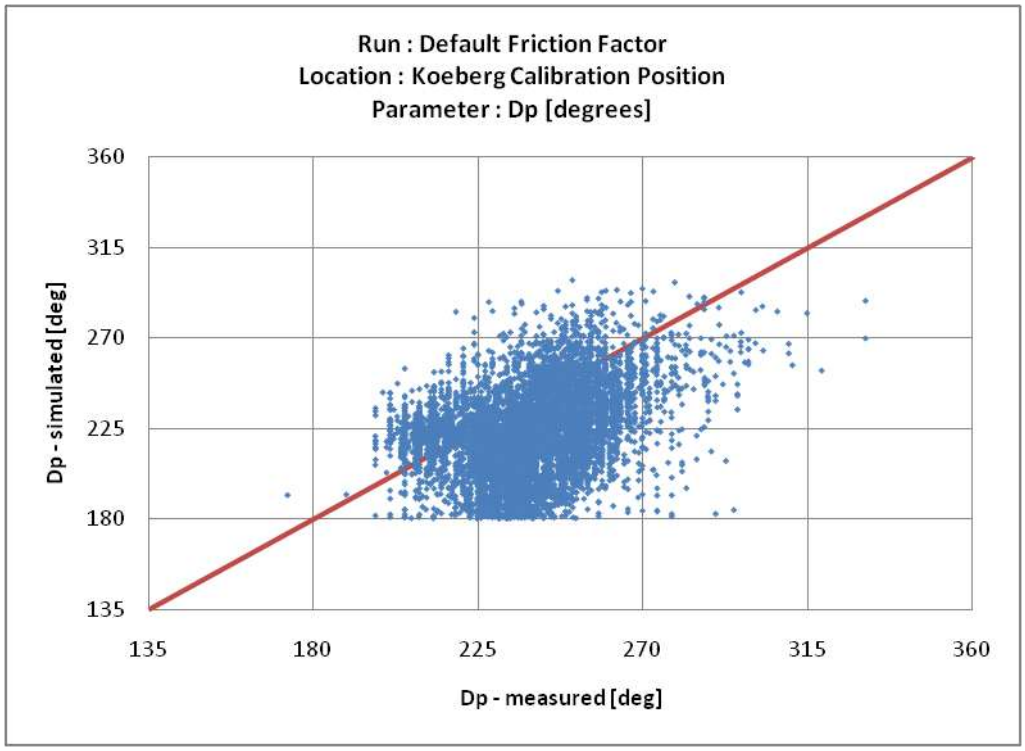

Similarly to the wave height comparison, the conclusion which can be drawn from this is that the bottom friction of the model is insufficient, since, if the bottom friction was correct, the waves would have refracted more, thereby turning more to agree closer with the measured wave direction.

The final calibration tool used to inform the decision regarding the choice of friction factor was a comparison of the individual time series, being H_{mo}, T_p and D_p. Figure A - 17below reiterates comments made during this discussion, namely that the simulated wave heights were too high and that the simulated wave directions were too low. By comparing the individual time series' however, it will be noticed that the difference between the simulated and measured wave heights were most prominent when the peak periods are large. It is clear from linear wave theory that a larger wave period causes a wave to "feel the bottom" in deeper water compared to short period waves. This therefore confirms that the friction factor has to be adjusted to increase the accuracy of the wave simulation model.

Figure A - 17: Time Series Comparison of Initial Spectral Wave Simulation

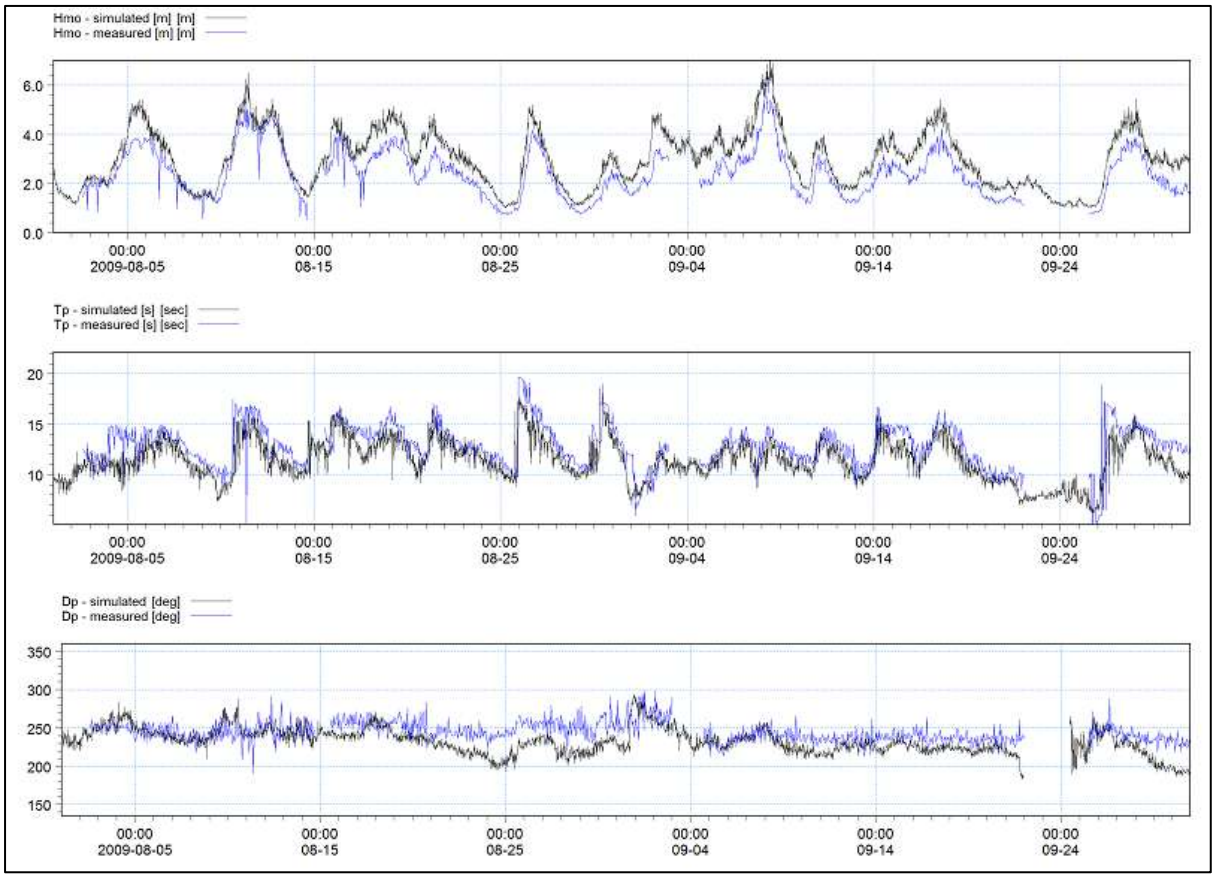

A.6.4 Calibrated Wave Model

The analysis described in the previous paragraph was repeated for each calibration run, investigating the accuracy of wave height and wave direction in order to refine the friction factor. Following numerous iterations, a friction factor of 0.1 was used to deliver satisfactory results.

Figure A-18 shows the wave height comparison at the Koeberg calibration position, using the final friction factor of 0.1. It is clear from this figure that the simulated and measured wave heights correlated well, and were generally within 10 % of each other. This was deemed a reasonable comparison, sufficiently accurate for the subsequent sediment transport calculations.

Comparing Figure A - 16 and Figure A - 19, it will be noticed that simulated wave directions had, in general, increased to agree more closely with the measured directions. Although there was a fair amount of scatter, a good correlation was identified.

As introduced previously, the final tool to determine the accuracy of the friction factor was to compare sections of the various time series. Figure A - 20 shows a significantly better correlation between simulated and measured wave height and direction can be made compared to the default wave simulation (Figure A - 17).

Figure A - 18: Friction Factor of 0.1, Koeberg Calibration Position, D_p Comparison

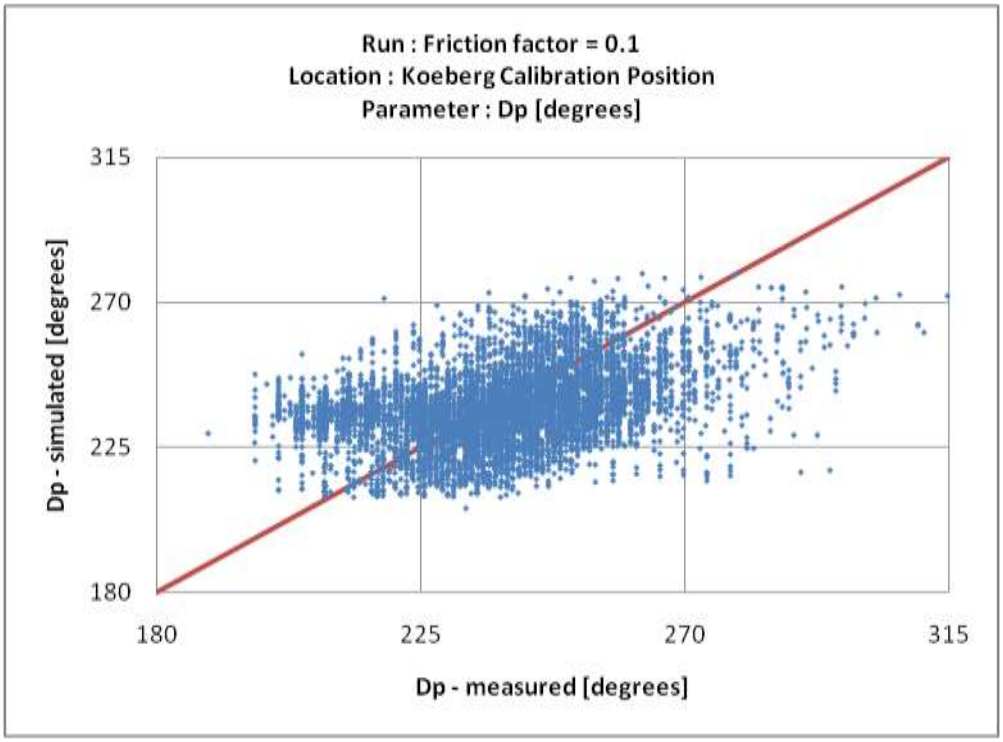

Figure A - 19: Friction Factor of 0.1, Koeberg Calibration Position, H_{mo} Comparison

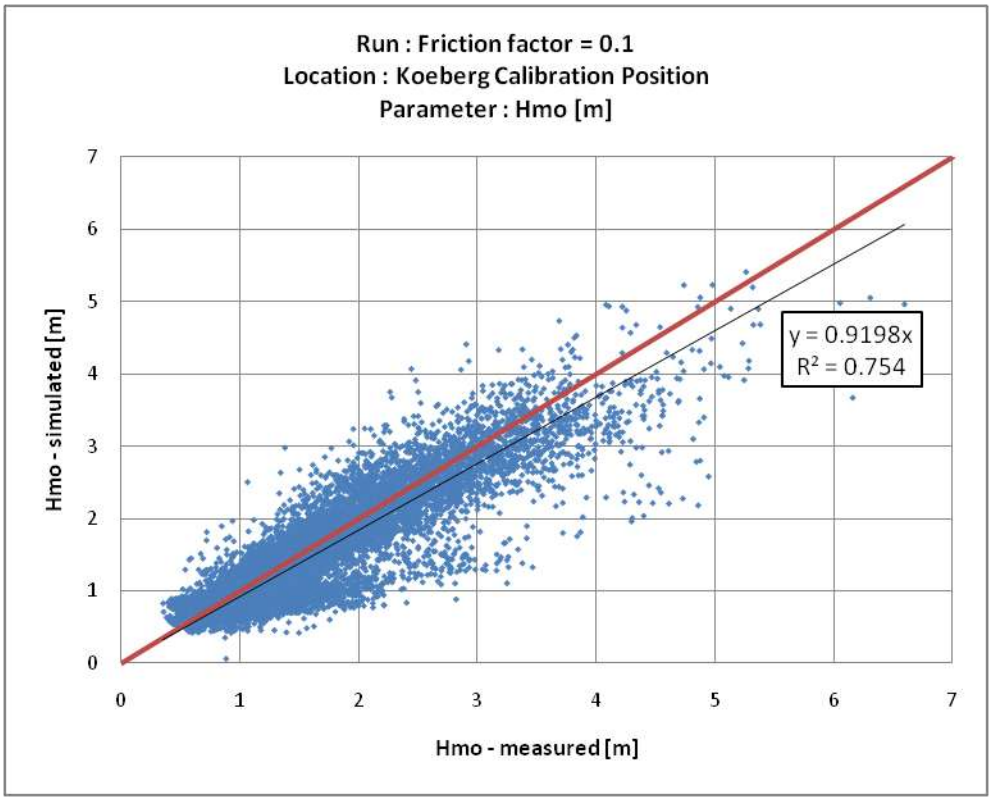

Figure A - 20: Time Series Comparison of Final Calibrated Wave Simulation

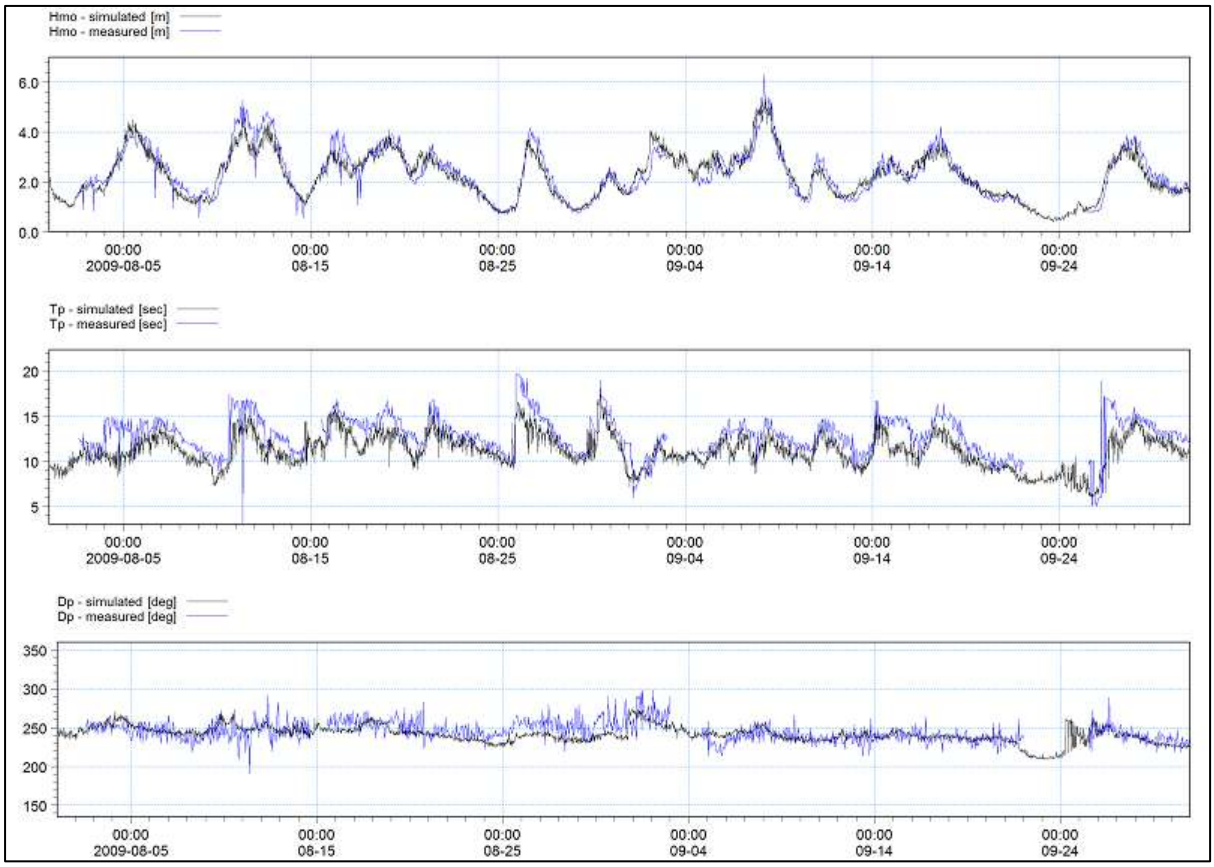

A.7 Production Run

Considering the wave modelling approach adopted during this study, no additional production runs were required to determine the nearshore wave climates needed for the sediment transport analysis. The calibrated refraction coefficients could be used directly to determine these climates directly without any additional simulations.

A.8 Summary and Conclusions

Wave refraction modelling has been performed by implementing the MIKE21 Spectral Waves software package. A one-dimensional spectral offshore wave dataset measured at the Slangkop and Cape Point wave measuring stations has been used as model forcing. An in-depth review of the offshore wave dataset has been performed, during which the measurements have been split into sea and swell components, with each component being refracted separately to the nearshore.

It has been shown that, by splitting the total wave energy up into sea and swell components, a more accurate representation of the nearshore wave climate is obtained. This is because the variance, in terms of both wave direction and frequency, are retained during the wave transformation modelling. Resulting sea and swell wave climates are then combined at the nearshore, to determine the total wave climate at that location.

A so-called look-up table approach has been used to perform the wave transformation modelling. During this approach, a matrix of refraction coefficients is generated, each of which describe the refraction characteristics of one particular offshore condition. In this way, simulation run times were significantly reduced, since each wave condition only had to be simulated once, regardless of the recurrence in the offshore wave time series. The real offshore wave time series was then refracted to the nearshore by applying the applicable refraction coefficients to each of the respective time steps.

The use of a fictional bathymetry was discussed. In this fictional bathymetry, all depths greater than -70 m MSL were fixed to be -70 m MSL. This has been done since the offshore wave data was located at a depth of -70 m MSL, whilst the offshore boundary of the wave transformation model was generally located in much deeper water than this. In such a way, refraction effects only commenced at the -70 m MSL depth contour.

It is concluded that by adopting the various numerical modelling methods and approaches, a representative nearshore wave climate has been determined, which could be used for the subsequent sediment transport modelling to investigate the impact of the Seli One shipwreck.

APPENDIX B – BLOUBERG BEACH SURVEY (3RD JULY 2011)

B.1 Introduction

One of the main objectives of the current study was to investigate the accuracy and applicability of numerical modelling software to identify and quantify the impact of the Seli One shipwreck on the Blouberg shoreline. To be able to perform this adjudication, the actual impact of the shipwreck on the shoreline needed to be measured. To this end, a beach survey was performed on the 3rd July 2011, which is covered in more detail in the following paragraphs.

B.2 Survey Methodology

B.2.1 Survey Approach

The survey was performed by the author by measuring the position of the beach along44 cross-sections, spaced intermittently along the Blouberg beachfront, comprising 441 individual survey points as shown in Figure B - 1. The top of each of the cross-sections was generally chosen to be on top or landward of the primary dune crest, whilst the bottom of the cross-sections was taken as low down the beach as possible. Since the survey was performed by foot, the lowest position that could be surveyed was generally in knee-deep water.

Between the upper and lower survey locations, points were chosen so as to accurately represent the beach shape, by surveying particular features and the location of a change in beach gradient.

Cross-sections were most densely spaced along the beach in the immediate lee of the wreck, becoming more widely moving away from the impact area of the wreck. The spacing in the lee of the wreck was in the order of 20 m, whilst this increased to approximately 100 m at the outer ends of the survey area.

The survey area extended from the northern side of the Dolphin Beach Hotel to the rock outcrop at the northern end of the Blouberg beachfront, a length of approximately 2.8 km.

The survey date of the 3rd July 2011 was chosen as this coincides with the spring tidal cycles in Table Bay. The lowest survey point in a cross-section is dictated by the water level, the lower the water level, the greater the survey coverage. The bottom of the surveyed cross-sections generally to between the 0 m MSL and -1 m MSL depth contours.

Figure B - 1: Beach Survey Area and Surveyed Cross-Sections

B.2.2 Survey Equipment and Survey Verification

A Differential Global Positioning System (DGPS) was used to perform the beach survey, supplied free of charge by Mr Aubrey Price of C&C Technologies. This instrument is comprised of a staff, a differential GPS mounted on top of the staff, as well as a data logger and user module connected mid-way on the staff. The equipment setup is shown in Figure B - 3.

The claimed accuracy of this system is 1 cm for the horizontal position, and 2 cm for the vertical position. Calibration of the instrument was not necessary, since it receives real-time RTK (Real Time Kinematic) corrections via the mobile cellular phone network.

Although calibration as such was not necessary, the measurements still had to be verified to ensure correctness. This was done by comparing the location, both in plan and elevation, of a fixed benchmark to the

surveyed location thereof. Details of the town benchmarks for the City of Cape Town were obtained from Mr Tim Painter of Lloyd and Hill Surveyors.

Numerous benchmarks are located near the Seli One. The one shown in Figure B - 2 was however the easiest to reach, and was therefore chosen for the comparison of the surveyed and fixed benchmark levels. As shown in the figure, the level of this benchmark as per the City of Cape Town database is +10.004 m MSL, whereas the surveyed level was +9.92 m MSL, a difference of 8 cm. It was assumed that the level as per the City of Cape Town is correct, which meant that surveyed levels were increased by 8 cm throughout.

Figure B - 2: Fixed City of Cape Town Benchmark versus Surveyed Benchmark

Cape Town benchmark as obtained from Lloyd and Hill Surveyors

Cape Town benchmark as surveyed during beach survey for current study

A separate point was surveyed at regular intervals throughout the course of the day, to test whether the equipment was “drifting”. The levels of this point ranged between +9.24 m MSL and +9.28 m MSL, which is within the acceptable tolerance of the equipment. It was therefore concluded that the instrument remained consistent throughout the course of the day.

Figure B - 3: Survey Equipment Used During Beach Survey

B.3 Survey Execution

Despite July being the middle of winter, the 3rd July 2011 turned out to be pleasant, partly cloudy, with no rain. The temperature was approximately 18°C. Wave conditions were mild, with breaking waves being judged to be between 1 m and 1.5 m in height.

The predicted tidal levels on the 3rd July 2011 were as follows (SANHO, 2011):

High tide	4:29 AM
Low tide	10:39 AM
High tide	16:54 PM

The survey commenced at approximately 8AM, approximately two and a half hours prior to the lowest water level. This was done since it was thought that the survey would take about five hours to complete, with the lowest water level aimed to occur approximately half-way through the survey.

Figure B - 4: The Author Surveying a Point on the Beach in the Lee of the Seli One Shipwreck

Figure B - 5: The Author Surveying the Bottom Portion of a Cross-Section

B.4 Survey Results and Conclusion

Results of the survey were processed by performing a linear interpolation of the individual survey points to generate a contour map of the beach from the Dolphin Beach Hotel to the rock outcrop at Blouberg. This is shown in Figure B - 6, from which a curvature in the lee of the Seli One shipwreck can be identified. These results were used during the evaluation of the shoreline evolution modelling component of this study.

Figure B - 6: Interpolated Beach Contours

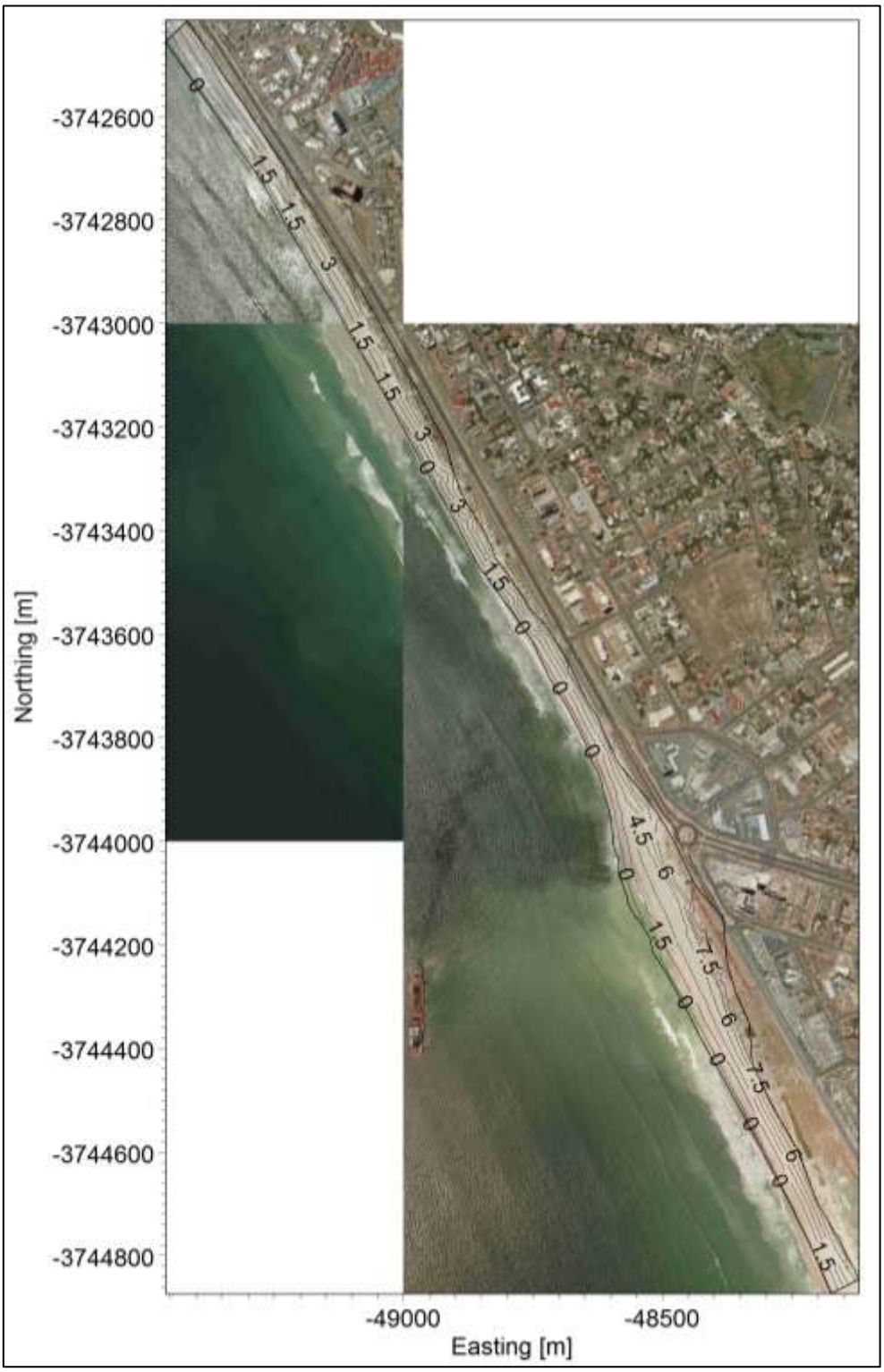

APPENDIX C – STUDY MAP (TABLE BAY)

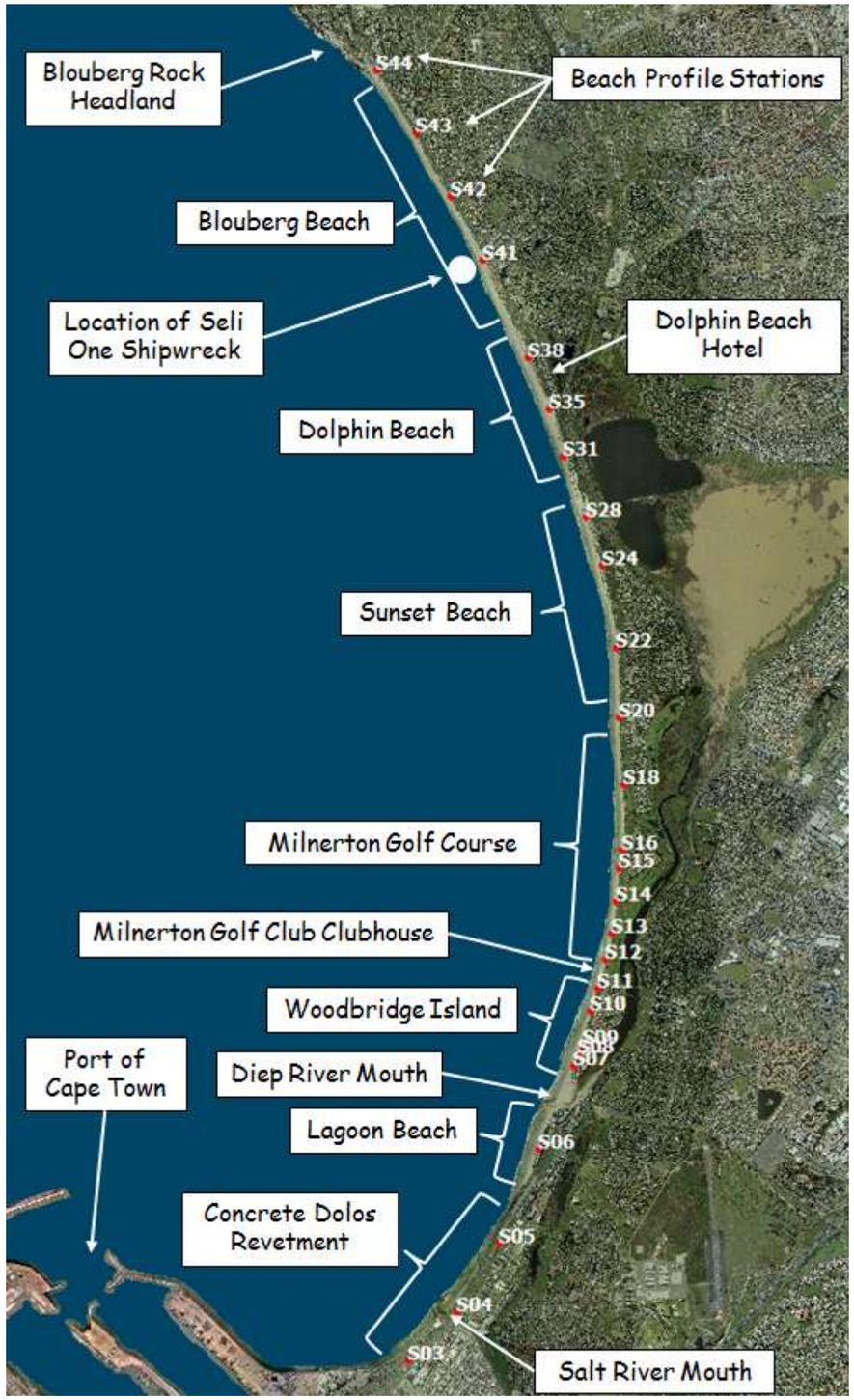

APPENDIX D – STUDY MAP (BLOUBERG ROCK HEADLAND TO MELKBOS ROCK HEADLAND)

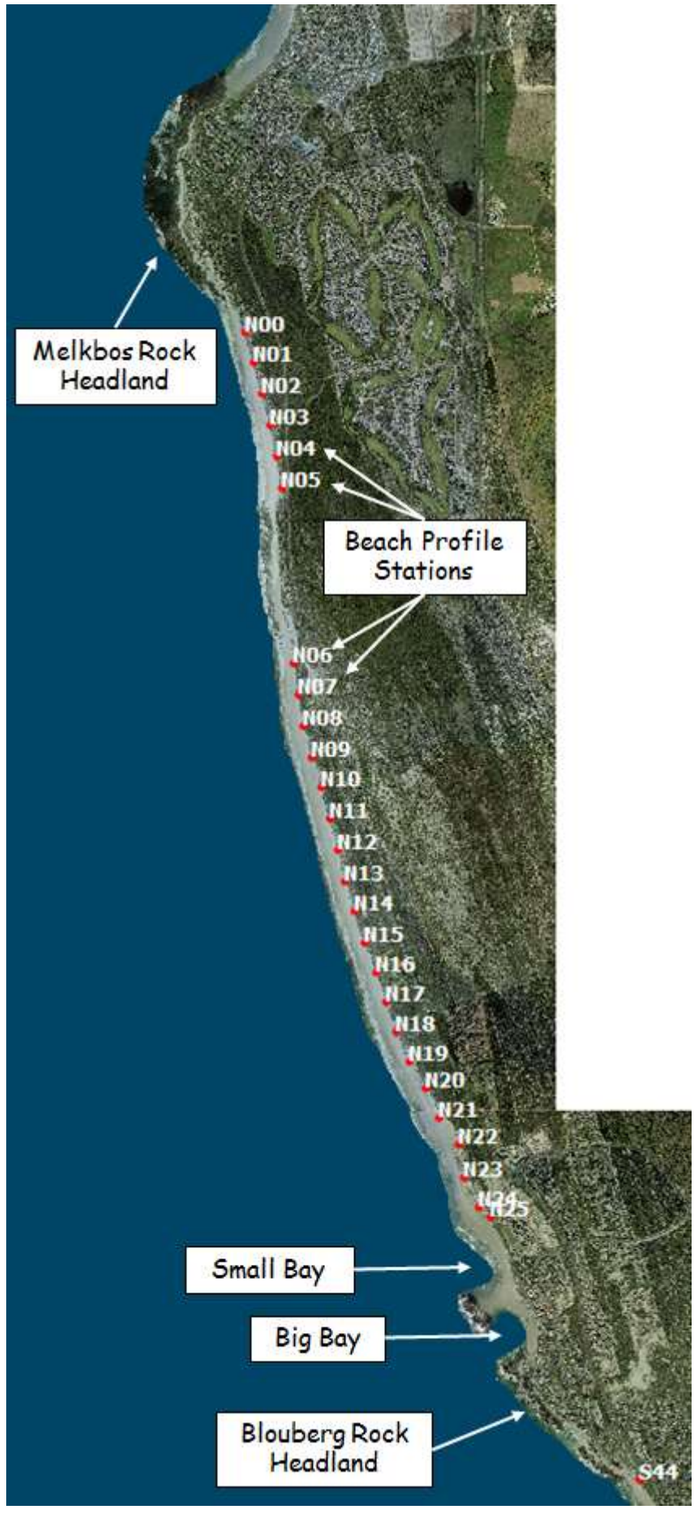

APPENDIX E – COASTAL SECTORS OF TABLE BAY